DEVELOPEMENT OF CONCEPTUAL FRAMEWORK FOR SHAPE MATCHING IN NESTING

by

PRASHANT S. RANE

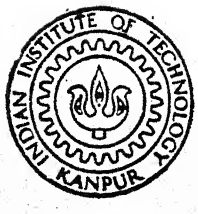

DEPARTMENT OF MECHANICAL ENGINEERING

INDIAN INSTITUTE OF TECHNOLOGY, KANPUR

JULY, 1989

DEVELOPEMENT OF CONCEPTUAL FRAMEWORK FOR SHAPE MATCHING IN NESTING

A Thesis Submitted
In Partial Fulfilment of the Requirements
for the Degree of
MASTER OF TECHNOLOGY

by

PRASHANT S. RANE

to the

DEPARTMENT OF MECHANICAL ENGINEERING
INDIAN INSTITUTE OF TECHNOLOGY, KANPUR

JULY, 1989

Certificate

This is to certify that the work entitled "Developement of Conceptual Framework for Shape Matching in Nesting", by Prashant Rane has been carried out under my supervision and has not been submitted elsewhere for the award of a degree.

Dr. J. L. Batra
Professor
Department of Mech. Engg.
I.I.T Kanpur.

ACKNOWLEDGMENT

I take this opportunity to express my gratitude to my professors and my friends in IIT Kanpur who guided and helped me in this thesis. Dr. Dhande helped me select the topic and gave the initial impetus for this work. Dr. J. L. Batra has been a continuous source of inspiration and encouragement during the past year. I am greatly indebted to him for his guidance and support. My friends are too numerous to be listed and acknowledged. I can not mention all of them because of sheer size. But some of them have loomed so large that they must be acknowledged. I thank Nitin Joshi, Shripad Ponkshe and Sunil Damle, without whose efforts this work could not have been completed. The dramatics and music group of my friends Sandeep Kulkarni, Subodh Harmalkar, Sandeep Nawathe, Prashant Phatak, Mukund Surange and Abhay Tarnekar culturally enriched the last two years. Sandeep Gupta, Amit Singhal, P. A. Balaji contributed greatly towards making my stay in IIT Kanpur an intellectually fruitful one. All the IME students, especially D. Ramkrishna and Anand were extremely helpful. Last but not the least, the discussions with Sanjay Apte and Vinayak Manohar went a long way in clarifying the concepts in my work.

Prashant Rane

CONTENTS

List of Figures

List of Tables

NOMENCLATURE

a : Approximation measure;

C, C_r : Criticality;

C_u : Concavity reduction factor;

C_{cv} : Concavity measure;

D : Deletion solutions;

D, D_f : Difference in deletion solutions;

Dw : Difference weightage;

G : Goodness of decomposition solution;

I : Intensity, Importance;

L, l : Length;

L_r : Largeness ratio;

L_c : Critical largeness;

P : Peripherality, Proximity;

P_r : Proximity ratio;

q : Quench Size, quench radius;

r, R : Radius of skeletal circle;

s : Distance along skeleton;

t : Fire front advance time;

$\bar{t}$: Unit tangent;

U : Usefulness of deletion solution;

V_q : Quench velocity;

v : Visibility;

W : Weightages;

θ, ϕ : Angles.

ABSTRACT

The problem of allocating irregular shapes on a plane sheet to minimise the required area has been studied extensively in literature. The important parameter affecting the nesting problem, that of the shapes of the pieces and the allocation area has not received sufficient attention. The present work is concentrated on the study of the range of two dimensional shapes from the view of matching the shapes for efficient nesting.

The aim of the work is to propose a comprehensive theory for a descriptive analysis of shapes, so as to facilitate shape matching. The shape description problem has been dissected in to subproblems of polygon decomposition, a classification of the decomposed primitives, the topological and geometrical inter-relations among the primitives, and recognition of shape features for nesting.

A complete polygon decomposition algorithm has been proposed which is aimed at giving a decomposition of the profile in to a set of convex polygons approximating the original profile; the objective of the decomposition is to provide a set of constituent polygons which would be useful for nesting oriented shape description.

A complete convex polygon classification and description has been proposed in the present work. It is based on the number of sides and the shape features such as prominent and sharp angles.

The topological and geometrical relations between the constituent convex polygons have been quantified, so as to provide simple nesting feature recognition criteria. With this, the shape

description is deemed to be complete.

The proposed theory and algorithms rely heavily on artificial intelligence and fuzzy theoretic techniques.

The present work is deemed to be a fundamental study of shapes, in addition to being a nesting problem solution. The concepts evolved in the thesis would be useful in the solution of allied geometrical problems such as the automatic machining sequencing problem in manufacturing. A conceptual level algorithm has been given in the appendix to illustrate the applicability the concepts to the allied problems.

Chapter 1

INTRODUCTION

1. Motivation of the Thesis :

Geometry problems are fundamental problems in mechanical engineering. They may appear as the main problem in mechanical engineering research; or as subproblems in course of some other research problem. They are encountered in almost all fields of mechanical engineering. Some of the more prominent fields in which geometry problems are crucial, are listed below.

Design and CAD : Any machine element design is finally a geometry specification for manufacturing. The geometry aspect of many of machine design problems has often been relegated to the level of determination of size parameters of some standard geometrical shapes. A full research on the possibilities offered by the 'shapes' of the bodies has rarely been done. Shape optimality of design is a field which would definitely be benefited by basic geometry investigations.

Solid mechanics : A solid mechanics problem of stress and strain analysis of a body has geometry problems in the guise of the geometry specification of the body to which various force fields are applied.

Finite elements method : Apart from the solid mechanics aplications of FEM, the other problems such as heat transfer through solids, have geometry aspects in the form of the boundary constraints for the differential equations. Also, the automatic mesh generation for FEM, is a mainly geometry problem.

Manufacturing process planning : Cutting processes can be viewed

as purely geometry problems, where in a given geometry of the stock is to be reduced the final geometry of the machined part. Any theoretical investigation in to geometry, clarifying the basic concepts, is likely to find applications in many of these fields.

2. The Nesting Problem :

The nesting problem, in its purely geometrical form, finds applications in optimum sheet layout for sheet metal processing; and in similar situations such as garment industry, leather industry.

Statement of the Problem :

The problem tackled in the present work is the two dimensional nesting problem.

A given set of two dimensional profiles along with the number of pieces of each of the profiles, and the specifications of two dimensional rectangular sheet, the profiles are to be allocated on the sheet, without any overlap between them, so as to minimise the area of the sheet utilised for allocations. The nesting efficiency is a measure of the area utilisation of the sheet. It may be defined as the ratio of the area of the profiles allocated to the utilised area of the sheet. Hence the objective function of the optimisation is the maximisation of the nesting efficiency.

The profiles considered in the present work are non-selfintersecting polygons, whose boundary is composed of straight line segments, without holes.

3. Basic Approach to the Nesting Problem :

The nesting problem can be viewed as an optimisation problem. The objective of the problem is to determine an allocation scheme to

minimise the area of the sheet. The constraints are the non-overlap of the allocated profiles with each other and with the exterior of the sheet.

Due to the extreme diversity of the shapes of the profiles, a formulation for closed form solutions seems impossible. Even application of classical search methods in optimisation would face very high difficulties at the formulation stage itself. Hence the possibilities of meaningful formulation of the problem as an optimisation problem and a successful application of a classical optimisation method seem bleak.

The nesting problem is solved in industry with little difficulty, by human experts. The solutions reached may not be optimal; but they are sufficiently good for practical purposes. An attempt at emulation of the qualitative reasoning carried out by human beings would be the best approach to tackle the problem.

The reasoning of a human expert, when solving a nesting problem is based on the 'shape' and 'size' qualities for identification of the profile best suited for an allocation in the complimentary area of the sheet, and a shape and size match for the eventual allocation.

The reasoning of a human expert is essentially vague and inexact in nature. Fuzzy theory is a very good theory available for the modelling of such vague and inexact processes.

A human expert bases his decisions on the experience gathered from the past attempts at nesting. The solution process is a search method with tentative decisions, backtracking. The decisions taken are based on heuristics.

The above discussion suggests an approach based on shape analysis

and matching. The algorithms for shape analysis and matching would be fuzzy algorithms. The nature of the algorithms would be of the type which may be classified as the heuristically guided search methods.

In the present work, basic elements of artificial intelligence and fuzzy theory have been used to model the qualitative, inexact and the tentative aspects of the problem. The main thrust of the work is on shape analysis. A fundamental study of shapes from geometric perspective has been attempted in this thesis.

4. Discussion on the Problem and Solution Approach :

The basic idea behind the nesting allocation algorithm is envisaged as follows.

After allocation of some profiles, the utilised region of the sheet takes the form shown in figure 4.1(a). The shaded area, is the complimentary area of the sheet, on which the next allocation is to take place. The complimentary area has some shape features, projection P_1 and bays B_1 and B_2 shown in the figure. The set of

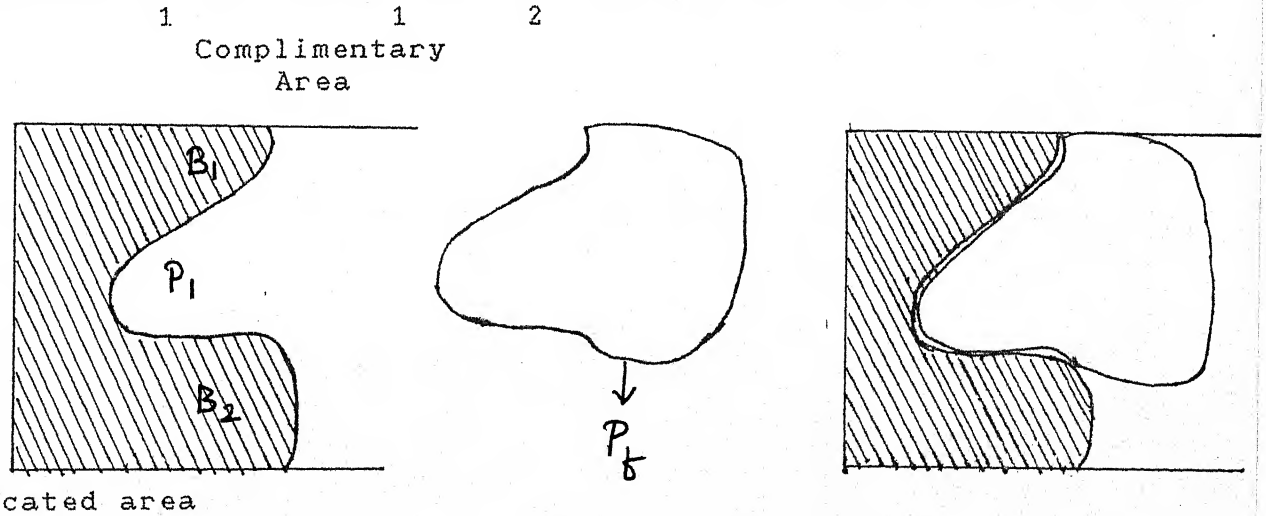

Fig. 4.1 Basic Idea of Nesting.

profiles yet to be allocated may contain profiles which may have similar shape features. A profile P_f, shown in figure 4.1(b), has a projection and a bay which may approximately match the projection P_1 and bay B_1 of the complimentary area. This profile, if placed in the complimentary area as shown in figure 4.1(c), would maximise nesting efficiency by minimising the wasted area. This approach entails an investigation of the following subproblems.

1) A profile description based on shape features such as projections and bays and their inter-relations. The profile description would be an enumeration of the features and their inter-relations.

2) Identification and description of the projection and bay features.

A profile may have extremely complex shape rendering a shape analysis for identification of features and their inter-relations correspondingly difficult. The difficulty is sought to overcome by decomposing the profile in to a set of convex polygons which are simpler and hence more amenable to analysis. The topological and geometrical relations among the constituent convex polygons are then analysed. Projection identification and description is done on the basis of the information available at this stage. Bays are identified by taking a convex hull of the profile. Bays are the differential areas between the convex hull and the profile. Bay analysis is done by treating the bays as independent profiles. The bays, projections and the geometrical and topological relations between them form the profile description.

Thus the following subproblems have been identified.

1) Profile decomposition in to a set of convex polygons.

2) Convex polygon description.

3) Formulation of geometrical and topological inter-relations among a set of convex polygons and their combinations.

4) Projection and bay identification and analysis. A shape description as the projection and bay features and the remaining constituent convex polygons, and their inter-relations.

5) Shape matching based on the profile description formulated in the steps given above.

6) Allocation of a profile based on the shape matching, subject to the constraints of non-overlap of the profiles.

The shape analysis and matching are the crux of the approach. The basic thrust of the present work is in shape analysis. The aim of the shape analysis is to give an abstract, qualitative shape description which is none the less complete. To give a rough analogy, the shape description gives a blurred picture. Some initial tentative decisions are taken on the basis of the blurred picture. As the solution proceeds, the picture is brought in to a sharper and sharper focus. The description is interpreted more and more exactly and quantitatively, as the decisions become more and more firm.

The description of a shape should necessarily have the following properties. The shape description should be unique to the profile being described. It should provide a one to one mapping from the space of all the shapes on to the space of descriptions. To preserve the abstraction and qualitative nature of the description

and at the same time satisfy the above criterion, the complete description should be composed of a number of sub-descriptions with varying degrees of, what could be termed as 'closeness to the profile' or 'goodness of description'. None of these sub-descriptions, by themselves, can provide one to one mapping. The conjunction of these descriptions with their individual 'goodness' gives the description of the profile. It should be noted that the solution methodology should, hence, produce multiple shape descriptions.

The shape matching is the matching of the descriptions. As opposed to a problem in machine vision, the shape matching here, is partial shape matching rather than full shape matching. A local region of the profile is to be matched against the complimentary space on the nesting sheet. Hence the local boundary features such as projections and bays should form the basis of the shape descriptions.

The shape analysis and matching should necessarily be general in nature. It should cover the whole range of possible two dimensional range. This is necessitated by the fact that though the shapes of profiles may be constrained in the problem definition. But the shapes generated in the complimentary area of the sheet during allocation of the profiles are beyond control. The complimentary area may assume any arbitrary shape even for the simplest of profiles. Hence any proposal or a study of nesting algorithms must be preceded by a complete study and analysis of arbitrary two dimensional shapes.

5. Heuristics in the Solution Methodology :

The advocated solution process is the process of attainment of a goal state from an initial state. The initial state is the specification of the sheet and the profiles. The goal state is the final optimal allocation of the profiles on the sheet. The goal state may not be unique.

The solution process is subdivided in to the subproblems stated in the previous section. Each of the subproblems may be treated as an independent problem, with its initial state and goal state. For many of the subproblems, the goal state evaluation is heuristic in nature. An attainment of multiple goal states is desirable, especially for shape descriptions and shape matching. Hence the algorithm can not terminate on reaching a goal state. Multiple paths need to be explored in the solution tree, to obtain multiple goal states.

The traversal from the initial state to the goal state may be modelled as a tree traversal, or a tree search problem for an optimal goal state. At every node of the tree, a number of solutions are generated, which are the children of the current node. The generation of the children at each of the nodes is done on the basis of the conceptual framework developed in the thesis.

The solution tree may be very large. Hence an exhaustive tree search is not advisable. The children nodes are evaluated using heuristic functions developed for the subproblem. The best of the children is explored first. On reaching a dead end or a goal state, the solution path is backtracked and multiple goal states are generated. The extent of backtracking i.e. up to which of the

nodes in the existing solution path should the backtracked, and the number of goal states, are determined again by heuristics.

The Solution method proposed, thus, may be called a heuristically controlled generative space search. The heuristic functions are applied for evaluation of the solutions and goal states, and for controlling the backtracking [28].

6. The Fuzzy Theory Application in the solution :

The fuzzy theory is a good tool to model 'vague', 'qualitative', 'inexact' reasoning. A good development of fuzzy theory has been given in standard textbooks on fuzzy theory [13, 14, 19 & 20]. In the present work, basic elements of fuzzy theory have been used to handle quantifications of the qualitative aspects of the shape analysis.

If the solution process is modeled as a decision tree, then at every decision node a number of decisions are possible. The heuristic functions evaluate the possible decisions i.e. the children of the current node. The quantity returned by the heuristic functions is taken to be the 'desirability' or 'goodness'' of the children. This is illustrated in the Fig. 6.1.

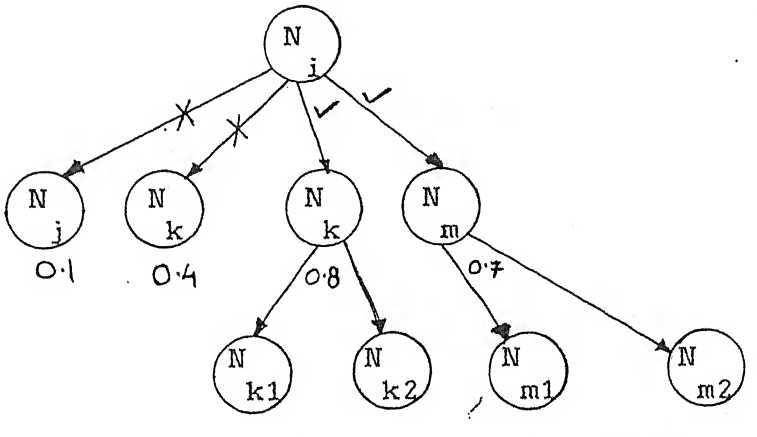

Fig. 6.1 Heuristic Decision Tree or Fuzzy Spawning Process The

node N_i has children N_j, N_k, N_l and N_m. Their goodness measures are given in the figure as 0.1, 0.4, 0.8 and 0.7, respectively. The node N_j and N_k have a low goodness. Hence they should be pruned. Nodes N_l and N_m have comparable and high goodness. They are both expanded, to explore the solution space. At each decision node more than one decisions may be followed, thus spawning a number of subprocesses. This type of processes have been termed as fuzzy spawning processes in the present work.

The goodness of the achieved goal may be evaluated independently by a heuristic function or it may be evaluated as a function of the goodness of the decision nodes in the path. This function, called the mapping function in literature, has to satisfy necessary constraints [19]. Sufficient conditions for the mapping functions have not been formulated. Some common mapping functions have been given in literature [13, 14, 19 & 20]. Both these approaches, for evaluation of goodness of the goal, have been advocated for different subproblems in the present work.

The heuristic functions which are the same as the fuzzy membership functions, are based on some qualities in the problem domain. They quantify the qualitative aspects. They are also termed fuzzy qualitative predicates as they detect the presence of a quality and return a number indicating the measure of the quality in the solution or decision alternative. On detection of a quality in the domain, a corresponding action is recommended by a rule. This action gives rise to a decision alternative.

The solution process may be viewed as a forward chaining of the fuzzy qualitative predicates, with fuzzy inferencing and with backtracking which is controlled by some fuzzy qualitative

predicates. The fuzzy spawning model fits in to this paradigm as a backtracking done to generate multiple goals. This paradigm is more convenient for implementation. The research done on fuzzy or possibilistic inferencing [14] will be useful for a thorough study of the problems through experimentation. The generalised modus ponens propounded in [14] is suggested as a fuzzy inferencing likely to give good results.

The general method followed for quantification of the qualitative aspects for the formulation of the fuzzy qualitative predicates is as follows. The rough quantity indicating a measure of the quality is taken, e.g. for largeness of geometrical size, a length or a radius may be chosen as the quantity. It is compared with a particular quantity of the same type characteristic to the profile under consideration, e.g. for a length, it may be longest distance between two boundary points of a profile. The normalised parameter obtained after comparison, is subjected to a fuzzy membership distribution for an evaluation of the qualitative predicate. Consider the predicate 'Long Length' for an example. The length to be evaluated under this predicate is normalised by taking a ratio with a characteristic length. Let the length ratio be L_r. The fuzzy membership distribution for 'Long Length' is shown in Fig. 6.2. The membership value is the value corresponding to the value of L_r. The fuzzy membership distribution functions embody the heuristics; they need to be refined by experimentation over a range of cases. For the beginning, a linear distribution of the type shown in Fig. 6.2 is proposed. This process is called fuzzy normalisation. In the thesis, a generic function 'fuzzy_normalise'

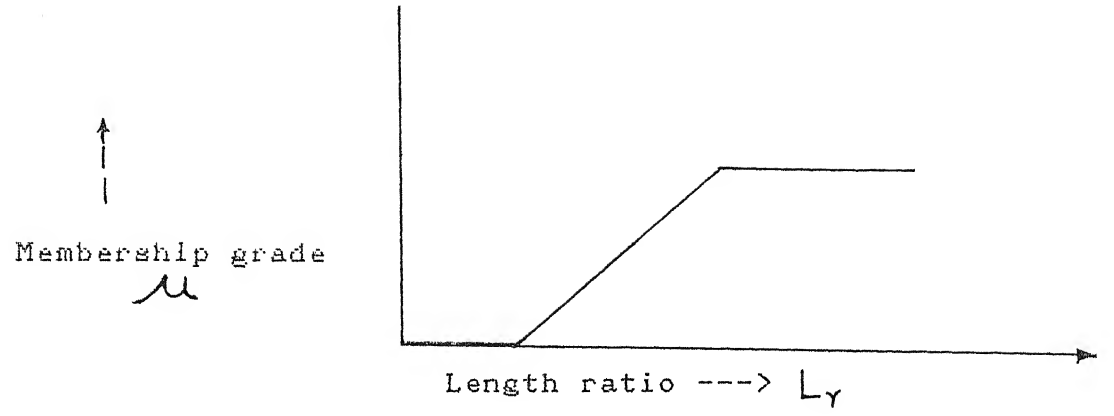

Fig. 6.2 A Fuzzy Membership Function.

has been used to indicate this process. The reference quantity, the characteristic length in the above example, is called the normalisation and comparison parameter.

7. Scope of Work :

The present work is limited to a development of the basic concepts required for a complete theoretical system for shape analysis Algorithms have been proposed; but they are more in nature of first proposals demonstrating the important niche of the concepts which have been developed. They should be treated as initial proposals providing fundamental guidelines for further work in the field. The algorithms have not been studied for complexity and implementation aspects. The attempt here has been to reduce the problems to the level of standard problems in the fields, such as path traversal in a graph, for which standard solutions are known to be available. Computational complexity has not been a consideration in any of the problems. Stress has been laid on the completeness of the theory, and correctness of approach, which appears to be missing in the research work in the field of shape analysis.

The present work is meant to be an exploration of a fundamentally new approach to geometry and shape handling in mechanical engineering problems. The concepts developed in the present work have a powerful potential for giving complete solutions of hitherto unsolved geometrical problems in mechanical engineering. As an example of the applicability of this approach, an algorithm, at a conceptual level, has been given for the solution of a process planning problem in the appendix.

The statement of problem has been given in section 2. A non-selfintersecting polygon, constrained by linear boundary segments, may have very short line segments in the boundary approximating a curved boundary. The curved boundary segments are identified and treated as curved rather than as being composed of line segments. Hence an arbitrary two dimensional shape can also be analysed by the proposed method.

The basic thrust of the present work is on shape analysis. The underlying philosophy of the approach has been to obtain an analysis consistent with human perception. The subproblem definitions have been proposed on this basis.

Shape matching for nesting should be based on local feature match such as the projections, bays and strings composed of projections and bays along the boundary. It is a partial and local shape match as against a complete and global shape match required in machine vision and part recognition systems. A complete and global shape match is not much relevant in nesting. A partial and local match is encountered more often; and hence description of the local boundary features and their inter-relations should form the basis of the shape description.

A large number of techniques may be devised for nesting and allocations. An explorative study of nesting problem and the possible algorithms would be very vast. It has not been attempted in the present work. A basic approach of shape matching, which is likely to be extremely fruitful, has been pursued.

The shape analysis is fuzzy in nature. The solution methodologies applied, are based on artificial intelligence techniques. The special problems of fuzzy algorithms and fuzzy inferencing have not been studied in depth. It has been assumed that mechanisms suitable for the proposed algorithms, may be selected from those available in literature. Some suggestions for the mechanisms have been given from time to time.

The artificial intelligence aspects of the problem are also not dominant. A very basic technique of heuristically controlled search has been applied. In this aspect also, an in depth study of heuristically controlled search has not been done. The proposed heuristics need to be tested and refined through wide ranging experimentation.

8. Comparison of the Approach in Present Work with some Standard Approaches :

The skeleton of a two dimensional profile [8] has been selected to be the basis of the whole shape analysis. The reasons underlying this selection have been laid out in section 1 of chapter 2.

Diverse approaches have been tried for shape analysis by various researchers. The details of these approaches are given in the literature review. The approach followed in the present work is an 'area analysis' approach, with profile decomposition and the

relations between the primitives formed by the decomposition,rather than a boundary analysis approach. A detailed discussion of this issue is given in the chapter 2.

Another rough classification of the approaches for shape analysis is between 'syntactic pattern recognition' and 'graph theoretic' approaches. The approach followed in the present work could be classified to be under the graph theoretic approaches.

One of the major problems with the syntactic approach is that it is, if not impossible, extremely difficult to develop computational grammars, which are applicable to the whole range of shapes. This problem has been mentioned in [18]. The most basic difficulties in this approach are the problems of discretisation of a continuum. For example, in a syntactic boundary analysis, the alphabet for the grammar is composed of short, directed vectors, of unit length. For a profile, in which the lengths of the linear boundary segments have a large range, say varying from one to fifty, the parse tree becomes extremely large. Attributed entities need to be used to overcome this problem, e.g. for boundary analysis, the length of the vector is the attribute of the vector. The next, and even more fundamental problem is that, what should be the orientation of the vectors. Obviously, unit vectors in all the directions can not included in the alphabet; the alphabet size would become infinite. The approach followed so far in the literature is that, either consider only polygons composed of boundary segments which are oriented in certain fixed directions only [17], or consider the boundary segments oriented in some range, say $0 < \theta < 90$, to be exactly the same [27]. None of these approaches seem satisfactory.

9. Literature Survey :

The literature review consists of review of the nesting algorithms for irregular shapes and the review of the subproblems and their solutions.

9.1. Nesting :

An exact formulation of nesting problem has been given by Bailleul et al [6]. It can be seen that the problem can not be solved analytically to get a closed form solution.

A nesting problem with just one shape falls under the category of lattice formation. An approach to nesting solution which constrains the solutions to single row, double row or in general a layout strictly forming strips has been explored in a lot of papers. An approach where in the profiles are enveloped in rectangles and the rectangles are allocated on the sheet has also been quite popular due to its relative simplicity. Such constrained nesting layouts, in general, would not give good nesting efficiency in all cases. Since the approach followed in the present work is extremely different from these approaches, they are not reviewed here. A good review of such approaches is given in [22].

Albano and Adamowicz [3] proposed an algorithm which clusters irregular shapes in to rectangular modules of minimum area, based on some heuristics, such as the best pairwise clustering is obtained by placing two pieces of the same profile next to each other along the width, aligning the lengths, and rotated through 180 degrees. The proposed rectangular module formation is an

extension of the pairwise clustering heuristic algorithm. Albano and Sappupo [4] gave a heuristic algorithm to allocate these rectangular modules on a sheet based on an estimation of the waste that will be generated by the future allocations. Maheshwari combined parts from both these algorithms and modified the heuristics to give a nesting algorithm which short listed profiles based on equality of lengths, giving priority to longer profiles and laying the short listed profiles from bottom left upwards [22]. Albano reported an interactive implementation of the algorithms in [3] [4], which allowed the user to control and modify the allocations proposed by these algorithms [2]. Bailleul and others followed more or less the same approach, i.e. creating strips by clustering profiles and allocating the strips on the sheet [6]. They have implemented an interactive program which presents allocation schemes of the user and allows him to select the one which is consistent with the anisotropic properties of the sheet and the profiles.

These nesting algorithms do not take in to consideration the basic property that dominates the nesting problem, that is the shape of the profiles and the shape of the complimentary area of the sheet. The first such attempt was done by Cai Yuzu et al [10]. They implemented an expert system for the shapes encountered in the garment industry, matching the projections and the bays of the pieces for allocation. The expert system does not analyse shapes but the shape knowledge, in the form of bays and projections, and allocation heuristics knowledge for previously known types of profiles is available, is encoded in the rules in the knowledge base. The expert function executes on the standard paradigm of

rule application and limited backtracking.

A nesting solution methodology should necessarily be based on shape analysis, as the property of "shape" forms the basis of the nesting problem. For a nesting solution to be considered a fully automated solution, it should be able to analyse and allocate diverse shapes and not a limited subset.

9.2. Shape Analysis Techniques :

Various techniques have been employed for shape analysis, such as thinning algorithms, statistical feature recognition and analysis techniques, Fourier Transforms of shapes, Syntactic analysis of the boundary and area, shape decompositions as area decompositions and boundary decompositions, and shape descriptions. The basic pattern recognitions methods applied in shape analysis are given in texts [16 & 25]. The special techniques evolved for shape analysis have been surveyed by Pavlividis in [24], and by Shapiro in [31]. The shape analysis work done in pattern recognition is mostly aimed at machine vision and automatic part recognition systems. Hence most of the research work is done on the assumption of closed world, i.e. a fixed set of well known profiles, or a class of profiles are analysed and matched for identification. Such work, where it is felt that it would be difficult to extend the techniques to diverse shapes, has not been included in the literature review.

Skeleton, alternatively called Medial Axis Transform (MAT), Symmetric Axis Transform (SAT) in the literature, is one of the basic techniques which have been quite popular with researchers in shape analysis. It is reviewed in the next section.

9.3. Skeleton :

The skeleton was proposed by Blum as a transform of two dimensional shapes [8]. Since then it has attracted a lot of attention from researchers in the shape analysis field. The skeleton and some of its basic properties can be found in standard texts on pattern recognition [15, 16 & 25]. Blum and Nagel investigated its properties and the possibility of its applications in shape analysis [9]. Some of its features such as the forking points, skeletal interaction zones have been mooted by Seng - Beng Ho and Charles Dyer [29]. Massone and Morasso have implemented a two dimensional shape editor based on a skeletal representation of shapes structuring a symbolic description of shapes and a shape topology [23].

As most of the work in shape analysis is aimed at machine vision, most of the algorithms for computation of skeleton work on digitised images. Digitisation, though it allows construction of simple algorithms for skeleton computation, produces its own problems, the foremost being that the skeleton is computed in the form of a set of pixels. A recovery of a line diagram description of the skeleton from the set of pixels is difficult and computationally complex. D. T. Lee has constructed a fast algorithm for computation of skeletons from direct boundary representation [21].

As the skeleton gives a good structurisation to multiferously branched shapes which is consistent with an intuitive concept, it has often been used to decompose profiles using the lines forming the skeleton, in to basic shapes and projections. Arcelli and di

Baja applied successive thresholding on the skeletal radius as the method of segmentation [5]. Pizer et al also used successive resolution reduction on object boundary resolution, by blurring the intensity extrema on a gray digitised image [26]. At every stage of the resolution, the skeleton is computed and a hierarchy is imposed on the lines forming the skeleton.

9.4. Polygon Decomposition :

Some of the polygon decomposition methods which directly use the skeleton have been mentioned in the above section. They are different from the standard polygon decomposition problem in the sense that they do not explicitly decompose the polygon in to a set of convex polygons. Even a convex polygon may be decomposed where as a resultant of the decomposition may not be a convex polygon. Hence these methods are not included in this section.

The polygon decomposition methods may be divided in to area decomposition methods and boundary decomposition methods. The first area decomposition method reported in literature is that of Pavlividis [25]. It follows the boundary of the polygon and eliminates concave vertices sequentially. The concave vertex elimination is restricted to cuts joining the concave vertex with some other vertex of the polygon.

Ahuja [1] has presented a decomposition method based on the Vornoi diagrams of the vertices of the profile. The concave vertices are eliminated by drawing a line (or lines) to the nearest Vornoi neighbour. Hence this algorithm can decompose the profile only in to convex polygons which are formed by joining the vertices. Chazelle [11] has formulated an algorithm which again follows the

boundary of the profile and eliminates the concave vertices. The concave vertices are eliminated by cutting the profile by a line lying within the reflex angle of the convex vertex, and joining the concave vertex with another vertex of the profile. The possibility of intersection of cuts has been considered. The intersecting cuts are modified so as to minimise the number of constituent convex polygon. The cuts may also be between a concave vertex and some points on the boundary, which are not the vertices. The results are very good for most of the examples given in the thesis. But as in all other methods, the factor of the identfiability of the constituent polygons has not been considered. Hence, though the decomposition may be optimal from the minimality of the number of convex polygons, it may not give results consistent with human perception.

The boundary decomposition method was first propounded by Shapiro and Haralick [32]. They have developed a graph theoretic clustering algorithm based on the mutual visibility of the vertices across the interior of the polygon, to decompose the boundary and then form the constituent polygons form the combinations of the decomposed boundary. This algorithm does not guarantee a decomposition in to convex polygons [24].

Bjorklund and Pavlividis [7] extended upon the boundary decomposition method by using a graph model for relations among the boundary elements in addition to the mutual visibility. The links of the graph, termed the similarity graph, are the adjacency and similarity relations between boundary elements. The complexity of the graph is curtailed by considering only the links with the k closest neighbours and deleting the rest of the links. The set of

approximately convex constituents are obtained by detecting the cycles in the similarity graph.

9.5. Convex Polygon Classification :

Most of the shape analysis methods either stop at decomposition or skip over the convex polygon description part and go on to the inter-relations among the components generated by decomposition. The survey of the literature indicates that the convex polygon description problem has been relegated to a backseat in the shape analysis field.

9.6. Shape Description and Matching :

After decomposition, and a description of the constituent convex polygons, the shape description depends on the inter-relations of the constituent polygons. Henderson and Davis [18] used a hierarchical syntactic approach for inter-relations among the constituent primitive shapes. The relations are modeled as discrete non-geometrical graphs. A stratified context free grammar has been employed to produce a parse tree of the relations. It has been tested for a class of shapes resembling aeroplanes. The results obtained are very good. The basic problem with this approach is that of constructing generalised production rules. This problem has been acknowledged in the paper [18]. The formulated production rules are only for the class of shapes resembling aeroplanes.

Shapiro [30] has developed 'intrusion' and 'protrusion' relations between the constituents. The relations are graph theoretic relations. A shape matching algorithm, using various heuristics such as weights and thresholding, has also been proposed in the

matching algorithm, for the relation graph matching. A structural description formalism has been proposed, which is used in the shape matching algorithm. Both, the description formalism and the shape matching algorithm give very interesting leads which may be useful in a complete theoretical formulation.

9.7. General Theoretical Background :

The application of the fuzzy theory and artificial intelligence methodologies is of a basic level in the present work. Hence a comprehensive literature review of these fields has not been included in the thesis. Basics of the fuzzy theory, used in the the present work, may be obtained from some standard texts [13, 14, 19 & 20]. The fuzzy classification of convex polygons is similar to the fuzzy clustering given in [20]. The inexact neighbourhood relations developed in the chapter 5, are similar to fuzzy graphs [13]. Possibilistic or inexact reasoning has been developed in [14]. The rudiments of heuristically controlled search methods may be referred from [28].

Graph theoretic concepts have been used liberally throughout the present work. These concepts can be referred from a standard text book on graph theory [12].

10. Organisation of the Thesis Report and Conventions :

10.1 Organisation :

The chapter one is the introductory chapter. The basic approach, literature review of similar problems are given in it. In the second chapter, the skeleton of a two dimensional shape, which forms the basis of the present work is elaborated. An algorithm for profile decomposition is proposed in the third chapter. An

analysis leading to a complete classification and description of general convex polygons is given in the chapter four. The relations between the constituent convex polygons of a profile are developed in the fifth chapter. Chapter six concludes the thesis by discussing the present work, stating the scope for further work on this problem. A solution of a process planning problem has been given in the appendix.

The sections in the chapters are numbered, starting from one, in each chapter. This is done as every chapter is essentially independent; also, to avoid long numbering, as the hierarchy of numbering is too deep.

10.2 Diagrams :

Since the present work is geometrical, it has been illustrated by ample diagrams. In the diagrams, very often, the skeleton of the profile is drawn along with the profile. The profile edges are labeled by the vertices V_i. In some diagrams, the profile boundary and its interior are distinguished from other lines by short hatching. The skeleton is drawn by a dot-dash line (centre line). The cuts and approximations are denoted by a section line. In chapter 5, the N-relations are indicated by a double arrowed line segment.

The diagrams are essentially illustrations of the principles explained in the respective sections. To maintain the link between chapter sections and diagrams, and to facilitate cross referencing, the diagram numbering is not contiguous. It follows the number of the section in which the figure appears.

Chapter 2

SKELETON

1. Requirements of a Basis for Shape Analysis :

Shapes of polygons can be extremely diverse. A precise analysis of shapes is a highly complex task. A feature based cluster analysis approach may be possible for a limited number of shapes. But when it comes to an analysis of all possible shapes, such an approach would produce a very high dimensionality; and also the generation of rigid and mutually exclusive partitions in the feature space denoting classes of shapes, as required in a crisp or non-fuzzy cluster analysis, would be impossible. Rather than a pattern of clusters of points, a continuous spectrum would be obtained. The selection of features, for such an analysis is extremely difficult. An approximate analysis using fuzzy partitioning in some form, is necessary.

Even before an approximate analysis is attempted, the shapes need to be transformed into a form more amenable to analysis, reducing the dimensionality and complexity. The transformation should necessarily ensure that there is no loss of information.

The features which form the basis of the shape analysis should be global rather than local. Features based on boundary analysis are likely to be local features influencing a small local region. Boundary analysis by definition follows the boundary of the profile. It can build only the relationships between parts of the boundary along the boundary. It can not build cross relations between parts of boundary across the interior of the profile. Such

cross relations can be extremely important. For example a boundary analysis may not differentiate between cases shown in Fig. 1.1. In part (a), the boundary points A and B are quite far apart from each other. There is no significant relation between them. In part (b), A and B are close by; they denote a constriction in the shape. Such relations can not be directly detected in boundary analysis. It does not have a mechanism to store such, across the interior, relations.

A transform, proposed by Blum on two dimensional shapes, variously called Skeleton, Median Axis Transform(MAT), or Symmetric Axis Transform(SAT) has been reviewed in literature survey (ref. chapter 1 section 9.3). This transform is well suited for shape analysis. It fulfills all the requirements above reasonably well. It preserves interaction across the interior along with interaction along the boundary. It reduces a shape into a more familiar domain of line diagrams which may be easier to analyse.

2. Skeleton Definition :

2.1 Definition of the Skeleton of a Profile :

Compute the minimum distance of every point in the interior of the profile from the boundary of the profile. With every interior point, at least one point on the boundary is associated, which is the foot of the line of minimum distance. The skeleton is defined as the set of interior points which are associated with more than one point on the boundary. In Fig. 2.1.1, the points P_1, P_2 and P_3 are associated with one point on boundary, points F_1, F_2, F_3 respectively. Point $P_{skeleton}$ is associated with points F_4 and F_5

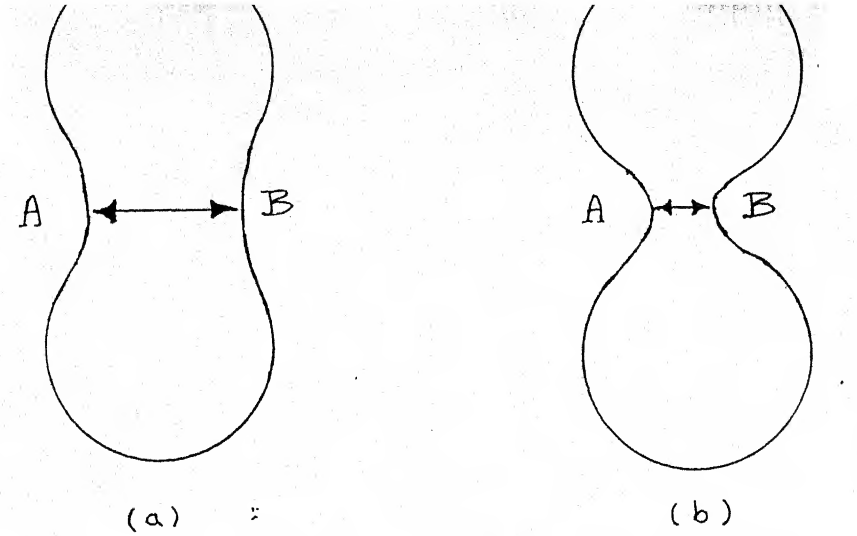

Fig. 1.1 Boundary Interactions Across Interior.

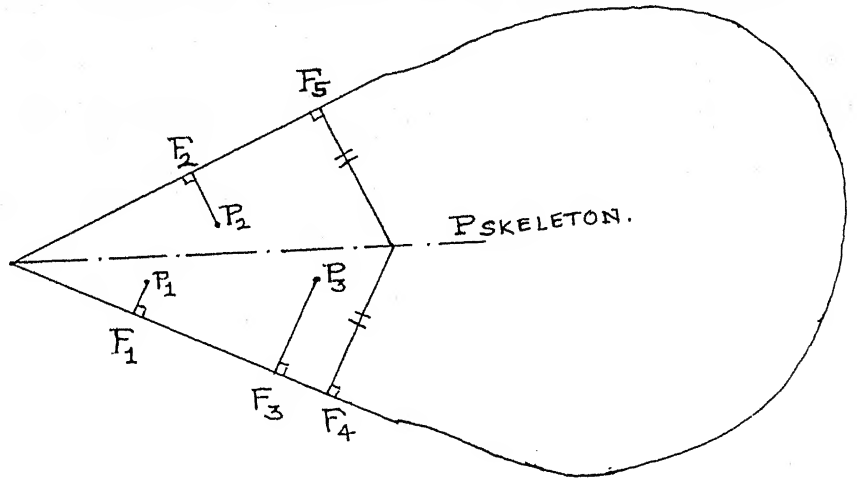

Fig. 2.1.1 Definition of Skeleton.

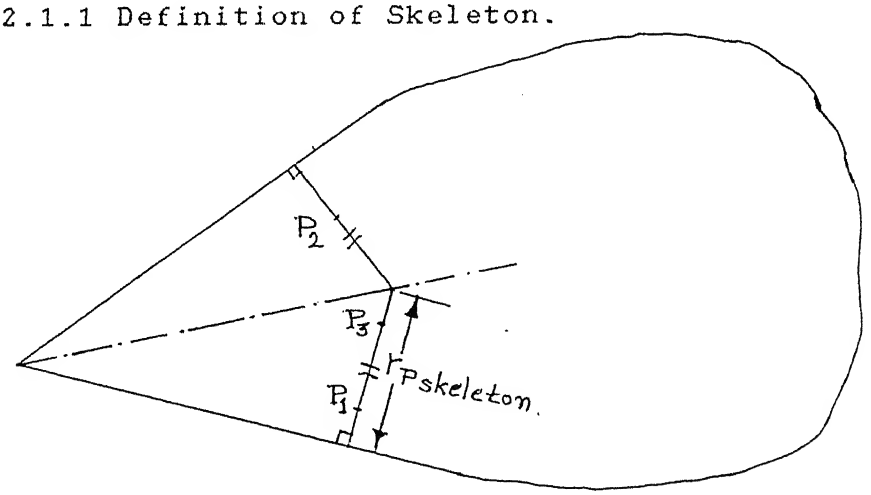

$$r_{P\,skeleton} > r_{P_3} > r_{P_2} > r_{P_1}$$

Fig. 2.2.1 Skeleton as the Set of Ridge Points.

as distance F_4 -$P_{skeleton}$ is the same as distance F_5 -$P_{skeleton}$.

2.2 Different perspectives on the skeleton :

The points forming the set are physically contiguous. The skeleton is a continuous line diagram. The skeleton, along with the distance associated with the constituent points, is completely equivalent to the profile. Hence the transformation is without any loss of information [9, 15 & 25].

The minimum distances of the interior points can be thought to to form a field in the interior. The ridge points of the distance field form the skeleton [25]. In Fig. 2.2.1, the distance of point $P_{skeleton}$ is the largest among the distances of points P_1, P_2, P_3 and $P_{skeleton}$. $P_{skeleton}$ is a ridge point of the distance field.
The skeleton can alternatively be thought of as a 'quench line of prairie fire'. If a field congruent to the profile is set afire at the boundary simultaneously, fire fronts advance from the boundary at the same rate. Wherever two fire fronts meet, a quench line is formed. The set of these quench lines is the skeleton [15]. In Fig. 2.2.2, the rectangle V_1 -V_2 -V_3 -V_4 is the profile. Fire fronts start from the rectangle V_1 -V_2 -V_3 -V_4 at time t = 0. At t = t', fire fronts reach the position V_1'-V_2'-V_3'-V_4', forming the quench lines V_1 -V_1', V_2 -V_2' V_3 -V_3' and V_4 -V_4'. The fire fronts advance through time t'' till they are completely quenched forming the skeletal lines V_1 -A, V_2 -B, V_3 -B, V_4 -A. This perspective on skeleton gives rise to an important parameter of the skeleton, the quench velocity. It is the rate of formation of the quench line with respect to the distance(q) through which the fire front advances.

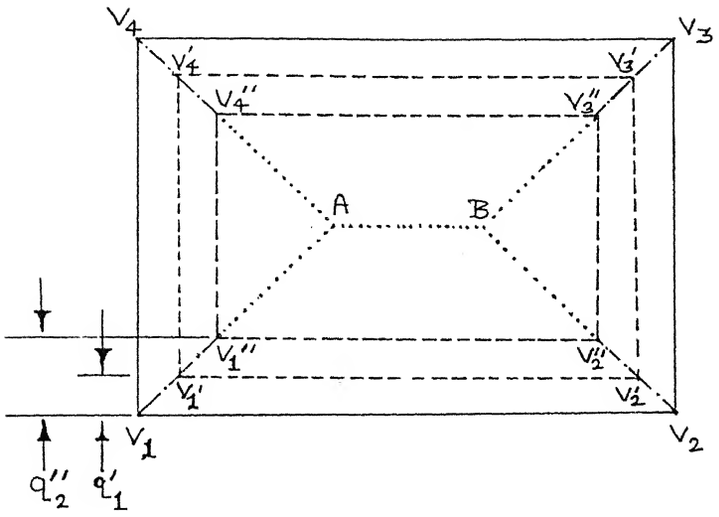

Time t'' > t' > 0

q' --> Fire front position at t'

q'' --> Fire front position at t''

Fig. 2.2.2 Skeleton as the Set of Quench Lines of Prairie Fire.

As the circle is swept along the skeleton its radius changes.

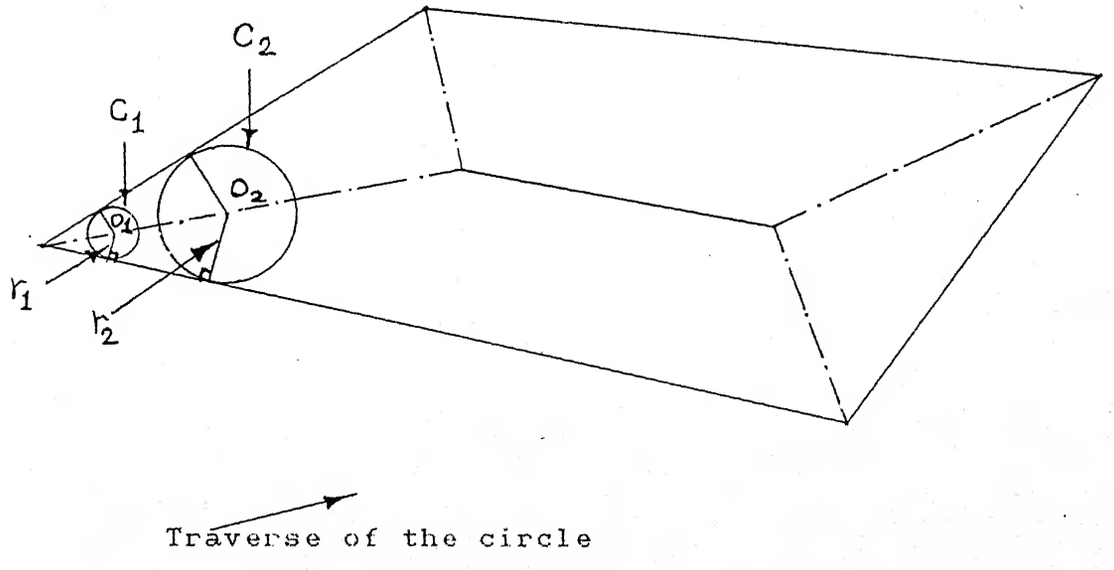

Traverse of the circle

Fig. 2.2.3 Profile Generation by a Circle Swept along skeleton.

Thus the quench velocity, $V_q = ds/dq = 1/(dq/ds)$; where s is the length of the formed skeleton, i.e. distance along the skeletal lines.

The shape can be deemed to be generated by a circular disc swept along the skeletal lines; the radius(r) of the circle being the minimum boundary distance associated with the skeletal points [15]. In Fig. 2.2.3, circle C is swept along the skeleton. At point O_1 on the skeleton, which is the centre of the circle (C_1), the circle has radius r_1. As it is swept to O_2, the radius increases to r_2. This view of the skeleton is particularly useful in shape analysis.

3. Discussion on Skeleton :

The skeletons of some common polygons are illustrated in Fig. 3.1. Skeleton of a polygon consists of mainly lines emanating from the convex vertices of the polygon. As the line is traversed, the radius of the circle increases. At some point the circle grows so large that it comes into contact with another boundary segment. At this point the skeletal line forks, giving forth skeletal lines produced by combinations of the boundary segments.

The concave vertices of the polygon may interact with a boundary edge, giving rise to curved skeletal segments. If two concave vertices interact, a linear skeletal segment is produced. The skeleton of a convex polygon consists of only straight lines.

A non-selfintersecting polygon without holes has a 'tree' skeleton [15,25]. The tree is geometrically located in the plane of the profile. The nodes of the geometrical tree are the forking points

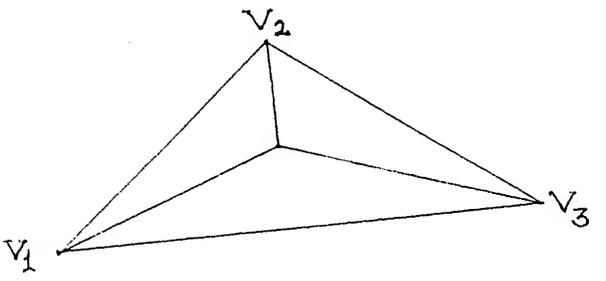

(a) Triangle

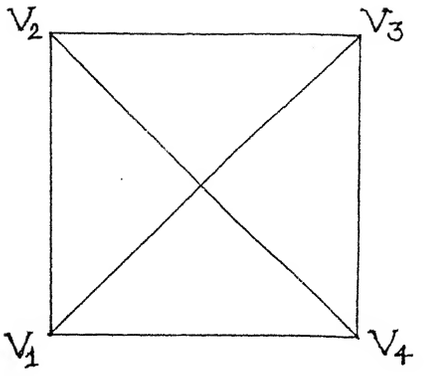

(b) Square

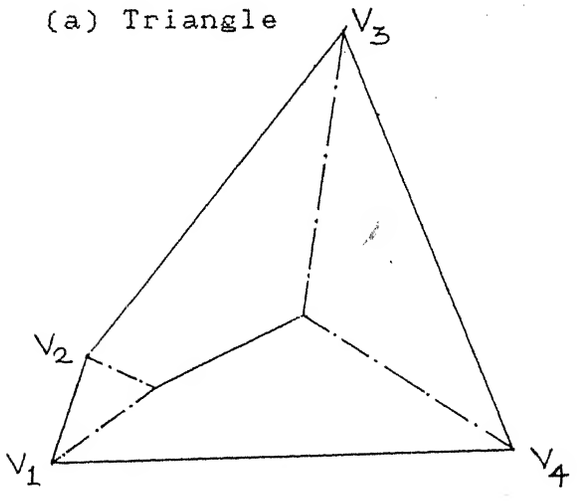

(c) Arbitrary quadrulateral

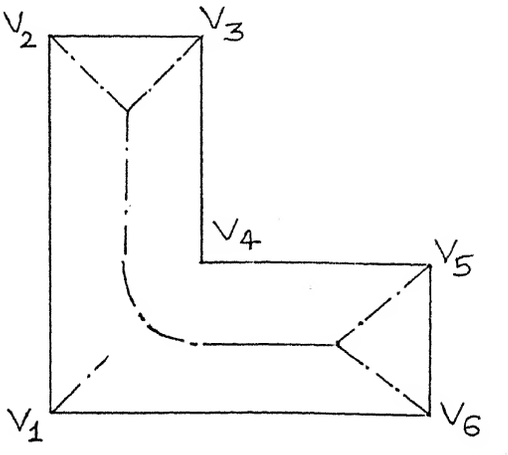

(d) 'L' shape

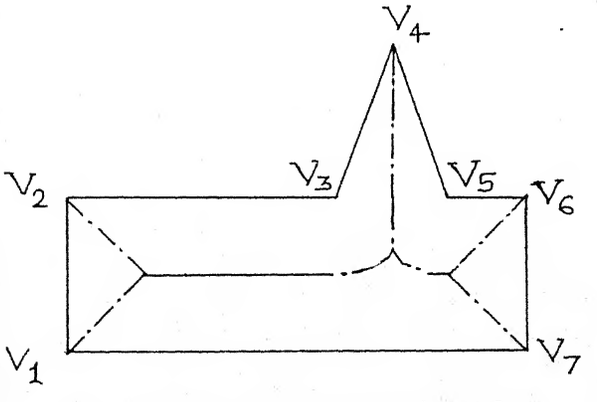

(e) Triangular projection on a rectangle

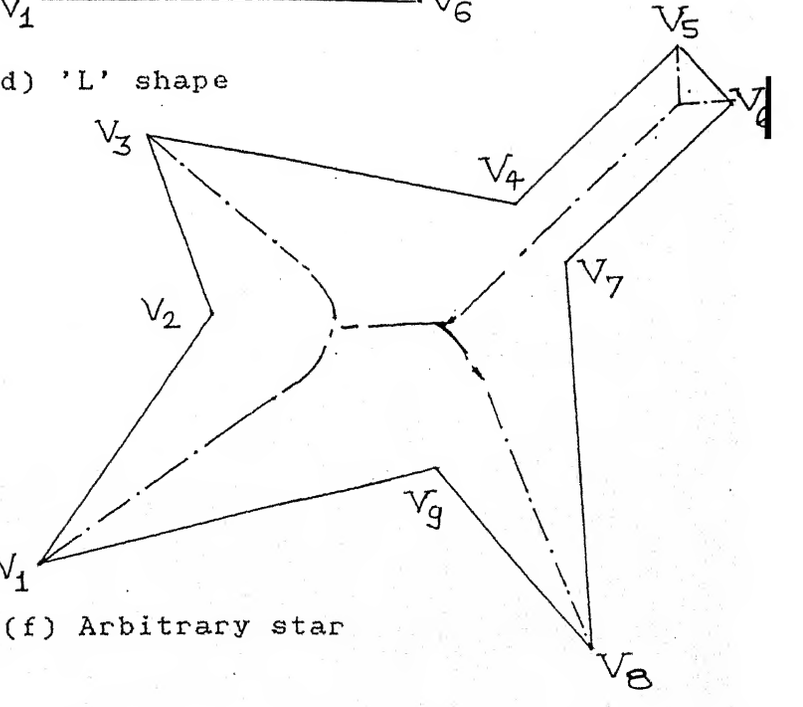

(f) Arbitrary star

Fig. 3.1 Skeleton of Some Shapes.

of the skeleton and the vertices of the polygon. The vertices form the leaf nodes of the tree. Its edges are the skeletal lines. The skeleton of a polygon with a hole is a planar graph [9],[15],[25].

Skeleton is sensitive to sharp minor boundary variations. A small notch in the periphery can distort the skeleton of a rectangle drastically. In Fig. 3.2(b), the notch $V_4 - V_5 - V_6$ in the rectangle $V_1 - V_2 - V_3 - V_7$, has disfigured the skeleton of the rectangle. The skeleton of the rectangle is shown in part (a) of the figure. A minor projection produces extra long lines in the skeleton due to interaction between the concave vertices as shown in Fig. 3.3. Hence the skeleton can not be directly used for shape analysis. An approximation method is needed to get rid of the disturbances due to minor variations.

Skeleton is based on the interactions of the boundary across the interior of the polygon. It does not consider interactions of boundary across the exterior of the profile. In Fig. 3.4, the points A and B are far apart in part (a). In part (b), they are quite close by. These relations are not detected in the skeleton. An elaborate analysis is needed to encapsulate these interactions. This analysis can not be based on the skeleton. It is based on an analysis of the convex hull of the profile and its differential area between the convex hull and the profile. It is the bay analysis proposed in the complete profile description, in chapter 5, section 2.

The concept of 'Visibility of Boundary Elements across the Interior of a Profile' has been expounded in literature [1,11&32].

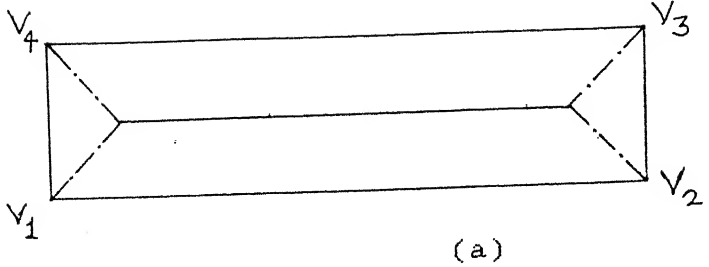

(a)

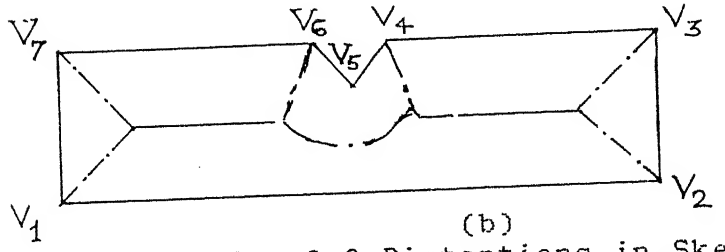

(b)

Fig. 3.2 Distortions in Skeleton.

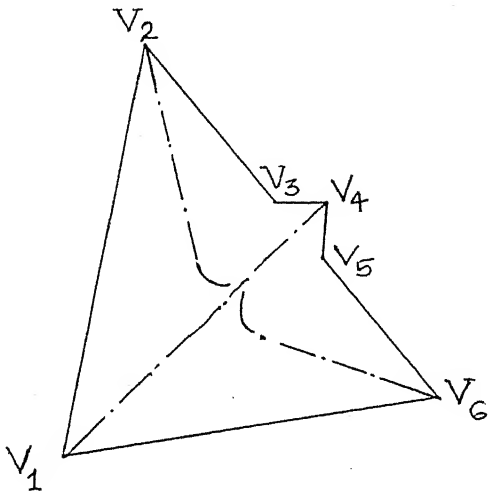

Fig. 3.3 Extraeneous Lines in a Skeleton due to a Small Projection

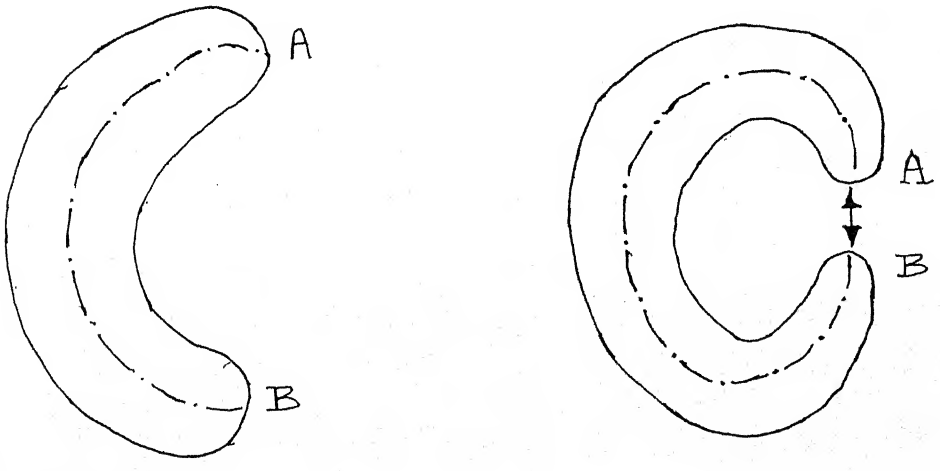

FIg. 3.4 Boundary Interaction across Exterior.

If the line joining two vertices of a profile lies fully within the profile then the two vertices are said to be visible to each other. This definition can be extended to any pair of boundary points. Skeletal interaction between a pair of boundary points is a more strict version of visibility. If a pair of boundary points interact to give rise to a point on the skeleton, they must necessarily be visible to each other. In Fig. 3.5, the boundary points P_1 and P_2 interact with each other to produce a skeletal point S. The skeletal circle of interaction is C, centered at S. As the circle C lies fully within the profile, the chord P_1-P_2 must also lie within the profile. Hence the points P_1 and P_2 are also visible to each other.

4. Skeletal interaction :

Skeletal interactions in a polygon can be of three types :

1) between two edges of the polygon,

2) between a concave vertex and an edge,

3) between two concave vertices.

4.1 Skeletal interaction between two edges :

The skeleton produced by two interacting edges is a straight line segment. It is the bisector of the angle between the two edges. The radius distribution along the skeletal line is linear. In Fig. 4.1.1, along segment PQ of the skeletal interaction between edges V_1-V_2 and V_1'-V_2'. The radius variation along PQ is linear from r1 at point P to r_2 at point Q. The quench velocity is constant.

$$V_q = S / r_2 = \sin(\theta/2).$$

Quench velocity reduces with increase in the angle between edges.

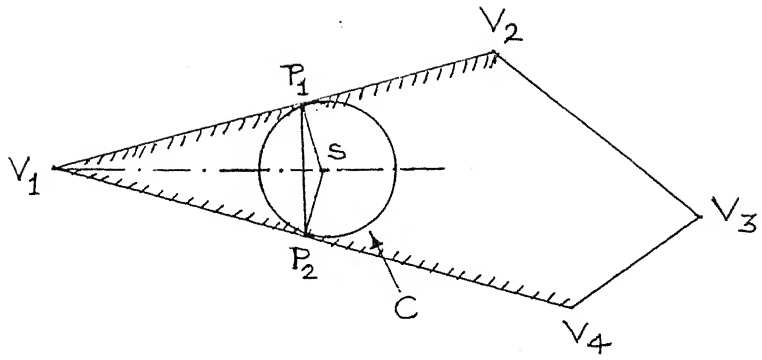

Fig. 3.5 Visibility and Skeletal Interaction.

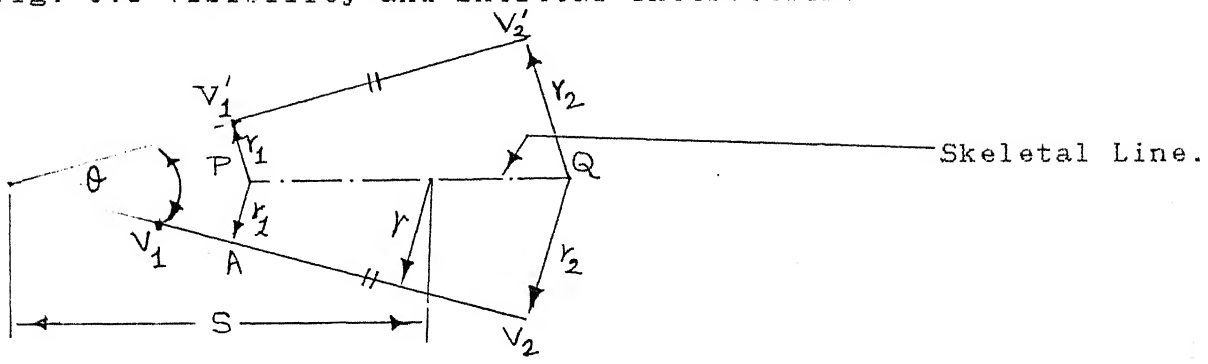

Fig. 4.1.1 Skeletal Interaction between Two Straight Lines.

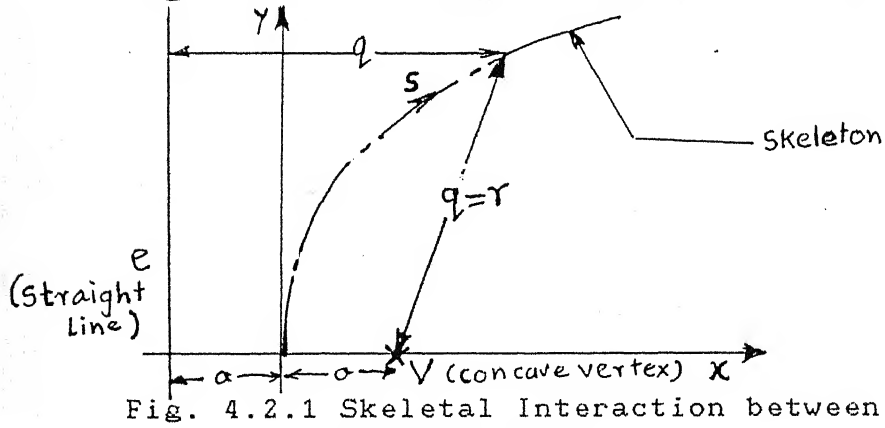

s --> distance along skeleton

q --> quench size (= radius 'r')

Fig. 4.2.1 Skeletal Interaction between a Concave Vertex and a Straight Line.

Skeletal circle, centred at O, radius = r.

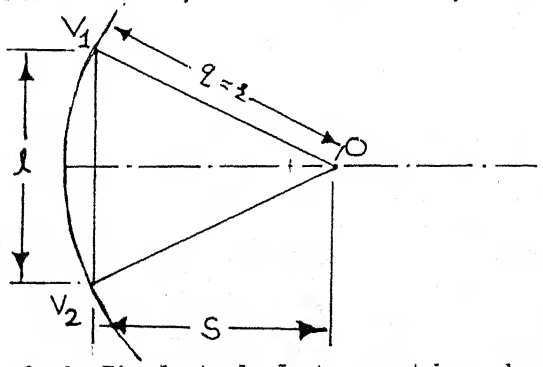

Fig. 4.3.1 Skeletal Interaction between two Concave Vertices

As $\theta \rightarrow \pi$, $V_q \rightarrow 0$, and

as $\theta \rightarrow 0$, $V_q \rightarrow$ infinity.

The quench velocity for skeletal line of two parallel edges is infinite, i.e. the whole line forms simultaneously as the fire front advances from both the edges.

4.2 Skeletal interaction between a concave vertex and an edge :

The skeletal interaction between a concave vertex v and an edge e is a parabolic arc as depicted in Fig. 4.2.1. The radius increases as the arc is traversed away from the concave vertex. The quench velocity reduces along the arc.

For the parabolic arc shown in the Fig. 4.2.1,

$y^{**}2 = 4ax$;

$q = x + a = y^{**}2 / (4a) + a$;

$$V_q = \frac{ds}{dq} = \text{sqrt}\left(\left(\frac{dx}{dq}\right)^{**}2 + \left(\frac{dy}{dq}\right)^{**}2 \right),$$

$V_q = \text{sqrt}(1 + (a/(r-a)))$.

$V_q > 1$, and as s -> infinity, r -> infinity, and $V_q \rightarrow 1$.

4.3 Skeletal interaction between two concave vertices :

The skeletal interaction is the perpendicular bisector of the line joining the vertices (Fig. 4.3.1). The radius distribution has a minimum at the midpoint of the line joining the vertices. The quench velocity has a maximum at the same point.

s = sqrt (q**2 - l**2/4) ;

$$V_q = \frac{ds}{dq} = \text{sqrt}\left(\frac{l^{**}2 / 4 + S^{**}2}{S^{**}2}\right) ;$$

$V_q > 1$, and as s -> infinity, V_q -> 1.

4.4 Interaction strings and zones :

A skeletally active polygon boundary element, an edge or a concave vertex, interacts with one or more other elements. These interactions are sequential i.e. if we start from an extreme of the interaction field of an element, the element interacts with only one element at a time. As the skeletal line is traversed, a point is reached where the circle comes into contact with another element. As we sweep past this point the contact with the earlier element is lost and the element starts interaction with the next element. This continues till the other extreme is reached. It is illustrated in Fig. 4.4.1 with explanatory notes for the sequence of interactions. Thus the total skeletal interaction of an element is a 'string of interactions'. The skeletal tree is composed of individual strings of interactions of all elements.

The skeletal string of segments in a string of interactions is again composed of the distinct zones of each interaction pair. In Fig. 4.4.1b, segment AB is the interaction zone of elements V_1 and e_1 on skeletal line, BC between V_1 and e_2, and so on. Segment PQ is the interaction zone on edge e_1, for e_1 and V_1. Angle AV_1B is the interaction zone at V_1, for V_1 and e_1.

The area bounded by the interaction zone and the skeletal line associated with the interaction zone is the skeletal interaction

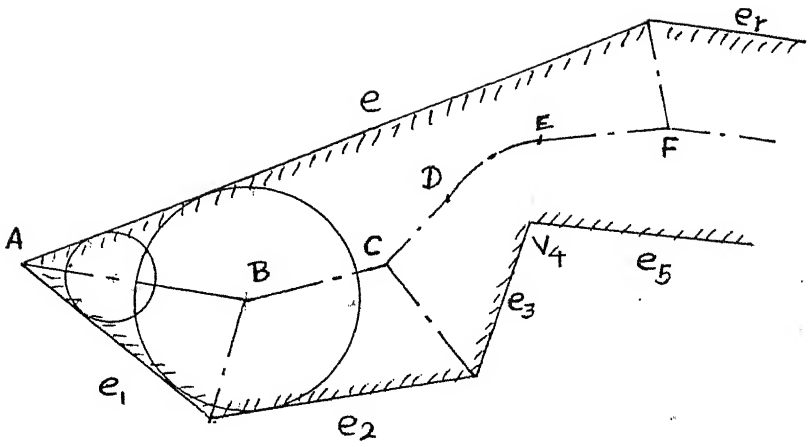

At A : Interaction e-e_1 starts
B : interaction e-e_1 ends; interaction e-e_2 starts
C : interaction e-e_2 ends; interaction e-e_3 starts
D : interaction e-e_3 ends; interaction e-V_4 starts
E : interaction e-V_4 ends; interaction e-e_5 starts
F : interaction e-e_5 ends; interaction e_r-e_5 starts

(a) String of interaction of edge 'e'.

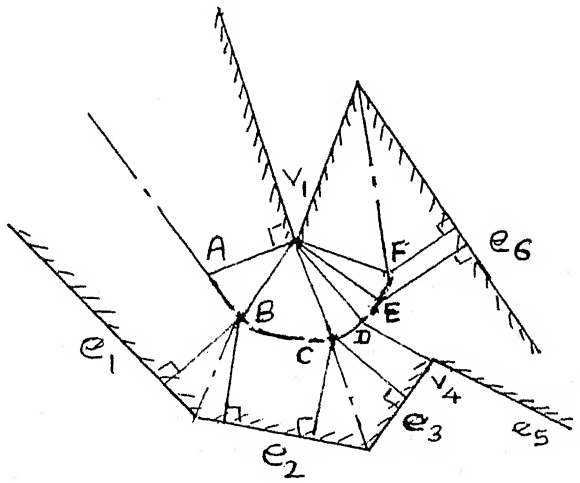

At A : Interaction V1-e1 starts
B : interaction V1-e2 ends; interaction V1-e2 starts
C : interaction V1-e3 ends; interaction V1-e3 starts
D : interaction V1-e4 ends; interaction V1-V4 starts
E : interaction V1-e5 ends; interaction V1-e6 starts
F : interaction V1-e6 ends; interaction er-e6 starts

(b) String of interaction of vertex V.

Fig. 4.4.1 Strings of Interaction.

area of zone. In Fig. 4.4.1(b), the area ABPQ is the skeletal interaction area for the interaction zone of the V_1-e_1 interaction for the edge e_1. Similarly, the area AV_1B is the skeletal interaction area for V_1-e_1 interaction for vertex V_1. The total area V_1APQB is the interaction area for the skeletal line AB. The sum of all the skeletal areas associated with an edge is the skeletal interaction area of the edge. Similarly skeletal interaction area is defined for a vertex.

5. Concavities in polygon and their effects on the skeleton :

It can be easily seen that the skeletal lines produced by interactions of the concave vertices are different from those produced by two polygon edges. The skeletal lines of interaction between two concave vertices are geometrically straight lines but the radius distributions and quench velocity are different from those for skeletal lines of interaction between two polygon edges.

The skeletal tree can be deemed to be composed of subtrees of different types, the convex skeletal interactions and the concave skeletal interactions. The convex skeletal interactions are homogeneous. They form strictly linear geometrical trees. In contrast the concave skeletal interactions are not homogeneous. The interactions between two concave vertices are different from those between an edge and a concave vertex. The concave interaction subtrees are composed of concave interaction strings.

The properties, such as quench velocity, radius distribution, geometrical size, of the convex and concave subtrees and strings, and their distribution through the skeletal tree are the important

features for shape analysis.

6. Properties of skeleton :

The features of skeleton which are important for shape analysis are defined below.

6.1 Characteristic lengths :

Various characteristic lengths are used in shape analysis. They are,

1) Maximum of the distances between two vertices of the polygon (L_1),

2) Maximum radius in the skeleton (L_2),

3) Maximum length in the skeleton + maximum diameter in the skeleton (L_3).

6.2 Properties of concave interactions :

6.2.1 Concavity measure :

The exterior angle of a concave vertex is a good measure of the concavity of the vertex. In Fig. 6.2.1.1, a part of a profile with edges e, e_l, e_r and a concave vertex V is shown. θ_e is the exterior angle between e_l and e_r. θ_p is the angle between perpendiculars to e_l and e_r. It is the angle of interaction for the skeletal interaction between V and e.

In Fig. 6.2.1.1, $\theta_p = \pi - \theta_e$;

concavity measure $C_{cv} = Fuzzy\_normalise(\theta_p, \pi)$. (ref. chapter 1 section 6 for the function fuzzy_normalise).

6.2.2 Peripherality :

A profile may have a lot of minor concavities giving it a jagged boundary. Such jagged boundaries must be smoothened before a shape

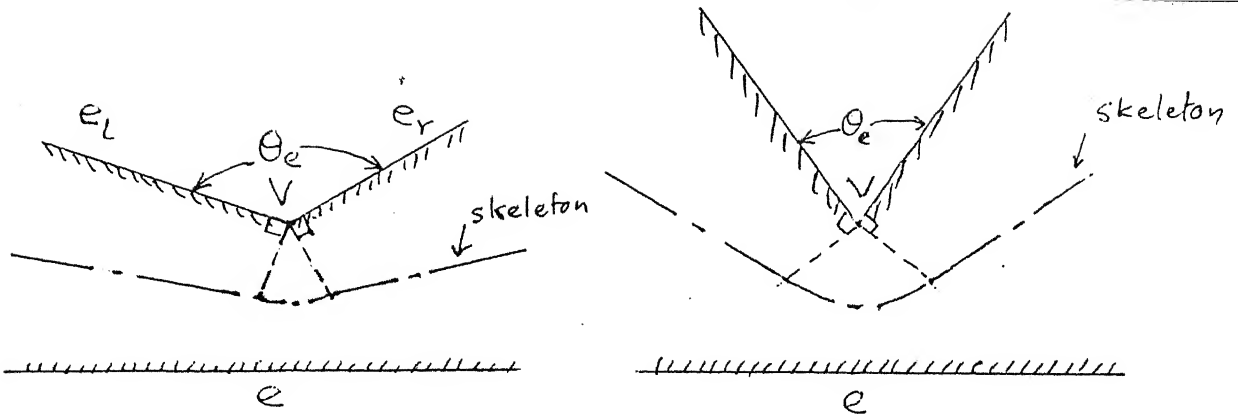

Fig. 6.2.1.1 Concavity Measure of a Concave Vertex.

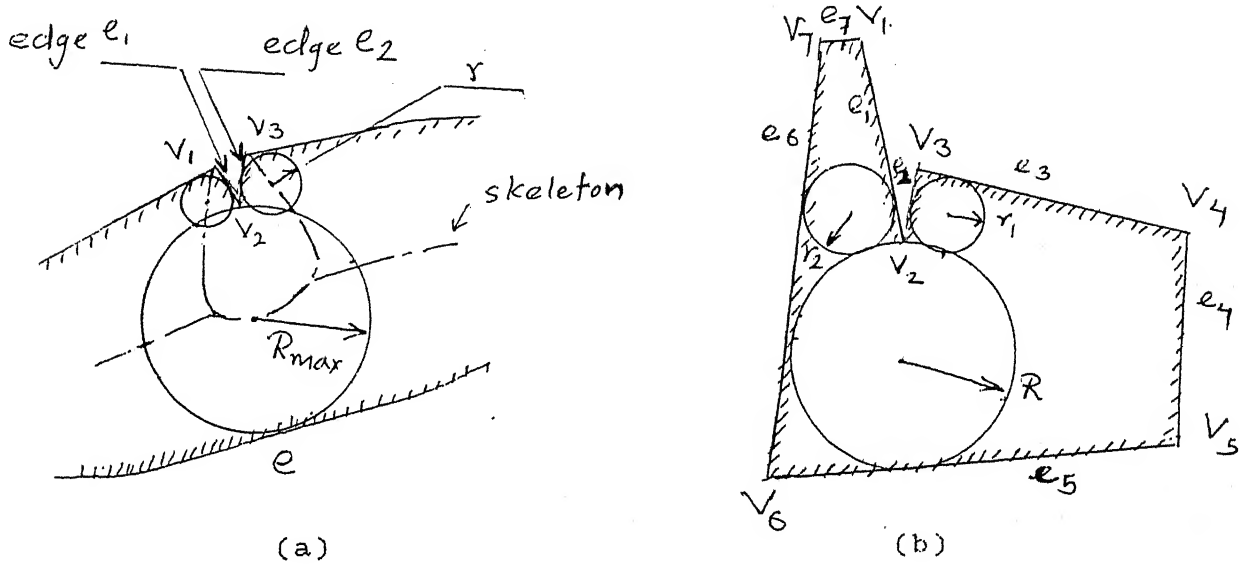

FIg. 6.2.2.1 Peripherality of a Concavity.

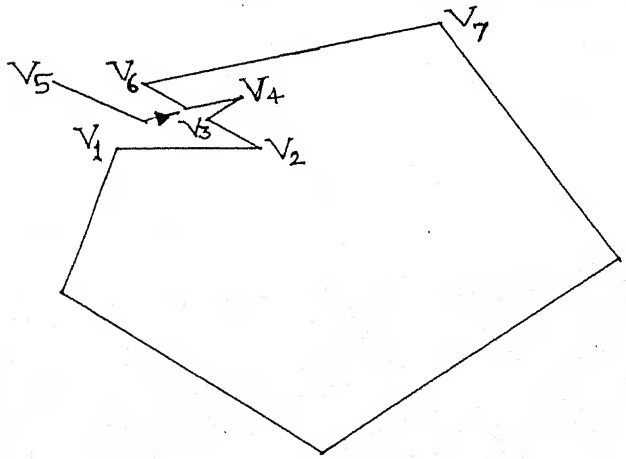

Fig. 6.2.2.2 Occluded Peripheral Concavity.

analysis as they do not contribute much to shape. On the contrary, they unnecessarily complicate the solution space and hence the shape analysis process.

An essential feature of the jagged edges is that the edges adjoining the concave vertex are small. But, this alone can not be the criterion for detection of jaggedness or 'peripherality' of a concavity. A smooth and curved boundary segment may be composed of a large number of small lines. The peripheral concavities are distinguished by their long interaction strings and presence of large radius sections interacting with boundary elements straight across the interior. In the Fig. 6.2.2.1, the notches V_1 $-V_2$ $-V_3$ in part (a) and V_2 $-V_3$ in part (b) have geometrically long interaction strings. The interaction starts with small radius r_1. The radius increases till it becomes much larger than r_1, upto the R_{max} in the figure; then it reduces again to r_2, which is again quite small compared to R_{max}. Presence of long interaction strings is also not a reliable criterion. Only the long range interactions across vast distances of interior areas give a strong indication of peripheral concavities. Some peripheral concavities may be hidden from the interior by presence of another peripheral concavity. In this case, the overlying peripheral concavity is identified as such first. The concept of peripherality is being used in the profile decomposition algorithm, developed in the next chapter. In the algorithm, the decomposition is achieved by deleting concavities (concave vertices) one by one. Hence, when this concavity is deleted, the other concavity gets identified as a peripheral concavity. In Fig. 6.2.2.2, the peripheral concavity

V_3 -V_4 -V_5 is occluded by the peripheral concavity V_1 -V_2 -V_3. In this case, V_1 -V_2 -V_5 will be identified as a peripheral concavity. After it is deleted, V_3 -V_4 -V_5 will be identified as a peripheral concavity and deleted.

Peripherality may be defined as the conjunction of smallness of the edges adjoining the concave vertex and existence of a large radius section. Determine the largest radius in the concavity interaction string. In Fig. 6.2.2.1, if R_{max} is the largest radius, then

peripherality, P_{pr} = (very_small(edge $_1$) OR very_small(edge $_2$)) AND large(R_{max}).

6.2.3 Importance of a concavity :

A concavity which penetrates the interior and divides the profile into two clear parts is an important concavity. On the contrary, minor peripheral concavities may interact with a large section of the boundary, with large radius, but they do not cleave the interior of the profile. Such a concavity V_1-V-V_2 is depicted in the Fig. 6.2.3.1. The general trend of the radius(r) versus distance along skeleton(s) characteristics of concavities within the interaction zone give an indication of cleavage. The r(s) curve is concave upwards. In Fig. 6.2.3.1b, the r(s) curve of the interaction of the concave vertex V, which cleaves the interior of the profile, is illustrated. Sharper the concave nature of the r(s) curve, clearer the cleavage. But this function fails to take care of situations where a smooth and curved concavity may be composed of a sequence of short line segments (Fig. 6.2.3.2a), and where a thin bridge connects two large polygons (Fig. 6.2.3.2b). In both these cases, though the interior is cleaved, the r(s)

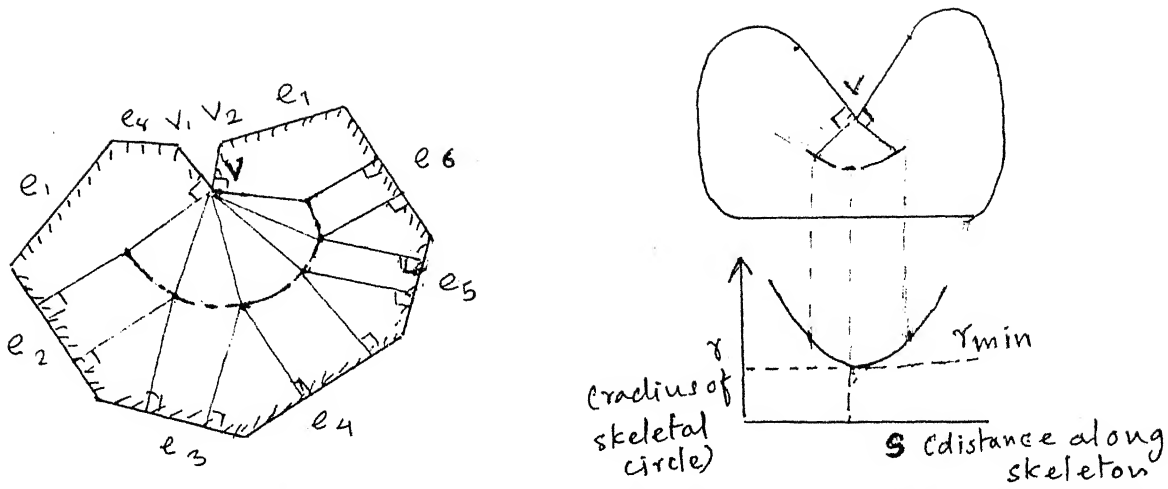

(a)Peripheral Concavity with large interaction (b) Concavity Cleaving profile

Fig. 6.2.3.1 Peripheral and Cleaving Concavities

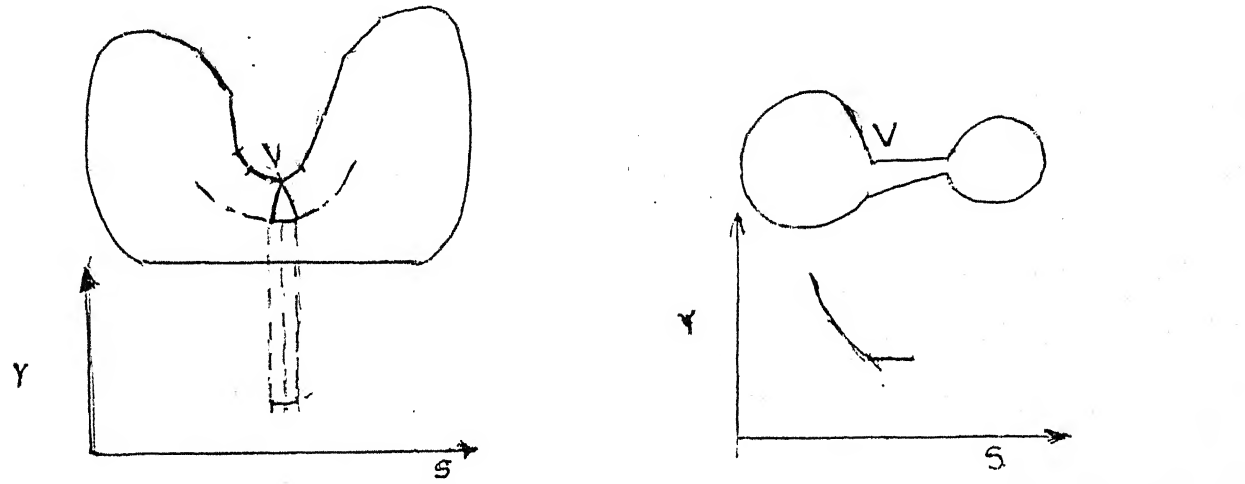

(a) Smoothly curved concavity (b) Bridge connected at concavity

Fig. 6.2.3.2 Cleaving Concavities.

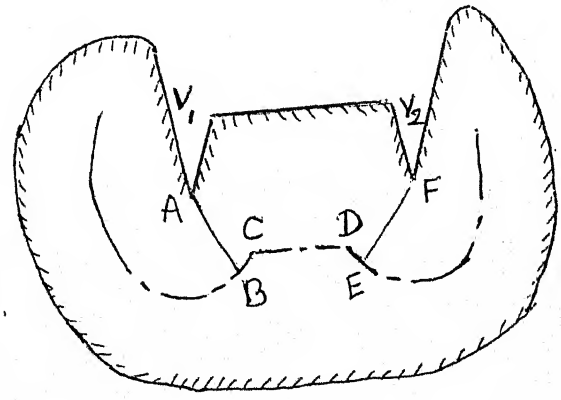

Fig. 6.2.4.1 Proximity of Concavities.

curve, as shown in Fig. 6.2.3.2, is not sharply concave upwards. This is due to the local nature of the interaction string of a concavity. In situations given in Fig. 6.2.3.2, the interaction string of the concavity reflect the situation in the local vicinity of the concave vertex. Cleavage is a global property. A global r(s) curve, of concave nature, truly reflects the cleavage. A global r(s) function may be extremely varied. Its study is would be a daunting task. Hence a scheme is proposed for importance evaluation which is not exact but it is very simple.

Cut the skeleton into two at the point of the lowest radius in the concave interaction string. Evaluate the largest radius on both parts of the skeleton. Evaluate the sequence of largest radius to the left (R_l), the smallest radius R_{min}, and the largest radius to the right (R_r), for a concave variation i.e. 'large-small-large' variation, as a conjunction of fuzzy predicates 'large' and 'small' applied to their respective arguments. The resulting fuzzy set membership grade gives the 'importance' of the concavity; that is,

Importance = Large(R_l) AND small(R_{min}) AND large(R_r).

It is suggested that the fuzzy conjunction be implemented as the average of the three fuzzy membership value.

6.2.4 Proximity of two concavities :

Proximity of two concavities is NOT of the relative distance between them, with respect to characteristic length L_3. The relative distance between the two concavities is the comparison of the sum of their radii at the closest points in their interaction strings and the distance along the skeleton between their interaction strings. For example, in Fig. 6.2.4.1, the distance

between V_1 and V_2 is the distance ABCDEF. BCDE is the skeletal line, whereas AB is the radial distance along the right extreme of the interaction zone of vertex V_1 with the opposite edge e.

Proximity P_x = NOT (Fuzzy_normalise (d, L_3)). (ref. chapter 1 section 6 for the function fuzzy_normalise).

Note that distance along skeleton is the distance between the nodes of a tree and hence can be easily determined.

6.3 Properties of convex interactions :

6.3.1 Forks :

The skeleton, as observed earlier, is a tree composed of geometrical lines. The nodes of the tree are the forking points of the line diagram. These nodes will be referred to as the 'forks' of skeleton in the further work. In Fig. 6.3.1, f_1 and f_2 are the forking points of the skeleton. They play an important role in the processing of the convex interactions.

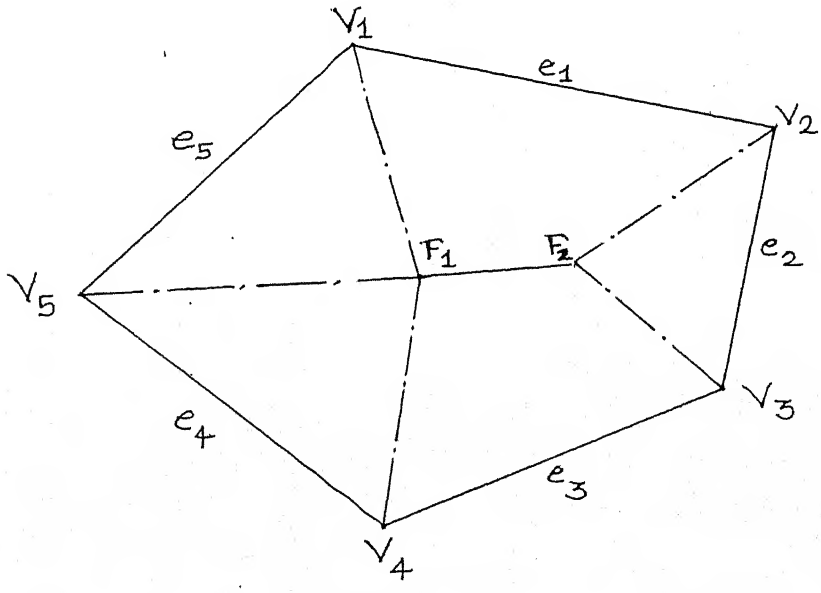

Fig. 6.3.1 Convex Skeletal Interaction Lines.

The 'Size' function in the last formula may be the 'Local_Size(fork)' or the 'Global_Size(fork)', in accordance with whether the largeness is to be local or global.

6.3.4 Proximity of Forks :

Proximity of two neighbouring forks is quantified as the length of the NACSIL connecting them compared to the locally largest radius, i.e. the larger of the radii of the two fork, or the globally largest radius in skeleton.

If l is the length of the NACSIL between forks f_1 and f_2, and Rg_{max} and Rl_{max} are the global and the local maximum radii respectively, then

$$\text{Local\_Proximity}(f_1, f_2) = \text{Small}(\text{Fuzzy\_normalise}(l, Rl_{max})),$$

$$\text{Global\_Proximity}(f_1, f_2) = \text{Small}(\text{Fuzzy\_normalise}(l, Rg_{max})).$$

6.3.5 Intensity of CSIL :

Intensity of the CSILs is a property indicating the importance of the CSIL in the skeleton. It combines the radius and length of the CSIL. It also depends, although indirectly, on the quench velocity.

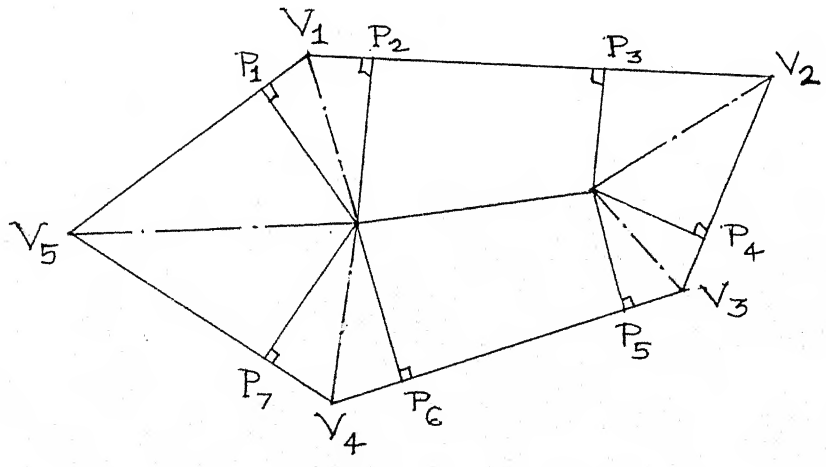

Fig. 6.3.5 Intensity and Skeletal Interaction Area.

Intensity is defined as the area associated with the skeletal interaction which generated the CSIL, compared to the total area of the polygon. In Fig. 6.3.5, the area $V_1 - P_1 - f_1 - P_2$ is the interaction area for the ACSIL $V_1 - f_1$; and the area $P_5 - P_3 - P_2 - P_6$ is the interaction area for the NACSIL $f_1 - f_2$.

The intensity 'I' is given by

I = Fuzzy_normalise(interaction area, area of the polygon).

6.3.6 Intensity of forks : Intensity of a fork is the sum of the intensities of the intensities of all the CSILs converging at the fork.

Chapter 3

PROFILE DECOMPOSITION

1. Objective :

The proposed nesting method is based on shape description and matching of the shapes on the basis of description, for profile allocation. A description scheme encompassing all possible shapes requires some structuring and classification of the shapes. Classification of all shapes is a highly complex task. The possible shapes are too numerous, too diverse and they have too many regions of complex ranges among the extreme cases. Hence as a first step in a structuring process, the profiles are decomposed into constituent convex polygons. Convex polygons are more amenable to imposition of classification. Shapes are described in terms of the constituent convex polygons (primitives), and their topological and geometrical relations.

The basic requirement of the decomposition scheme is that the decompositions should be consistent with human perception of the shape. Various decomposition schemes have been proposed in literature. All the schemes have been briefly reviewed in the literature survey (ref. section 9, chapter 1). The results of some representative decomposition algorithms Pavlividis [25], Ahuja [1] and Chazelle [11], are discussed here., The objective of these schemes is to decompose the profile into a minimum number of convex polygons. These schemes are exact in nature. Hence small disturbances in the boundary lead to large and undesired variations in the decompositions. It is illustrated in Fig. 1.1.

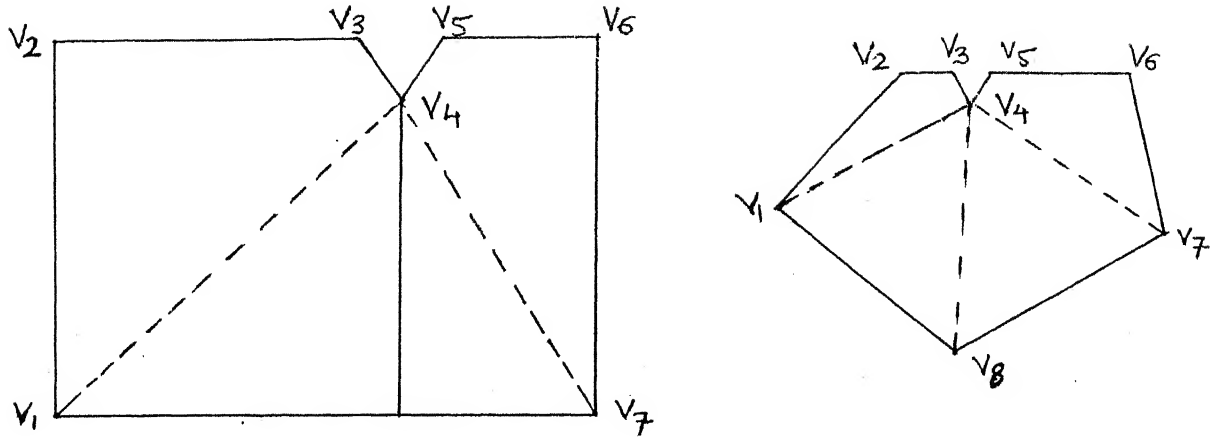

(a) (b)

Fig. 1.1 Need for Smoothening before Polygon Decomposition.

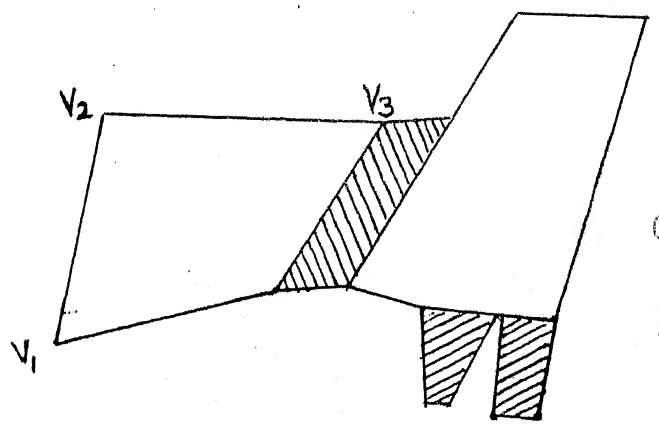

(a) Pavlividis algorithm.

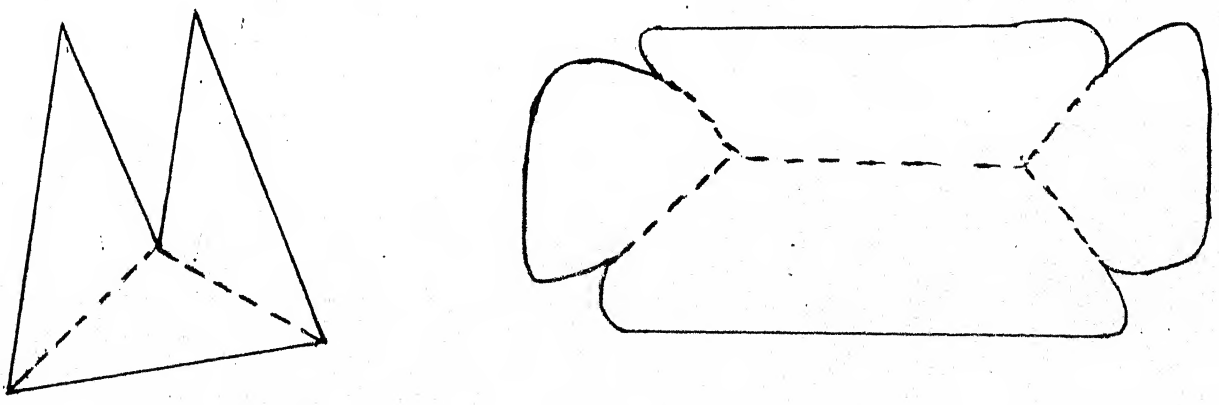

(a) Ahuja algorithm. (b) Chazelle algorithm.

Fig. 1.2 Results of Some Decomposition Algorithms.

Part (a) shows a rectangle with a very small notch in the boundary. The small notch induces decompositions as shown by the dashed lines. A similar effect is seen in the part (b) also. The small notches should be smoothened out to maintain consistency with perception. In the decomposition algorithms mentioned above, for some simple profiles, the decompositions obtained are not consistent with human perceptions. Some such profiles are shown in Fig. 1.2. Part (a) depicts the result of the application of the Pavlividis algorithm [25]. Some of the constituent convex polygons are shaded. It can be easily seen that the decomposition does not yield much information about the shape features. Especially the decomposition in the left half of the profile, producing the quadrilateral $V_3 - V_4 - V_{11} - V_{12}$ seems too artificial. In part (b), the results of application of Ahuja decomposition algorithm to the profile $V_1 - V_2 - V_3 - V_4 - V_5$ are shown [1]. The decomposition into three triangles again is not natural. A decomposition in to two quadrilaterals, by dropping a perpendicular from vertex V_3 on to the edge $V_5 - V_1$, would be much better. The results of the Chazelle algorithm are shown in the part (c) [11]. The presence of a long cut running through the interior of the profile again belies the perception. The drawbacks in the Pavlividis and Ahuja algorithms are mainly due to the fact that only vertex to vertex cuts are used for decompositions. In the Chazelle algorithm, some of the drawbacks of the other two algorithms have been overcome. But still, the decompositions may seem artificial in some cases. This drawback arises due to a strict adherence to the objective i.e. decomposition into minimum number of polygons.

2. Important Concepts for Decomposition Problem :

We propose modifications in the formulation of polygon decomposition problem. It is not sufficient to obtain solutions which will decompose the profile into a minimum number of convex polygons. The optimisation criterion should also ensure that the constituent polygons are such that they are easily identifiable in the profile. It can be seen from Fig.s 1.1 and 1.2 that the decomposition schemes do not guarantee it. The resultant decompositions which might be minimal in terms of the number of polygons. But a shape description based on these constituent polygons and their interrelations, will not be useful for nesting.

The 'ease of identifiability' of constituent polygons depends upon the way the profile is 'cut up' in decomposition. The 'cuts' are extraneous to the profile. If the cuts are kept to a minimum it will increase the identifiability of the constituent polygons. It is illustrated in Fig. 2.1. The cut $A\text{-}V_3\text{-}B$ produces three convex polygons which are more easily identifiable than the convex polygons produced by the other cuts. The length of the cut $A\text{-}V_3\text{-}B$ is smaller than that of the other cuts. The convex polygons generated by the cut $A\text{-}V_3\text{-}B$ have boundaries which are more exposed to the exterior of the profile than the boundaries of those generated by the other cuts. It may be inferred from these examples that for a decomposition to produce easily identifiable constituent convex polygons, the boundary of the constituent polygons should be largely composed of the boundary of the profile. To express it in different words, the constituent polygons should be 'maximally exposed to the outside'; or,

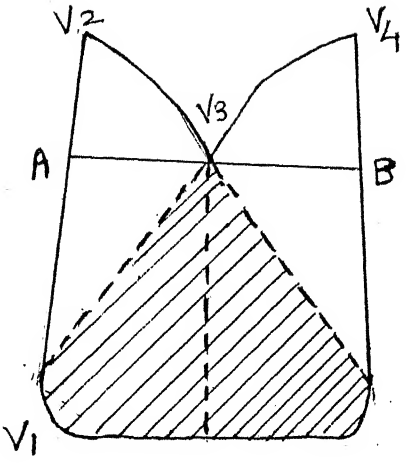

Decompositions based on the identifiability of consituent polygons.

Decompositions based on the minimum number of constituent polygons.

Fig. 2.1 Identifiability of Constituent Polygons.

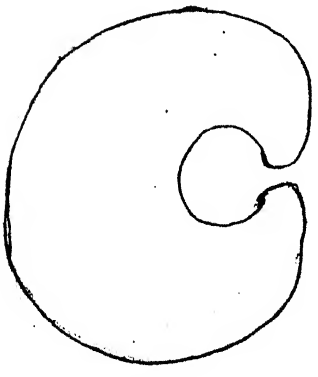

(a) Simple 'lagoon'

(b) Irregular 'lagoon'

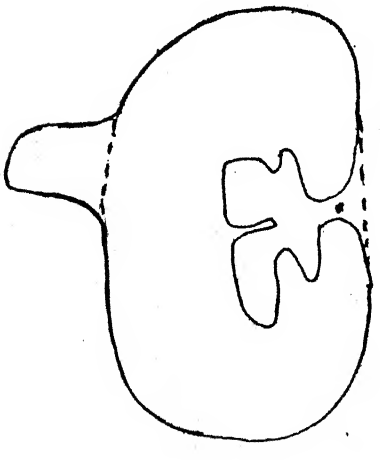

(c) Approximate decomposition

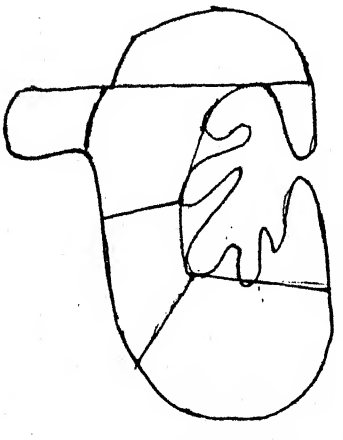

(d) Exact decomposition

Fig. 2.2 External Visibility - 'Lagoon'

expanding further, the constituent polygons should be 'maximally visible' form far, in the plane of the profile.

The concept of 'maximum external visibility' along with ease of identifiability, also incorporates another concept. A profile may have a large 'lagoon' almost closing the profile onto itself (ref. Fig. 2.2(a)). Though it is possible that this lagoon may be used in nesting, it is quite unlikely that there will be another profile with a narrow 'neck' with a large body attached to the neck, fitting the lagoon. The lagoon is most likely to be wasted, especially so if its boundary is irregular. For example, the probability of another profile which may fit in to the lagoon of the profile in Fig 2.2(b) is quite low. Since the proposed shape description does not consider the effects of the cross relations of profiles the possibility of nesting of the lagoon can be neglected. Hence an approximate decomposition scheme closing the lagoon and neglecting its presence would be better suited for nesting (ref. Fig. 2.2c). The exact decomposition given in part (d) of the figure is unnecessarily complex. It should be noted that the external visibility of the lagoon, from a large distance, is low.

The quantification of the concept of 'external visibility from far' would require probabilistic or possibilistic analysis considering the random possibility of nesting of some other profiles into the concavities. It is not attempted in the present work. A simplified version 'external visibility from close quarters' is used. It neglects the 'lagoon cases' and their effects altogether. It embodies the 'ease of identifiability' in

terms of 'cut minimality'. All hitherto references to external visibility should be taken to mean this concept.

Cut minimality is represented by the minimality of the total length of the cuts. External visibility can be represented by the ratio of total length of the line diagram formed by the profile and the cuts to the total length of the original line diagram i.e. the perimeter of the profile.

Another essential feature of the decomposition into convex polygons is that some minor variations in the boundary should not induce large discontinuous changes in decomposition. In Fig. 2.3(a), the edges V_2-V_3 and V_5-V_6 are collinear. A line joining V_3 and V_5 completes the decomposition. In part (b), the two edges are slightly offset. Two cuts are needed to decompose the profile, as shown. Thus a very minor variation has induced a major change in the decomposition. In a decomposition algorithm, the minor variations should be smoothened out and approximated. They may not be neglected altogether. But their effects should be reduced ensuring continuous variations in decompositions. This is especially important for small concavities on the boundary. Small concavities such as very shallow bays and very sharp notches, which are not likely to be affect the nesting efficiency much, may be covered by 'straightening up' the profile boundaries. In Fig 2.4, a sharp notch is covered up by an approximating edge. Also, a sequence of minor concavities, if not approximated, would give rise to a large number of small constituent polygons, thereby destroying usefulness of the decomposition of the profile.

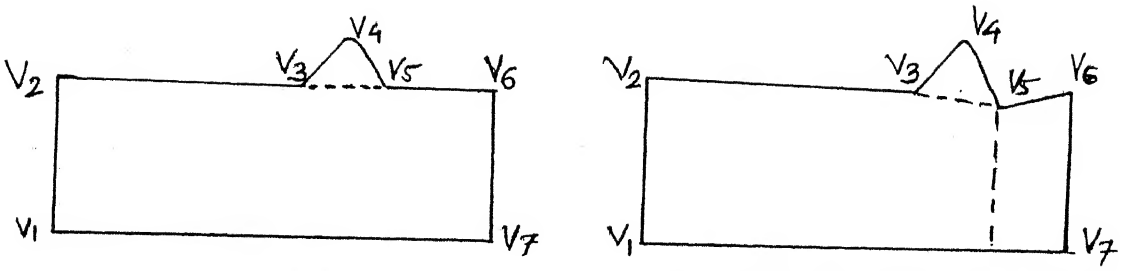

V2-V3-V5-V6 are collinear.

(a)

V2-V3 & V5-V6 are slightly offset.

(b)

Fig. 2.3 Minor variations in boundary affecting decomposition.

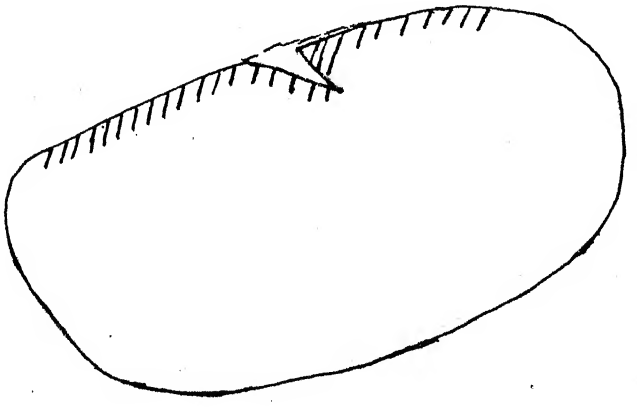

Fig. 2.4 Straightening Up / Approximation.

It is important to note that if small projections are simply ignored, it could be fatal for nesting. Approximations should be done only on concavities. This implies that the approximations will strictly be external envelopes of the profile.

The extraneous areas introduced by 'straightening up' could be taken to be a measure of approximation. As the approximation is always an external envelope of the profile, the possibility of spurious 'good approximations' due to cancellation of positive and

negative approximations, is absent. Hence ratio of original area to area of approximation gives a good measure of the accuracy of the approximation.

3. Formal Statement of the Problem :

The profile decomposition problem can be stated as follows : Given an arbitrary polygon P_o approximate it by an aggregate of convex polygons P_i, $i = 1...n$, so that the objective function, 'goodness', $G(v,a)$ is maximised, where 'v' is a measure of the external visibility of the constituent polygons, and 'a' is a measure of the accuracy with which P_o is approximated. Note that the approximation is by external envelopes.

External visibility measure 'v' is taken to be

$$v = \frac{\text{Perimeter}(P_o)}{\text{Perimeter}(P_o) + L_c} ;$$

where L_c = total length of cuts.

Accuracy measure 'a' is taken to be

$$a = \left(1 + \frac{\text{Area}(P_o)}{\sum_{i=1}^{n} \text{Area}(P_i)} \right) ;$$

The objective function, 'goodness', $G = v * a$.

Explanation of Measure of Accuracy Formulation :

During shape description, if the extraneous area introduced by approximation is described as a bay then there exists a possibility that this area could be utilised in nesting. Thus the extraneous area may not be completely wasted. If it is utilised

fully, the approximation is not really an approximation and the accuracy measure should be one. If the area is not utilised at all, then the approximation accuracy could be taken to be the area ratio. In absence of any information on the possibility of utilisation of this area, the chances of both the cases are taken to be the same and an average value is taken.

If on the contrary, the extraneous area is not described as a bay, then it will not be utilised. In this case the approximation accuracy should be taken as just the area ratio.

4. Exploration of the Solution Space :

This problem could be viewed as a problem of deletion of the concavities in a profile by a judicious combination of cuts and approximations. In absence of approximations, atleast one cut should originate at or pass through a concave vertex. In figure 4.1, some cuts required to delete the concavity at the vertex V are shown. More than one cutting line will be required if the cutting line does not fall within the reflex angle of the vertex. In such a simple case, a procedure of concavity deletion one at a time, with selection of the locally best solution at each deletion could be sufficient. The possibility of intersection of two cuts increases the complexity of the solution space and thus rules out such simple solution methods.

Approximations add another dimension to the complexity of the solution space. The boundary lines of constituent polygons now need not pass through the concave vertices. In figure 4.2, a portion of the boundary of a profile is shown as the edges connecting vertices V_1 to V_8. The approximate decomposition line,

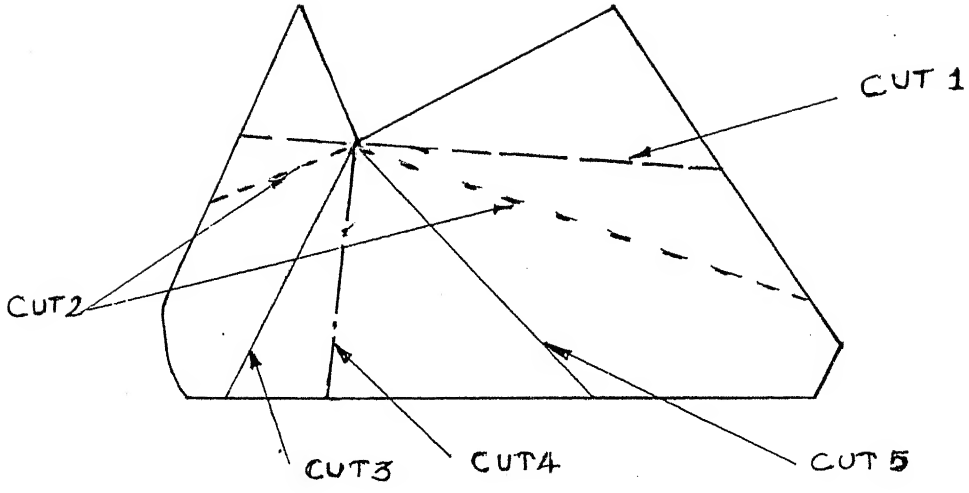

Fig. 4.1 Cuts at a Concave Vertex.

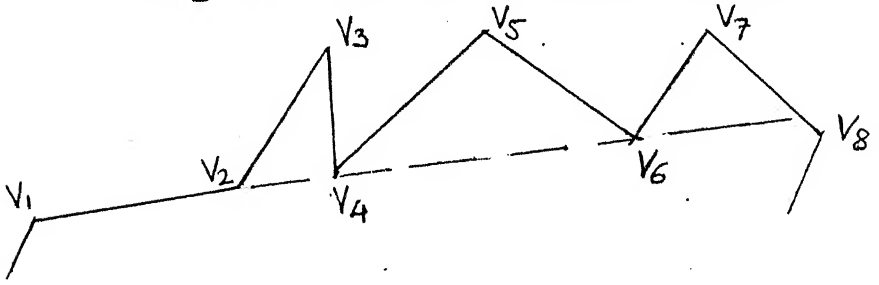

Fig. 4.2 An Approximate Decomposition Line at a Concave Vertex.

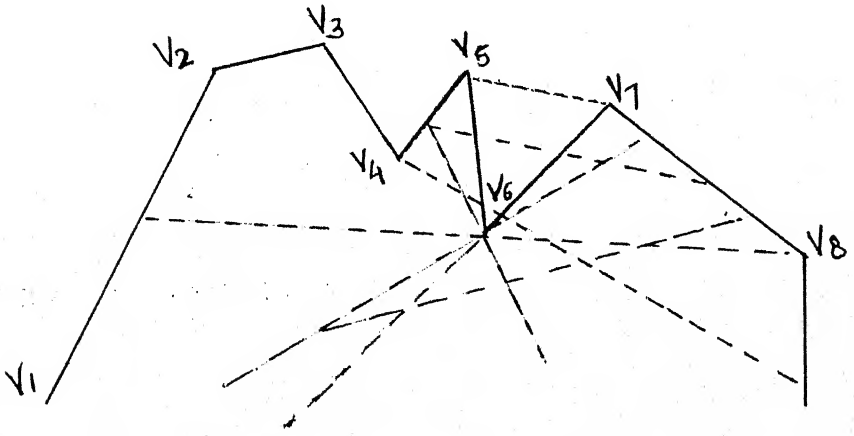

Fig. 5.1 Range of Possibilities at a Concave Vertex.

shown dashed in the figure, does not pass through the concave vertices V4 and V6. Hence the solution space, with this provision, becomes the space of all possible geometrical graphs - geometrical line diagrams, produced by the combinations of the line segments in the plane, which either lie within the profile or terminate on the profile boundary.

5. Method of Solution :

A meaningful mathematical formulation of the problem for application of the classical optimisation methods seems impossible. A combination of heuristic and combinatorial search methods is a promising avenue for optimisation. The search over the solution space could be divided into search over the cuts and approximations for each concavity for the concavity deletion, and a search over the sequence of deletion of concavity. The advocated algorithm for decomposition is based on some ordering of the concavities for deletion and deletion of one concavity at a time. With each deletion, the profile is subdivided in to two or more subprofiles which may or may not be convex. The decomposition is complete when every subprofile is a convex polygon.

The search space in each concavity deletion is uncountably infinite. In figure 5.1, a portion of the boundary of a profile is shown as edges from V_1 to V_8. A number of approximate cuts are shown, all of which may delete the concave vertex V6.It has discrete regions wherein the problem characteristics change discontinuously from region to region. But they vary continuously within each region. The proposed solution method is to locate 'most likely' cuts and approximations in each region using

heuristics. Then the problem could be solved by heuristically guided combinatorial search method.

Different concavity deletions may have cross effects giving rise to the problems such as cut intersections, and interaction of cuts and approximations, and interaction between two approximations. They are illustrated in figure 5.2. In part (a), cuts cut1 and cut2 intersect. The problem is which of them is to terminated at the intersection point, and which one should be extended to the boundary. In part (b), the approximation is done for the new concave vertex at V5 generated by the cut, which has been applied earlier. The cut now becomes redundant. In part (c), a chain of concave vertices V_2 to V_7 is being straightened up by approximations at various combinations of the vertices. These approximations intersect and create a few more possible approximations. These complications are taken care of by heuristic rules; and the different deletions are effectively isolated.

The process can now be modelled as a generative search method. The search nodes at each step are generated by rules for cuts, approximations and their cross relations. The solutions are evaluated by heuristic evaluation criteria. The heuristic evaluation criterion is the 'usefulness' of the solution. The best solution node is explored first.

If a dead end is reached or the goal state is not sufficiently good enough, then the solution tree is backtracked. A dead end is a solution with a low objective function 'goodness' value.
For complex shapes, likely to be encountered as complementary area

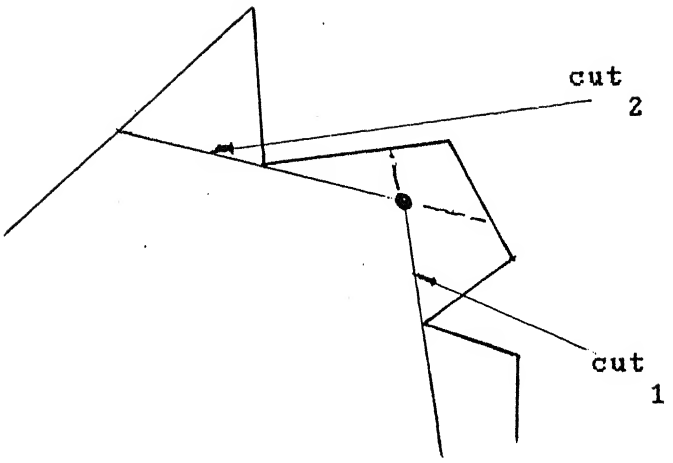

(a) Cut intersection.

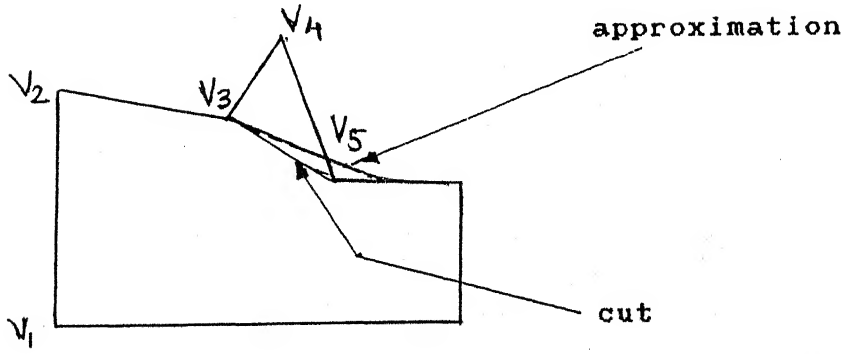

(b) Cut modifications.

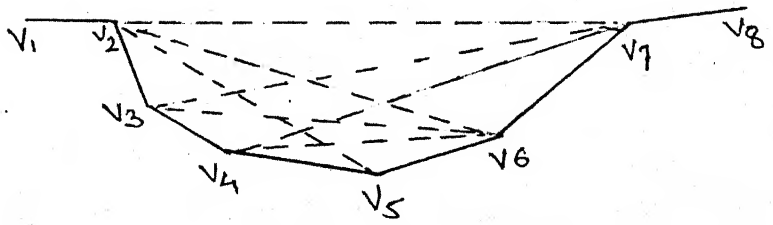

All the dotted lines are the interacting apprximations.

(c) Interacting Approximations

Fig. 5.2 Cross Effects of Deletions.

in nesting, the solution tree may become very large. Large amount of backtracking may become necessary to obtain a good solution. If the solution is quite bad then the process may spend time unnecessarily searching and backtracking over similar solutions which may not offer any significant improvement. To avoid such a condition it is necessary to identify the critical decisions, which when backtracked, would offer significantly different solutions. The factors affecting the 'criticality' of a decision are the importance of a concavity, degree of difference of the solutions, and the local 'goodness' of the possible solutions.

Multiple shape descriptions are necessary for nesting. Also the simplifications in the optimisation problem erode the confidence in the final solution. The goodness of the solution depends upon the heuristics, which can't be guaranteed to work equally well across the whole range of shapes. Hence it is necessary to obtain multiple solutions in the decomposition process.

The multiple decompositions should be sufficiently different from one another. They should be comparably 'good'. This can be achieved by developing all of the most critical solution nodes. Then finally the best comparable few solutions can be reported as the decompositions.

In the fuzzy spawning paradigm (ref. chapter 1, section 6), the pruning of the decision alternatives for decomposition is based on the high usefulness. Additional pruning is introduced in the form of the backtracking control. The goal state evaluation is the heuristic function goodness of decomposition. The backtracking control is based on the difference criticality. The heuristic

functions or the fuzzy qualitative predicates are the goodness, usefulness, criticality etc.

6. Discussions on Concavity Spectrum and Concavity Deletion :

Concavities in a profile may assume diverse shapes and sizes. These concavities also interact with the non-concave regions of the profile and with other concavities in the profile. These features give rise to a complex range of profiles. An attempt at spanning the range of these features is presented below.

6.1 Shape and Size of a Concavity :

Here, only an isolated concavity with smooth monotone borders is considered, i.e. there are no intervening local projections or second order concavities on the border.

1) General shape of the concavity : A sharp notch (Fig. 6.1.1(a)), a gentle bay (Fig. 6.1.1(b)), a vary shallow depression (Fig. 6.1.1(c)).

2) Nature of the boundary : Its boundaries may be smooth (Fig. 6.1.2(a)), or composed of long straight line segments(Fig. 6.1.2(b)).

3) Size with respect to the other profile features : The concavity may be dominating - large, or negligible - small.

6.2 Multiple Concavities :

1) Distribution of features listed in section 6.1, over the concavities.

2) Consecutive concavities along a border which may give rise to a concave curve (Fig. 6.2.2).

3) Concavities interspersed with various different convex regions.

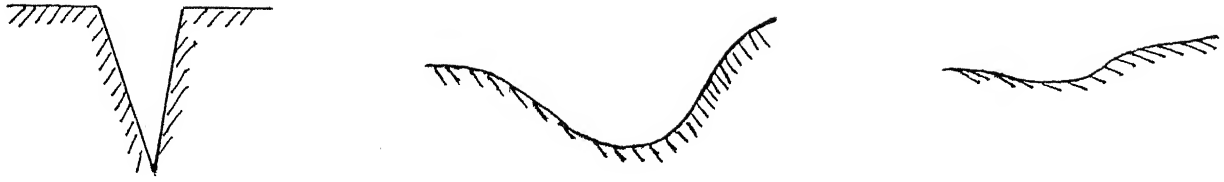

(a) (b) (c)

Fig. 6.1.1 Different Concavities.

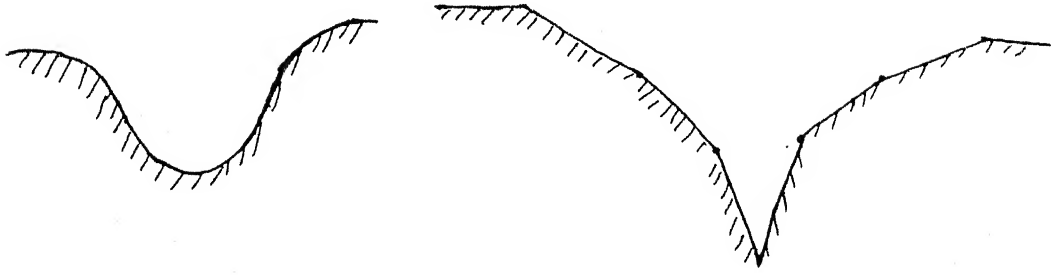

(a) (b)

Fig. 6.1.2 Boundary of a Concavity

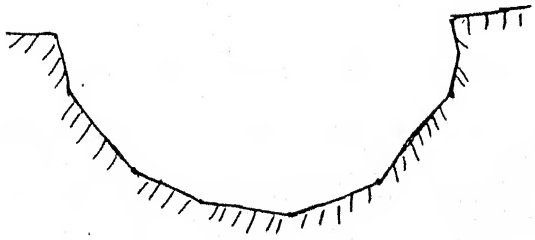

Fig. 6.2.2 Multiple Concavities

6.3 Geometrical Arrangements of Concavities in the Border :

1) The sequences described in section 6.2 may be restricted in one region of the profile boundary.

2) Sequences scattered over the profile boundary.

6.4 Geometrical Arrangements of Concavities Across the Interior :

1) Skeletal interaction among concavities giving rise to necks (Fig. 6.4.1).

2) Skeletal interaction between concavities and convex regions of the profile (Fig. 6.4.2).

6.5 Concavity Deletion :

The concavity deletion process should be capable of handling the whole spectrum of concavity possibilities. We propose two disparate methods for the concavity deletion. They are, 'Cuts' and 'Approximations'.

We propose to delete concavities one at a time. These concavities are the local concavities between adjacent edges. The cases of concavities with smooth curved boundaries (ref. Fig. 6.1.2) are handled by sequences of successive applications of the two deletion methods. The sequences are generated by the successive nodes of the generative space search. That is, each concave vertex in the profile is deleted independently.

The vertices of profile with interior angle greater than π are the concave vertices. Each of these concave vertices is deleted by application of a 'Cut' or an 'Approximation'.

6.3 Geometrical Arrangements of Concavities in the Border :

1) The sequences described in section 6.2 may be restricted in one region of the profile boundary.

2) Sequences scattered over the profile boundary.

6.4 Geometrical Arrangements of Concavities Across the Interior :

1) Skeletal interaction among concavities giving rise to necks (Fig. 6.4.1).

2) Skeletal interaction between concavities and convex regions of the profile (Fig. 6.4.2).

6.5 Concavity Deletion :

The concavity deletion process should be capable of handling the whole spectrum of concavity possibilities. We propose two disparate methods for the concavity deletion. They are, 'Cuts' and 'Approximations'.

We propose to delete concavities one at a time. These concavities are the local concavities between adjacent edges. The cases of concavities with smooth curved boundaries (ref. Fig. 6.1.2) are handled by sequences of successive applications of the two deletion methods. The sequences are generated by the successive nodes of the generative space search. That is, each concave vertex in the profile is deleted independently.

The vertices of profile with interior angle greater than TT are the concave vertices. Each of these concave vertices is deleted by application of a 'Cut' or an 'Approximation'.

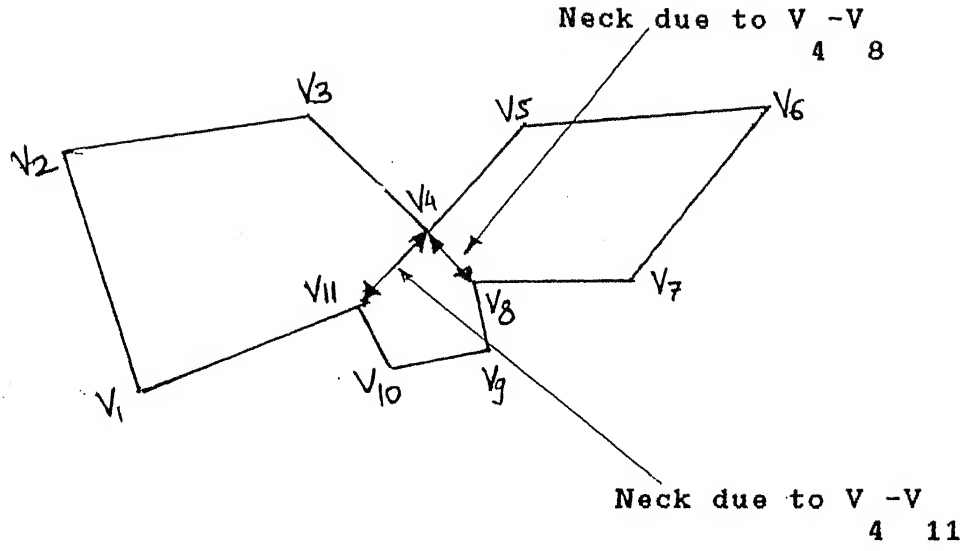

Fig. 6.4.1 Interaction between two Concavities

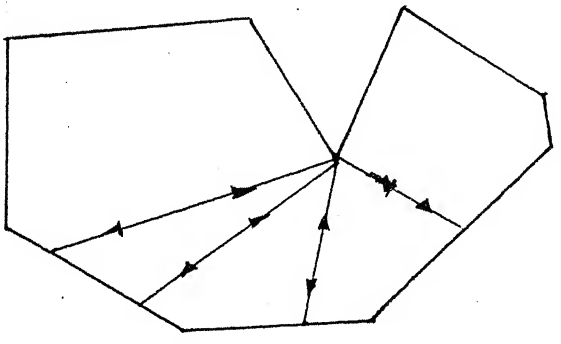

Fig. 6.4.2 Interaction between Concavity and a Convex Region

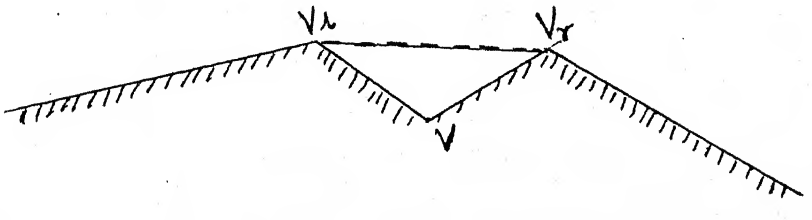

Approximation of concave vertex V

Fig. 6.5.1.1 Definition of an Approximation.

6.5.1 Approximations :

It can be seen from discussion given above that profiles can have great variations and may be extremely complex. A profile may have a large number of major and minor variations in the boundary. The minor and not so minor disturbances would tend to clutter up a decomposition solution with a large number of constituents. It will reduce the usefulness of the shape description. This situation can be avoided by a careful use of the approximations. The minor concavities are straightened up or deleted by 'enveloping' by approximations.

Approximations, as a method of concavity deletion, are in the form of 'straightening'. In Fig. 6.5.1.1, the vertices V_l and V_r, adjacent to the concave vertex being deleted, V, are joined by a straight line and thus the concavity is deleted. A sequence of cuts and 'straightening up' approximations in the decompositioning process, illustrated in Fig. 6.5.1.2, may give other types of desirable approximations.

Approximations of different concavities may overlap or otherwise interact with each other (ref. Fig. 6.5.1.3). The concavity deletion order becomes critical when the approximation interaction are feasible.

6.5.2 Cuts :

Cuts are taken to originate at the concave vertices. A cut, if it lies in the reflex angle of the concavity, consists of only one line. Else it consists of two lines (Fig. 6.5.2.1). The cuts are

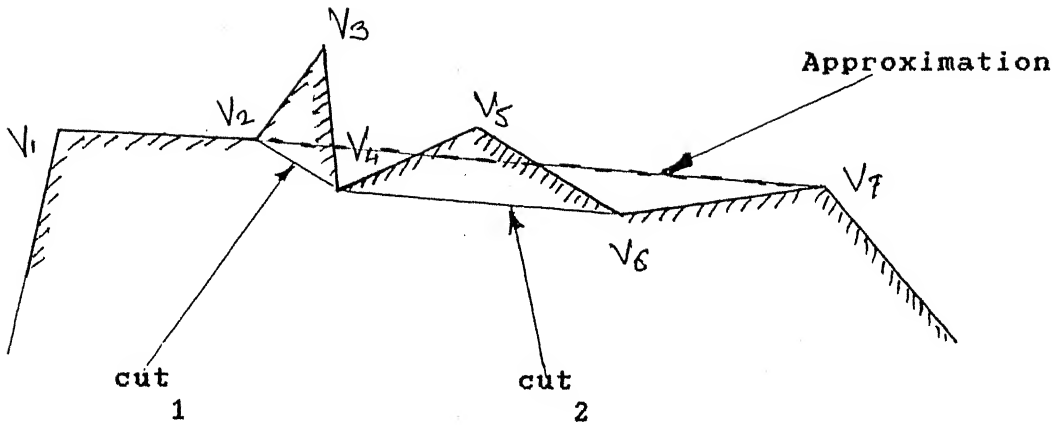

Fig. 6.5.1.2 Sequence of Approximations and Cuts.

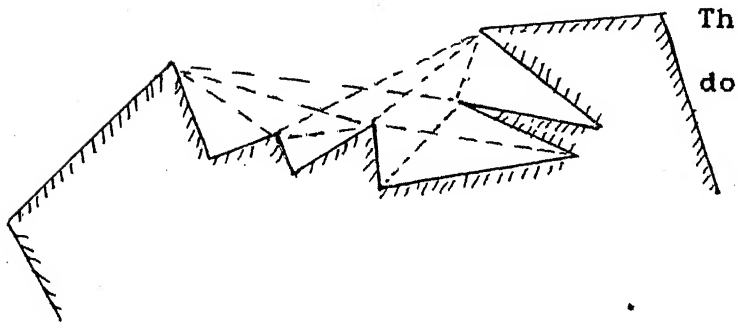

Fig. 6.5.1.3 Overlapping and Intersecting Approximations.

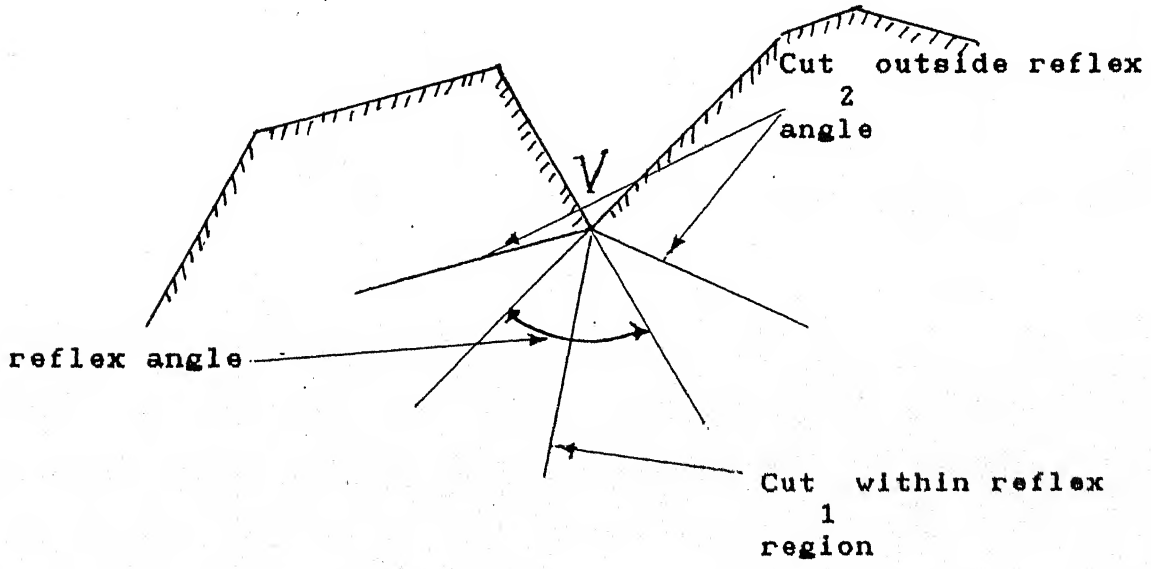

Fig. 6.5.2.1 A Cut at a Concave Vertex.

generated by application of the heuristic rules stated in section 7.

A cut could theoretically, lie anywhere in the interior angle. The heuristics generating the cut should locate the most probable regions of the interior angle which would give maximal external visibility i.e. minimal length cuts. We propose that the skeletal interactions give a good basis to locate these regions. These are the skeletal interactions of the concave vertex being deleted. In another words, the concave skeletal interaction strings of the skeleton are being replaced by convex skeletal interaction lines. If a ray is passed from the concave vertex till it intersects the boundary of profile, and scan the whole range of the interior angle, the length of the ray and its variation with the angle would yield a lot of information about the possible cuts. The cut should be located in the minimum length regions or in the regions where the characteristics of the length variation undergo major changes. These regions are roughly located by the skeletal interactions. In Fig. 6.5.2.2 the skeletal interaction of the concave vertex V_0 is shown. A cut should be located in the zone delimited by the angles θ_2 to θ_5. With in this zone, $\theta 3$ completely and regions of $\theta 4$ are ruled out if the cut is to end on the skeletal interaction regions of vertex V_0 on its interacting edges, i.e. segments AB on edge V_1-V_2 and segment CD on edge V_5-V_6. Thus, it can be seen that the skeletal interaction regions of the concave vertex, on the edges interacting with the concave vertex, are the regions where the foot of the minimum length cut are likely to lie.

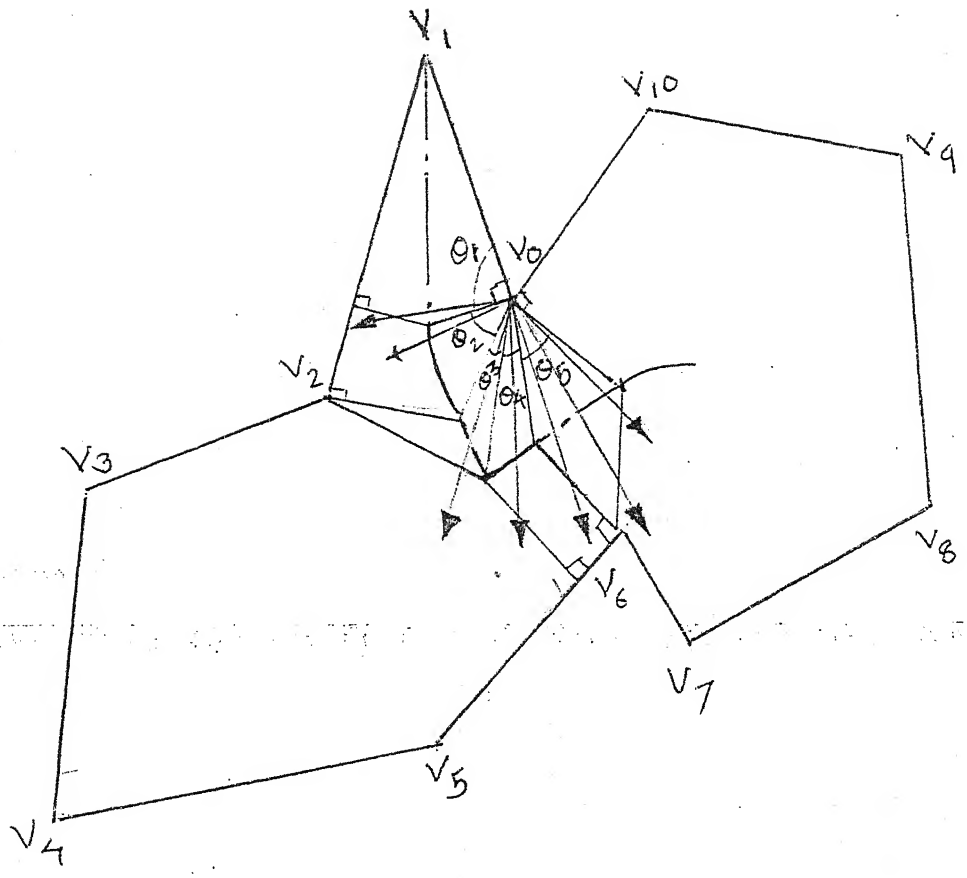

Fig. 6.5.2.2 Skeletal Interaction Basis for a Cut.

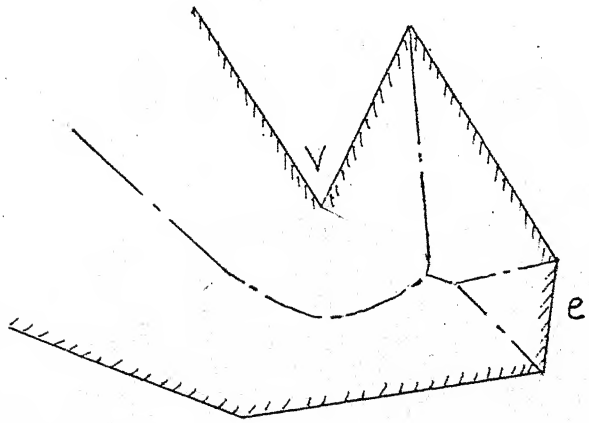

Vertex V just missed a skeletal interactionwith edge e.

Fig. 6.5.2.3 Missed Interactions

Apart from passing rays at discrete angular interval, checking the intersections and scanning the interior angle, there is no alternative to skeletal interaction for exploration and study of cuts. The process of passing rays would be computationally too expensive. The skeletal interaction inherently takes care of whole diverse concavity spectrum. Thus, to minimise cut length, cuts should be based on the geometrical regions of the concave skeletal interaction strings.

There may exist situations where an interaction between the concave vertex and a boundary segment is just missed; e.g. vertex V and edge e in Fig. 6.5.2.3. A good and viable decomposition could result from these missed interactions, as is apparent in the figure. The identification and an appropriate handling of these cases should be done on the basis of a fuzzy or possibilistic definition the skeleton. It is beyond the purview of the present work.

Exploration of the Skeletal Interaction Regions and Formulation of Cut Rules :

A concave vertex interacts with a sequence of profile edges and other concave vertices. These separate interactions produce disparate regions with differing characteristics. Each of these regions should contribute atleast one cut to the set of solution nodes. In each interaction region, cuts connecting the concave vertex with the extremes and the centre of the interaction region, and the minimum distance cut should be generated.

If the cut lies outside the reflex angle of the concave vertex,

then another cut line on the other side of the reflex angle is generated by application of the same heuristic rules (ref. Fig. 6.5.2.1).

6.5.3 Cut Interactions and Cut Modifications :

Cut Interaction : Cuts taken during a particular concavity can not interact with each other. They are exclusive of each other. In Fig. 6.5.3.1, the skeletal interaction and the interaction regions of the concave vertex V are shown. The cuts C_1, C_2 and C_3 lie in the angular interaction regions of V with edges V_1-V_2, V_2-V_3 and V_3-V_4 respectively. Hence they can not intersect with other. After a concavity is deleted, the profile changes. It may be replaced by an envelope, or it may be decomposed into multiple polygons. The skeleton of the new profile is determined afresh. In the new skeleton, the interaction zones are also different. Thus a cut may interact with cuts taken in a previous concavity deletion; e.g. cut taken in deletion of vertex V_1 and cut taken in deletion of vertex V_2 in Fig. 6.5.3.2.

Cut Modifications : A cut modification results from an interplay between a cut and a subsequent approximation across the interior edges created by the cut (Fig. 6.5.1.2). (Interior edges are those which lie inside the original profile boundary.) In such a case the earlier cut is obliterated and the new cut resulting from the approximation is retained.

6.5.4 Heuristic Evaluation of the Intermediate Solutions :

The 'goodness' measure of the intermediate solutions generated by the heuristics could be used as the heuristic evaluation function 'usefulness'. This would turn the decomposition process into a hill climbing process with its attendant pitfalls like foothill climbing. To overcome these drawbacks, the 'goodness' measure is modified by the 'concavity reduction measure'. This introduces the possibility of not following of the locally best path every time. Hence, with a good heuristic intermediate solution evaluation function, foot hills may be avoided.

As the name suggests, the concavity reduction measure is a measure of how many concavities are being reduced by the cut and to what extent. It may be noted that a cut might only reduce a concavity, and might not delete it. Also, more than one concave vertices may be affected by one cut, as the cut C in Fig. 6.5.4.1. This factor should be designed to increase the usefulness of a cut joining two concave vertices. It should also enhance the usefulness of the cuts which reduce the concavity to a large extent and those which completely delete the concavity. The exact evaluation of the concavity reduction measure is given later, in section 7.1.

6.5.5 Criticality of a Concavity Deletion :

The criticality of a deletion is an indication of how different the possible decomposition results are from each other. It also depends on the importance of the children solutions. The useful solutions, which may be developed further, if they are drastically different from one another, may give rise to highly different

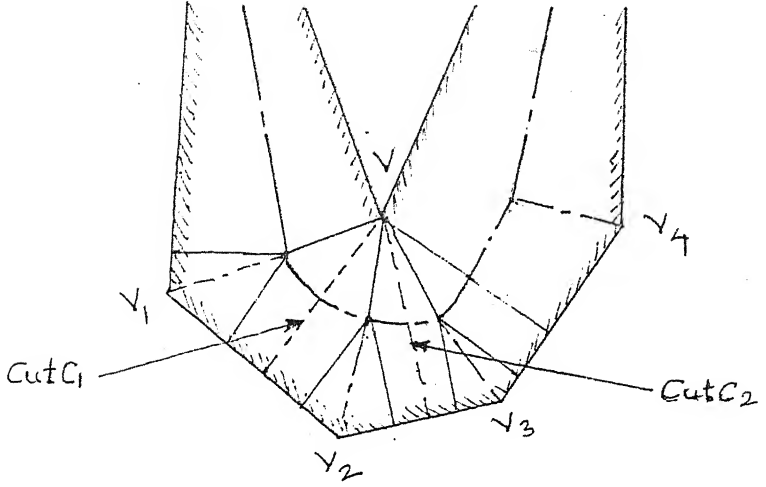

Fig. 6.5.3.1 Non-interaction of the Cuts of a Concavity with one another

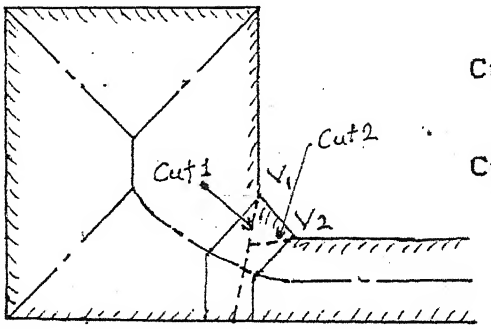

Cut 1 deleting V_1

Cut 2 deleting V_2

Fig. 6.5.3.2 Interaction of Cuts of Different Concavities.

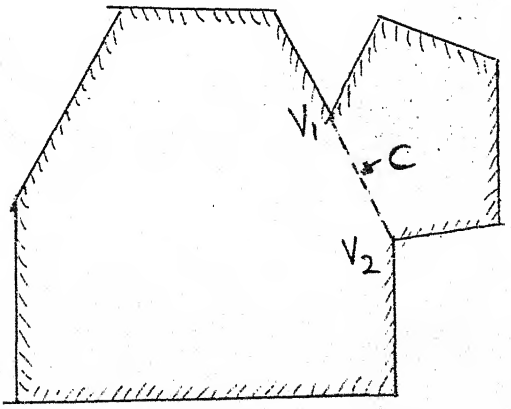

Cut 'C' deleting V_1 and V_2

Fig. 6.5.4.1 A Cut Affecting Two Concavities.

decompositions. Hence these solutions are critical for the generation of multiple and different decomposition solutions. Multiplicity of decompositions is necessary to generate multiple and varied descriptions for a profile. The success of shape matching approach to nesting depends upon the ability to generate multiple descriptions.

During the decomposition process, at a particular concavity deletion, from the possible solutions, the 'most useful' solutions are shortlisted. All the most useful solutions can be checked against the solution with highest usefulness for difference. The criticality of the deletion is the largest difference and the importance of the concavity.

The difference between two deletion solutions can be a difference between a cut and an approximation or difference between two cuts. A cut and an approximation are absolutely different. The difference between two cuts depends upon whether the two cuts are 1) vertex to edge cuts or vertex to vertex cuts, 2) one line cuts or two line cuts, 3) angular separation between the cuts. The first two sources of difference are combinatorial in nature, whereas the last one is continuous. A heuristic difference evaluation function combining these sources of difference and returning a difference measure needs to be formulated. The combinations of first difference can be given weightages. The difference is the weighted sum of the normalised angular separation. The exact formulation of the heuristic difference evaluation functions is given in section 7.3.

6.6 Sequence of Concavity Deletion :

Sequence of concavity deletion becomes extremely important with the possibility of cut interaction, cut modifications and approximation interaction, hence forward generically called deletion interaction. If there is no likelihood of either of deletion interaction, then the order of deletion is immaterial.
As cuts are restricted to the skeletal interaction zone, cut interactions are possible only for the concavities which are visible to each other across the interior of the profile (ref. section 3, chapter2). Approximation and cut modifications are possible for concavities proximal along the boundary of the profile. Since cuts are based on the skeletal interaction, the proximity of the concave skeletal interaction string regions increases the possibility of cut interaction. Due to the nature of the skeleton, proximity of the concavities along boundary is bound to reflect in proximity of the skeletal lines. Thus deletion ordering is highly important for concavities with skeletal lines in proximity.

As noted earlier, a complex profile may have large number of minor concavities. The deletion interaction of such minor concavities is not likely to produce significantly different decompositions. Accordingly, the concavities present in the polygon have been given properties of 'peripherality' and 'importance' (ref. section 6.2, chapter 2). These two properties of concavities can be used in combination to decide the deletion order.

The peripheral and not important concavities are merely disturbances on polygon boundary. These should be deleted first to

give a smoother boundary; otherwise they will unnecessarily interfere in the deletion process of important concavities, complicating the solution space.

Among the non-peripheral concavities, the order of deletion of 'not important' concavities does not substantially affect the final decomposition solutions. The important concavities are deleted first and then finally the non-peripheral and unimportant concavities.

The properties of the concavities are evaluated with respect to the particular polygon to which they belong (ref. section 5). This necessitates an ordering of the constituent polygons. This problem is circumvented by taking the global reference values for the property evaluation, e.g. for peripherality and importance evaluations, the reference length with respect to which the 'smallness' or 'largeness' of radius is to be evaluated, is taken with respect to the whole skeleton and not the skeleton of the particular profile. This ensures that large polygons are processed more carefully than the small polygons.

For the high peripherality and low importance concavities, the order is not much important. For non-peripheral concavities, the deletion will in general be in a decreasing order of importance. When multiple concavities are seen to be equally important, all are presented for deletion. The 'usefulness' of deletions then decide which one will be explored before others. If any of these concavities are proximal then the decision is mark d as critical. The critical decisions are used for generation of multiple

decomposition schemes, by exploring all the useful alternatives at the critical decision.

Criticality of Deletion Order :

The deletion order is critical in the high importance phase of the decomposition process. In this phase, a deletion decision which has multiple candidates is a critical decision. The proximity and importance of the candidates for deletion decide the criticality of the deletion order decision.

6.7 Process Control Strategy :

The decomposition process is designed for production of multiple decompositions of equal goodness. Heuristic function 'usefulness' is used to guide the process in local decisions. Another heuristic function 'criticality' is used to guide the backtracking and to produce multiple goal states.

At each decision node, concavities are short listed for deletion on the basis of the ordering heuristics. The criticality of deletion order is evaluated. Deletion heuristics are applied to each of the candidate concavities. The resulting solution nodes are evaluated for usefulness. The criticality contribution by the deletion is evaluated. The total criticality of the decision, function of both deletion criticality and order criticality, is evaluated. The most useful solution is followed.

In case of a dead end, the decision tree is backtracked to the previous critical decision. After a satisfactory decomposition is achieved, the most critical decision nodes are explored further to

produce more decompositions of equal goodness.

7. Complete Formulation of Heuristic Rules and Procedures :

The proposed heuristic rules and functions carry out the quantification of the qualitative concepts discussed so far. The heuristics are based on study of some situations. They are quite ad hoc in nature as they represent a tentative embodiment of qualitative principles guiding the development. Carefully planned experimentation, over a wide range of shapes, is needed to refine and improve the heuristics.

7.1 Rules for Cut :

More than one cuts are generated at the deletion of each concave vertex .

1) A cut is generated for all the profile boundary elements skeletally interacting with the concave vertex being deleted.

2) If the element is a concave vertex then the cut is the straight line connecting the two vertices.

3) If the element is a profile boundary edge then generate four cuts by connecting the concave vertex with :

a) centre of the interaction zone.

b) the extremes of the interaction zone (two cuts).

c) the minimum distance line between the concave vertex and the profile boundary within the interaction zone, if it is not already generated in the above cuts.

4) If the cut lies outside the reflex angle then,

produce cuts over all other interacting profile boundary elements. Reject those lying inside the refle angle or on the same side of the reflex angle as the first cut line.

5) Usefulness evaluations of cut :

Usefulness is the 'Goodness' G, modified by concavity reduction factor. i.e.

$$U = G * C_u ;$$

where $G = V * A$,

and C_u is the concavity reduction factor of the cut.

$$C_u = \sum_{i=1}^{m} (W_i * C_{ui}) ;$$

'm' is the number of concave vertices being affected by the cut,

W_i is the important weightage of the i'th concave vertex,

C_{ui} is the concavity reduction of the i'th concave vertex.

Note that a cut joining two concave vertices reduces the concavity at both the vertices.

Evaluation of C_{ui} :

a) For the concave vertex being deleted :

C_{ui} is a function of the final angle at the vertex being deleted. This function is plotted in Fig. 7.1. θ_e is the exterior angle of the profile at the concave vertex V. θ_f is the final interior angle at the vertex V after the cut i.e. angle between the two lines forming the cut. θ_c is the compliment of θ_e . If the cut lies in the reflex angle of the vertex, then the final angle is zero. This factor allows some concavity to remain after the deletion action. In the Fig. 7.1,

$$\theta_c = \pi - \theta_e ;$$

$$\theta_1 = \pi + \theta_d .$$

θ_1 is the limit on θ_f above which the C_{ui} is zero. Value of θ_d is proposed to be $\theta_c / 2$.

b) For other concave vertices : A concave vertex other than the one being deleted may be affected by a cut. For these vertices, taking complement of the exterior angle to be the measure of the concavity ($\theta_c = \pi - \theta_e$; ref. Fig. 7.1),

C_{ui} = (θ_c before_cut) - (θ_c after_cut)) / π;

if the concavity is deleted then (θ_c after_cut) = 0.

7.2 Rules for Approximations : (ref. Fig. 6.5.1.1)

1) Straightening up :

Draw the approximation line by connecting the two vertices flanking the vertex being deleted.

2) Cut modification :

If any of the edges being eliminated by the approximation is an interior edge then the constituent polygon with the interior edge is modified to the new edge formed by the approximation.

3) Approximation interaction :

The last approximation overrides the previous approximations.

4) Usefulness :

The usefulness of an approximation is the goodness value G (ref. section 3) of the decomposition.

7.3 Deletion Criticality :

Let C be the concavity being deleted.

Let D_i , i = 1,...,N_d , be the most useful deletion solutions.

Let $HUD_{hi} = D_i$, $i <= h_i < N_d$, be the deletion with the highest usefulness value.

Let D_{fi} , $i /= h_i$, be the difference measure of the HUD with D_i .

7.3.1 Evaluation of D_{fi} :

The difference evaluation is commutative, i.e. $D(D_f, D_i, D_j) = D(D_f, D_j, D_i)$.

1) If the two deletions are a cut and an approximation then $D_f = 1$.

2) Difference weightages for types of cut, D_W :

(ref. section 6.5.5 for sources of differences and their combinations.)

Vertex to vertex cut : $D_W = 0.8$.

Vertex to edge cut : $D_W = 0.6$.

This reflects the observation that a vertex to vertex cut is more different from other cuts than a vertex to edge. The numbers proposed for D_W are ad hoc; they are adjusted so as to lie within the lower and upper bounds of zero and one respectively. The bounds are the same as those normally used in fuzzy membership functions.

Combinations of two cuts may be,

a) one line and one line,

b) one line and two lines,

c) two lines and two lines.

3) Difference evaluation between two one line cuts :

The situation is illustrated in Fig. 7.3.1.3. The concave vertex V is being deleted from the profile. θ_i is the interior angle at the vertex, and θ_d is the angle between the two one line cuts being compared for difference evaluation.

Cut C_1 has difference weightage D_{W1} and C_2 has D_{W2}.

$D_f = D_{W1} * D_{W2} * (\theta_d / \theta_i)$.

D_f is bounded, $0 < D_f < 1$.

4) Difference between a one line cut and a two line cut :

The case is illustrated in Fig. 7.3.1.4. V is the concave vertex being deleted from the profile. The line L_2 and L_3 form the two line cut cut2 The cut is the one line cut.

Cut C has difference weightage D_{W1},

Line L_1 of cut C_1 : D_{W2},

Line L_3 of cut C_2 : D_{W3}.

$D_f = (D_{W1} * D_{W2} * (\theta_{12} / \pi) + D_{W1} * D_{W3} * (\theta_{13} / \pi))$.

D_f is bounded. Minimum $D_f = 0$.

For maximum D_f,

$\theta_{12} = \pi$,

$\theta_{13} = \theta_d$ (ref. section 7.1, number 5)

with $\theta_e \rightarrow 0$, $\theta_{13} \rightarrow \pi / 2$,

substituting, maximum $D_f = 0.96 < 1$.

5) Difference between two two line cuts :

The case is illustrated in Fig. 7.3.1.5. V is the concave vertex being deleted from the profile. The line L_1 and L_3 form the two line cut cut . The cut is formed by lines L_1 and L_2.

Cut C is a two line cut comprised of lines L_3 and L_4.

Cut C_1 is a two line cut comprised of lines L_1 and L_2.

Cut C_2 is a two line cut comprised of lines L_3 and L_4.

Line L_1 of cut C_1 has difference weightage D_{W1},

Line L_2 of cut C_2 has difference weightage D_{W2},

Line L_3 of cut C_3 has difference weightage D_{W3},

Line L_4 of cut C_4 has difference weightage D_{W4}.

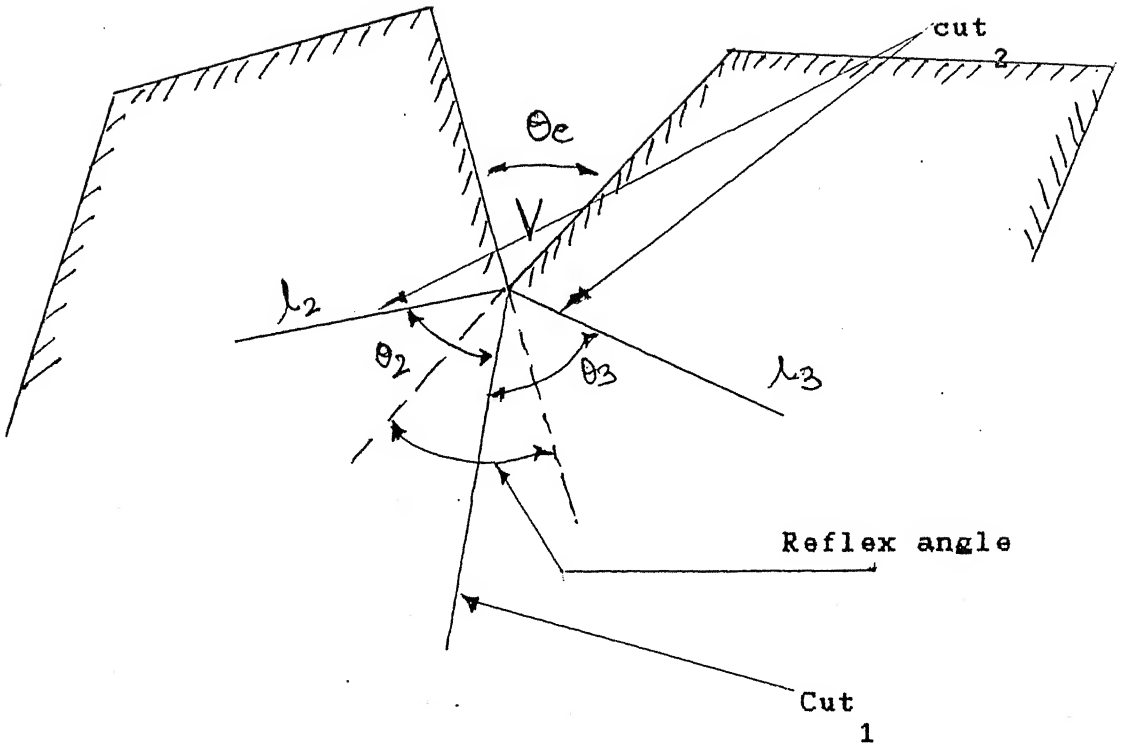

Fig. 7.3.1.4 Difference between a One Line Cut and a Two line Cut

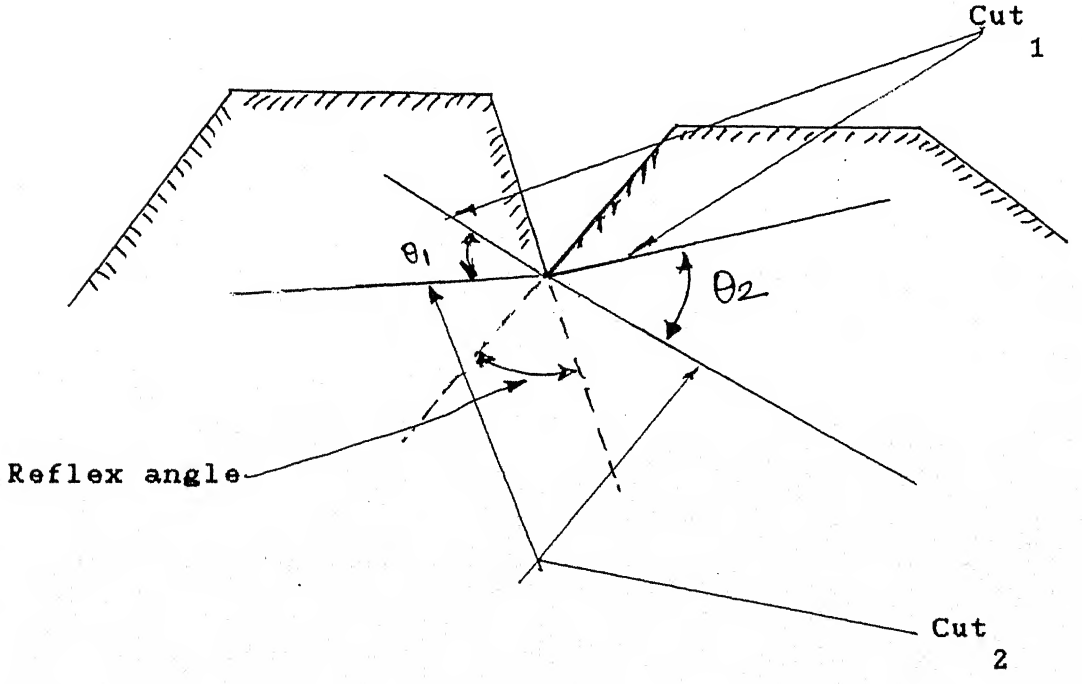

Fig. 7.3.1.5 DIfference between Two Line Cuts.

$$D_f = \left(\frac{\theta_1}{\pi - \theta_e} \right) * D_{W1} * D_{W3}$$

$$+ \left(\frac{\theta_2}{\pi - \theta_e} \right) * D_{W2} * D_{W4} .$$

D_f is bounded. Minimum $D_f = 0$.

For maximum D_f

$\theta_e \rightarrow 0$, $\theta_1 + \theta_2 \rightarrow \pi + \theta_d$ (ref. section 7.1, number 5),

i.e. $\theta_1 + \theta_2 \rightarrow 3 * \pi / 2$,

substituting, maximum $D_f = 0.96 < 1$.

7.3.2 Criticality Evaluation for D_i :

The deletion criticality $C_r(D_i)$, between pairs of the HUD and D_i is the fuzzy logical conjunction of importance of the concavity Imp(C), difference D_{fi}, and equality of usefulness of HUD and D_i i.e. the fuzzy predicate

equal(usefulness(HUD),usefulness(D_i)).

$C_r(D_i)$ = Imp(C) AND D_{fi} AND equal(usefulness(HUD),usefulness(D_i)).

7.3.3 Deletion Criticality Evaluation :

It is the fuzzy logical disjunction over all the D_i.

$C_r = OR\ C_r(D_i)$, $i = 1,\ldots,N_d$, $i \neq h$.

7.4 Rules for Deletion Order :

1) Classification of concavities into four types :

a) High peripherality and low importance.

b) High importance and high peripherality.

c) High importance and low peripherality.

d) Low importance and low peripherality.

It is the application of the fuzzy logical functions;

$$type_1 = high(peripherality)\ AND\ low(importance);$$

$$type_2 = high(importance)\ AND\ high(peripherality);$$

$$type_3 = low(peripherality)\ AND\ high(importance);$$

$$type_4 = low(peripherality)\ AND\ low(importance).$$

2) Check existence of concavities of type one by taking an alpha cut [13] [19,20] on the set of membership grades of type one. The suggested value of the alpha cut is 0.2. If there are no type one concavities then process the concavities for type two, three and four as given in the following parts 3 and 4; else select the concavity with highest type one membership.

3) Shortlist the important concavities from the profile,

$$IC_i,\ i = 1,2,...N_{ic}.$$

4) Select the most important concavity (concavities) from them. All of the most important concavities are presented for deletion.

$$MIC_j,\ j = 1,2,...,N_{mic}.$$

5) Evaluate the proximity of the most important concavity with the important and the most important concavities. Deletion order criticality of a concavity pair is the fuzzy logical conjunction of proximity and importance; i.e.

$$C_r(C_i,C_j) = P_r(C_i,C_j)\ AND\ Imp(C_i,C_j).$$

The order criticality of the deletion order decision is the fuzzy disjunction of all the pairs; i.e.

$$C_r = OR\ C_r(C_i,C_j).$$

The concavities for which the order of deletion is critical, are noted, along with the criticality. The order of deletion is taken to be the descending order of importance of the concavities. The deletion order criticality is utilised in deciding upon the backtracking (ref. section 7.5).

7.5 Rules for Process Control :

1) Criticality of a decision :

It is the fuzzy logical disjunction of the deletion criticality C_{rd} and the order criticality C_{ro}, $C_r = C_{rd}$ OR C_{ro}.

2) Judgment on solution state :

Dead end recognition : It is the fuzzy predicate 'low' applied to the local goodness value; i.e. low(goodness(HUD)).

Goal state recognition : The necessary condition is that all the concavities are deleted. It is the fuzzy logical 'satisfactory' applied to the goodness of the final decomposition solution, satisfactory(goodness(Solution)).

3) Critical decision recognition and backtracking :

Critical decision recognition is the application of the fuzzy predicate 'high' to the decision criticality list. Backtracking is done upto the last 'high' criticality decision.

8. Complete Algorithm :

1) Evaluation of the skeleton and its properties.

2) Generation of Concavity deletion solutions :

a) Deletion order analysis to determine Concavities for deletion.

b) Deletion of concavity.

c) Usefulness evaluation of each solution.

d) Criticality of the decision.

The most useful explored first.

The decision stored on stack.

3) Goal state / dead end / end of process recognition.

4) If none of the three go back to skeleton evaluation.

5) if goal state,

a) Determine and analyse the bays formed by approximations.

b) store the final results,

c) Get the list of most critical decisions,

d) backtrack to the last of them,

e) go to skeleton evaluation.

6) If dead end,

a) Get the list of most critical decisions,

b) backtrack to the last of them,

c) go to skeleton evaluation.

7) if it is the end of the process then quit.

9. Example of Decomposition :

The decomposition algorithm is illustrated by an example. Consider the profile given in the Fig. 9.1.

The concavities are V_4 , V_7 , V_9 .

Importance order (descending) of concavities (ref. section 6.2.3, chapter 2) :

V_7 and V_9 have approximately same importance. V_4 has much lower importance.

$V_7 > V_9 > V_4$.

Peripherality of all the concavities is low (ref. section 6.2.2, chapter 2).

Candidates for deletion are V_7 and V_9.

V_7 and V_9 have good proximality (ref. section 6.2.4, chapter 2); hence the order of deletion of V_7 and V_9 is critical.

1) Deletion of V_7 in First Step :

V_7 interacts with edge E_4 and vertex V_9. Hence two cuts are possible; (Note that the three cuts between V_7 and E_4 (ref. section 7.1) are reduced to one cut at the centre of the zone of interaction.) Cut between V_7-E_4 and Cut V_7-V_9. Approximations have low usefulness and hence are not considered.

Usefulness order (ref. section 7.1) :

The usefulness of the two cuts is almost the same. But,

Cut V_7-V_9 > Cut V_7-E_4 .

It may be noted that the cut V_7-V_9 does not eliminate the concavity at V_9 ; but it only reduces the concavity.

Hence V_7 may be deleted by the cut V_7-V_9 or by cut V_7-E_4 .

2) Deletion of V_7 by cut V_7-V_9 :

Now the profile is decomposed in to two profiles, as shown in Fig. 9.2. The subprofile P_2, has concavities V_4, V_9, V_7. All have low importance and low peripherality. The order is also not critical.

Hence let the order be V_9-V_7-V_4.

For V_9 deletion, Cut V_9-V_4 is the most useful (ref. Fig. 9.2).

Now only V_7 is the concavity. The approximation V_9-V_6 is the most useful for deletion of V_7. The resulting final decomposition is shown in Fig. 9.3.

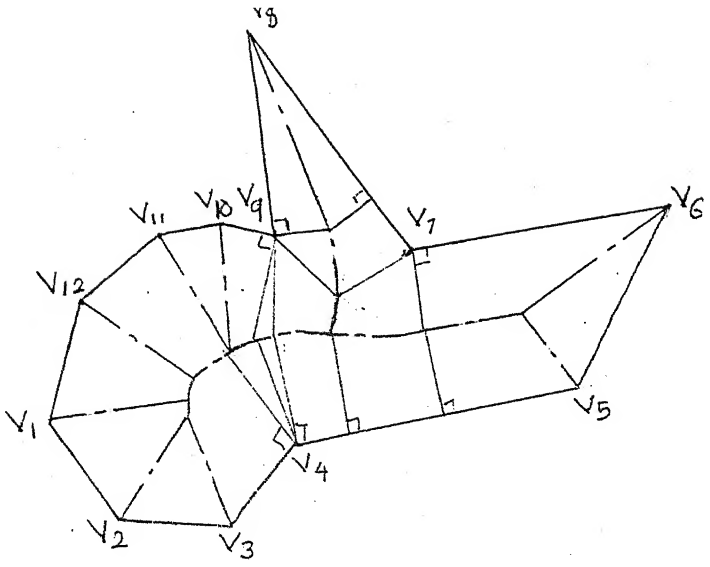

Fig. 9.1 Profile in Example

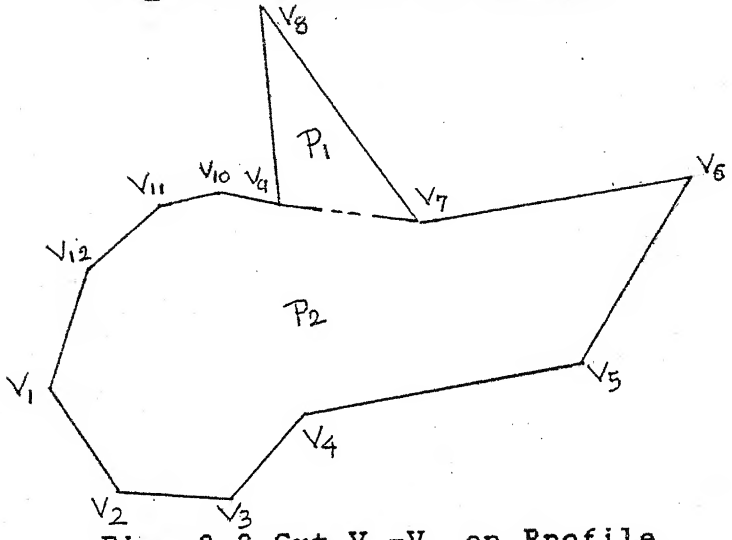

Fig. 9.2 Cut V -V on Profile

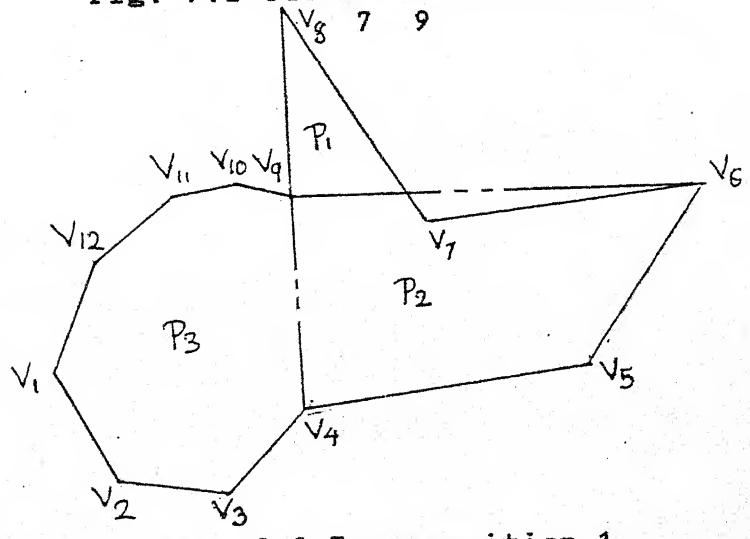

Fig. 9.3 Decomposition 1

3) Deletion of V_7 by cut V_7-E_{74} :

The profile is decomposed in to two subprofiles as shown in Fig. 9.4. The subprofile P has concavities V_2, V_9, V_4. Both the concavities have similar low importance and low peripherality. The order of deletion is not critical. Let V_9 be deleted first. Of the possible cuts and approximations, cut V_{94} has highest usefulness, outstripping the remaining alternatives by a large margin. Hence cut V_{94} is taken. The resulting decomposition is shown in Fig. 9.5.

4) Deletion of V_9 in First Step :

As the deletion order of V_7 and V_9 is critical, the solution is backtracked to the first step and V_9 is deleted in the first step. V_9 interacts with edge E_{74}, vertices V_7 and V_4. The possible cuts are $V_{9-E_{74}}$, V_{97}, V_{94}, V_{97}. Cut V_{97} is the same as the deletion of V_7 by cut V_{97}, in the first step. It will lead to the same solutions.

Usefulness order : Cut V_{94} > Cut $V_{9-E_{74}}$. The usefulness of cut V_{94} is appreciably larger than that of cut $V_{9-E_{74}}$ as the cut V_{97} deletes concavities at both V_4 and V_9.

Hence V_9 is deleted by cut V_{94}. The profile is now decomposed in to two subprofiles, P_1 and P_2 (ref. Fig. 9.6). Subprofile P_2 has concavity V_7. The concavity interacts with edges E_{9-4}, and E_4. The cut $V_{7-E_{74}}$ produces a decomposition which has been produced earlier. Hence the concavity V_7 is deleted by the cut $V_{7-E_{9-4}}$. The resulting decomposition is shown in Fig. 9.7.

Thus the given profile is decomposed in to three different decomposition schemes, given Fig.s 9.3, 9.5, 9.7. In this case, the three decompositions are not much different from one another.

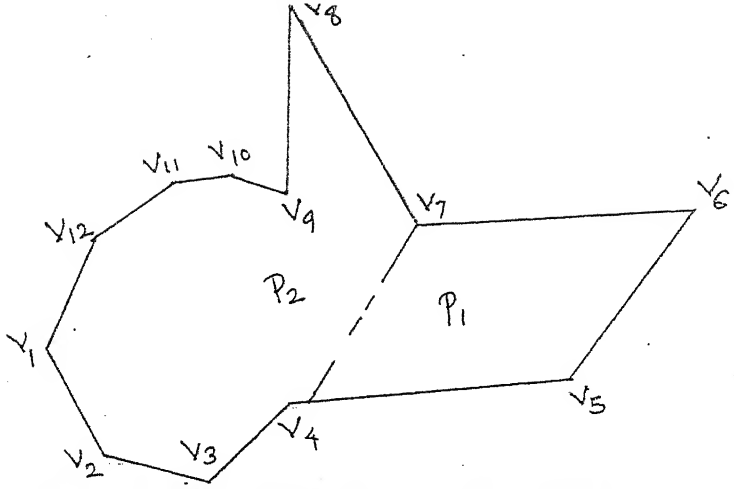

Fig. 9.4 Cut V -V on Profile
7 4

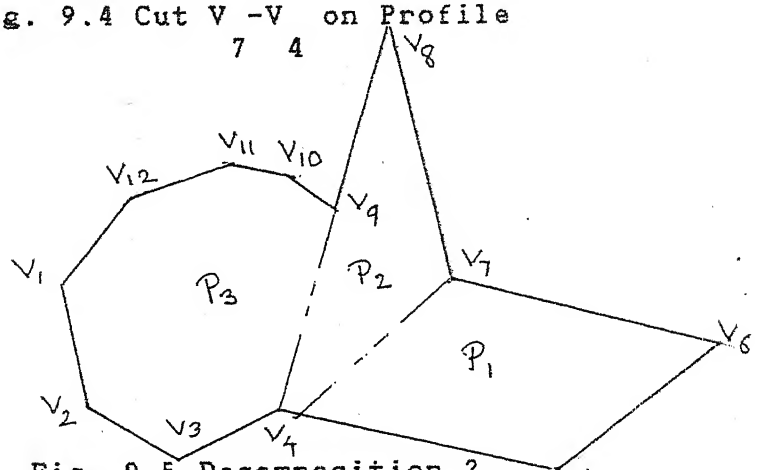

Fig. 9.5 Decomposition 2

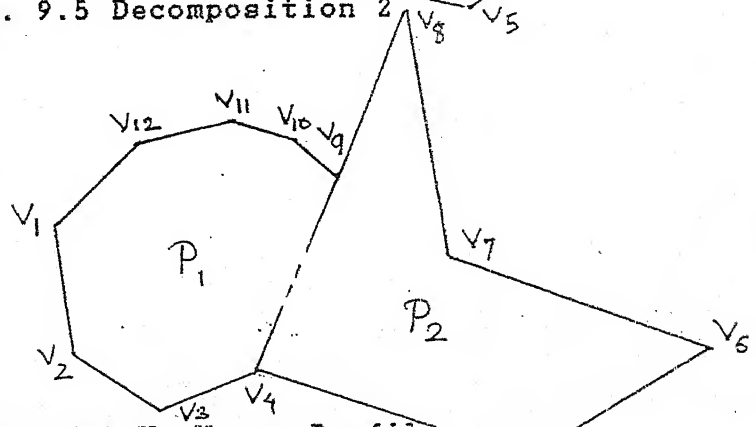

Fig. 9.6 Cut V -V on Profile
9 4

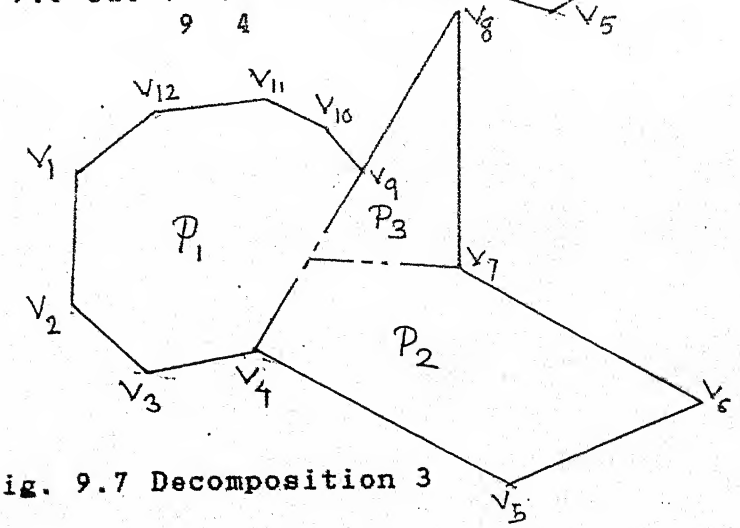

Fig. 9.7 Decomposition 3

Chapter 4

CONVEX POLYGON DESCRIPTION

1. Introduction :

Convex polygon description is a stage in the shape description of a profile. After the profile is decomposed into a set of constituent convex polygons, a description of the constituent polygons is obtained based on its qualitative aspects. In case of a convex profile this description itself becomes the shape description. For profiles with concavities, description of constituent polygons is useful in projection matching during the allocation.

The description of a convex polygon can not be only qualitative. It must combine both, the qualitative as well as the precise quantitative geometric features of the polygon. Polygon description is a complex, structured geometrical knowledge. An approximate global description neglecting minor features, may be used as a criterion to pare down and delimit the feasible solution space for allocation. Then the exact description is used for final allocation in the reduced solution space.

1.1 Objective of Convex Polygon Description :

A polygon description should be independent of translation, rotation and mirror imaging transformations. It should identify features of the polygon which are likely to be helpful in nesting. It should also be capable of representing the geometrical relations between the features. The features and their geometrical interrelations together constitute a complete polygon description.

1.2 Shape and Size of a Polygon :

A polygon is characterized by its shape and size. Shape of a polygon may be specified by the shape features and their interrelations. Shape is a necessarily qualitative property. Size is a quantitative property. Size can not be defined as a single global quantity. Size specification must be done with reference to the shape. Thus size and shape are intricately and inextricably woven together. They together define the polygon. We propose to define size of a polygon as the size of its shape features. The size of the dominant features and their combinations will be used as the global polygon size.

1.3 Basic Approach to Description :

Convex polygon description is based on classification of the polygons into a set of well defined shape classes. The proposed shape classification is hierarchical in nature . It can be modeled as a decision tree based on the features detected in the convex polygon. The proposed shape classes completely cover the whole shape space. They are based on shape features and their geometrical interrelations. The features and interrelations form the basis of the shape space. They span the whole shape space. The coordinate directions of the shape space are divided into different regions. The shape space is classified into different groups formed by combinations of these regions. The division and the subsequent classification are based on qualitative rules. The rules are in turn based on a systematic shape space exploration carried out by studying features and their interrelation regions and their combinations.

All the divisions and the classifications are fuzzy in nature.

This preserves the continuity of shape variation from one class to another by allotting grades of membership of classes to the polygons. A polygon may have nonzero membership grades for many classes. Thus the complex relationships among classes of shapes can be modeled in this approach, which may not be possible in a crisp approach.

This approach is best illustrated by an example. The polygon in Fig.1.3.1 could be described as just an approximate regular hexagon or a regular hexagon with a projection. Either of the two would be an approximate description. Neither of them alone would be sufficiently accurate. In the present work, both the descriptions are maintained; and the polygon is given different grades of membership or different confidence values for both the descriptions. For example, it may be described as a regular hexagon with say, 0.7 confidence and a regular hexagon with a projection with 0.75 confidence value.

An extremely simplified illustration of a general case is given in Fig. 1.3.2. The feature space is just two dimensional i.e. only two features are considered. X_1 , X_2 ,...,X_m are the zones of the feature 'X' along x axis. Y_1 , Y_2 ,...,Y_n are the zones of the features of the feature 'Y' along the y axis. Combinations of these zones give us classes C_1 , C_2 ,... . A profile P_1 lying halfway between C_2 and C_5 has equal membership grades for C_2 and C_5 and zero membership grades for the other classes. The profile P2 may have same membership grades for C_2 and C_5 , but it has nonzero membership grades for C_1 and C_4 also. The whole set of class descriptions and the membership grades together describe the

profiles.

If the description process is modeled as a decision tree, at each decision node some alternatives may be ruled out altogether. All the remaining alternatives need to be explored. The decision process spawns one or more subprocesses at each of the nodes. In each subprocess, the decision taken at the parent node to spawn the process is firm. In Fig. 1.3.1, at a decision as to whether the profile is to be a hexagon or a hexagon with a projection, both the decisions will be taken, each one spawning its own subprocess. In the subprocess spawned by the decision of hexagon with a projection, in all further analysis, the profile will be treated as a hexagon with a projection and similarly for decision of the profile being just a hexagon. If the projection were to be very minor then the alternative of hexagon with a projection would be neglected altogether. Only when the profile is such that it lies somewhere halfway in between two classes, both the classes would be considered. This type of analytical process will be referred to as a fuzzy spawning process in further work.

1.4 Shape Features :

A convex polygon may be deemed to be formed by the process of distortion of a regular convex polygon with the same number of sides. The distortions take the form of different stretching operations on the regular polygon. The stretching operations may result in formation of long sharp projections, mild projections, or elongations of the polygon. The stretching operations on a regular polygon are illustrated in Fig. 1.4.1. A regular polygon has only one fork in its skeleton. All the ACSILs converge to that fork. NACSILs are absent. The fork and the skeletal circle of the

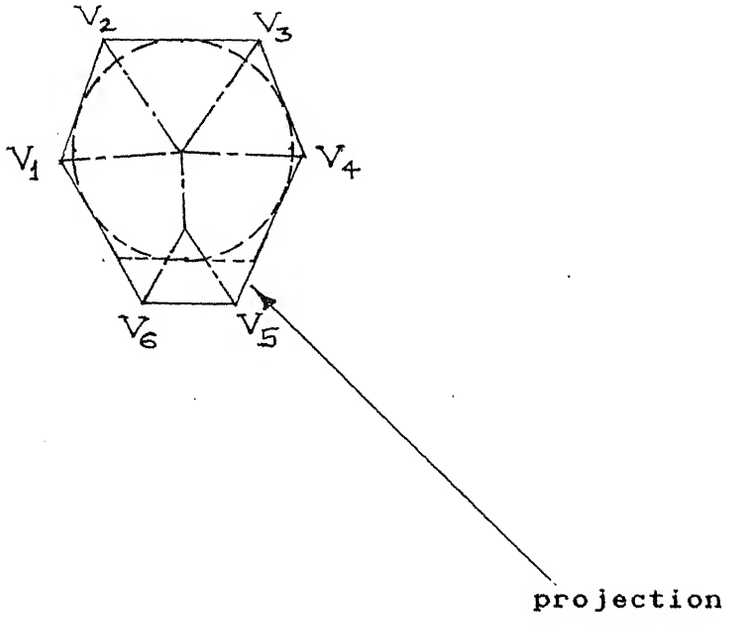

Fig. 1.3.1 Hexagon / Hexagon with a Projection.

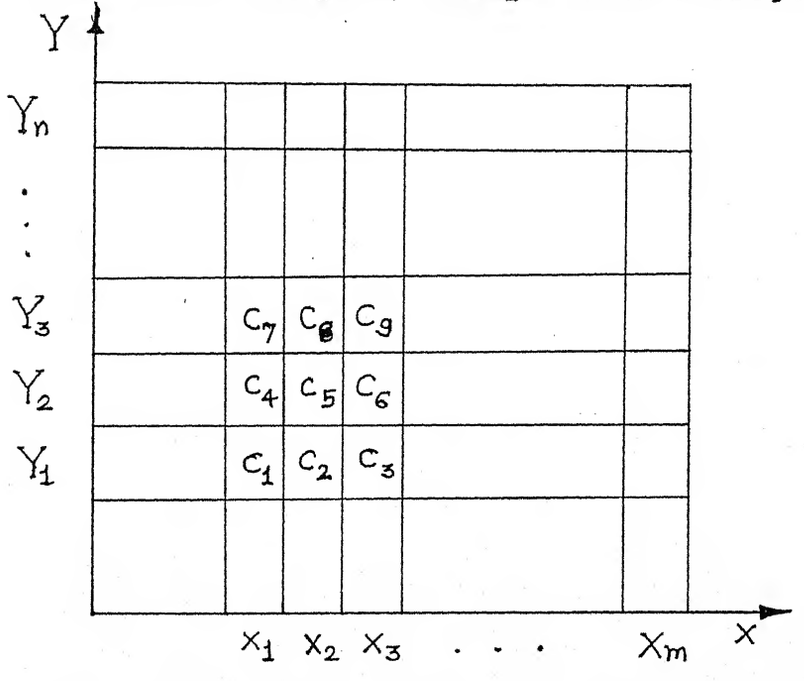

Fig. 1.3.2 An Illustration of a Feature Based Classification

regular polygon are drawn in the figure. Only the sides of the polygon undergoing the stretch operation are shown to avoid cluttering.

In Figure 1.4.1a, vertex V_2 is pulled out pushing back vertices V_1 and V_3 along the skeletal circle. The length of sides V_1V_2 and V_2V_3 increases at the expense of the other sides of the polygon. The angle ϕ is reduced to a small value. The symmetry of the skeleton of the regular polygon is disturbed. The angles and the lengths of the skeletal lines are no longer equal. A long sharp projection, a beak, emanates at the vertex V_2. In Figure 1.4.1b, a similar but weaker distortion results in a mild projection, a bulge. This type of stretch operations is referred to as type one stretch operation henceforth.

In Figure 1.4.1c, the edge e_2 is pulled out maintaining its orientation. The interior angles of the regular polygon remain the same. But an extra skeletal line is formed due to interaction between edges E_1 and E_3. It results in an elongation of the polygon. It also generates additional forks and the NACSILs in the skeleton. This type of stretch operations is referred to as type two stretch operation henceforth.

The two stretch operations mentioned above can produce, on repeated applications in different order combinations, all the possible variations in the skeleton of a convex polygon. Hence they can span the whole shape space.

The resultants of stretching operations, i.e. beaks, bulges and elongations, are important shape features. Very weak stretch operations result in minor distortions. Minor projections and minor elongations do not greatly affect the shape. They can be

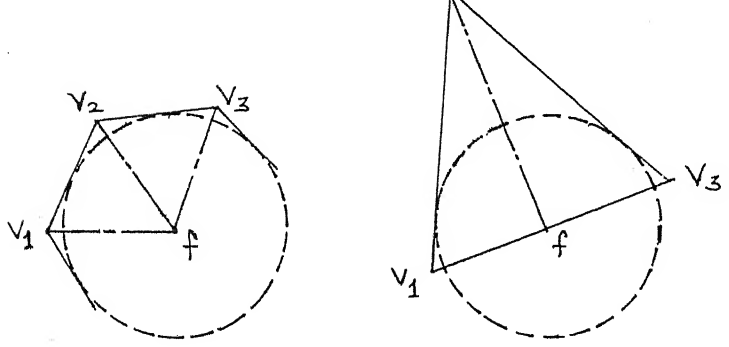

(a) A major type 1 stretch operation

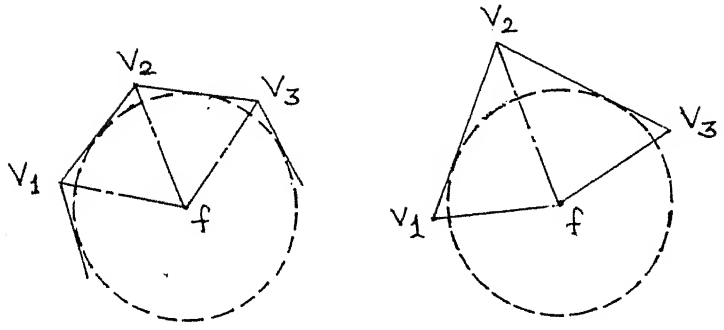

(b) Minor type 1 stretch operation

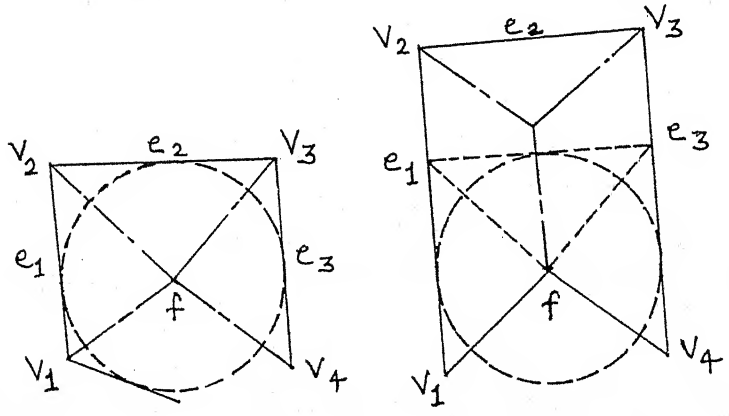

(c) Type two stretch operation

Fig. 1.4.1 Stretch Operations

approximated out to simplify the polygon and its skeleton. On the other hand, if the stretch operation is very strong, then the other features pale into comparative insignificance. The stretch operations dominate the shape. It is the middle level resultants of the stretch operations, beaks, bulges and elongations as listed above, are most important shape features. These important shape features and their interrelations form the basis of the shape space for explorations.

Of the shape features, beaks and bulges are the result of the same type of stretching operations, whereas elongation represents an entirely different operation altogether. It is contended that the sequence of application of these two operations can be separated into two distinct sequences. This contention is more rigorously justified later on in this chapter, in section 2.6.12. These two operations and their sequences can be explored separately. They are classified separately and finally combinations of these classes are used to classify the convex polygons.

For regular polygons, as the number of sides increases, the polygon becomes more and more similar to a circle. The difference in shape of a polygon, produced by addition of an extra side, is negligibly small if the number of sides is large. Regular polygons with five or more sides are treated as circles. This introduces extra approximation. But it is necessary to curtail the complexity of the convex polygon classification problem. Triangle and quadrilaterals are treated as such.

1.5 Polygon Simplification :

The minor features need to be approximated out of the polygon to simplify it and thereby make it amenable for analysis.

Approximations are done as a prelude to any attempt at shape analysis. A long sequence of minor stretch operations, applied in different directions, may distort the shape in vastly different ways. A thorough analysis of the effect of such sequences would be quite complicated. It is not attempted in this work. Long sequences of minor stretch operations are approximated by short sequences of major stretch operations.

Minor type one stretch operations give rise to irregular polygons which are very similar to the regular polygons (ref. Fig. 1.5.1). In Fig. 1.5.1, polygon in (a) has been distorted to (b), by an operation near vertex V_6. Vertices V_1 and V_5 are pulled towards vertex V_6. In the process, V_2 and V_4 are also affected. V_1 and V_6 maintain their positions. The ACSILs of the skeleton are shifted from their positions and the angular symmetry is disturbed. It can be seen that the shape of the polygon is hardly affected. The resultants of such operations are neglected altogether in classification. Minor type one stretch operations, when coupled with some major stretch operations, or just application of some major stretch operations may give rise to rounded corners (ref. Fig. 1.5.2). In Fig. 1.5.2, two major type one stretch operations have produced two beaks. These two operations have generated a rounded corner $V_1 - V_2 - V_3$.

Minor type two stretch operations produce small elongations. Again these stretch operations hardly affect the shape of the polygon (ref. Fig. 1.5.3). Extremely strong type two operations are illustrated in Fig. 1.5.4. It can be easily seen that they generate rounded corners. A sequence of minor type two operations

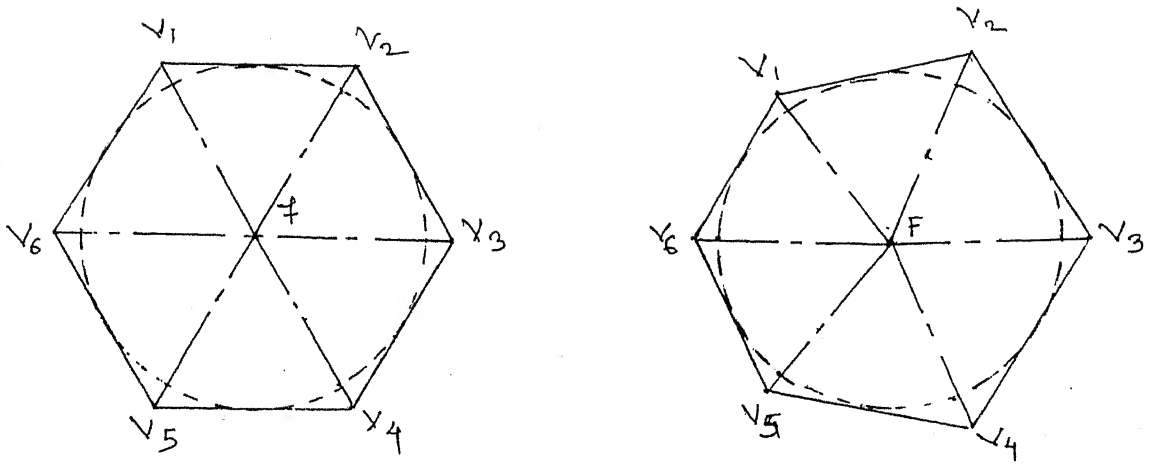

Fig. 1.5.1 Minor type 1 Stretch Operation

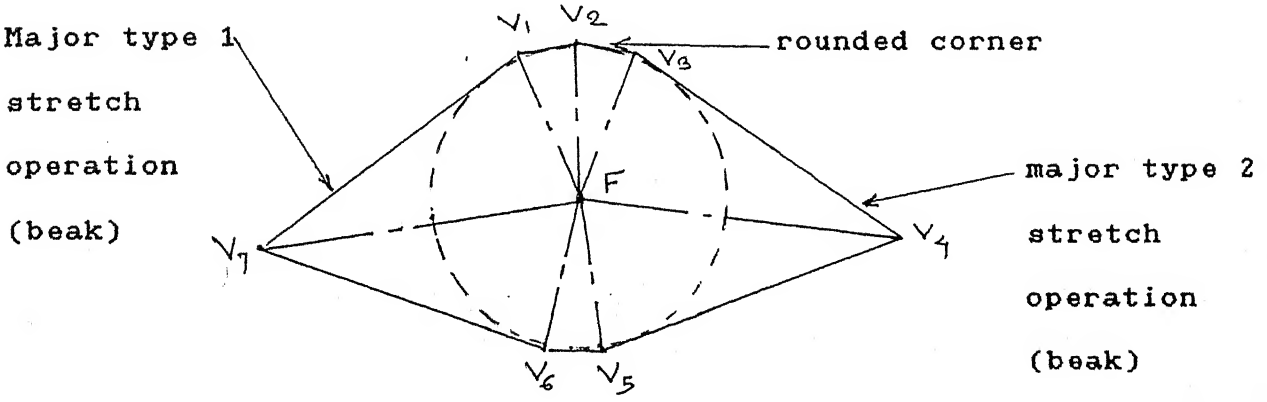

Fig. 1.5.2 Two Major Type 1 Stretch Operations.

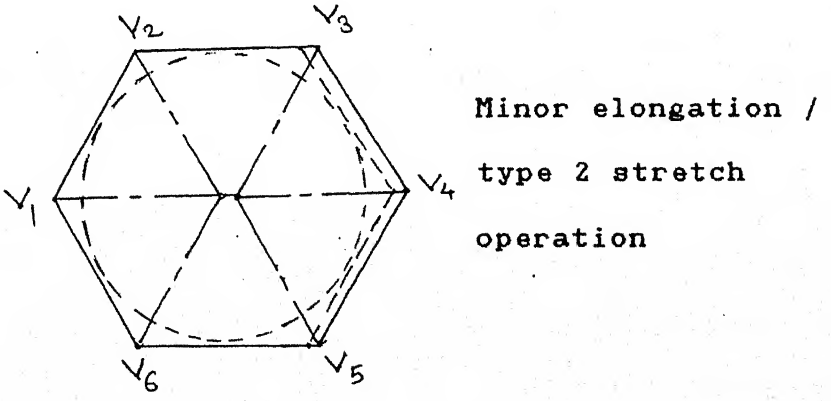

Fig. 1.5.3 Minor Type 2 Stretch Operation

(ref. Fig. 1.5.5) generates a boundary pattern which closely resembles a curved boundary.

2. Skeletal Basis for Description Process :

The skeleton and skeletal properties provide a very good basis for detection and replacement of features to be approximated. Identification of shape features and their interrelations is facilitated by skeletal characteristics.

2.1 Description of Convex Polygon Skeleton :

The skeleton of a convex polygon is devoid of any concave skeletal interaction. It is composed of only convex skeletal interaction lines, i.e. CSIL as they are referred to in the chapter 2. The skeleton is again a geometrical line diagram. It is a geometrical tree. The nodes of the tree are the forks, and the end points of the adjacent edge convex skeletal interaction lines i.e., the ACSILs. The edges are the CSILs. The non-adjacent convex skeletal interaction lines i.e. the NACSILs are the edges between the forks and the ACSILs are the edges between forks and the ACSIL endpoints.

2.2 Observations on the Properties of Convex Polygon Skeleton :

The skeletal circle radius(r) as a function of the distance(s) along the skeletal lines has some important properties.

2.2.1 The Unimodality of r(s) :

Along a path in the tree from a leaf node to another leaf node, r(s) is strictly unimodal; it is increasing - decreasing. It is not concave upwards. In Fig. 2.2.1, as the skeletal path from V_1 to V_5 is traversed, the r increases from zero till it reaches its maximum at fork f_1 and starts decreasing again till it reaches zero again at V_5.

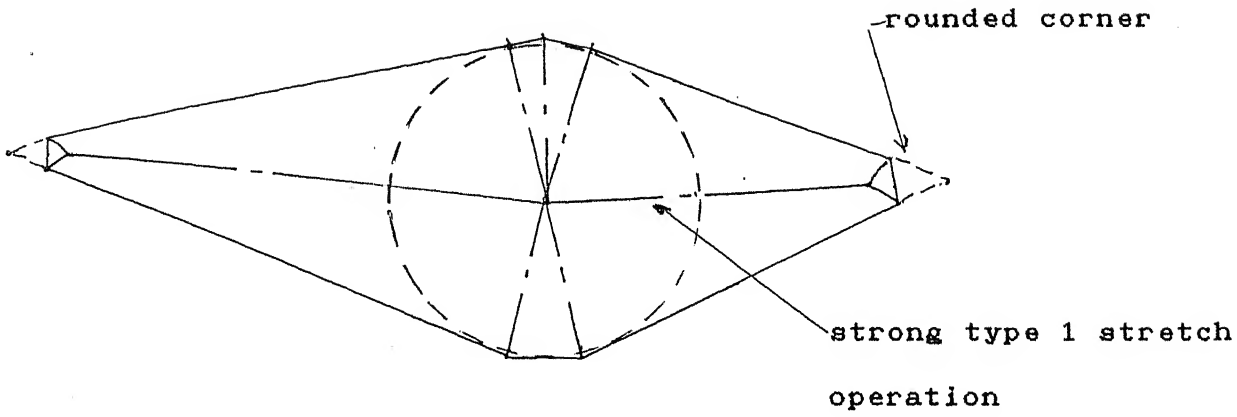

Fig. 1.5.4 Extremely Strong Type 2 Stretch Operation

Curved boundary

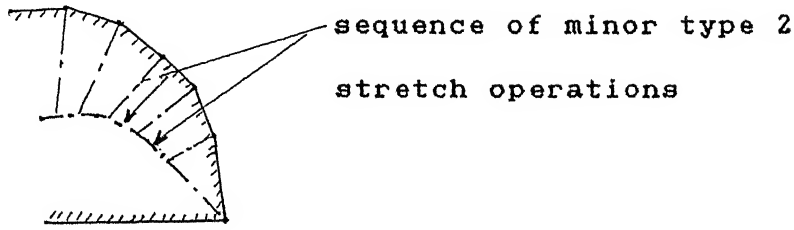

Fig. 1.5.5 A Sequence of Type 2 Stretch Operations

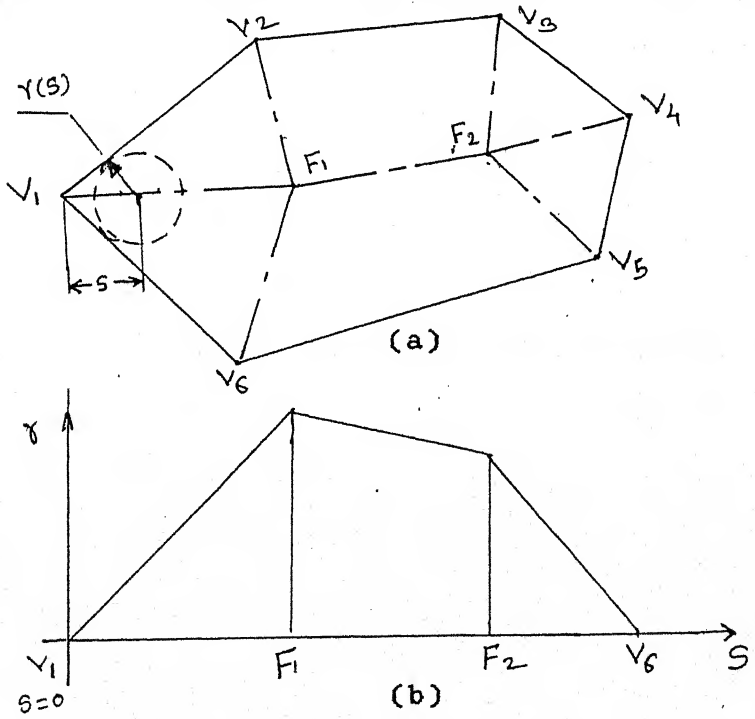

Fig. 2.2.1 Unimodality of r(s)

Along any other path, r(s) is either monotone increasing, monotone decreasing, or unimodal and convex upwards.

2.2.2 The Convexity of r(s) :

The dr/ds is also unimodal, convex upwards along a path from a leaf node to leaf node. The area underneath the r(s) distribution is convex. In Fig. 2.2.2, any edges of the convex polygon, lying to the right of the V_2 -V_4 line, must necessarily lie within the shaded region. The angles between the edges must be larger than the angle ϕ between e_{12} and e_{34}. As the dr/ds is given by

$$\frac{dr}{ds} = \left(\frac{1}{ds/dr} \right) = \left(\frac{1}{\text{quench velocity}} \right) = \sin(\theta/2) \; ;$$

(ref. section 4.1, chapter 2, for quench velocity formulation.)

as the path is traversed to the right of C_1, i.e. s increases, the magnitude of dr/ds will increase as $(\theta/2) > (\phi/2)$. But as r is decreasing with increase in s, $dr/ds < 0$; and hence as s increases dr/ds decreases. This is the situation to the right of the location of the maximum r. To the left of maximum r, the situation is reversed, and the dr/ds increases with increase in s. Thus the dr/ds is also unimodal. This implies that the area under the r(s) curve is convex.

Along any other path, dr/ds is either monotone increasing, monotone decreasing, or unimodal, convex upwards.

2.2.3 Continuity of NACSILs :

The NACSILs in the skeletal tree are continuous. They are not fragmented into physically disparate units. If only the NACSILs are considered neglecting the ACSILs, then the resulting line diagram is also a tree. In Fig. 2.2.3, it can be seen that all the ACSILs start from a fork and terminate in a vertex, or a leaf node

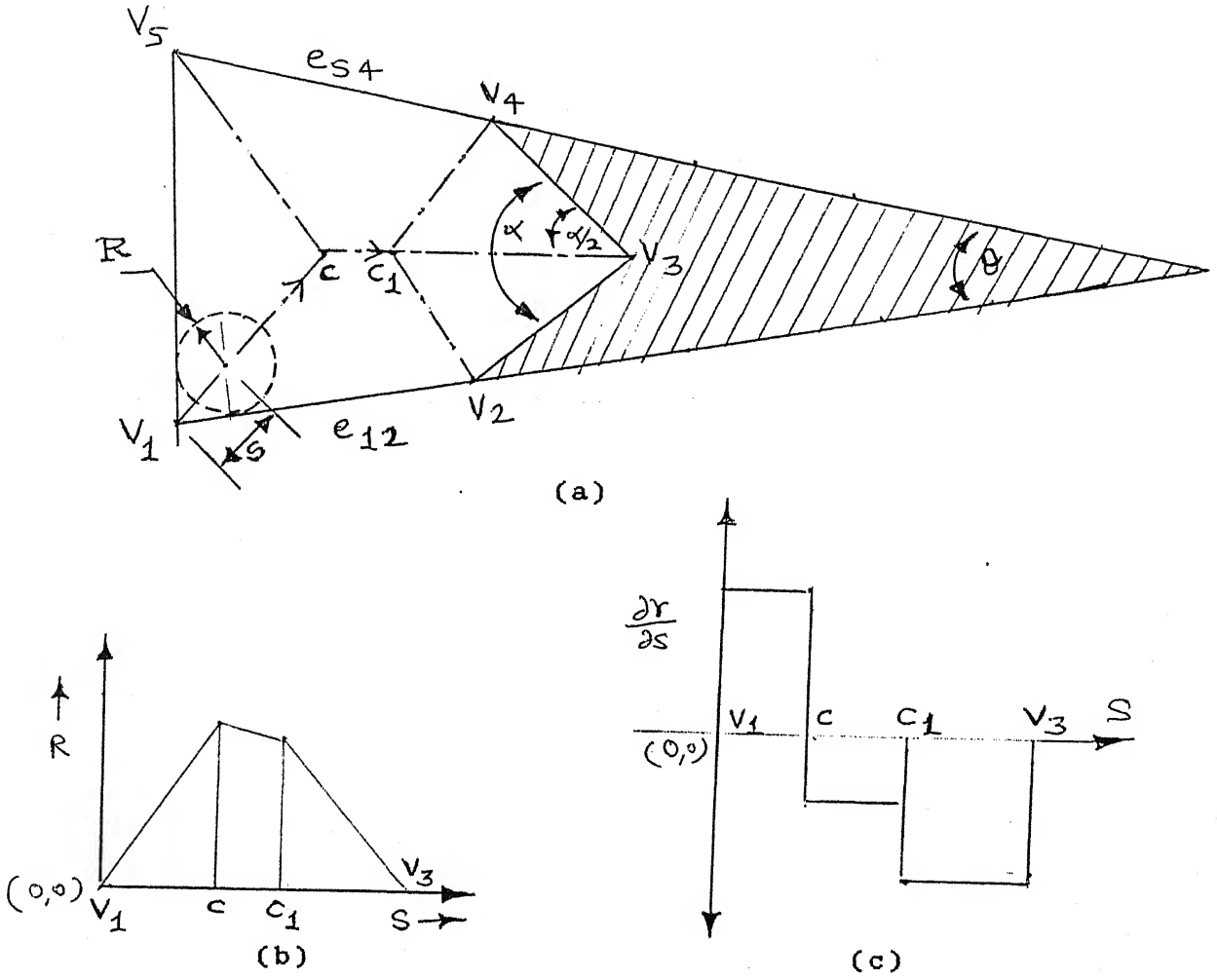

Fig. 2.2.2 Convexity of r(s)

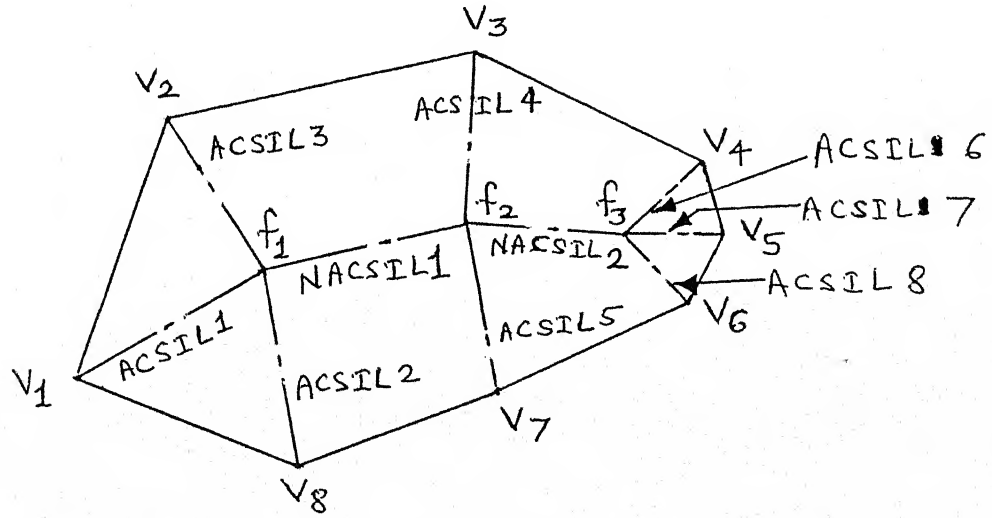

Fig. 2.2.3 Continuity of NACSILs

of the skeletal tree. An NACSIL could not exist at the vertex end of an ACSIL. It can occur only at the fork end, where it would be connected to the other NACSILs at the fork.

2.3 Fork - NACSIL Tree :

If the ACSILs converging at a fork and the fork are considered to be one unit and the NACSILs are considered to be the different entities, the effects of the two types of stretch operations can be discerned separately. The result is again a tree, with the units of fork with its ACSILs as the nodes and the NACSILs as the edges. This proposition is based on observation given in section 2.2.3. This tree has some important properties useful for convex polygon classification. The skeletal tree forks with their ACSILs, are the nodes of this tree. They are henceforth referred to as the forks in this chapter. The forks of the skeletal tree and these forks are almost the same; the only difference being the ACSILs. Hence the same terminology is retained, rather than introducing new terms.

The tree is referred to as the fork - NACSIL tree. A fork - NACSIL tree is illustrated in Fig. 2.3.1. Fig. 2.3.1(a) shows the skeletal tree of a convex polygon. The fork - NACSIL tree of the polygon is given in Fig. 2.3.1(b). The ACSILs of fork f1 in part (a) of the figure, i.e. ACSILs $f_1 - v_1$, $f_1 - v_2$ etc., are merged into fork f_1 in part (b).

2.4 Properties of the Fork - NACSIL Tree :

In the fork - NACSIL tree, the fork size and proximity definitions remains the same as in the skeletal tree. The intensity of the fork is defined as the sum of intensities of the ACSILs at the fork.

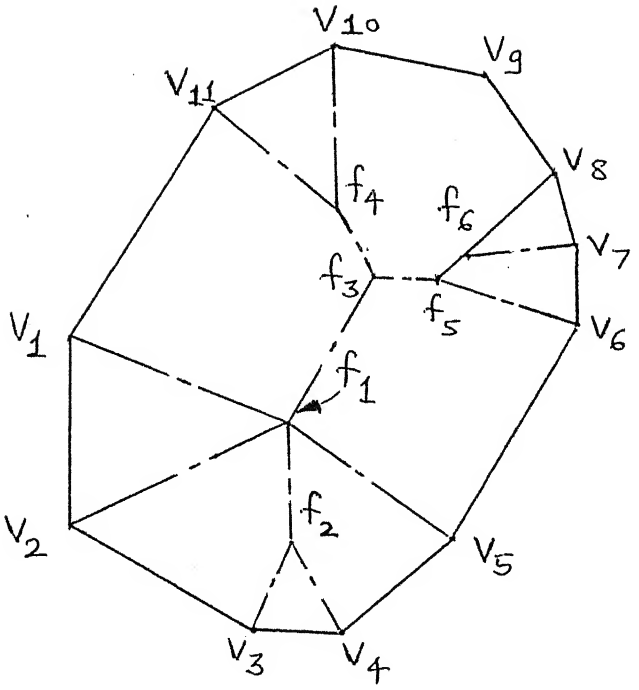

(a) Skeletal tree of polygon

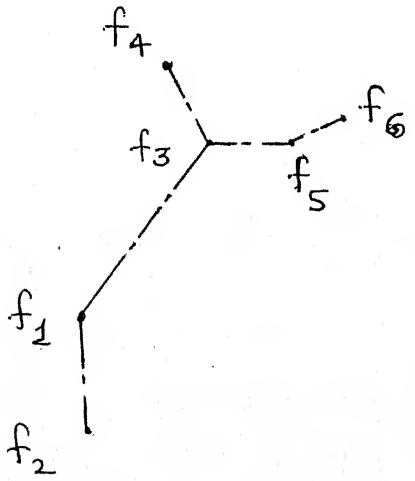

(b) Fork - NACSIL tree of the polygon in (a)

Fig. 2.3.1 Skeleton and Fork - NACSIL Tree

A path in the fork - NACSIL constitutes a string of forks. A string of forks or, a fork string, may be geometrically long or geometrically short, depending on the physical distances in the string. The physical distances are the lengths of the NACSILs. A fork string may be called long or short depending on the number of forks in it. In a dense fork string, the neighbouring forks are proximal to each other. In a sparse fork string neighbouring forks have a low proximality i.e. they are far flung apart.

2.5 Symbols Used in Representation of Fork - NACSIL Tree :

The following set of symbols is used to represent the fork - NACSIL tree and its various subtrees.

1) A locally large fork is represented by LL. 2) A globally large fork is represented by GL. 3) A locally small fork is represented by LS. 4) A globally small fork is represented by GS. 5) Proximity between a pair of forks is denoted by a short line joining the two forks. Distant pair is denoted by a long line joining the two forks.

For example,

LL------LS represents a distant or not proximal pair of locally large forks.

GL--GL represents a proximal pair of globally large forks.

The same set of symbols may be used with the skeletal tree without any conflicts as the two trees are essentially the same; they are different representations of the same tree.

2.6 Observations on the Properties of Fork - NACSIL Tree :

The observations on the fork - NACSIL tree are equally valid on the skeletal tree. All the observations essentially follow from

the observations in section 2.2. The observations form the basis of the approximation and classification process. Detection of situations for approximation, the actual approximations and the ordering of the approximation process is done on the basis of observations from sections 2.6.1 to 2.6.10. The classification and description is based on the rest of the observations.

The observations are in the form of logic propositional rules, i.e.

if 'A' then 'B'

where A is a feature of the fork - NACSIL tree or skeletal tree, and B is a shape or boundary feature. The tree features are qualitative fuzzy predicates such as 'a string of locally large forks'. As a result, the feature detected are not mutually exclusive. The same tree feature may satisfy more than one qualitative predicates with different confidence values.

The approximation and classification process is by and large a fuzzy spawning process. In case of border line cases of the qualitative predicate values, all the alternatives ensuing thereof are followed up and expanded. For example, for a fork pair which is ambiguous predicate values of say, around 0.5 and 0.6 for all of LL--LL and LL------LL and LL------LS, all the three solutions will be followed. Some of these solutions may in later analysis give very low confidence values for all decisions thereof. These will be discarded; but the rest will be followed. In the final description, all the descriptions of not very low confidence values, spawned by these three predicates will be present. This strategy is in conformance with the classification scheme expounded in section 1.3. It ensures that the approximations will

not be too damaging to the description.

The features of the fork - NACSIL tree and the skeleton tree analysed in the following observations completely cover all the possible ranges of the features of the tree. The fuzzy approach to the feature categories ensures completeness.

2.6.1 Location of Small Forks :

Small forks are always located at the extremes of the strings. This observation follows directly from sections 2.2.1 and 2.2.2. For a string from a leaf node to leaf node, the larger forks are in the middle of the string. The large forks dominate the shape of the polygon. The small forks can be approximated out by a pair of polygon edges and the ACSIL between them.

It can be seen from Fig. 2.6.1, that the small forks must lie at the extremes, else the convexity of the polygon will be violated. In the figure, dur to convexity of r(s), $r_1 < r_2$, and

$r_2 > r_3 > r_4$.

2.6.2 Relation between Size, Proximity and Angle between Interacting Edges :

In the Fig. 2.6.2, edges e_{12} between vertices V_1 ad V_2, and e_{34} between vertices V_3 and V_4, give rise to a fork f_1 at point O. Their interaction continues till point O' where the edge e_{23} between vertices V_2 and V_3 stops their interaction, giving rise to another fork f_2 at O'. The radii of the skeletal circles at forks f_1 and f_2 are R and r respectively. The distance between the forks is d. In the figure,

$l(OQ) = R / \sin(\phi)$;

$l(PQ) = r / \sin(\phi)$;

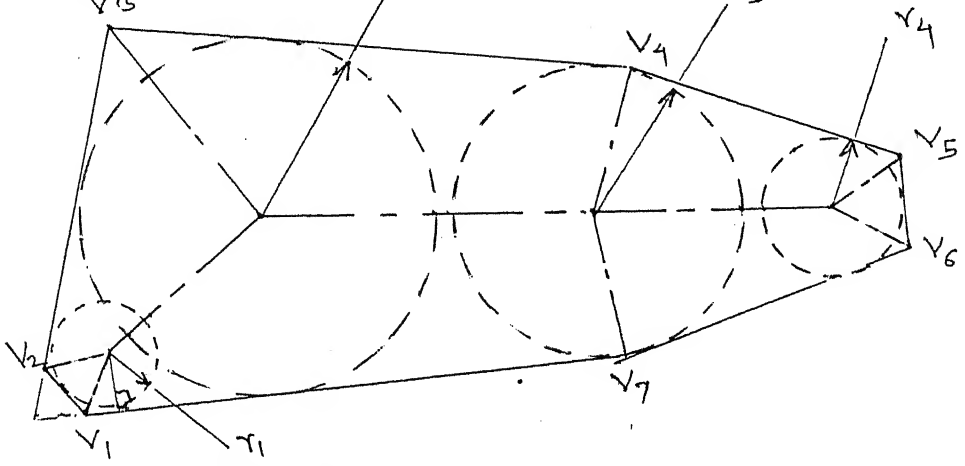

FIg. 2.6.1 Location of Small Forks

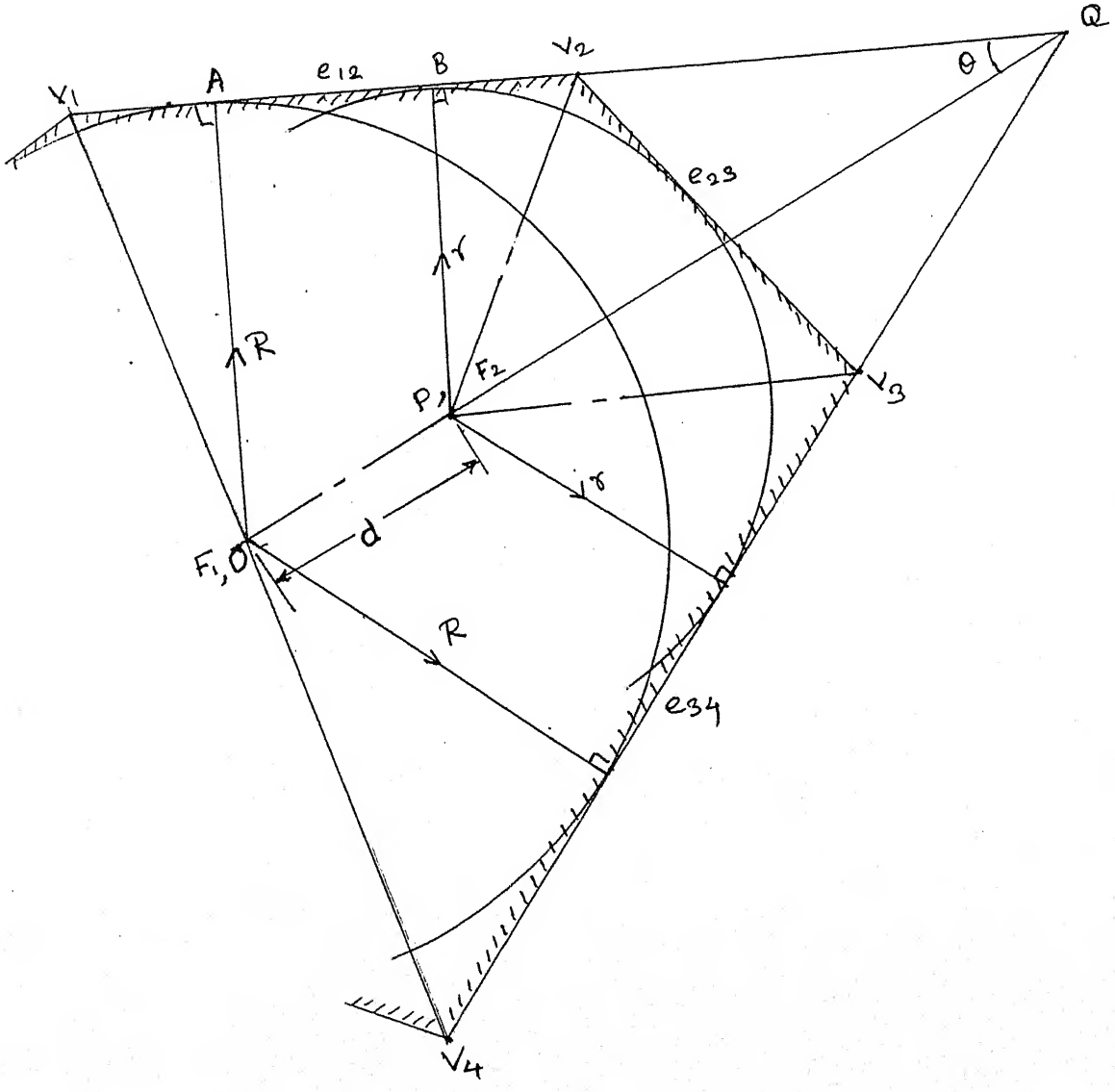

Fig. 2.6.2 Relation between Size, Proximity and angle in a Fork Pair

By similarity of the triangles QOA and QPB,

$$\frac{(R \;/\; \sin(\phi)) - d}{(R \;/\; \sin(\phi))} = \frac{r}{R} \;;$$

i.e.

$$R - d * \sin(\phi) = r \;;$$

Proximity ratio P_r is defined as $P_r = d / R$, $0 < P_r < \text{infinity}$;
Largeness ratio L_r is defined as $L_r = r / R$, $0 < L_r <= 1$;
As ϕ is half the edge angle, $0 < \phi < 90$;

$$P_r * \sin(\phi) + L_r = 1. \qquad \text{(----------2.6.2.)}$$

The proximity ratio and the largeness ratio are in conformance with the definitions of proximity and size given in the chapter 2. Hence the relation 2.6.2 can be used as an indicative of the relations between size, proximity and quench velocity.

2.6.3 Uneven Size Proximal Fork pairs :

In a pair of forks, for a locally large fork to be proximal to a locally small fork, the angle ϕ must be quite large. For a locally large and small pair of forks, L_r is low. For a low L_r, $P_r * \sin(\phi)$ must be high, from relation 2.6.2. For a proximal pair, P_r should be low. Note that P_r lies between 0 and infinity. Low P_r does not mean that it should be low compared to one. A low P_r may be close to one (ref. section 7.2, definitions of the fuzzy qualitative predicates). ϕ should also be quite close to one, to satisfy the relation 2.6.2. Hence the angle ϕ should be comparable to 90. Such a situation is illustrated in Fig. 2.6.3. It may be treated as a rounded corner. The edges e_1 and e_2 may be extended till they meet, to approximate and simplify the polygon, as the area approximations involved will be quite small (ref. section 7,

for the exact area approximations).

2.6.4 Uneven Size Distant Fork Pairs :

In a LL------LS fork pair, the small fork can be neglected without any appreciable loss of accuracy.

The locally small forks indicate rounded corners and they can be approximated out by a pair of edges and an ACSIL between the edges. In the Fig. 2.6.4, the large fork f_1 is a major feature of the shape. The small fork f_2 lies very close to the tip, and is the result of a cut off tip.

2.6.5 Proximal Fork Pairs :

A proximal fork pair is the result of a minor type two stretch operation. It must necessarily be LL--LL. The proposition in section 2.6.3 takes care of the LL--LS fork pair. The two proximal forks can be treated as one fork without appreciable loss of accuracy. The two forks can be merged into one fork. All the skeletal lines are preserved, but they, instead of emanating from the two original fork points, emanate from one fork point lying somewhere halfway between them. The basic angle properties of the skeletal lines such as 'skeletal lines bisect angle between the edges' and so on, remain approximately true.

In Fig. 2.6.5, the two forks f_1 and f_2 are large and are very close to each other. The overall shape of the profile is not disturbed much by the minor type two stretch operation. It resembles a regular hexagon.

2.6.6 Global Size of Forks :

Globally small forks are indicators of very strong type two stretch operations. The stretch operation is so extreme that the edges stretched out become very small in comparison with the rest

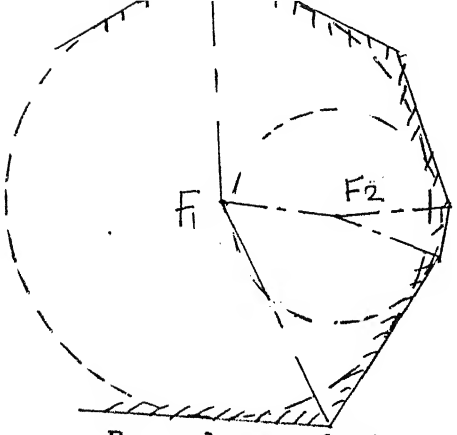

F_1 = large fork, F_2 = small fork

FIg. 2.6.3 Uneven SIze Proximal Forks

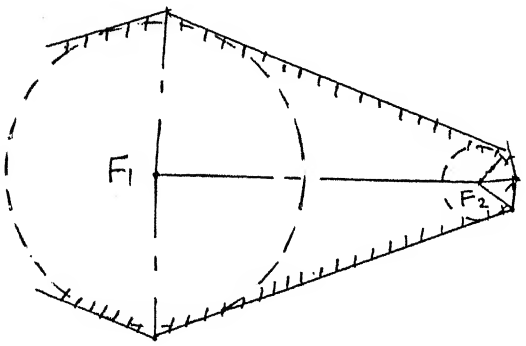

F_1 = large fork, F_2 = small fork

Fig. 2.6.4 Uneven Size Distant Forks

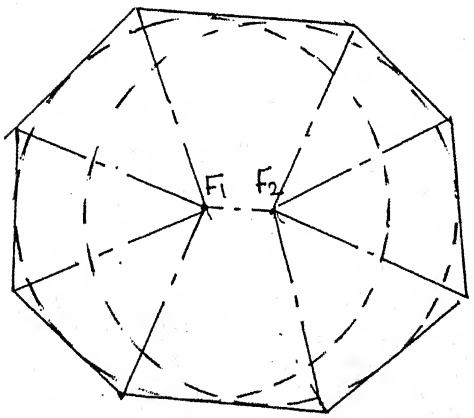

F_1 and F_2 are comparable.

Fig. 2.6.5 Proximal Fork Pair

of the polygon. They represent rounded corners in the polygon and hence can be approximated as the rounded corners detected in the earlier observations. This observation is in line with the one given in the section 2.6.4.

2.6.7 Subtree of Forks :

It may be noted that the propositions outlined in sections 2.6.1 to 2.6.6 may be used to simplify fork pairs. As a result, only LL------LL fork pairs are left in the skeleton. Concatenation of these pairs may give rise to fork string or fork trees.

LL------LL pairs have large values of the proximity ratio(P_r) and largeness ratio(L_r). It can be inferred from relation 2.6.2 that ϕ should be quite small. The fuzzy qualitative predicates are so defined that the LL------LL pair exists only at ϕ below 50 (ref. section 2.7). The number of CSILs with low ϕ emanating from a fork is limited. It can be seen from Fig. 2.6.7.1 that the angles θ' must sum upto 360. Hence only three CSILs can maximally be present in a fork with ϕ of about 60. As LL------LL fork pairs can not exist at ϕ equal to 60, a subtree of large trees can not exist in skeleton.

A subtree of large forks can occur only if they are proximal. Subtrees of forks can be reduced to one fork by repeated application of proposition in section 2.6.5. A subtree of large forks, f_1, f_2, f_3, and f_4, is illustrated in Fig. 2.6.7.2.

A subtree of large forks can not have distant forks. Thus, if a compact subtree is taken care of by approximations, the NACSILs resulting from type two stretch operations will be in the form of a set of strings rather than forming an arbitrary tree. This argument is again similar to that in sections 2.6.4 and 2.6.6.

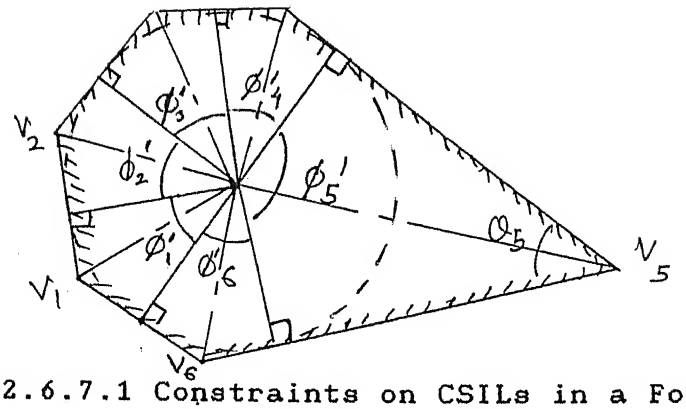

FIg. 2.6.7.1 Constraints on CSILs in a Fork

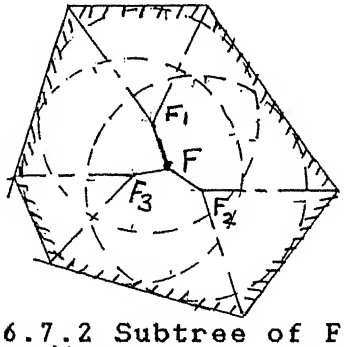

Fig. 2.6.7.2 Subtree of Forks

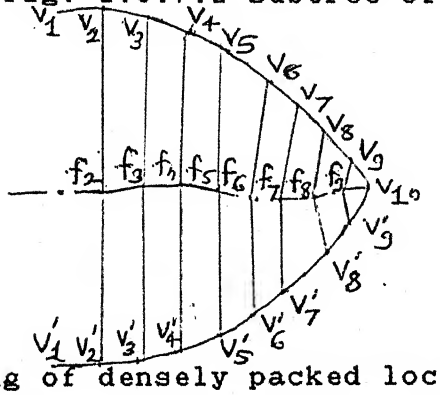

(a) String of densely packed locally large forks

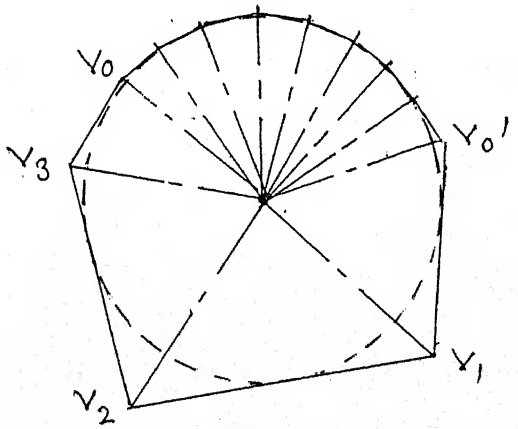

(b) Closely packed low intensity ACSILs

Fig. 2.6.8.1 Curved Boundary

2.6.8 Curved Boundary :

A numerically short dense string indicates the presence of a small curved boundary segment which can be treated as a rounded corner. The definition of the numerical shortness is that the string should have less than five forks. The rounded corner may be approximated by extension.

A numerically long dense string indicates the presence of a curved boundary. In Fig. 2.6.8.1(a), the curved boundary from vertex V_2 till vertex V_2' produces a skeletal interaction wherein a large number of locally large forks are densely packed in a small length of the skeleton. This is the result of a type two stretch operation on an approximately circular boundary.

The ACSILs of the forks are of very low intensity, as the angles between them are close to 180. A curved boundary on both the sides of the skeleton produces closely packed low intensity ACSILs, emanating from almost every fork, on both the sides. For a curve only on one side, such ACSILs are restricted only on the side of the curve. Both the cases are illustrated in Fig. 2.6.8.1. Replacement of a string will be complete when all the curves it generates are approximated.

A dense long string of large forks may be a part of larger substrings (ref. Fig. 2.6.8.2). The substring f_1-f_2 is part of strings V_1-V_3, V_1-V_4 and so on. In such a case, it is necessary to identify the curve limits on the boundary and the string which gives rise to the curve. We propose to identify the string and the curve by determining the minimum of the areas enclosed by the string and the curved boundary segment associated with it. In the Fig.2.6.8.2, the curve V_2-V_3 will be associated with the upper

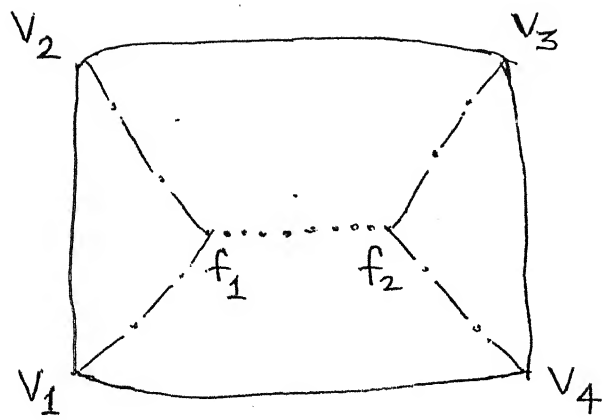

Fig. 2.6.8.2 A 'Rectangle' Formed by Curved Boundary

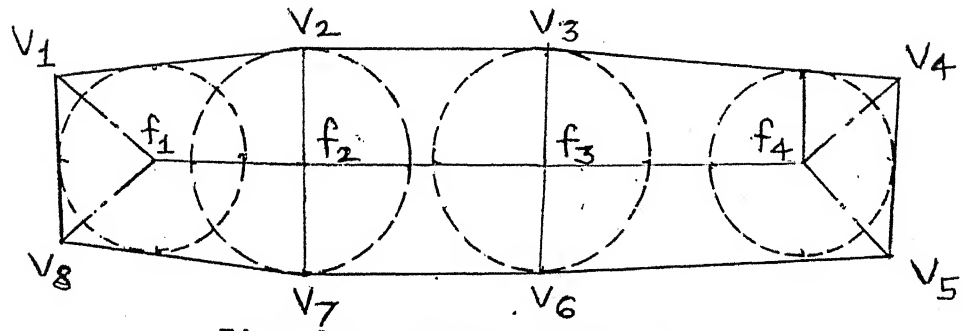

Fig. 2.6.9 Sparse Strings of Forks

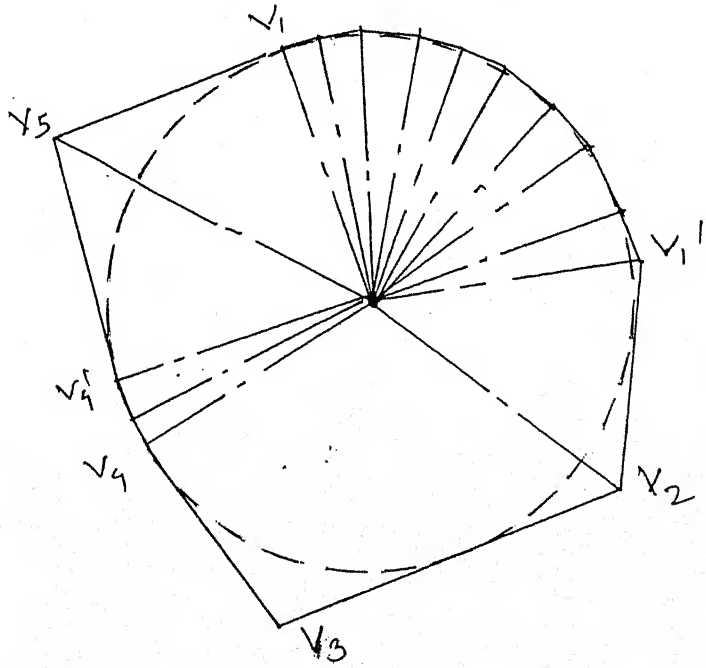

Fig. 2.6.11 Curved Boundary Segments in a Polygon.

Sparse strings interspersed with dense strings are reduced to only sparse string by proposition in section 2.6.8.

After all the approximations outlined in sections 2.6.1 to 2.6.8 are carried out, the dense strings, all the small forks and hence the small fork strings are deleted from the fork - NACSIL tree. The tree is composed of only sparse strings. Since the sparse strings can not be branched, more than one sparse strings can not exist in the tree. The fork - NACSIL tree is composed of only one sparse string.

2.6.10 Order of Application of Rules Formulated from Observations :

Repeated applications of the propositions stated in sections 2.6.5 and 2.6.6 to a dense string can produce quite erroneous results. Hence dense strings need to be detected and replaced before any other approximations are applied.

2.6.11 The ACSILs in a Fork :

A sequence of large number of very low intensity ACSILs within a fork represents a circular curve in the boundary.

If a circular curve is delimited on either sides by an ACSIL showing a sharp increase in intensity and the angle between the extremities of the curve is low, then it is a rounded corner. In Fig. 2.6.11, the boundary segment $V_1 - V_1'$ is a circular curve and $V_4 - V_4'$ is a rounded corner.

2.6.12 Separation of the Elongations from the Polygon :

Type two stretch operations preserve the angular relations between ACSILs and the polygon edges. Their effect is restricted to generation of additional forks and NACSILs joining the forks. The change in lengths of the polygon in these operations is a result

of these changes. It is not the fundamental distortion in shape; rather it is a secondary distortion.

The type one stretch operations basically distort the angular relations. The length changes can be treated as the results of the angular distortions. For a given fork radius, the angle specifications are sufficient to completely reproduce the profile. Hence the type one stretch operations can be treated as basically angular distortions.

A separation of elongations by merging all the forks together, preserves all the angular relations. Feature analysis for beak and bulge features can be carried out on the merged fork as well, as it could be on the unseparated tree. These two feature analyses would be exactly equivalent. The separation of elongations does not affect the feature analysis.

separation thus cleanly sifts two distinctly different phenomena. It helps in simplifying the analysis preceding the classification and description of convex polygons.

By means of separation, the tree and hence the polygon is is divided into a one fork polygon and the elongation line diagram. These two are explored and analysed separately. The subtrees of the fork - NACSIL tree, are merged into the single fork. They are thus taken care of.

The separation is illustrated by two examples (Figures 2.6.12.1 and 2.6.12.2). In Fig. 2.6.12.1, the original polygon and the skeleton are given in part (a). For simplicity, it does not contain small forks and dense strings. The fork - NACSIL tree is separated into unifork (b) and elongation (c). Fig. 2.6.12.2 runs

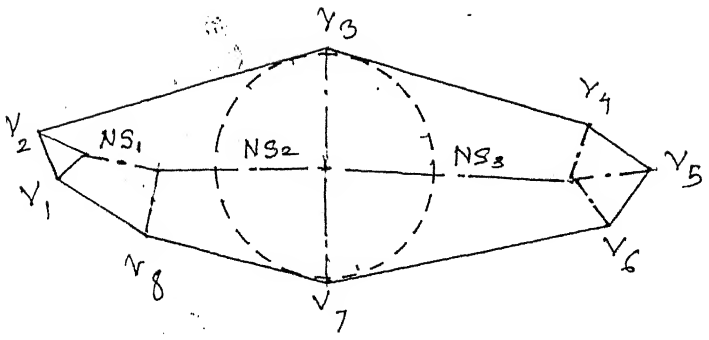

(a) Original polygon and its fork - NACSIL tree

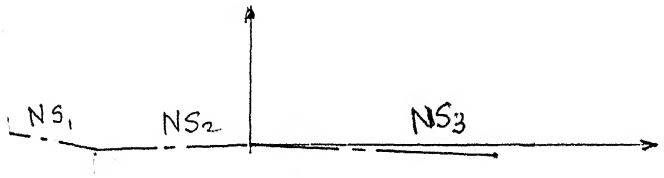

Elongation

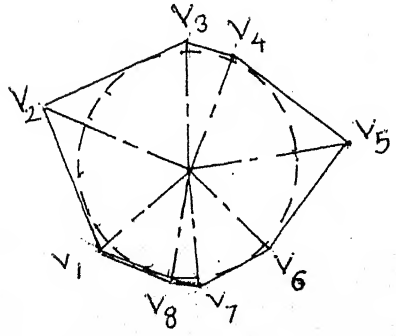

Unifork polygon and its skeleton

(b) Seperation

Fig. 2.6.12.1 Separation of Unifork and Elongation - I

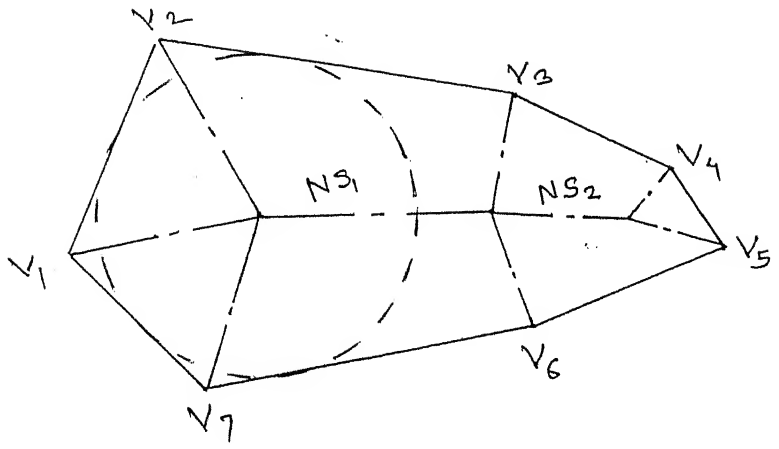

(a) Original polygon and its fork - NACSIL tree

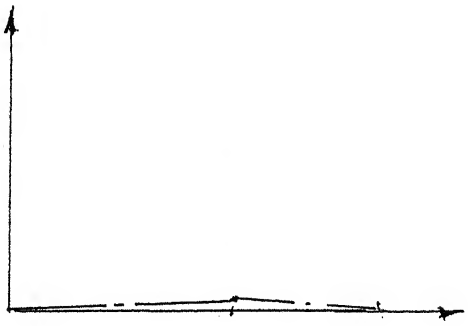

Elongation

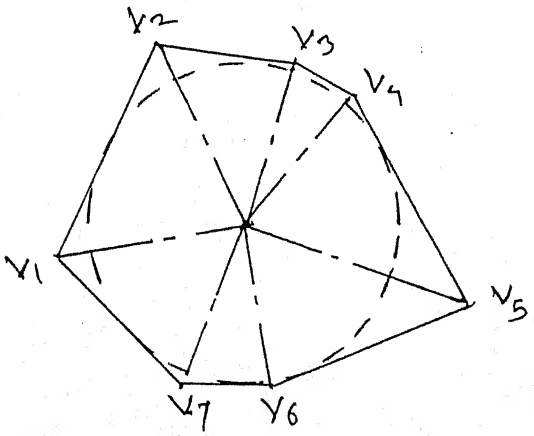

Unifork polygon and its skeleton

(b) Seperation

Fig. 2.6.12.2 Separation of Unifork and Elongation - II

along similar lines. Its elongation is along only one direction instead of two directions as in section 2.6.12.1.

2.6.13 Unifork :

The single fork into which the forks of the fork - NACSIL tree are merged, and the polygon it represents, is referred to as the unifork in this chapter. The exact meaning will be clear from the context of usage.

As observed above, all the angular relations of the polygon are preserved in the unifork. For a given radius of the unifork, the angles uniquely determine the edge locations. This implies that the beaks and bulge features of the original polygon are completely preserved in the unifork.

The unifork analysis and classification requires extensive work and is expounded in section 3.

2.6.14 Elongations :

As observed earlier, the elongations i.e. the NACSILs are continuous. The line diagram of elongations is a tree. Observations given in sections 2.6.1 through to 2.6.9 and their resulting approximations imply that the elongation tree will not be excessively branched. After the approximations only one sparse string is left in the fork - NACSIL tree. The approximation process being a fuzzy spawning process, fork subtrees will either give rise to rounded corner approximations or they will be merged together as one fork before separation. Due to this processing, the elongation tree is extremely simplified. It has only the major elongation corresponding to the sparse string, which by observation 2.6.9, can not be branched. Hence elongation tree is

only a string of NACSILs.

Elongations are illustrated in Fig. 2.6.12.1 and 2.6.12.2. At the center, corresponding to the unifork location, the elongation string has at the most two major branches as evident in the figures.

The angles between successive NACSILs in an elongation strings, are very large, almost close to 180. It can be observed in Fig.s 2.6.12.1 and 2.6.12.2. This observation relies on the propositions given above. The justification for the proposition is as follows.

In Fig. 2.6.14.1, edges e_1 and e_2 form an NACSIL P_1-O. It terminates at the skeletal circle centered at O, of radius R, in fork f_1. The next NACSIL in the elongation string O-P_2, starts from O. The edges e_3 and e_4 form the NACSIL O-P_2 . O-P_2 ends in fork f_2 at P_2. For the sake of simplicity, the fork f_2, its ACSILs and the edge between e_3 and e_4 are not shown. The edges e_3 and e_4 are extended till they meet at Q . e_1 is parallel to e_1. e_2' is the extension of e_1' till it meets the edge e_2 at Q . e_3 is the extension of e_1 till it meets e_4 at Q . P_1'-O is the NACSIL that would be produced by edges e_1' and e_4. If C is the angle between e_1 and e_2', C/2 is the angle between P_1'-O and P_1-O as the NACSILs are the angle bisectors of the edges. The rest of the angles are as shown in the figure. The relations between the angles which are shown, can be easily proved on the basis of elementary geometry.

As P_1-O is parallel to e_1',

$$A - C / 2 - D + E = 180;$$

in triangle Q_1-Q_2-A, $2 * \phi$ is the exterior angle, hence,

$$E = \phi - B;$$

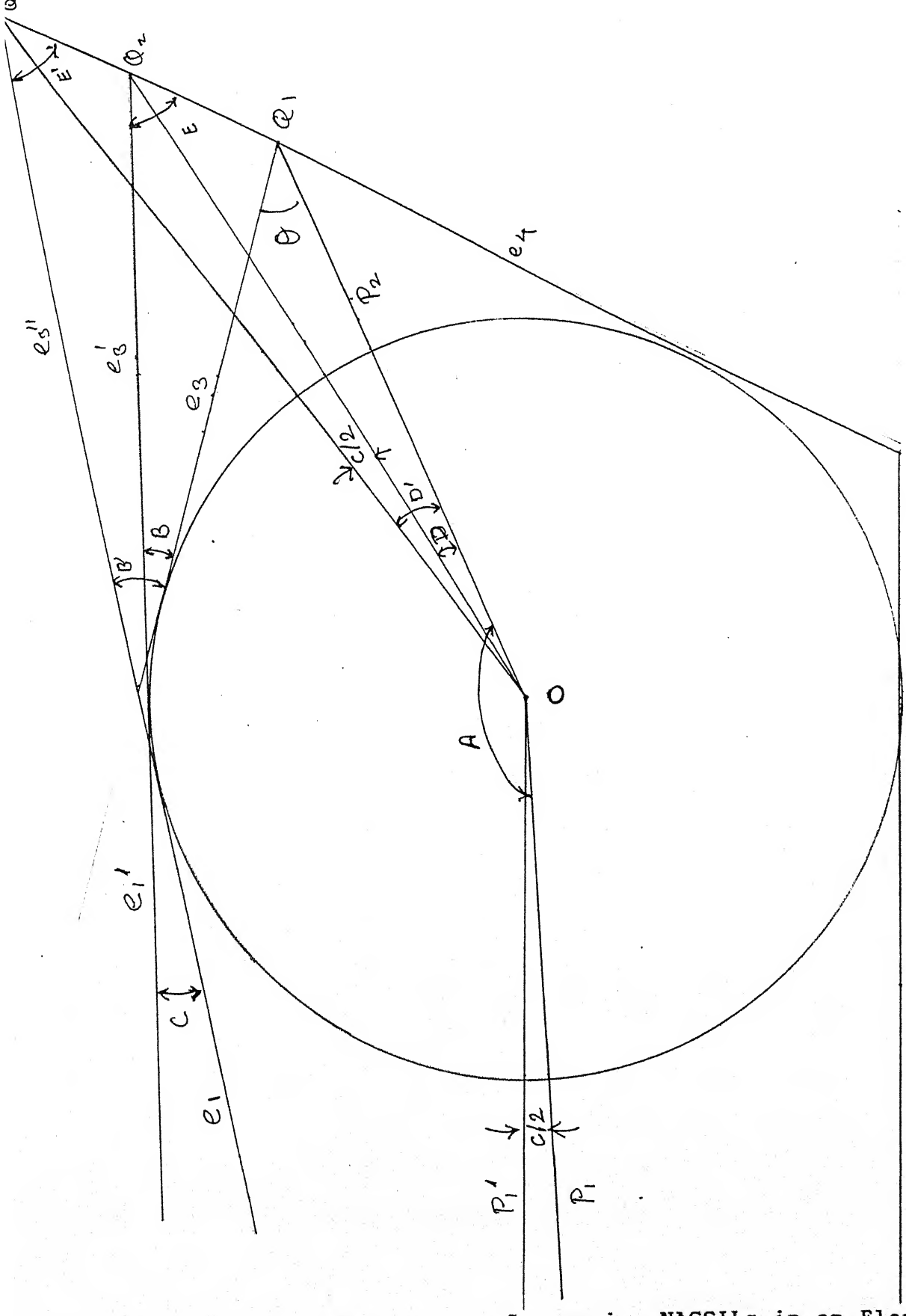

Fig. 2.6.14.1 Angle between Successive NACSILs in an Elongation

Substituting in the first relation,

$$A - C / 2 - D - B / 2 + \phi = 180.$$

For smallest A, C, D, B all should be zero, i.e.

$$A_{min} = 180 - \phi \qquad (----------2.6.14.1).$$

As A becomes smaller, ϕ increases. At A = 150, ϕ = 60. It will be proposed in section 2.7 that at around ϕ = 60, the proximity and size qualitative predicates will be so adjusted to treat the fork pair f_1 $-f_2$ as a large proximal pair, to be merged into one fork, or an uneven size pair, to be treated as rounded corner. Due to this treatment, the angle ϕ must be quite small to generate a LL------LL pair, which will lead to a sparse string. As observed above, only sparse strings lead to elongations. Hence, the angle ϕ must be quite smaller than 60, i.e. A must be larger than 150. Thus A must be quite close to 180.

At the terminal elongations also the same situation prevails as described above. If the angle A becomes too small, the fork pair is either merged or it is treated as rounded corner. Hence, even though the A may not be very close to 180, it can not be much smaller either.

Elongation classification is developed in section 4.

2.7 Exact Definitions of the Qualitative Predicates :

The propositions given above obviously require a definition of the qualitative predicates which will keep the approximations to a minimum for the description process to give good results. The definitions should be such that the approximations are kept to a minimum even in the worst case. The critical predicates are exactly defined in this section. The exact definitions of the remaining predicates are not so critical and are largely self-

evident. they should be refined by experimentation on a large number of different shapes.

The worst case for the propositions is that of an almost regular hexagon with three elongations on three alternate edges. This comes closest to a subtree of large and distant forks. It is illustrated in the Fig. 2.6.7.2.

A general elongation is illustrated in Fig. 2.7.1. $O\text{-}V_1\text{-}V_2'\text{-}V_3'\text{-}V_4$ is the elongation of a polygon, corresponding to the pair of forks f_1 and f_2 at O and O' respectively. $V_2\text{-}V_3$ is an edge the polygon without an elongation. In the figure,

$l(OQ) = h$ = height of triangle $P\text{-}V_2'\text{-}V_3'$;

$l(OO') = d$ = distance between forks f_1 and f_2;

$l(OV_1) = R$ = radius of the skeletal circle at fork f_1;

$l(O'Q) = r$ = radius of the skeletal circle at fork f_2;

From triangles $P\text{-}Q\text{-}V_2'$ and $Q\text{-}V_2'\text{-}O'$,

$r = h \tan(\phi) \tan(45 + \phi / 2)$;

$l(OP) = R / \sin(\phi)$; $l(V_1P) = R / \tan(\phi)$;

Area of $O\text{-}V_1\text{-}P\text{-}V_4 = A = R^{**} 2 / \tan(\phi)$;

Area of triangle $P\text{-}V_2'\text{-}V_3' = A' = h^{**} 2 * \tan(\phi)$.

Let $A = k * A'$, $k > 1$, where k is the approximation area ratio.

Hence, $h = (1 / \text{sqrt}(k)) * R / \tan(\phi)$;

and $r = (1 / \text{sqrt}(k)) * R * \tan(45 + \phi / 2)$.

Largeness ratio $L_r = (1 / \text{sqrt}(k)) * \tan(45 + \phi / 2)$;

(----------2.7.1)

and proximity ratio $P_r = (1 / \sin(\phi) - 1 / \text{sqrt}(k) \tan(\phi))$.

(----------2.7.2)

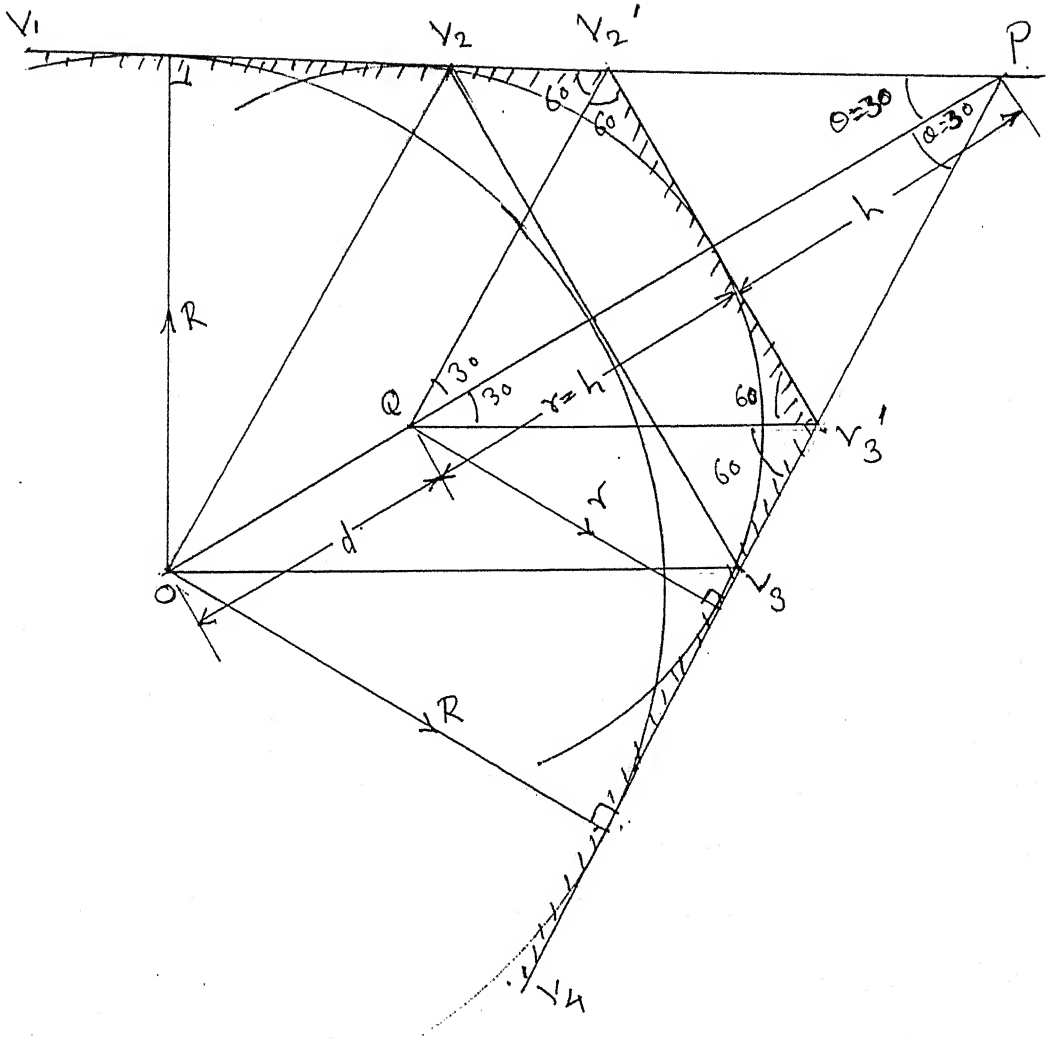

Fig. 2.7.1 Size and Proximity in a Fork Pair.

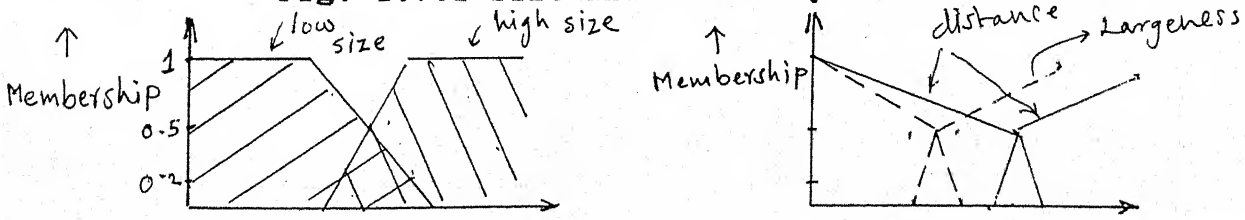

(a) Size Grade Membership for largeness and distance (b) Relation between Largeness and distance "sizes".

Fig. 2.7.2 Largeness and Distance of Forks, Fuzzy Distributions

For the polygon in Fig. 2.6.7.2, which is closest to a subtree of distant large forks, ϕ = 30. We propose that the approximation area ratio k = 4 is a sufficiently close approximation in this case. For the elongation V_1-V_2'-V_3'-V_4 the position of edge V_2'-V_3' about midway between an extreme elongation and a minor elongation. It gives a critical value for L_r for the transition between 'largeness' and 'smallness' of forks.

The critical largeness ratio L_{rc} = sqrt(3) / 2;

and the corresponding proximity ratio P_r = 2 * (1 - sqrt(3) / 2).

At L_{rc}, the smallness and largeness should be at least 0.5 to ensure a good fuzzy spawning. The proximity size quality distributions is such that the LL------LL situation is ruled out at ϕ = 30. The desired relation between the size quality distributions for L_r and P_r against length along NACSIL OO', for ϕ = 30, are shown in Fig. 2.7.2(a). It can be seen that this relation between L_r and P_r size quality distributions rule out LL------LL at ϕ = 30. Thus, a subtree of large distant forks can not exist in the skeleton.

The exact size quality distributions of L_r and P_r are given in Fig. 2.7.2 (b) and (c). These distributions should be tested for a large number of situations for fine tuning and refinements.

3. Unifork Classification :

A feature analysis approach is adopted for Unifork classification. The features are the interior edge angles of the polygon. The angles, in conjunction with the radius of the unifork, completely represent the unifork polygon. Hence a unifork description must

give the shape classification based the angles and the size in the form of the radius. The size may also be given in some other parameters such as the lengths of beaks and combinations thereof. As stated earlier, the classification is based on combinations of the ranges into which each feature is divided. The feature range division is approximate and not exclusively exact.

It may be noted that the classification based on the feature analysis is a fuzzy spawning process.

3.1 Effect of Number of Sides in Classification :

The unifork polygons with large number of sides are very similar in shape to circles. When the number of sides is small, the deviation from circular shape is too large. We propose to analyse triangles and quadrilaterals apart from the polygons with circular shape. Pentagons and hexagons are border line cases. A detailed exploratory spanning of shape space and concomitant analysis required for pentagons and hexagons is complicated. It is not attempted in the present work. They are treated as circular polygons instead.

The number of sides is decided on the basis of the number of 'not_low' intensity ACSILs in the unifork. The low intensity ACSILs produce very minor and gentle projections in the polygon. In Fig. 3.1.1, the low intensity ACSIL $O\text{-}V_2$ produces a gentle projections in what otherwise would be a triangle. It is isolated from other ACSILs and hence has not been approximated by applying rules developed in section 2.6.11.

The decision of the number of sides is a fuzzy spawning process. In ambiguous cases, where the ACSIL intensity is not low and not

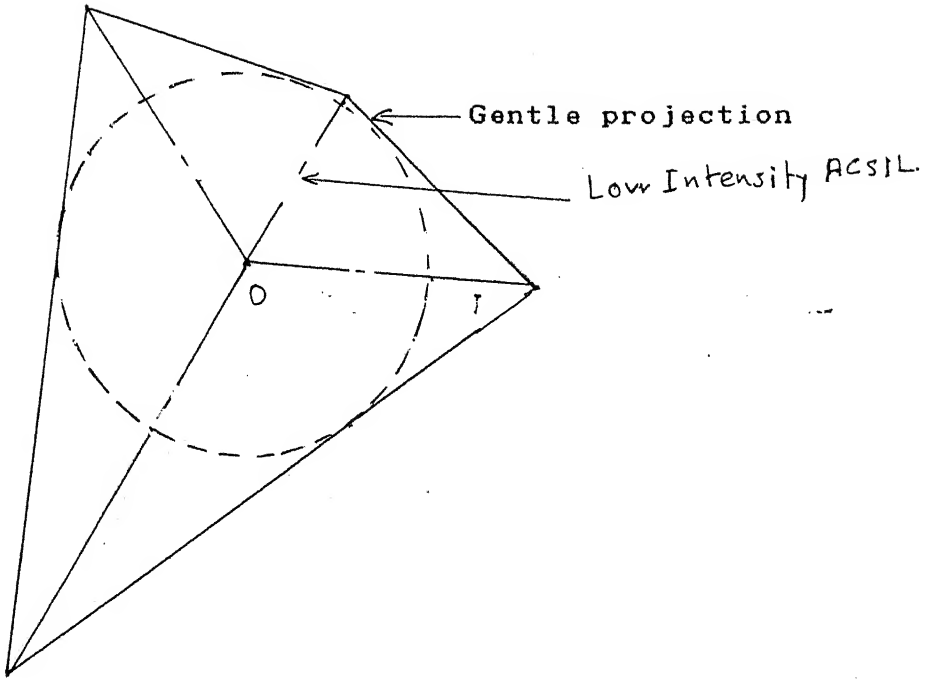

Fig. 3.1.1 A Gentle Projection due to a Low Intensity ACSIL.

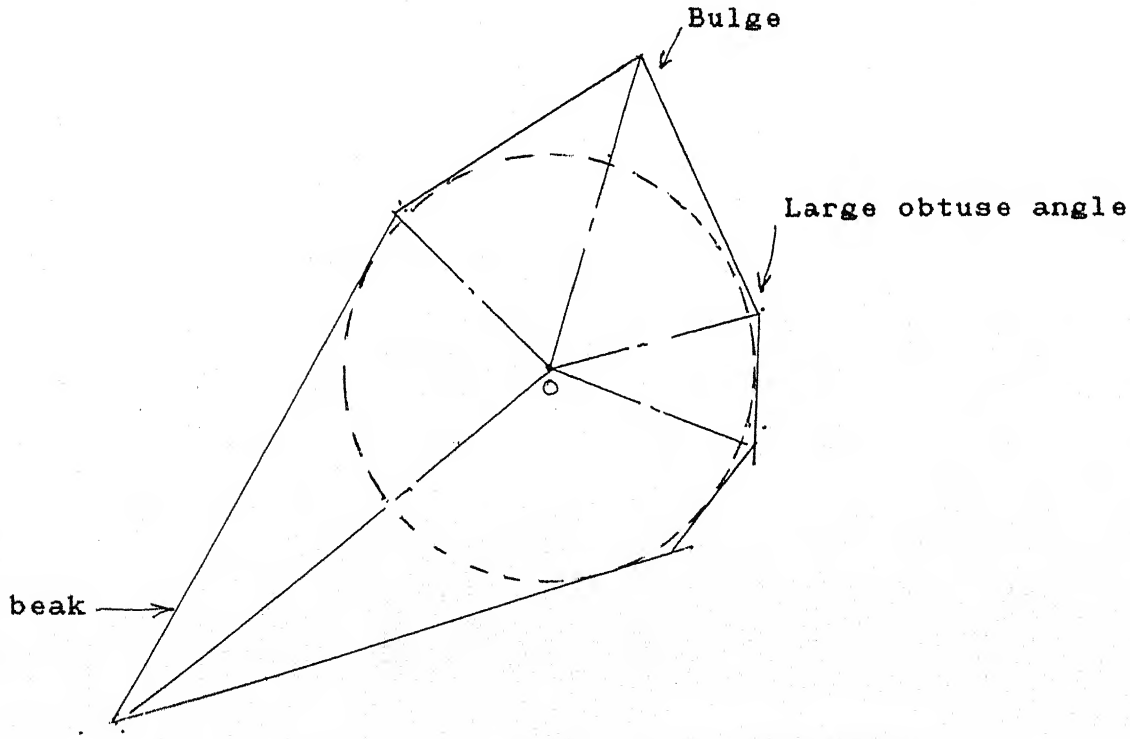

Fig. 3.2.1 Angle Features of Unifork

'not_low', it generates two decision trees, one with the ACSIL being treated as a low intensity, and the other with the ACSIL being treated as a 'not_low' intensity ACSIL.

3.2 The Shape Features :

Shape features are the distinctive angles which dominate the shape of polygon. Angles are directly related to the quench velocity (ref. section 2.2, chapter 2). The angle features can be detected by the quench velocities of the ACSILs of the unifork.

The small angles in the unifork give rise to sharp projections, the 'beaks'(ref. Fig. 3.2.1). The large obtuse angles approximate the circular curve. They do not affect the shape of the polygon. The middle level angles produce projections not as sharp as the beaks. They are called the 'bulges'. They are detected by the qualitative predicates 'Small_angles' and 'Middle_angles'. The ranges of the angles are defined as fuzzy ranges :

beak : $0 < \phi < 60$; bulge : $60 < \phi < 100$;

where ϕ is the interior edge angle.

The feature identification is a fuzzy spawning process.

3.3 Properties of Convex Polygon :

1) The sum of angles of a convex polygon with 'n' sides = 180 (n - 2).

2) The sum of any three angles of a convex polygon is greater than or equal to 180. If the sum is equal to 180, the polygon is a triangle.

The proofs of the above propositions are trivial and hence omitted. These propositions have been used extensively, explicitly as well as implicitly, in the classification.

3.4 Classification of Triangle :

Triangle classification is based only on beaks. Upto three beaks may be present in a triangle. Beaks are further subdivided into three ranges :

Prominent beaks (PB) : $0 < \phi < 30$;

Middle level beaks (MB) : $30 < \phi < 50$;

Incipient beaks (IB) : $50 < \phi < 60$;

where ϕ is the interior edge angle.

The combinatorial classes are :

1) One Prominent beak (ref. Fig. 3.4.1(a)).

2) One Middle beak (ref. Fig. 3.4.1(b)).

3) Two Prominent beaks (ref. Fig. 3.4.1(c)).

4) PB - MB (ref. Fig. 3.4.1(d)).

5) PB - IB (ref. Fig. 3.4.1(e)).

6) MB - MB (ref. Fig. 3.4.1(f)).

7) MB - IB (ref. Fig. 3.4.1(g)).

8) IB - IB (ref. Fig. 3.4.1(h)).

9) IB - IB - IB (ref. Fig. 3.4.1(i)).

3.5 Classification of Quadrilateral :

The approach employed in classification is different from that for triangles. As a quadrilateral has four angles, the combinations would mushroom into a large unmanageable number. The angles used for classification are not wholly the edge angles of the polygon. The angles between the ACSILs are also used in the exploratory spanning of the quadrilateral shape space.

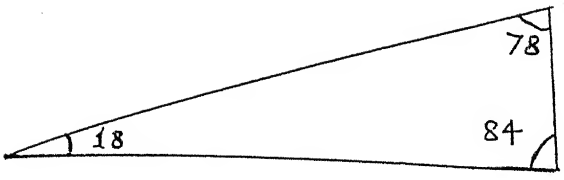

(a) One PB

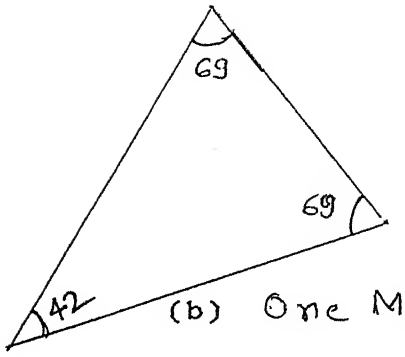

(b) One MB

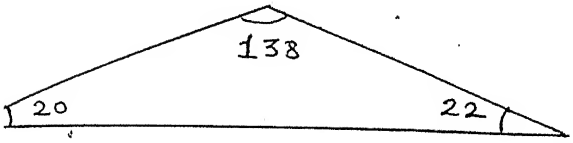

PB - PB (c)

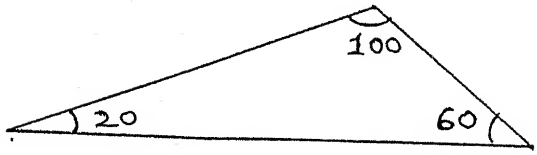

(d) PB - MB

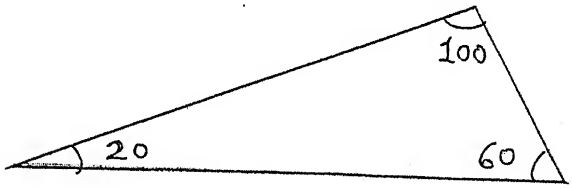

(e) PB - IB

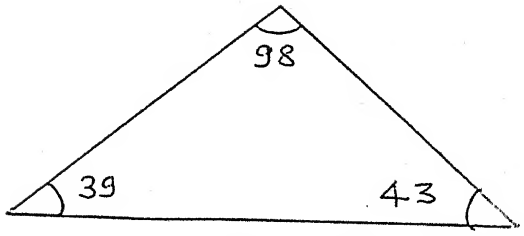

(f) MB - MB

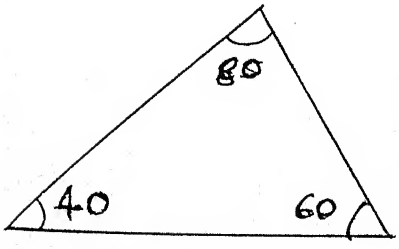

MB - IB (g)

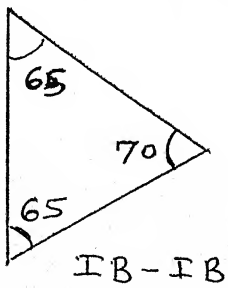

IB - IB (h)

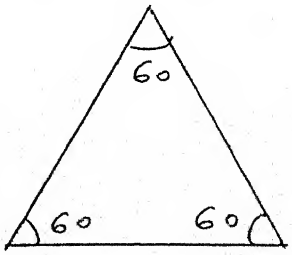

(i) IB - IB - IB

Fig. 3.4.1 Classes of Triangles

3.5.1 Shape Space for Quadrilaterals :

All the angles and their nomenclature are shown in the Fig. 3.5.1.1.

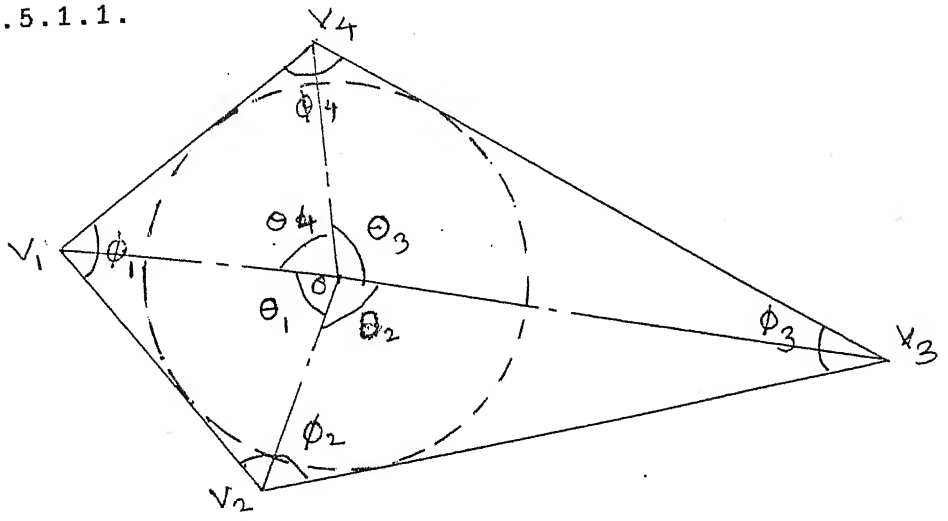

Fig. 3.5.1.1 Nomenclature for Quadrilateral Shape Feasible Space

The constraints on the angles are,

$$0 < \theta_i < 180 \; ; \; 0 < \phi_i < 180; \; i = 1, 2, 3, 4. \qquad (\text{----------3.5.1})$$

The governing equations for the angles are,

$$\theta_1 + \theta_2 + \theta_3 + \theta_4 = 360 \; ; \qquad (\text{---------- 3.5.2})$$

From triangle $V_1\text{-}O\text{-}V_2$,

$$\phi_1/2 + \phi_2/2 + \theta_1 = 180 \; ; \qquad (\text{---------- 3.5.3})$$

From triangle $V_2\text{-}O\text{-}V_3$,

$$\phi_2/2 + \phi_3/2 + \theta_2 = 180 \; ; \qquad (\text{---------- 3.5.4})$$

From triangle $V_3\text{-}O\text{-}V_4$,

$$\phi_3/2 + \phi_4/2 + \theta_3 = 180 \; ; \qquad (\text{---------- 3.5.5})$$

From triangle V_4-O-V_1 ,

$$\phi_4/2 + \phi_1/2 + \theta_4 = 180 \ ;$$

(---------- 3.5.6)

Equations 3.5.2 to 3.5.6 represent a system of linear equations, with five equations and eight variables. Three variables may assume random values, subject to the constraints expressed by relations 3.5.1, to generate a solution i.e. it has three degrees of freedom. Quadrilateral shape space exploration is done by systematically spanning the solution space over three basic variables.

θ_1 , θ_4 and $\phi 1$ are selected as the basis variables. The remaining five variables can be expressed in terms of these variables :

$$\theta_2 = 180 - \theta_4 \ ; \qquad (----------3.5.6)$$

$$\theta_3 = 180 - \theta_1 \ ; \qquad (----------3.5.7)$$

$$\phi_2 = 360 - 2\theta_1 - \phi_1 \ ; \qquad (----------3.5.8)$$

$$\phi_3 = \phi_1 + \theta_1 + \theta_4 - 180 \ ; \qquad (----------3.5.9)$$

$$\phi_4 = 360 - 2\theta_4 - \phi_1 \ ; \qquad (----------3.5.10)$$

Expressing the constraints in 3.5.1 in terms of these basis variables :

$$2\theta_1 + \phi_1 < 360 \ ; \qquad (----------3.5.11)$$

$$2\theta_1 + \phi_1 > 180 \ ; \qquad (----------3.5.12)$$

$$\phi_1/2 + \theta_1 + \theta_4 < 270 \ ; \qquad (----------3.5.13)$$

$$\phi_1/2 + \theta_1 + \theta_4 > 180 \ ; \qquad (----------3.5.14)$$

$$2\theta_4 + \phi_1 < 360 \ ; \qquad (----------3.5.15)$$

$$2\theta_4 + \phi_1 > 180 \ ; \qquad (----------3.5.16)$$

The feasible quadrilateral shape space boundaries are drawn in Fig.3.5.1.2. The polyhedron ABCDEF is the feasible shape space.

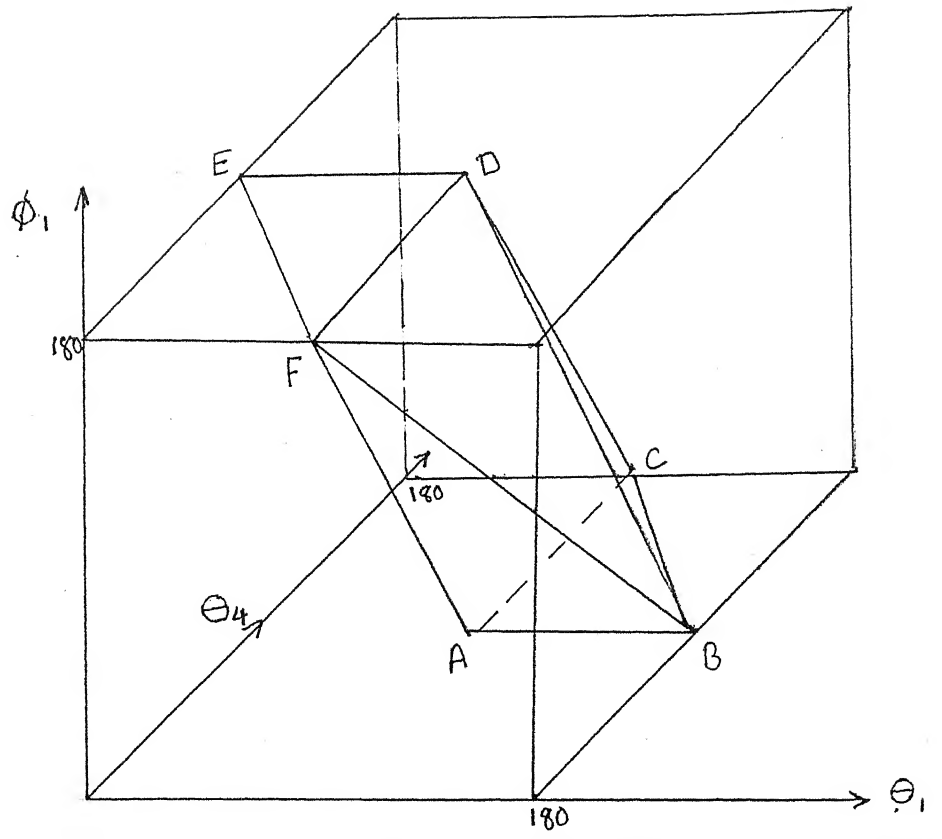

Fig. 3.5.1.2 Quadrilateral Shape Feasible Space

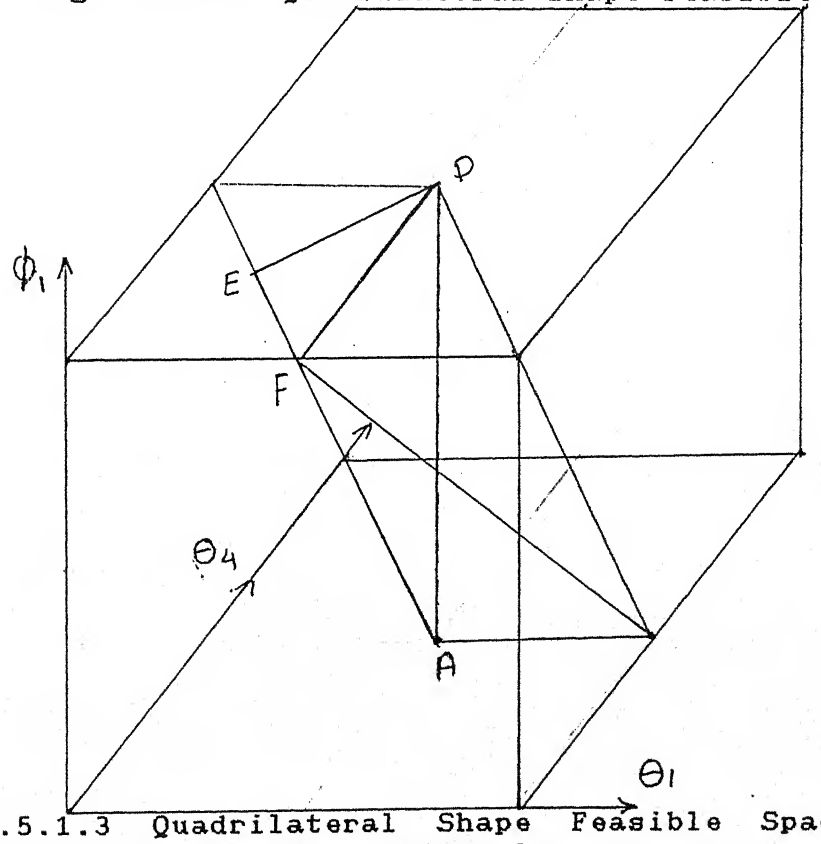

Fig. 3.5.1.3 Quadrilateral Shape Feasible Space, Reduced by Symmetry Considerations

As the nomenclature is arbitrary i.e. any of the angles could be the first angle and the nomenclature could be clockwise or anticlockwise, quadrilateral shapes are repeated in the feasible space under different nomenclature schemes. To pare down the feasible shape space to its exact size avoiding repetitions, the nomenclature scheme needs to be fixed uniquely.

The nomenclature is fixed uniquely by specifying that θ_4 should be the smallest of θ_i and θ_1 should be the next smallest. This implies that

1) the feasible space polyhedron is cut by the plane $\theta_1 = \theta_4$ and the polyhedron with $\theta_1 > \theta_4$ forms the feasible space.

2) From this polyhedron, the part with $\theta_1 > \theta_3$ i.e. $\theta_1 > 90$ is removed.

The resulting pyramid AEFD is shown in the Fig. 3.5.1.3.

3.5.2 Exploration of the Shape Space :

The pyramidal space AEFD has special quadrilateral categories at the vertices, edges and faces. They are illustrated in Fig. 3.5.2. In the figure, typical representative cases are drawn. In case of some of the categories, when an interior edge angle of the quadrilateral is zero, the angles shown are close to zero, about 10 degrees, but not zero.

1) Vertex A :

In the vicinity of the vertex A, the quadrilateral has two very sharp beaks at angles ϕ_1 and ϕ_3 (ref. Fig. 3.5.2(a)). At the vertex A, $\theta_1 = \theta_2 = \theta_3 = \theta_4 = 90$; $\phi_1 = \phi_3 = 0$; $\phi_2 = \phi_4 = 180$.

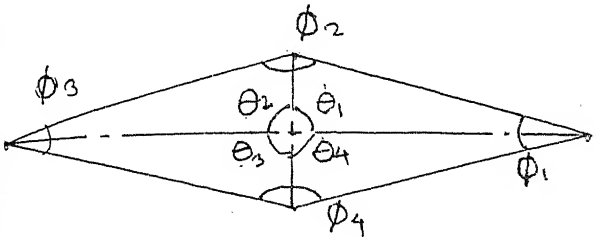

(a) Vertex A

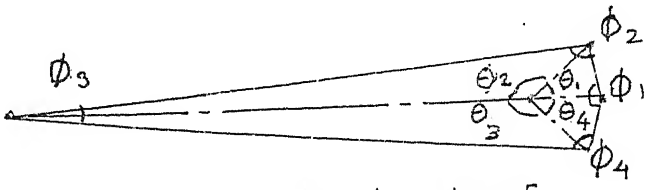

(b) Vertex E

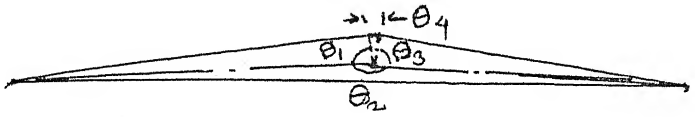

(c) Vertex F

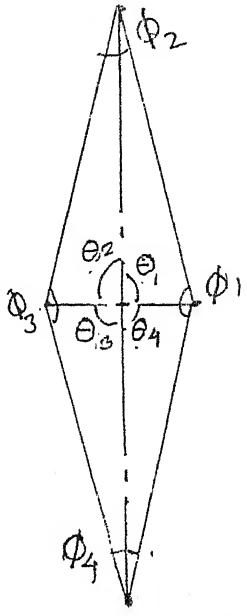

(d) Vertex D

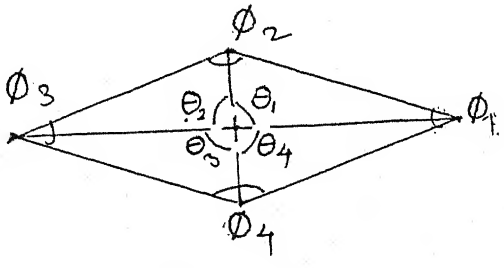

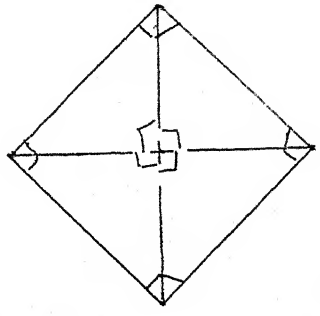

at 'H' – Square

(e) ~~the~~ edge AD

Fig. 3.5.2 Classes of Quadrilaterals (continued on next page)

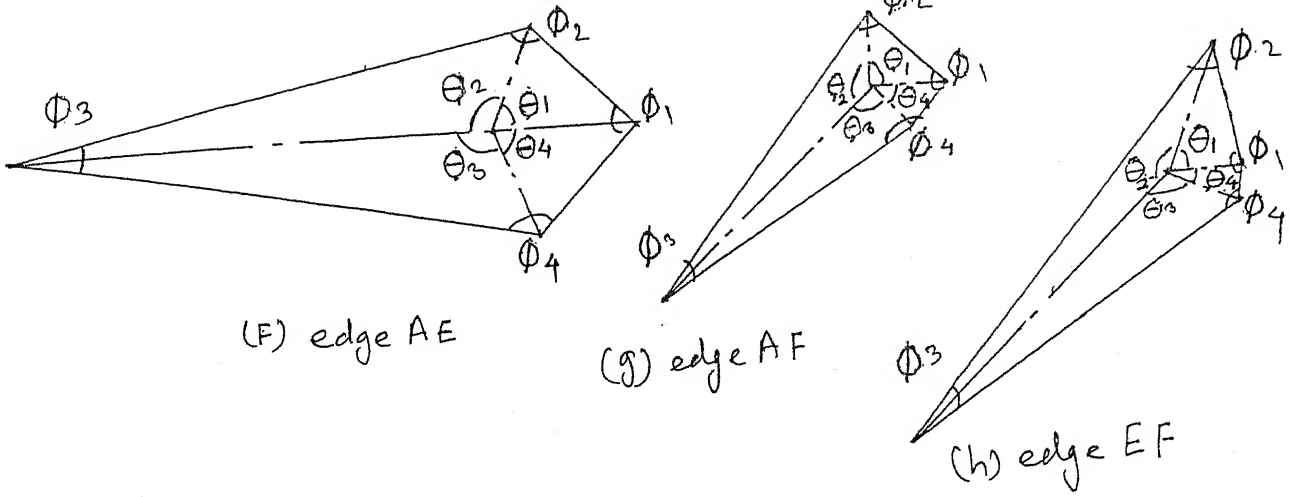

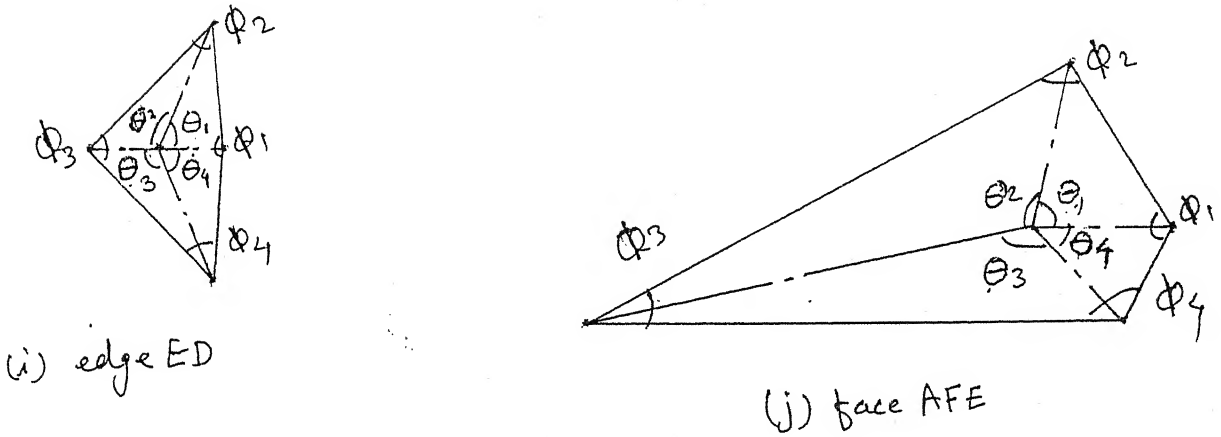

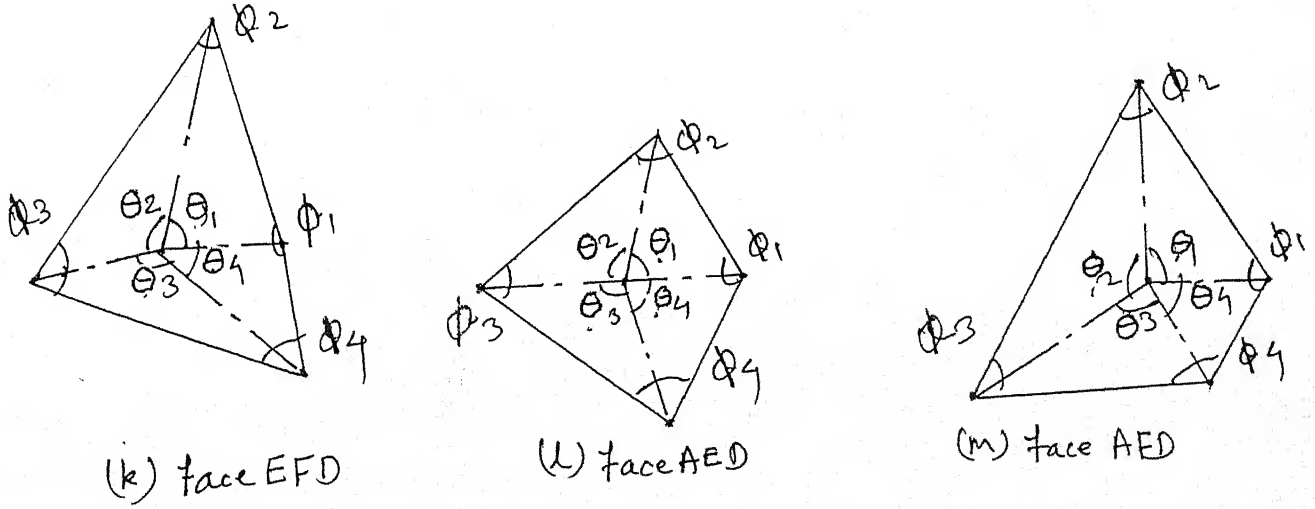

Fig. 3.5.2 Classes of Quadrilaterals (continued from previous page)

2) Vertex E :

In the vicinity of vertex E, the quadrilateral has a sharp beak at angle θ_3 (ref. Fig. 3.5.2(b)). At the vertex E, $\theta_1 = \theta_4 = 45$; $\theta_2 = \theta_3 = 135$; $\phi_1 = 180$; $\phi_2 = \phi_4 = 90$; $\phi_3 = 0$.

3) Vertex F :

The quadrilateral has two sharp beaks at ϕ_2 and ϕ_3 (ref. Fig. 3.5.2(c)). At F, $\theta_1 = \theta_3 = 90$; $\theta_4 = 0$; $\theta_2 = 180$; $\phi_1 = \phi_4 = 180$; $\phi_2 = \phi_3 = 0$.

4) Vertex D :

The quadrilateral has two sharp beaks at ϕ_2 and ϕ_4 (ref. Fig. 3.5.2(d)). At D, $\theta_1 = \theta_2 = \theta_3 = \theta_4 = 90$; $\phi_1 = \phi_3 = 180$; $\phi_2 = \phi_4 = 0$.

5) Edge AD :

The quadrilateral is a rhombus (ref. Fig. 3.5.2(e). Along the edge , $\theta_1 = \theta_2 = \theta_3 = \theta_4 = 90$; $\phi_1 = \phi_3$; $\phi_2 = \phi_4$. At the midpoint of the edge H , $\phi_1 = \phi_2 = \phi_3 = \phi_4 = 90$. It is a square.

6) Edge AE :

The quadrilateral is symmetrical about one of the diagonals, a shape resembling a kite, with a sharp beak at $\phi 3$ (ref. Fig. 3.5.2(f)). Along the edge, $\theta_1 = \theta_4$; $\theta_2 = \theta_3$; $\phi_2 = \phi_4$; $\phi_3 = 0$.

7) Edge Af :

The quadrilateral is a trapezoid with a sharp beak at ϕ_3 (ref. Fig. 3.5.2(g)). Along the edge $\theta_1 = \theta_3 = 90$; $\phi_3 = 0$.

8) Edge EF :

The quadrilateral has a large angle, almost 180 at $\phi 1$, and a sharp beak at ϕ_3 (ref. Fig. 3.5.2(h)). Along the edge, $\phi_1 = 180$; $\phi_3 = 0$.

9) Edge ED :

The quadrilateral is a kite with one large angle, almost 180, at ϕ_1 (ref. Fig. 3.5.2(i)). Along the edge, $\phi_1 = 180$.

10) Edge FD :

The quadrilateral is a trapezoid with a large angle and a sharp beak (ref. Fig. 3.5.2(j)). Along the edge, $\theta_1 = \theta_2 = 90$; $\phi_1 = 180$; $\phi_2 = 0$.

11) Face AEF :

The characteristic of face AEF is that the angle $\phi_3 = 0$. A typical quadrilateral is shown in Fig. 3.5.2(k).

12) Face EFD :

Face EFD is a degenerate face representing triangles as the angle $\phi_1 = 180$. A typical quadrilateral lying very close to the face is shown in Fig. 3.5.2(l). The quadrilaterals lying very close to the face and near the center will be approximated as triangles.

13) Face AED :

The quadrilaterals on this face are 'kites' (ref. Fig. 3.5.2(m).

14) Face AFD :

For this face, $\theta_1 = \theta_3 = 90$ which implies that the quadrilaterals on this face are trapezoids. The proof of this statement is trivial. A typical quadrilateral lying close to the center of the face is shown in Fig. 3.5.2(n).

3.5.3 Regions in Shape Space and Classification :

The regions are those close to the vertices and point H representing square, and the edges and faces. The regions are defined as qualitative predicate values of the specifications of the points, edges and faces. The predicates are defined for faces first. The edges are an 'AND' conjunction of the faces which intersect to produce the edges. Similarly, the vertices are

defined as conjunctions of the edges. Point H is taken as the midpoint of edge AD. The region between point H and vertex A is the same as the region between H and D for membership grade for this class; otherwise they differ in their relationship with other classes.

The central regions of edges are defined as conjunction of the edge predicate and negations of vertices predicates. For example, the central region of edge AE is defined as (ϕ_3 = 0) AND (ϕ_1 = 180) AND (θ_1 /= 90) AND (θ_4 /= θ_1). All the comparisons and the conjunction are fuzzy. The fuzzy ranges of the angle values are shown in Fig. 3.5.3. The fuzzy membership functions shown are for the particular quality such as θ_1 = 90. The angles observed in the polygon say, θ_1, has its membership function as shown in part(d) for θ_1 and θ_4. The application of the predicate is the conjunction of fuzzy sets.

The classes and their predicates are listed in table 3.5.3.

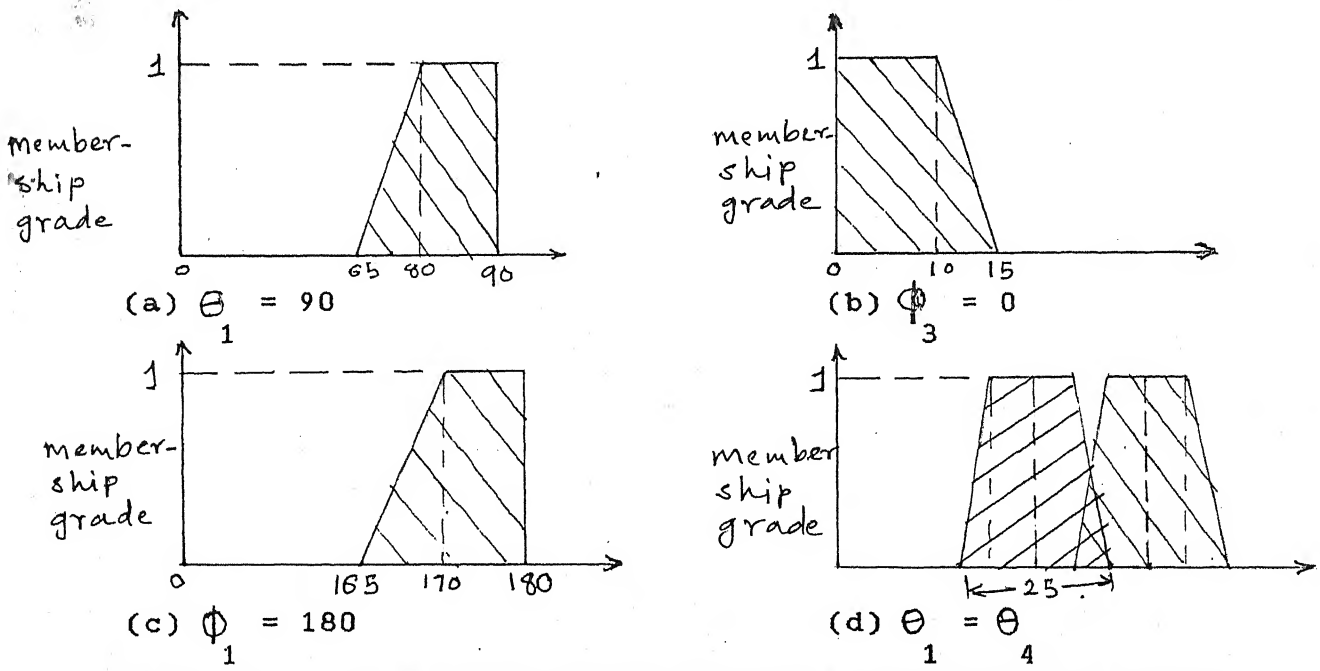

Fig. 3.5.3 Fuzzy membership Functions for Quadrilaterals

Table 3.5.3

Quadrilateral classes and their predicates :

Angle Quality :	$\Theta 1 = 90$	$\Theta 1 = \Theta 4$	$\phi 1$	$\phi 3$
1) Interior	NOT	NOT	/= 0	/= 180
2) Vertex A	YES	YES	= 0	= 0
3) Vertex F	YES	NOT	= 180	= 0
4) Vertex E	NOT	YES	= 180	= 0
5) Vertex D	YES	YES	= 180	= 180
6) Edge FD	YES	YES	= 180	/= 0
7) Edge AF	YES	NOT	/= 180	/= 0
8) Edge ED	NOT	YES	= 180	/= 0
9) Edge EF	NOT	NOT	= 180	= 0
10) Edge AE	NOT	YES	/= 180	/= 0
11) Edge AD :				
a) Point H : $\Theta 2 = \Theta 4$	YES	YES	/= 180	/= 0
b) Zone HA : $\Theta 2$ /= $\Theta 4$	YES	YES	/= 180	/= 0
c) Zone HD : $\Theta 2$ /= $\Theta 4$	YES	YES	/= 180	/= 0
12) Face AFD	YES	NOT	/= 180	/= 0
13) Face AFE	NOT	NOT	/= 180	= 0
14) Face EFD	NOT	NOT	= 180	/= 0
15) Face AED	NOT	YES	/= 180	/= 0

3.6 Classification of Polygons with Higher Number of Sides :

The classification of convex polygons with more than four sides (note that the number of sides is the one left after various approximations) is based on the beak and bulge features and their geometrical relations with each other. The definitions of beaks and bulges is the same as that given in section 3.2.

3.6.1 Classification Basis :

The number of beaks and bulges in a convex polygon are constrained by the angles subtended by them at the center of the unifork. In Fig. 3.6.1, the lines OP_i, $i = 1,\ldots,n$, where n is the number of sides, are perpendicular to the edges E_i. Let θ'_i be the angle between OP_i and OP_{i+1}. Then,

$$\theta'_1 + \ldots + \theta'_i + \ldots + \theta'_n = 360; \qquad (3.6.1)$$

$$\theta'_i + \phi_i = 180; \qquad (3.6.2)$$

where ϕ_i is the angle between Ei and Ei+1. Thus θ'_i and ϕ_i are directly related. Beaks and the bulges can be detected using angles θ'_i. The beak and bulge definitions in terms of θ'_i are,

$$\text{Beak} : 180 > \theta'_i > 120 ; \qquad (3.6.3)$$

$$\text{Bulge} : 120 > \theta'_i > 90 . \qquad (3.6.4)$$

The number of beaks and bulges is constrained by the relation 3.6.1. This limits the number of possible combinations of beaks and bulges and allows combinatorial approach to remain within manageable limits.

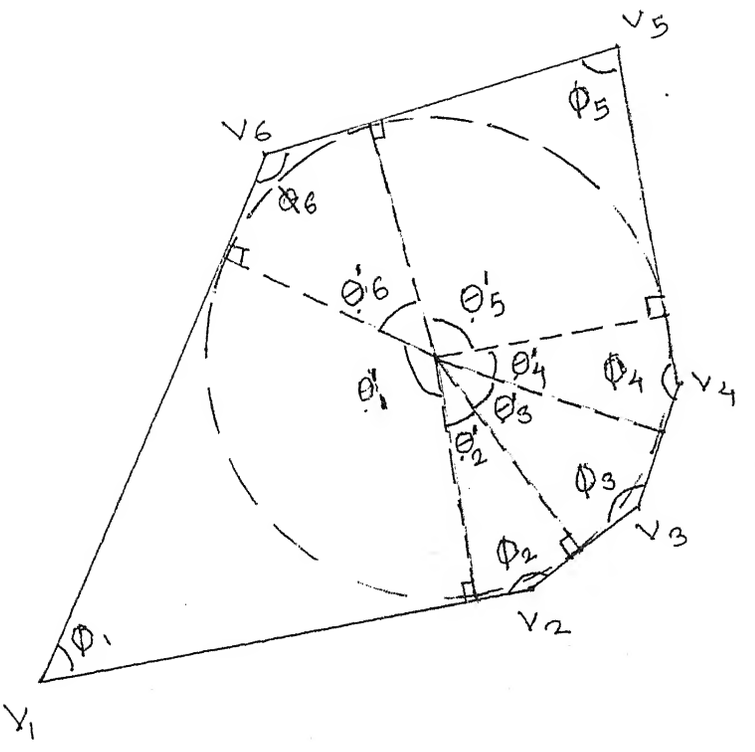

Fig. 3.6.1 Constraints on beaks and bulges

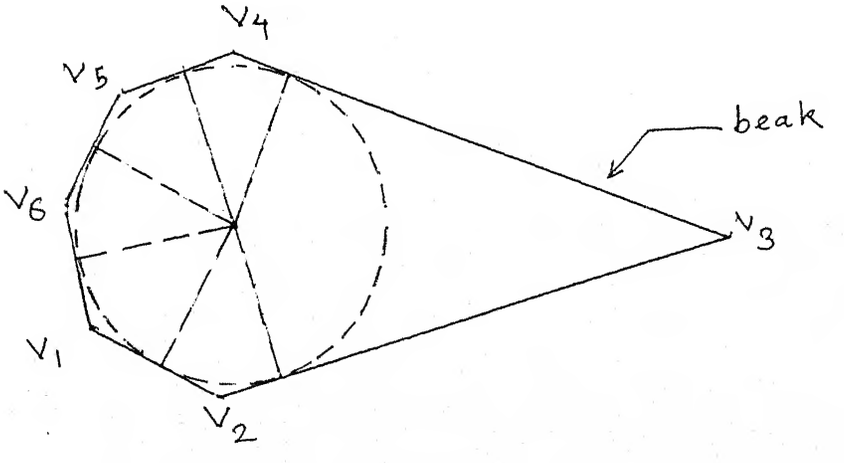

Fig. 3.6.2.1 Unifork Polygon with a Beak

3.6.2 Combinatorial Classes :

The possible combinations are,

1) One beak

2) Two beaks

3) One bulge

4) Two bulges

5) three bulges

6) One beak and one bulge

7) One beak and two bulges

The cases of three beaks, four bulges, two beaks and one bulge are not possible, as they entail very low intensity ACSILs separating the features; these cases would be treated as triangles or quadrilaterals, as the case may be, with very gentle minor projections.

A brief discussion and illustrations of the classes are given below. In the illustrations, the fork point of the unifork, its skeletal circle and the perpendiculars from the fork point onto the sides are drawn. The skeleton is not drawn unlike the previous figures.

1) One beak :

It is illustrated in Fig. 3.6.2.1. As there are no other features, geometrical relations are absent.

2) Two beaks :

There are two classes of polygons with two beaks, depending on the geometrical positions of the beaks. In Fig. 3.6.2.2(a), the beaks are opposite each other, the minimum angle (θ' of section 3.2.1) between them being 60. In Fig. 3.6.2.2 (b), the angle between the beaks is close to 0.

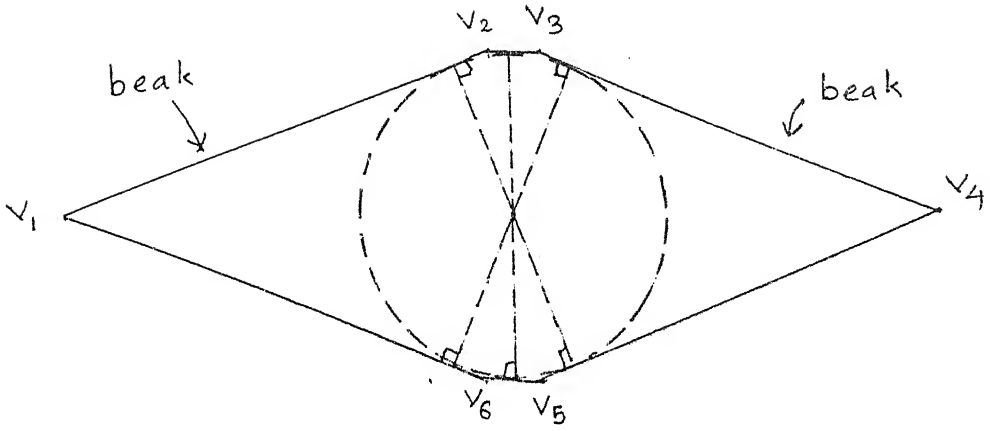

(a) Two beaks, opposite each other

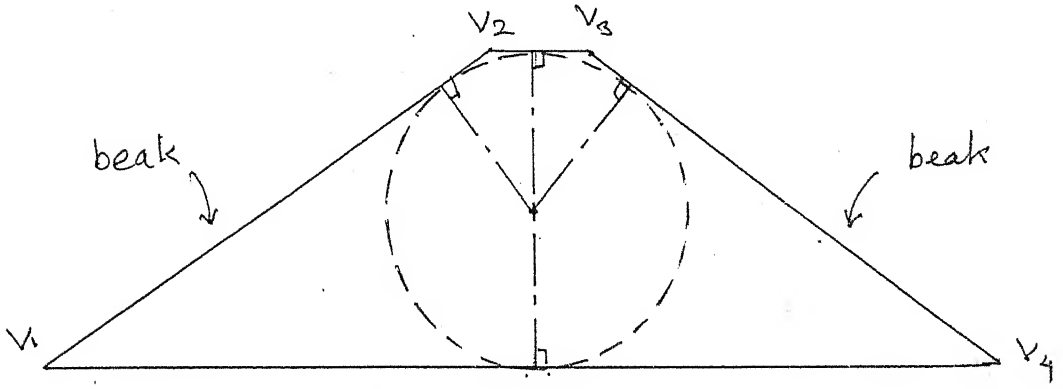

(b) Two beaks adjacent to each other

Fig. 3.6.2.2 Unifork with Two Beaks

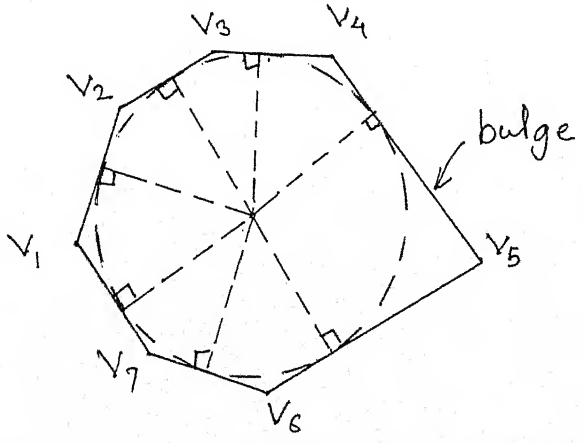

Fig. 3.6.2.3 Unifork Polygon with a Bulge

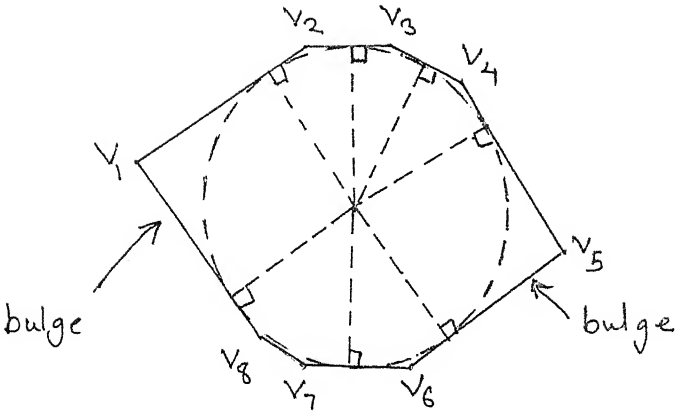

(a)

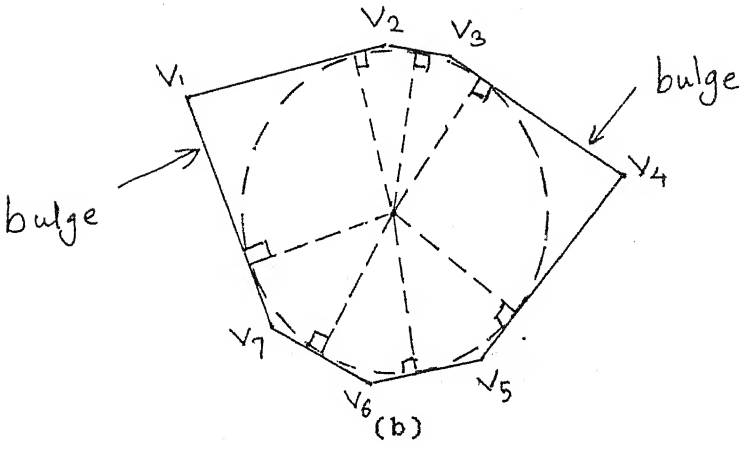

(b)

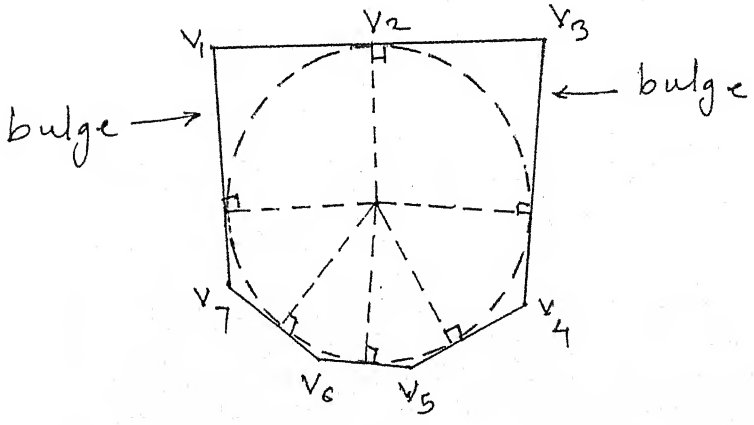

(c)

Fig. 3.6.2.4 Unifork with Two Bulges

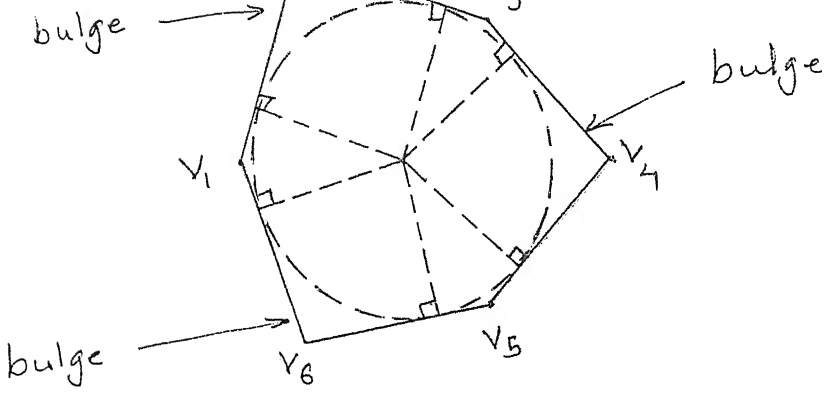

(a)

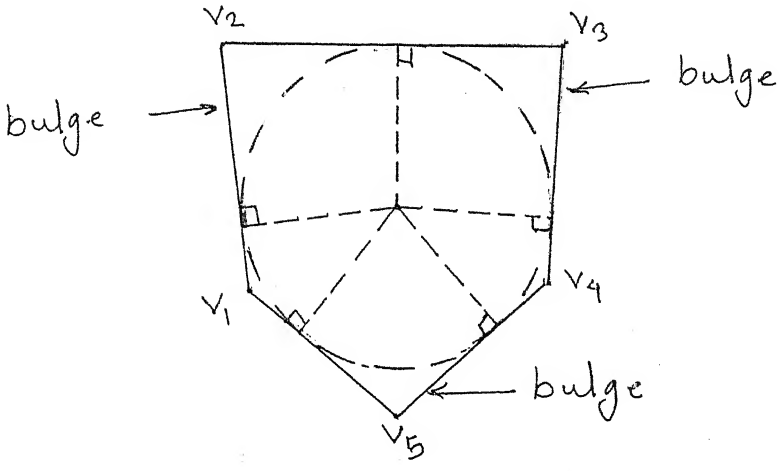

(b)

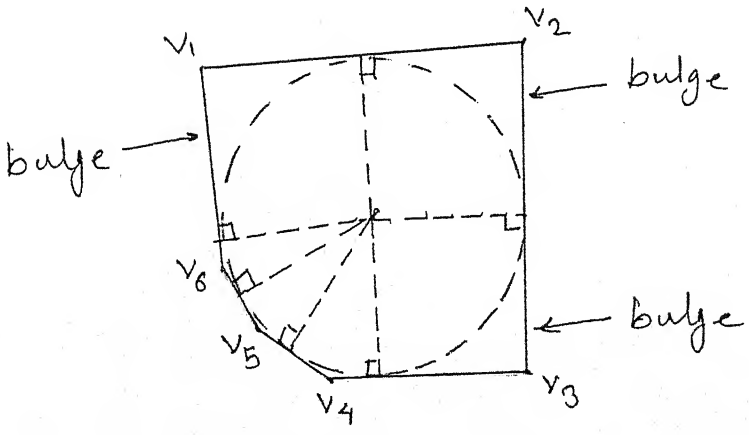

(c)

Fig. 3.6.2.5 Unifork with Three Bulges

3) One bulge

It is illustrated in Fig. 3.6.2.3. As there are no other features, geometrical relations are absent.

4) Two bulges

There are three classes of polygons with two bulges, based on the geometrical positions of the bulges. In Fig. 3.6.2.4(a), the bulges are opposite each other, the minimum angle (θ' of section 3.2.1) between them being 90. In Fig. 3.6.2.4 (b), the angle between the bulges is close to 45. In part (c), the angle is 0.

5) three bulges

With three bulges, atleast 270 degrees of the total angle are in the bulges. The remaining 90 degrees may be distributed as 30,30,30 in between the bulges, or 0,45,45 or 0,0,90. Correspondingly, there are three categories of polygons with three bulges. They are illustrated in Fig. 3.6.2.5.

6) One beak and one bulge

There are three categories of a polygon with one beak and one bulge. The beak and bulge may be close to one another with angle between them almost 0 (ref. Fig. 3.6.2.6(a)). The angle may be around 35 (ref. Fig. 3.6.2.6(b)), or the angle may be around 75, with the beak and bulge exactly opposite each other (ref. Fig. 3.6.2.6(c)).

7) One beak and two bulges :

There are totally five categories of the class. The total hi' contribution by the beak and bulges is around 300. By relation 3.6.1, the remaining angles must sum to around 60. These 60 degrees are to be distributed in three angles between the beaks and bulges. Hence the categories are,

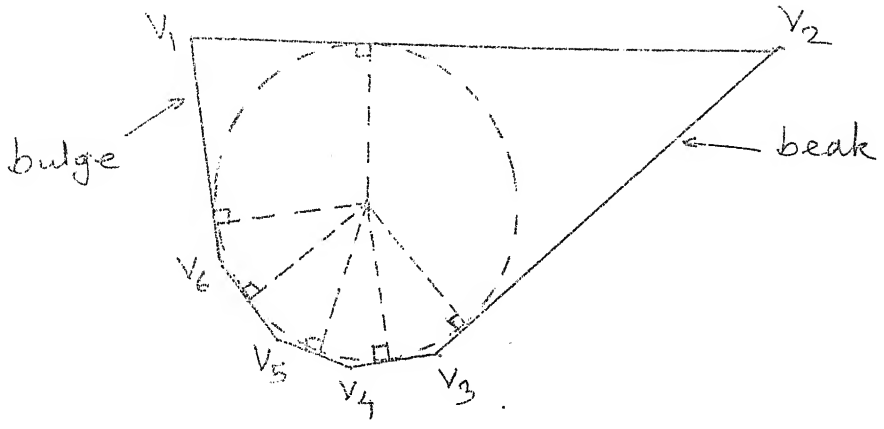

(a)

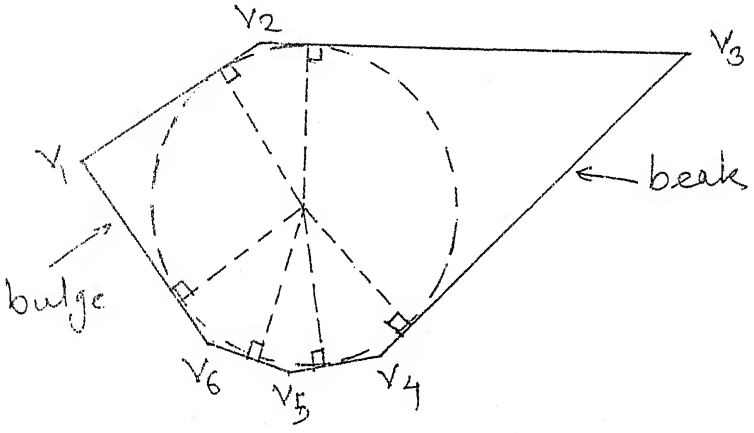

(b)

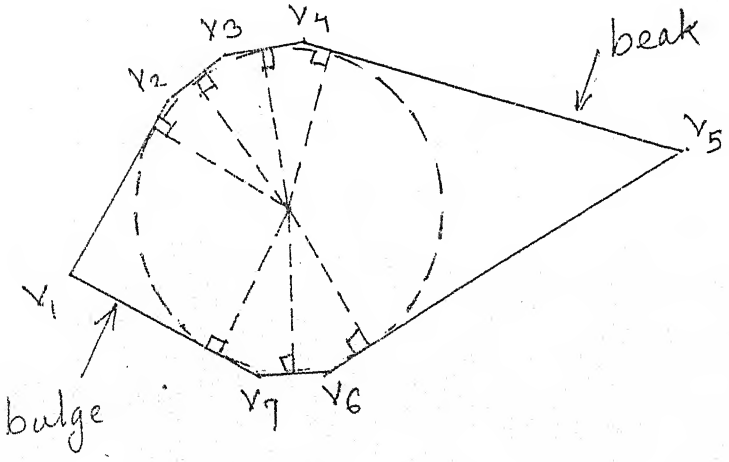

(c)

Fig. 3.6.2.6 Unifork with One Beak and One Bulge

a) angle distribution : 0 - 0 - 60; two subcategories due to the asymmetry. (ref. Fig. 3.6.2.7, parts (a) anb (d)).

b) angle distribution : 0 - 30 - 30; two subcategories due to asymmetry (ref. Fig. 3.6.2.7, parts (c) and (d)).

c) angle distribution : 20 - 20 - 20; (ref. Fig. 3.6.2.7(e)).

4. Elongation Classification :

Elongation is a string of long or middle length NACSILs, split into two by the unifork point. The two substrings thus formed, henceforth referred to as the elongation branches, are almost collinear. Successive NACSILs in the branches, have a very large angle, almost 180 degrees, between them. The angles in the branches, henceforth referred to as bends, result in deviation of the elongation from rectilinear form. The branches, may be almost rectilinear, with successive bends in opposite directions, or they may curve in one direction. These features in addition to the lengths of the branches, are used to classify elongations.

The classification scheme is hierarchical. The number of elongation branches, and lengths of the elongation branches give the first level of classification. The bend features are then combined with the first level classes to give final classification.

Before proceeding with classification, a number of new concepts representing some elongation properties and entities need to be defined.

4.1 Definitions of Elongation Properties :

1) Mean elongation line : Mean elongation line is defined for each of the elongation branches. It is defined as the line passing through the origin and with inclination which is the weighted

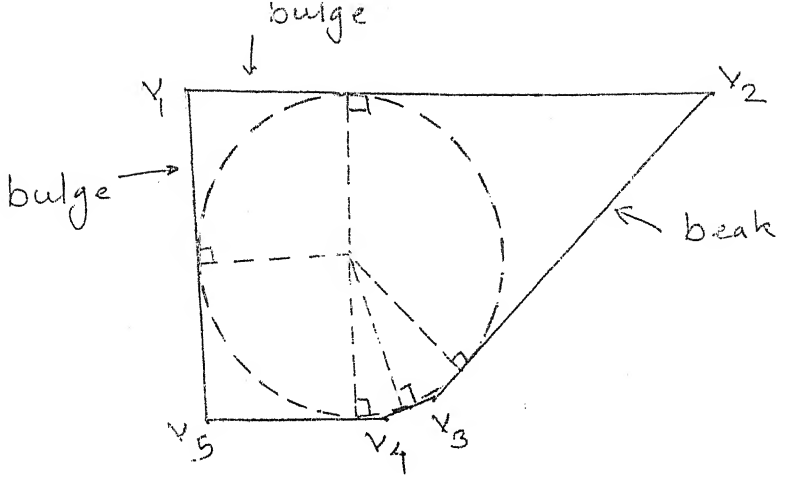

(a)

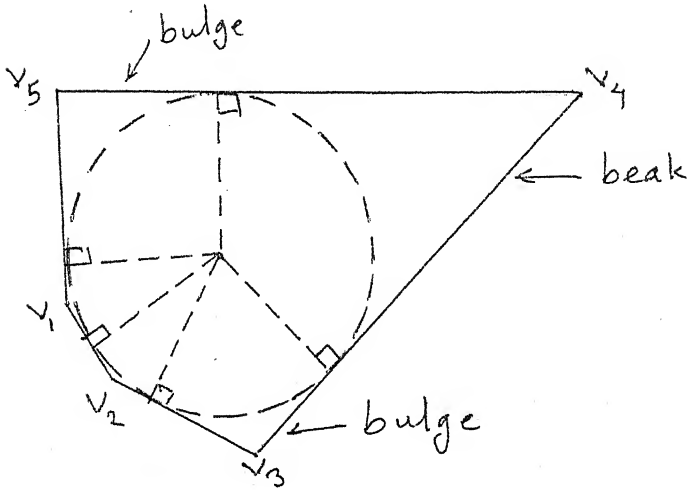

(b)

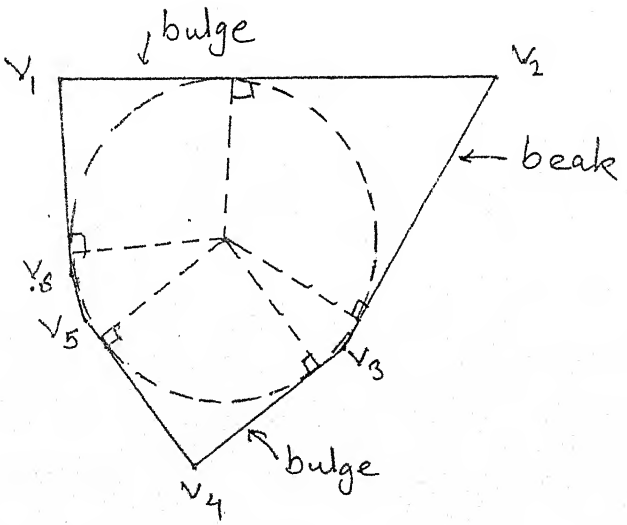

(c)

Fig. 3.6.2.7 Unifork with One Beak and Two Bulges (contd.)

average of the NACSILs in the branch, the weights being the intensities of the NACSILs. The length of the mean elongation line is the rectilinear distance between the unifork point and the tip of the elongation branch. In Fig. 4.1.1, the elongation branch O-P -P -P -P starts from the origin which is the unifork point. The line O-P is the mean elongation line. It is used as a rough approximation of the elongation branch. It gives a reasonably good approximation as the elongation branch can not have sharp bends and does not contain short lines.

An overall mean elongation line is defined for the whole of elongation along exactly the same lines as for the individual mean elongation lines for the elongation branches.

2) Elongation deviation : It is the standard deviation of the inclinations of the NACSILs from the inclination of the mean elongation line, weighed by the intensities. It is an indicator of the closeness of the approximation in the mean elongation line.

4.2 The Number and Lengths of Branches :

The number of branches may be one or two. The length of branches is the length of the mean deviation lines of the branches. It is divided into fuzzy long and short categories, the normaliser and comparator for the qualitative division being the unifork radius. The combinations of these give the classes.

4.3 Bends in Elongation Branches :

The bends in the branches are analysed for curve trends. They are classified as with a curve trend and without curve trend.

A curve is indicated by monotonic inclinations of the NACSILs. Local deviations from the curve trends are approximated by cutting across the deviations. In Fig. 4.3.1 the NACSILs forming an

elongation branch are drawn as the lines OP1, P1-P2, and so on. The local deviation from the curve trend, $P_2-P_3-P_4$, is approximated by substituting the segment $P_2-P_3-P_4$ by the line P_2-P_4. All local deviations are successively approximated. As the elongation branches are not complicated, this simplistic method can give good results for most of the cases. For the cases where it is complicated, for example in an extremely elongated polygon having a large number of NACSILs in its elongation branches which are quite randomly disposed, the elongation branch will be considered to be a line with a large deviations.

The value of the curvature of the resulting elongation branch would indicate the curve trend. The local curvature of a 'curve' formed by a set of line segments joined end to end, can be defined by considering the line segments to be approximating a curve. Consider two line segments, L_1 and L_2, have lengths S_1, S_2; if the unit vectors along the lines are $\bar{t}_1$ and $\bar{t}_2$. (Note that $\bar{t}_1$, $\bar{t}_2$ are the unit tangent vectors.) If L_1 and L_2 are located end to end, then the local curvature could be defined as the length of the normal vector $\bar{N}$, given by

$$\bar{N} = (\bar{t}_1 - \bar{t}_2) / ((S_1 + S_2)/2) ; \qquad (----------4.3.1)$$

where the denominator is the length of the region of the line segments associated with the 'local curve' which gives the local curvature.

The average of the local curvatures is assumed to give the curve trend. This assumption is justified as the inclination change, and hence the range of local curvatures is quite small in an

elongation branch. The standard deviation of curvature, weighed by the intensities of the NACSILs, gives the mean deviation from the curve trend and thus it is a measure of the confidence value of the curvature.

The average curvature and its standard deviation together define the two bend classes, curve trend and rectilinearity. The curve trend is defined as 'large' curvature and rectilinearity is defined as 'low' curvature.

4.4 Elongation Classes :

As stated earlier, the elongation classes are combinations of the features given above. In addition to the combinations given above, the direction of curvature of the two branches, gives classes of 'curved towards each other' and 'curved away form each other'. Table 4.4 lists the elongation classes.

Table 4.4 Elongation classes

Symbols :

L :- long, S :- short, R :- rectilinear, C :- curved,

T :- curved towards one another

A :- curved away from one another.

One branch : LR, LC, SR, SC.

Two branches :

LR-LR	LR-LC	LR-SR	LR-SC
LC-LR	LC-LC-T , LC-LC-A	LC-SR	LC-SC-T , LC-SC-A
SR-LR	SR-LC	SR-SR	SR-SC
SC-LR	SC-LC-T , SC-LC-A	SC-SR	SC-SC-T , SC-SC-A

5. Convex Polygon Description :

Convex polygon description is based on the shape classification, size parameters of the polygon, and identification of the 'favoured directions' in the polygon. Shape classification has been elaborated upon in the discussion so far. The size parameters have been briefly mentioned in the section 1. The concept of favoured directions in the polygon has not yet been introduced. As the size parameters are dependent on favoured directions, the concept of favoured directions will be expounded first.

5.1 Favoured Directions :

Favoured directions may be said to be the directions along which a nesting allocation is likely. Favoured directions may be the approximate symmetry and stretch operation directions of the polygon. They are utilised in the entire profile description for the relations of the constituent convex polygons which are the result of the polygon decomposition.

Favoured directions are the stretch axes, e.g. the mean elongation lines, the beak and bulge ACSILs, and the axes of symmetry. The stretch directions are directly available from the earlier analysis. Symmetry axes lie in between the adjacent stretch axes. Favoured axes are geometrical lines located in the plane of the polygon . Favoured directions are illustrated in Fig. 5.1.1. In part (a) the CSIL O_1-O_2 is a favoured axis. In part (b), line OP is a symmetry axis, and hence a favoured direction.

For the stretch axes, the measure of 'favouredness' may be the intensity of the CSIL along the stretch axis. For the mean elongation lines, it is the sum of the intensities of the NACSILs forming the elongation or elongation branches.

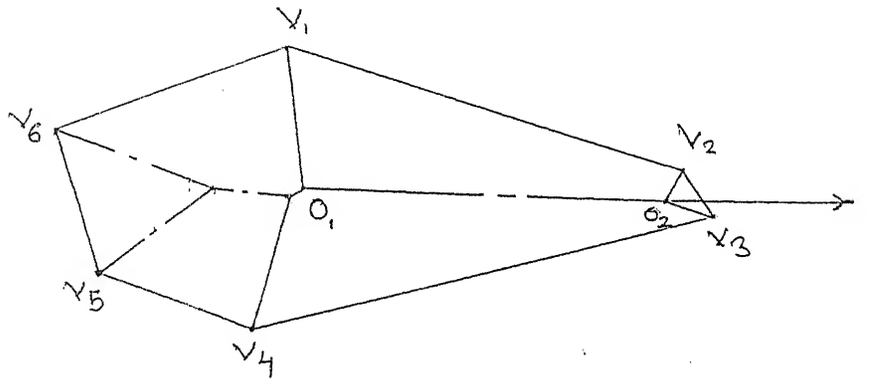

(a)

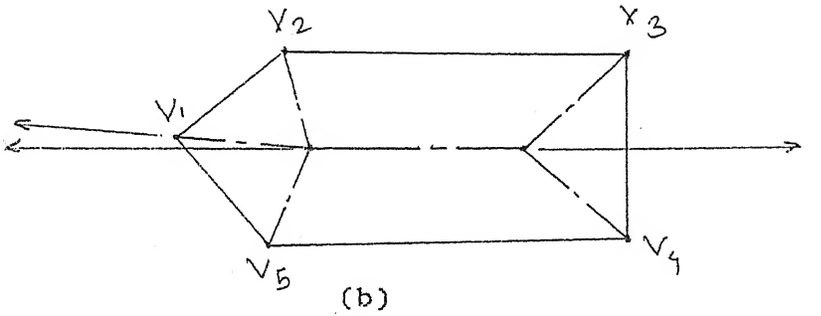

(b)

Fig. 5.1.1 Favoured Axes

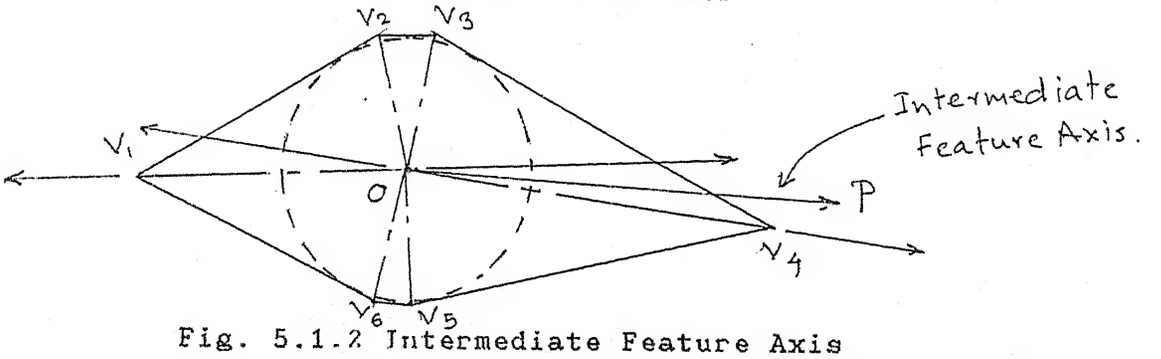

Fig. 5.1.2 Intermediate Feature Axis

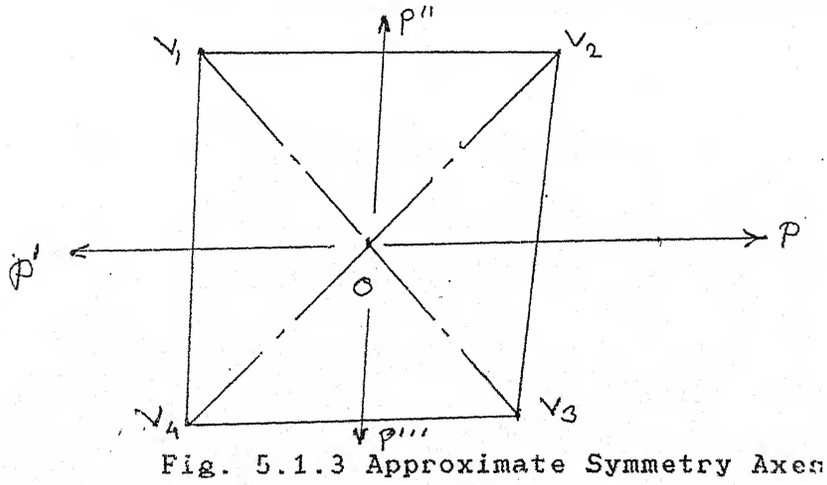

Fig. 5.1.3 Approximate Symmetry Axes

A favoured direction may be formed by more than one features of stretch. In this case, the favouredness is the sum of the contributions by the features. If equally favoured two feature axes have almost equal inclinations then the angle bisector of the two axes is also a favoured axis, called an intermediate feature axis. If the two feature axes are parallel, then the line equidistant to them is the intermediate feature axis. The favouredness of the intermediate feature axis is the average of the favouredness of the two feature axes. In Fig. 5.1.2, CSILs $O-V_1$ and $O-V_4$ are almost collinear. Line OP is the intermediate feature axis.

The symmetry axes generally lie either along a stretch feature or between two stretch features. Approximate symmetry axis is the angle bisector of two equally favoured feature axes. The favouredness of the symmetry axis is the average of the favouredness of the two feature axes. In Fig. 5.1.3, the feature axes $O-V_1$ and $O-V_2$ generate the approximate symmetry axis OP. Intermediate axes and symmetry axes are determined only for highly favoured axes.

5.2 Size Parameters of Shapes :

In the proposed shape classification scheme, the unifork radius, the elongations and the information on which of the sides of the unifork form the NACSILs of the elongations, are sufficient to determine the approximated skeleton and hence the approximated polygon. Thus, from completeness of the description issue, just the unifork radius and the elongation branches, in addition to the classes, are sufficient.

We propose to take the unifork radius and the length of the

polygon along its favoured directions as the size parameters. As favoured directions are associated with classes, with each class for which the polygon has an acceptable class membership grade, atleast one size parameter will be associated. It plays an important role in matching of profiles.

5.3 Overall Classification :

The overall classification is the combination of the unifork classification and the elongation classification. It is a hierarchical classification scheme. The classification decision tree is formed by attaching the whole of elongation decision tree to each of the leaf nodes of the unifork decision tree. It is a fuzzy spawning decision tree.

The final classes which occur at the leaf nodes of the decision tree, may be treated as a descriptive string rather than a homogeneous entity. For example, the class 'Two beaked circular polygon with one rectilinear long elongation branch' is a description of the polygon. The class is a fuzzy conjunction of the qualitative predicates forming the description strings. The membership grade of the polygon for the whole of the class is the application of fuzzy conjunction of the qualitative predicates. The membership grades for each of the predicates forming the string are individually preserved. The dominance of any of the features represented by the predicate is given by the product of the grade and the intensity of the feature. The relative dominances of a combination of the predicates with respect to the others are defined likewise. Not all the possible combinations are allowed. Only those representing a continuous path in the decision

tree and forming a step in the classification process are relevant.

With the final classifications, the area approximations that were done during the approximation process to produce the classifications are preserved as the ratio of original area to the approximated area. Different approximation areas are possible as some of the steps in the approximation process are also fuzzy spawning steps, producing different approximations.

5.4 The Description :

Convex polygon description consists of the overall shape classification, the area approximation measures, size parameters and the favoured axes.

The overall shape classification generates multiple class membership for the polygon. All the classes must be preserved in the description in toto. None of the classes by itself would be a complete shape description.

The convex polygon description is a complex system of multiple classes, their memberships, their internal dominance relations and the size parameters and the favoured axes.

6. Convex Polygon Description Algorithm :

The convex polygon description process is based on the propositions given in section 2. It is a fuzzy spawning process, producing multiple descriptions. The simplifying approximations are done before the two pronged feature analysis of unifork analysis and elongation analysis. It is structured into functionally different steps. Each step completely deletes a particular type of manifestation of minor stretch operations, by

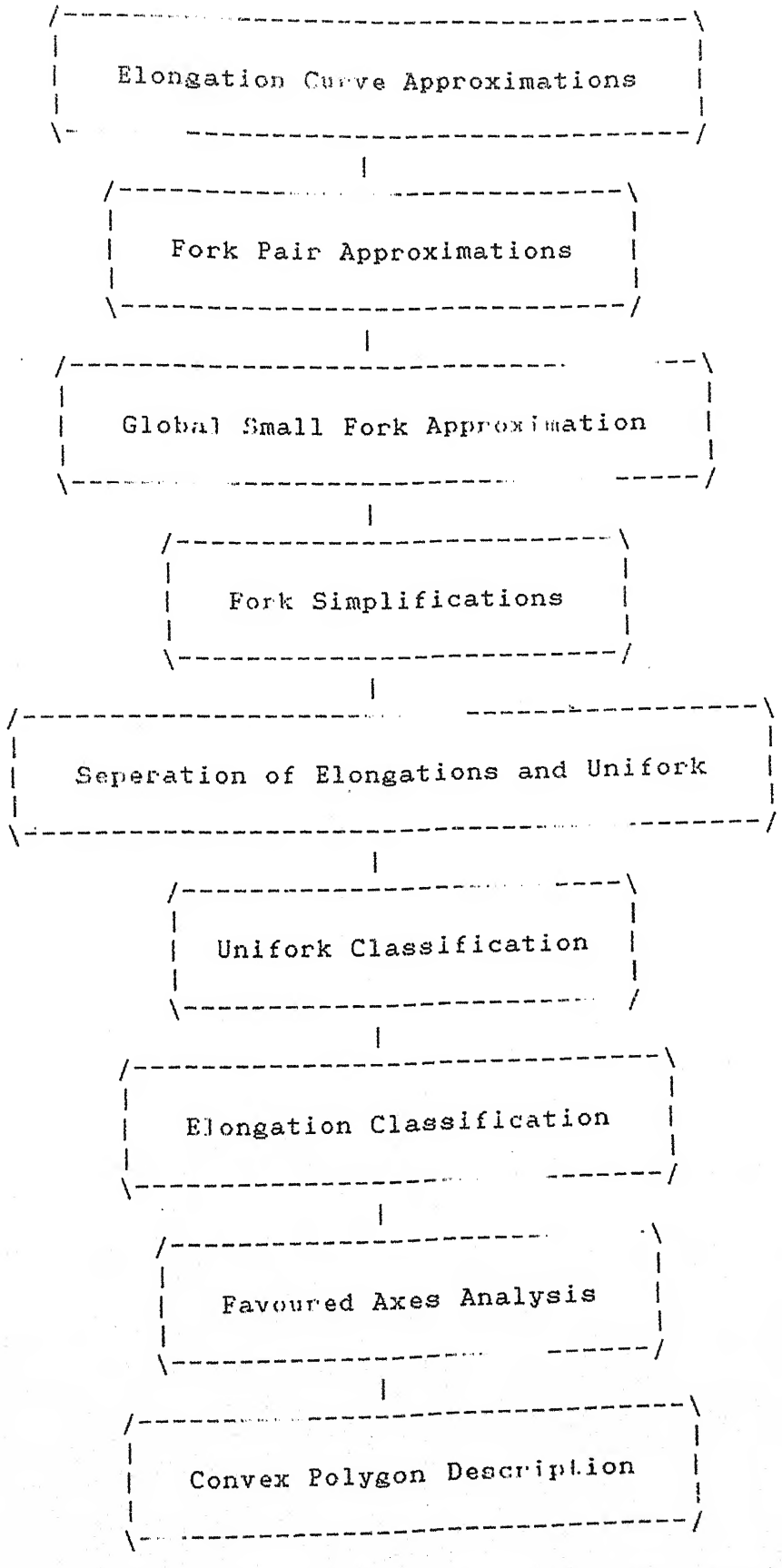

Fig. 6.1 Block Diagram of convex polygon Algorithm.

approximating it. The steps from 1 to 4 are approximation steps. Steps 5 to 7 are classification steps. Steps 8 and 9 give the description. The algorithm is given in the form of a block diagram in Fig. 6.1. All the steps are later elaborated upon and presented in the form of procedural algorithms in sections 7 to 14.

The description process is sequentially broken down into the following steps :

1) Elongation curve approximations : The curves in the NACSILs are detected and replaced. It is based on the observation in section 2.6.8. The fork - NACSIL tree is devoid of dense strings at the end of this step.

2) Fork pair approximations : The LL--LS, LL------Ls and LL--LL fork pairs are replaced in this step. It is based on sections 2.6.1 through to 2.6.7. It is fuzzy spawning process. The LL--LL are the small elongations and LL------LS are the rounded corners. The small elongations are approximated by merging the forks and adjusting the length of ACSILs in the forks. It is based on observations in sections 2.6.5 and 2.6.7. All the small elongations are deleted from the fork - NACSIL tree in this step. The rounded corners are approximated by extensions of appropriate edges of the polygon.

This step deletes all the small elongations and the locally small forks.

3) Global Small fork approximation : The globally small forks are approximated. It is based on observations in sections 2.6.1 through to 2.6.5. All the globally small forks are deleted in this step.

4) Fork simplifications : The corners rounded by circular curves

in forks are detected and replaced. It is based on observation in section 2.6.11. As a result of this step, in conjunction with step 2, all the rounded corners are deleted from the fork - NACSIL tree.

5) separation of elongations and unifork : The major fork is located. All the other forks are merged into it and the NACSILs are separated from the resulting unifork.

6) Unifork classification : The beak and bulge features of the unifork are identified and a classification based on the number of sides and the features is accomplished. The classification has already been proposed in section 4.

7) Elongation classification : The elongation line diagram is classified on the of the angular distribution and the lengths of the elongations. The elongation classification has already been proposed in section 5.

8) Favoured axes analysis : The favoured axes are determined on the basis of the propositions given in section 5.1.

9) Description : The final classification is done as a combination of unifork classification and elongation classification. The favoured directions are noted and the complete description is stored.

Control of the description process :

The process is modeled as a fuzzy spawning process (ref. chapter 1, section 6). The steps given above, are different sequential parts of the process, which may be viewed as independent subprocesses.

The fuzzy qualitative predicates for each of the subprocesses are

elaborated in the respective discussions. The pruning of the process is based on the membership grade returned by the fuzzy qualitative predicates. The goal state evaluation should be done by a mapping function of the quality grades. The suggested mapping function is the weighted average of the fuzzy quality grades, the weights being the intensities of the CSILs or profile boundary edges involved in the quality evaluation.

In the artificial intelligence paradigm, convex polygon classification is a heuristically guided generative space search. The solution generation is done by the application of the fuzzy qualitative predicates and the rules for the action to be taken thereof. Backtracking is controlled by the mapping function which is viewed as a heuristic function guiding the backtracking.

7. Procedure of Elongation Curve Analysis :

The procedure consists of a unique identification of a curve based on a string and the string delimitation; followed by its replacement. This process is not a fuzzy spawning process. It is a direct irrevocable algorithm.

7.1 Elongation Curve Identification :

1) Identify all the numerically long, dense strings of locally large forks. Identify the curves associated with it by the presence of low intensity ACSILs emanating from most of the forks and ending on the curve. The curve is delimited by the extreme low intensity ACSILs.

2) Calculate the areas enclosed by the string and its associated boundary curve segment. Note that a string may have two curved boundary segments and hence two areas will be calculated in such

cases. If one of the curve has already been replaced, it will not be considered in further processing.

3) Sort the strings in ascending order of areas. For strings with two unresolved curves, the smaller of the two areas will be considered for sorting.

4) Replace the curve associated with the first string. If two unresolved curves are associated with the string, the smaller area curve will be replaced. Mark the boundary as resolved.

5) If all the curves are replaced, the process is complete; otherwise go to step 3.

7.2 Curve Replacement :

Curve replacement is by external envelopes. It is an iterative process.

1) Extend the two extreme edges till they meet (ref. Fig. 7.2).

2) Determine the additional area, the shaded area in the Fig. 7.2. If the additional area is small compared to the area enclosed within the string and the curve, then the curve replacement is complete. The smallness of additional area is a qualitative predicate for 'good approximation'.

3) If the additional area is not small, then split the curve into two. Replace the two curves. For the replacement of these two curves, the good approximation criterion should be applied to the total area rather than individual application to each of the curves.

4) Curve splitting : The curve is split at the point on the boundary which is at the maximum distance from the chord (the dotted line in Fig. 7.2).

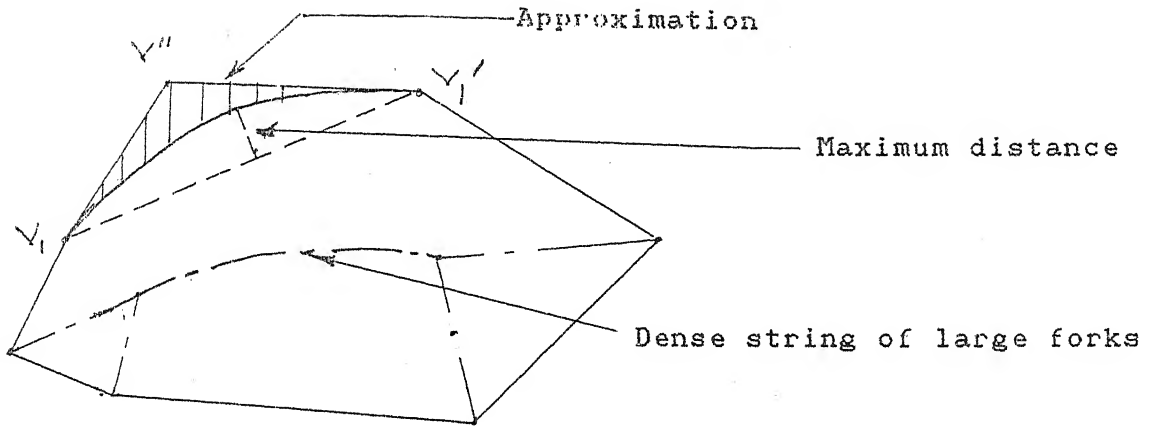

Fig. 7.2 Curve Approximation

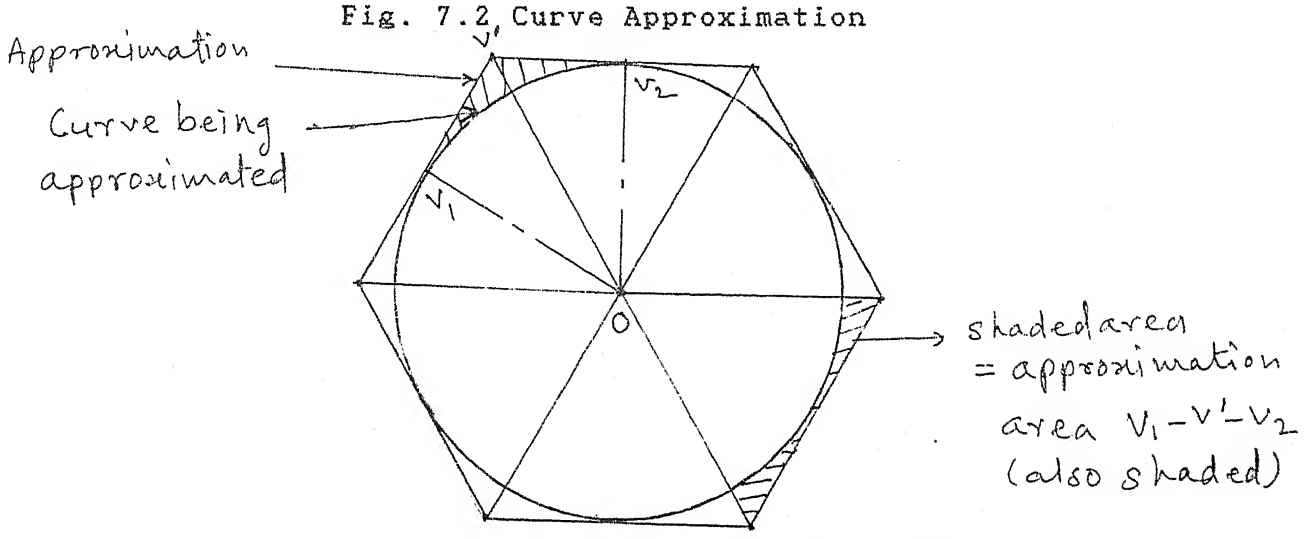

Fig. 7.3 Curve Approximation Closeness

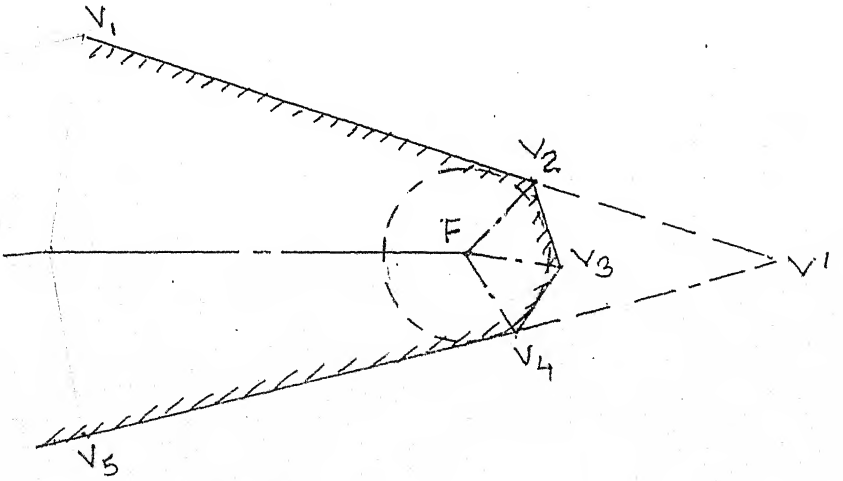

$V_2 - V_3 - V_4$ replaced by $V_2 - V' - V_4$.

Fig. 8.1 Rounded Corner Approximation

5) The numerically short curves are approximated as rounded corners as in the step 2 of the section 8.

7.3 Closeness of Approximation :

This criterion is adjusted as per the requirements of section 10. A circle can at worst be reduced to a hexagon. In Fig. 7.3, a closeness approximation would be the ratio of the shaded area to the area of the sector O-V -V . The ratio R , is given by,

$$R_g = \frac{r^{**}2 / \text{sqrt}(3) - II * r^{**}2 / 6}{r^{**}2 / 6}$$

$$= 2 * \text{sqrt}(3) - II = 0.3225;$$

Hence the closeness can be defined as 'less_than 0.3225 '.

8. Procedure of Fork Pair Approximation :

The LL--LS, LL------Ls forks are detected as rounded corners and LL--LL forks as small elongations. The rounded corners are approximated by extension of the polygon. The small elongations are approximated by merging the forks. It is a fuzzy spawning process. The fork pairs which have a reasonably good confidence value of both the classes spawn two children processes. It is also a sequential process in the sense that the forks are examined one by one.

1) Examine a fork for LL--LS, LL------LS or LL--LL categorisation. If it is LL--LS or LL------Ls then go to step 2. If it is LL--LL go to step 3.

2) LL--LS and LL------Ls rounded corner replacement : Extend the edges forming the NACSIL in the pair till they meet. Delete the small fork from the fork - NACSIL tree and the skeletal tree. In the Fig. 8.1 the small fork f_2 is deleted as shown by deleting the edges e_{12} and e_{34} till they meet at new vertex V_5.

3) LL--LL small elongation merging : Merge the two forks into one fork at the point on the NACSIL dividing the NACSIL into a ratio of intensities of the two forks. The CSILs in the two forks also deviate accordingly (see Fig. 2.6.12.1 and Fig. 2.6.12.2 for the exact deviation in the CSILs).

9. Procedure for Global Small Fork Approximation :

It is a direct sequential process in which the globally small forks are detected and approximated as rounded corners.

1) Examine a fork for global smallness.

2) Determine the larger of the two neighbouring forks. Delete the fork under consideration by extending the edges forming the NACSIL between the fork and the largest neighbouring fork. The extension is the same as that in section 5. (ref. Fig. 8.1)

10. Procedure for Fork Simplifications :

The circular curved boundary sections in forks may be rounded corners or curves. The curves are replaced first and then the rounded corners.

The curves are detected by application of the qualitative predicate stated in section 2.6.11. They are approximated as in section 7.2. The criterion for the acceptable approximation closeness is adjusted so that a circular polygon with large number of sides does not get reduced to a quadrilateral, but remains a circular polygon. It is a simple sequential process.

The rounded corners identification and replacement is also a simple sequential process.

1) Rounded corner detection : Examine a fork for a circular rounded corners, by applying the qualitative predicate for

detection as stated in section 2.6.11.

2) Replacement : It is the same as that in section 5.

11. Procedure for separation of Elongation and Unifork :

The separation of elongation and unifork is basically a tree traversal problem. The largest fork is located first and it is treated as the root of the tree for tree traversal.

1) Location of the largest fork : The fork - NACSIL tree may have two forks with the same largest radius. In such a case a new fork is created at a point on the NACSIL between the two forks, dividing the NACSIL in the ratio of the respective fork intensities. This fork is treated as the root for separation.

2) The tree is scanned in a depth first traversal. The NACSILs are recorded to form the elongation tree. The ACSILs are shifted to the root node to form the unifork.

12. Procedure for Unifork classification :

The unifork classification is a fuzzy spawning process in all its steps. The number of sides is determined first. Then the appropriate feature detection and classification is followed. Feature detection is common for triangles and polygons with more than four sides. For a quadrilateral, the classification is based on the angles between the ACSILs.

12.1 Determination of the Number of Sides in a Polygon :

The number of sides in the polygon = number of 'not low' intensity ACSILs. As explained in section 10, if an ACSIL is on the border of 'not low' intensity, two branches of the decision tree are created, one treating the ACSIL as 'not low' intensity, and the other treating it as low intensity.

12.2 Feature Identification :

The beak and bulge detection is done on the basis of the quench velocities of the ACSILs. The quench velocity range division is fuzzy.

Beak : $V_q > 1 / \sin(30)$;

Prominent beak : $V_q >= 1 / \sin(15)$;

Middle level beak : $1 / \sin(15) < V_q <= 1 / \sin(25)$;

Incipient beak : $1 / \sin(25) < V_q <= 1 / \sin(30)$;

Bulge : $1 / \sin(30) < V_q <= 1 / \sin(45)$.

The proposed fuzzy membership distribution functions, in terms of the polygon interior edge angle ϕ are given in Fig. 12.2.

Feature identification for quadrilaterals is the comparison of various angles with constants and among themselves. The fuzzy membership functions for these features have already been proposed in section 3.5.3.

The feature detection process is sequential i.e. the features are detected one by one. It is also a fuzzy spawning process.

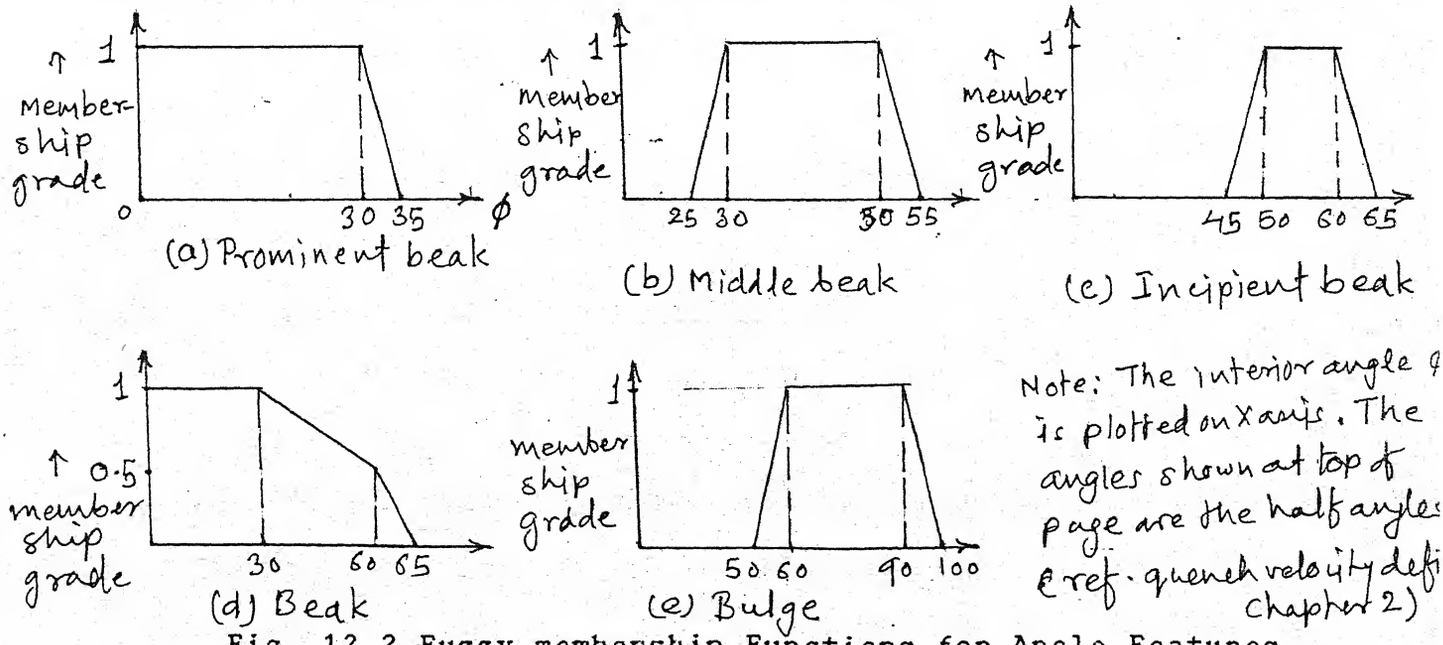

Fig. 12.2 Fuzzy membership Functions for Angle Features

12.3 Unifork Classification :

Unifork classes may be considered to be hierarchical. The classification process is a fuzzy spawning traversal of a path in the decision tree of the hierarchy. The decision tree of the hierarchy is very simple to construct. The first decision is based on the number of ACSILs which is the same as the number of sides. If the unifork is a triangle, then the further decision tree is based on the classification given in section 3.4. If it is a quadrilateral, the further decision tree is based on the classification given in section 3.5. For a polygon with higher number of sides, the tree is based on the classification in section 3.6.

13. Procedure for Elongation Classification :

Elongation classification is also a hierarchical scheme. The first level of the hierarchy is the number and length combination decision. Then the curve trend analysis is done and the resulting combinations with number and length classes are the final classes of elongation.

Evaluation of the mean elongation line and the mean deviation precede the classification process.

13.1 Number and Lengths of Elongations :

Elongation branches may be on or two in number. The length of elongation is the length of the mean elongation line. It is compared with the unifork radius for relations of 'much larger' and 'comparable' length. These two are the length classes, called respectively 'very long' and 'long'. The combinations of the number and length classes are the first level classes. In addition

to these, a category of two very long elongation branches which are at an angle with one another and the category of two very long collinear elongation branches are also formed. The mean elongation line is considered for the purpose of angle evaluation.

13.2 Curve Trend :

Monotonic inclinations represent a curve trend. The average curvature value and a low inclination deviation for curvature give the curve trend.

The inclination trend is followed from the unifork origin till the tip of the elongation branch. At each local reversal in trend of inclination, inclinations may be increasing or decreasing, the deviations are smoothened out, as stated in section 4.3 (ref. Fig. 4.3.1). This is continued till a uniform increasing or decreasing trend is obtained through out the elongation branch. The average curvature and the mean inclination deviation are calculated. A curve is detected by a high curvature and low mean inclination deviation. The sign of curvature indicates whether it curves upwards or downwards.

The presence or absence of a curve, and its direction of curvature in relation to the other curve if it is present, form the basis of the classes.

14. Procedure for Favoured Direction Analysis :

1) Stretch axes determination :

Stretch axes are the ACSIL lines of beaks and bulges, and the NACSILs of elongations. The mean elongation line is also taken to be a stretch axis. The measures of favouredness of all the stretch axes are calculated.

2) Intermediate feature axes determination :

Pairs of highly favoured feature axes with close inclinations are detected. The intermediate feature axes and their favouredness are calculated as stated in section 5.1.

3) Symmetry axes determination :

Pairs of highly favoured axes with equal favouredness measure, and which do not have close inclinations, are detected. The Symmetry axes and their favouredness are calculated as stated in section 5.1.

15. Procedure for Description :

The classifications are based on the features detected and their geometrical relations. The proposed classification is hierarchical in nature. The process of classification can be modeled as a decision tree with fuzzy spawning. The decisions are based on the detected features and the geometrical interrelations among them. These have already been expounded earlier.

The decision trees are different for each of unifork classification of triangles, quadrilaterals and polygons with higher number of sides, and the elongation classification. The exact codification of the decision trees and the process of their combinations to form the complete decision tree is self evident from the proposed classification scheme.

The complete convex polygon description consists of the multiple classes, their membership grades and the area approximation measures, their internal dominance relations, favoured axes and the size parameters. The multiple classes and the memberships are generated by the classification procedure given in sections 7 to 12. The internal dominance relations within a class are generated

in the same process. The favoured axes generation procedure is given in section 13. The size parameters are determined along with the favoured axes determination.

The fuzzy spawning can be modeled as backtracking upto a marked decision for the purpose of program design. Hence essentially the process model for program design is the same as that for polygon decomposition.

16. Example of Convex Polygon Description :

The examples of description are taken from the first decomposition, of the profile given in the example of decomposition algorithm (ref. chapter 3, section 9. Fig. 9.3). All the three CCPs of the profile, C_1, C_2 and C_3, are described here.

1) CCP C_1 is shown in Fig. 16.1. It is a triangle with angles θ_1 = 32, θ_2 = 56 and θ_3 = 92. As there is only one fork, no approximations are needed. It can be directly classified.

Beak analysis (ref. section 3.4) :

θ_1 : Prominent Beak , 0.45 membership, and Middle Beak 0.55 membership.

θ_2 : Incipient Beak 1.0 membership.

Hence the given CCP C_1 is a triangle, of class

a) PB-IB with 0.45 membership,

b) MB-IB with 0.55 membership.

The feature axes are along the CSILs emanating from the fork. They are,

a) CSIL $F\text{-}V_1$: size 21 mm,

b) CSIL $F\text{-}V_2$: size 13 mm,

c) CSIL $F\text{-}V_3$: size 8 mm.

Feature axis in a) is the most important as the corresponding CSIL has maximum intensity.

2) The CCP C_2 has two forks F_1 and F_2 (ref. Fig. 16.2). The fork pair is LL------LL. Hence there are no approximations. The separated unifork and elongations are shown in Fig. 16.2 (b). The polygon is a quadrilateral.

Unifork Analysis (ref. section 3.5) :

$\Theta_1 = 87$, $\Theta_2 = 109$, $\Theta_3 = 93$, $\Theta_4 = 71$;
$\phi_1 = 130$, $\phi_2 = 56$, $\phi_3 = 88$, $\phi_4 = 86$.

Application of the rules for classification :

$\theta_1 = 90$, $\Theta_1 \neq \Theta_4$, $\phi_1 \neq 0$, $\phi_4 \neq 180$.

Hence from table 3.5.3, the convex polygon is of unifork type 12, with unifork radius of 12.6 mm.

Elongation analysis :

The polygon has only one elongation line (line F_1-F_2 in Fig. 16.2 (a)). It's length is comparable to the unifork radius. Hence it is 'long' elongation (ref. section 13.1). There are no curves in elongation.

Feature axes :

The feature axes are, in descending order of importance, F_1-F_2, F_1-V_2, F_2-V_3, F_2-V_4, F_1-V_1. The sizes along the feature axes are, F_1-F_2 : 18 mm, F_1-V_1 : 13.5 mm, F_1-V_2 : 25.5mm, F_2-V_3 : 19 mm, F_2-V_4 : 19mm.

3) The CCP C_3 (ref. Fig. 16.3) is a convex polygon with large number sides. It has no elongation curves, as there are no long strings of locally large proximal forks (ref. section 7.1). It has the following fork pairs.

F_1 -F_2 : Largeness ratio L_r = 0.934,
Proximity ratio P_r = 0.23, LL-- LL;

F_2 -F_3 : Largeness ratio L_r = 0.961,
Proximity ratio P_r = 0.205, LL--LL;

F_3 -F_4 : Largeness ratio L_r = 0.738,
Proximity ratio P_r = 0.57, LL------LS;

F_4 -F_5 : Largeness ratio L_r = 0.748,
Proximity ratio P_r = 0.4, LL------LS.

Fork pair approximation (ref. section 8) :

F_3 -F_4 and F_4 -F_5 are approximated by rounding of the corners, i.e. by extending the edges V_9 -V_4 and V_{12} -V_{11} till they meet at V_{13} (ref. Fig. 16.3 (b)). F_1 -F_2 and F_2 -F_3 are now negligibly small. They are merged in to the CSIL F_3 -V_{13} .

There are no more approximations. The next step is separation. The unifork radius is 15 mm. The NACSILs are very minor, and they have already been merged in to the neighbouring CSILs. Hence elongations are absent.

Unifork Classification :

There is only one beak at V_{13}, ϕ = 54, Incipient Beak.

Hence the given CCP is a polygon with large number of sides and with one incipient beak.

Feature axes :

One important feature axis along CSIL F_3 -V_{13}, size 32 mm.

The low intensity axes are :

F_1 -V_4 : size 15.5 mm, F_1 -V_3 : size 15.5 mm, F_1 -V_2 : size 15.5 mm,
F_2 -V_1 : size 17 mm, F_3 -V_{12} : size 15mm.

The profile and CCPs after approximations are shown in Fig. 16.4.

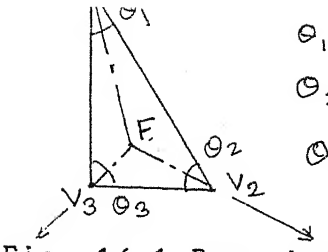

$\Theta_1 = 32^\circ$; F-V$_1$ = 21 mm ;
$\Theta_2 = 56^\circ$; F-V$_2$ = 13 mm ;
$\Theta_3 = 92^\circ$; F-V$_3$ = 8 mm ;

Fig. 16.1 Description of a Triangle

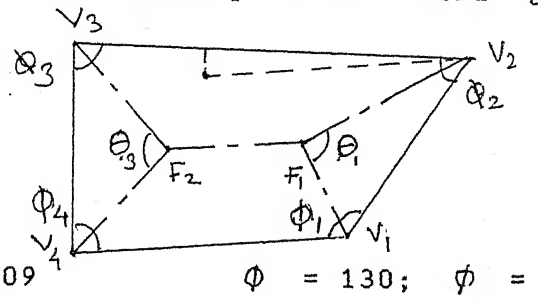

$\Theta_1 = 87$; $\Theta_2 = 109$; $\Theta_3 = 93$; $\Theta_4 = 71$

$\Phi_1 = 130$; $\Phi_2 = 56$; $\Phi_3 = 88$; $\Phi_4 = 86$

Fig. 16.2 Description of a Quadrilateral

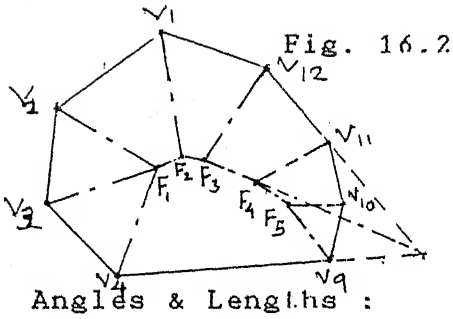

F$_1$ = 14.1 mm; F$_2$ = 15.1 mm;
F$_3$ = 14.5 mm; F$_4$ = 10.7 mm;
F$_5$ = 8 mm.

Angles & Lengths :

F$_1$ - V$_4$: 132, 15.5 mm;
F$_1$ - V$_3$: 130, 15.5 mm;
F$_1$ - V$_2$: 130, 15.5 mm;
F$_2$ - V$_1$: 125, 17 mm;
F$_3$ - V$_{12}$: 150, 11 mm;
F$_4$ - V$_{11}$: 153, 8 mm;
F$_5$ - V$_{10}$: 153, 8 mm;
F$_5$ - V$_9$: 107, 10 mm;,
F$_5$ - F$_4$: 80, 5 mm;
F$_4$ - F$_3$: 54, 8 mm;
F$_3$ - F$_2$: 54, 8 mm;
F$_2$ - F$_1$: 33, 4mm.
F$_1$ - F$_2$: L$_r$ 0.934, P$_r$ 0.23; LL--LL
F$_2$ - F$_3$: L$_r$ 0.961, P$_r$ 0.205; LL- LL
F$_3$ - F$_4$: L$_r$ 0.738, P$_r$ 0.522; LL------LS
F$_4$ - F$_5$: L$_r$ 0.75, P$_r$ 0.4; LL------LS

Fig. 16.3 Description of a Polygon with High Number of Sides

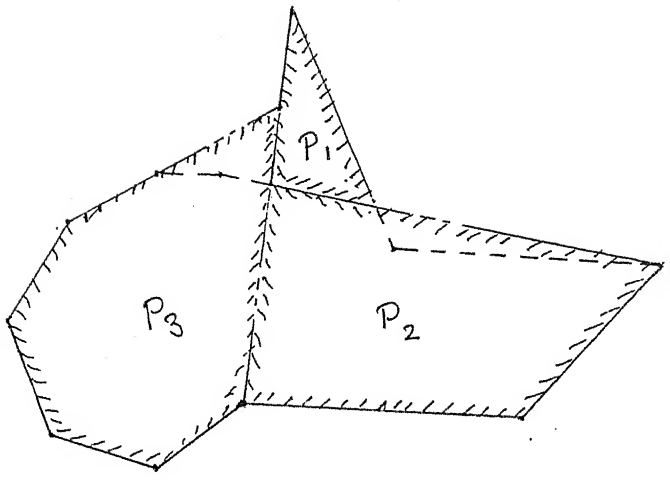

Fig. 16.4 Approximated Profile and its CCPs

Chapter 5

PROFILE DESCRIPTION

1. Introduction :

The approach of the present work towards nesting is based on a shape and size matching of profiles. A description of the profiles to be allocated is to be matched against the description of the complimentary area of the allocation sheet formed by previous allocations, to maximise nesting efficiency. Profile description is the crux of the approach.

Proposals for decomposition of profile in to the 'Constituent Convex Polygons', henceforth abbreviated as CCPs, and description of the CCPs have been outlined in the previous chapters. After the conclusion of these analyses, the profile model is in the form of a union of the CCPs, and their descriptions. The proposed profile description is based on the following :

1) A further analysis of the concavities of the profile, henceforth referred to as bays.

2) Identification of shape features likely to be useful in nesting. Only the projections of the profile are considered in the present work. Boundary features such as long straight edges for edge justification in juxtaposition of profiles has not been considered.

3) A study of the geometrical and topological relations among the projections and the bays of the profile.

Description of the profiles for matching and concomitant nesting is enumerative in nature rather than a classification as was done

for the convex polygons. A classification is not attempted in the present work as it would be extremely complex.

The basic requirements to be satisfied by profile description :

A profile may be rotated, displaced along the X and Y directions in the nesting plane, or it may flipped for allocation. Hence the description of a profile must be independent of rotation, displacement and mirror imaging transformations in the nesting plane.

2. Bay Analysis :

The aim of the description of the shape of a profile is that the description should be useful in the nesting allocation of the profile. A nesting allocation needs an identification of the 'projections' and the 'bays' of the profile which may be fitted snug against the bays and projections respectively of the profiles already allocated. The projections and bays of a profile could be matched against the projections and bays of the 'complimentary profile'. In the Fig. 2.1, the profile P_f, is being allocated. The shaded area is the region of the sheet on which the earlier allocations of profiles have been done. The unshaded area of the sheet is the complimentary profile with which the profile P_f is to be matched, and on which P_f is to be allocated. It can be seen that not only the projections of P_f and the complimentary profile may be matched, but also the concave parts of the two profiles may be matched for nesting efficiency. P_f has projections P_1, P_2, P_3 and bays B_1, B_2 lying in between the projections. The projection P_1 is matched with a projection of the complimentary profile. The projections P_2 and P_3 do not match exactly with the projections of the complimentary profile but the bay B_2 matches with a bay of the

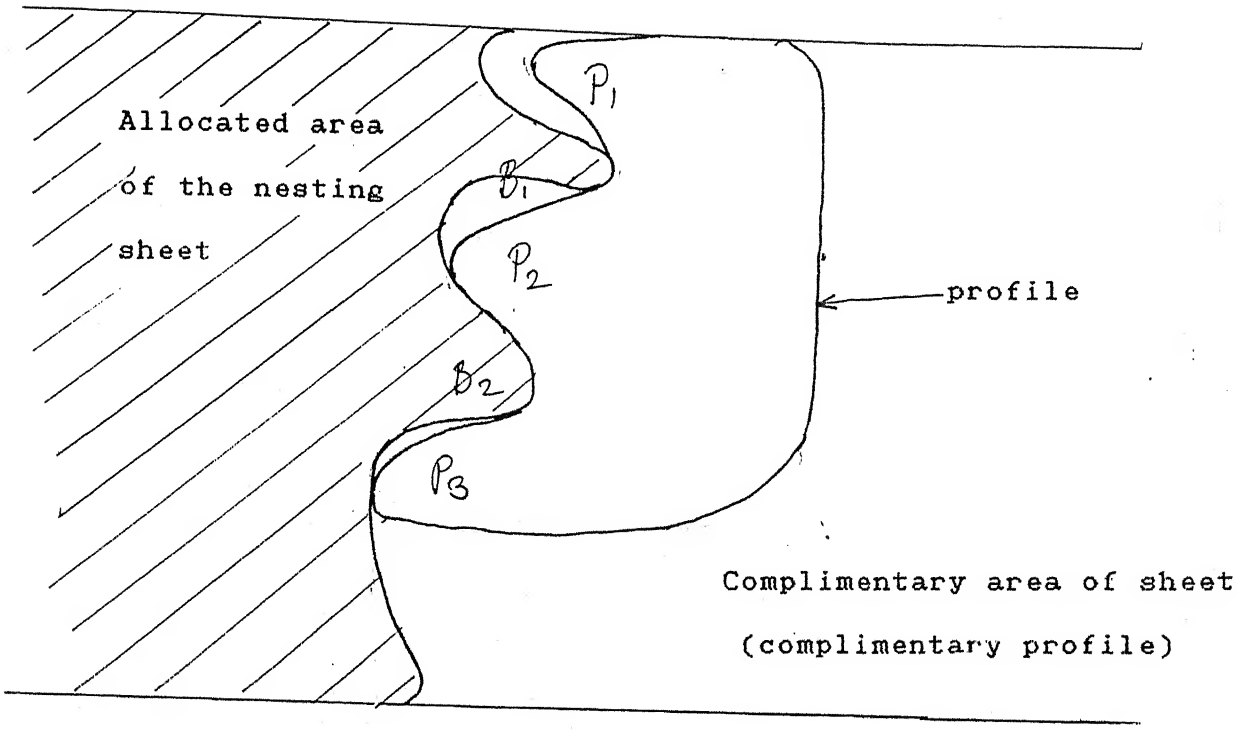

Fig. 2.1 Bay Matching in Nesting

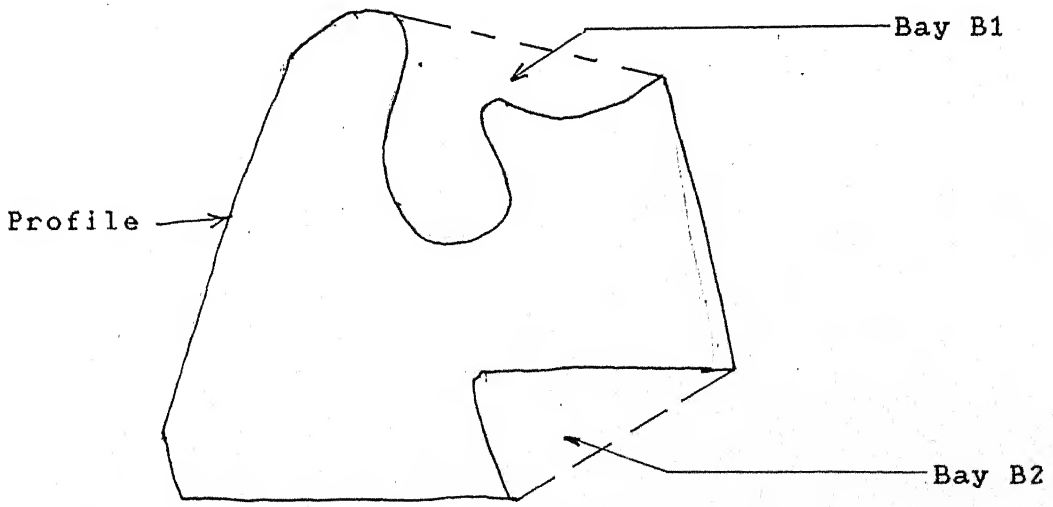

Fig. 2.1.1 Definition of Bays

complimentary profile.

A description of a profile can not be truly complete without a consideration of the bays of the profile. The bays give the interactions of the profile boundary across the exterior (ref. section 3, chapter 2).

2.1 Discussion on bay analysis :

Bays form an integral part of the shape of a profile. Bays are regions of the exterior of the profile delineated by the projections of the profile. Alternatively, bays can be thought of as the projections of the exterior of the profile or projections of the complimentary area of the profile, in the plane of the profile.

Bays could be detected by a decomposition of the complimentary area of the profile along the same lines as the decomposition of the profile. A simpler approach is proposed in the present work. Bays may be defined as the complimentary regions of a profile in the convex hull of the profile. In Fig. 2.1.1, the convex hull of the profile P_f is shown in dashed lines. B_1 and B_2 are the complimentary regions of the profile in the convex hull. They are the bays of the profile. This definition exactly delineates bays as two dimensional profiles which are exactly located in the plane with respect to the original profile. The problem of identifying the bays is that of obtaining the set of cycles in the geometrical graph formed by the boundary of the profile and the convex hull of the profile. Due to the definition of the convex hull, it is guaranteed that the bays, i.e. the cycles in the aforementioned graph, are mutually exclusive. The problem of identification of

such cycles is a standard problem and standard solutions exist in the literature [12].

As bays themselves are profiles, they can be analysed in the same way as the profiles. The integration of the two analyses may be used as a description of the profile. The shape analysis of a bay differs from the shape analysis of a profile only in the details of the approximations done in the analysis process. The approximations in the analysis of a profile are of the form of external envelopes; whereas the approximations in the analysis of bays are, what may correspondingly be called as the 'internal envelopes' of the polygon. The exact meaning of this term will be clarified in the next section where the 'internal envelope approximations' are proposed.

The difference between approximation method arises because of the basic nature of nesting. The most basic constraint on allocation of profiles is that there should be no overlap of the profiles. External envelope approximations in shape analysis of profile guarantee that if the approximated profile is allocated, checking the constraint satisfaction, there would be no overlap of the exact profiles. Similarly, internal envelope approximations in bay analysis ensure that the approximate bays and their descriptions may be used in allocation.

2.2 Bay analysis algorithm vis a vis profile shape analysis :

As stated above, bay analysis is the same as the profile shape analysis, except for the approximation methods, it suffices to just give the 'internal envelope approximations' of the bay, to lay down the procedural algorithm for bay analysis, after the bays have been identified. The algorithm is as follows :

2.2.1 Identification of bays :

1) Determine the convex hull of the approximated profile. These approximations are the external envelope approximations outlined so far in chapters on profile decomposition and convex polygon description.

2) Bays are the complimentary areas of the approximated profile with its convex hull.

3) Bays are analysed as independent shapes upto and including the neighbourhood relationship analysis given in section 3.

2.2.2 The approximations in shape analysis of bays :

1) Approximations in decomposition of bays into constituent convex polygons :

The 'straightening up' approximations (ref. section 6.5.1, chapter 3) are the same as 'cuts' (ref. section 6.5.2, chapter 3). A cut divides the profile in to two or three constituent polygons. The criterion to distinguish between a cut and a straightening up approximation is that one of the polygons resulting from the cut should have a small area in comparison with the area of the other polygons. The polygon with small area is neglected altogether.

2) Curve approximation in convex polygon description :

Curve approximations (ref. section 7, chapter 4) for bays are illustrated in Fig. 2.2.2.1. The curve V_1 -V_1 ' is approximated by the pair of lines V_1 -A and A-V_1 '. The point A is the point on the curve V_1 -V_1 ' at the maximum distance from the chord V_1 -V_1 '. The procedure for approximations and the definition of closeness of approximation remain the same.

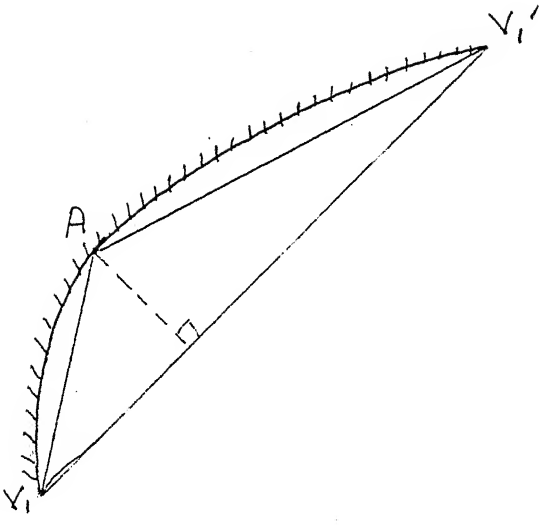

Curve $V_1 - V_1'$ approximated by
line segments $V_1 - A\ V_1'$
Point A is at maximum distance
from $V_1 - V_1'$

Fig. 2.2.2.1 Curve Approximation in Bays

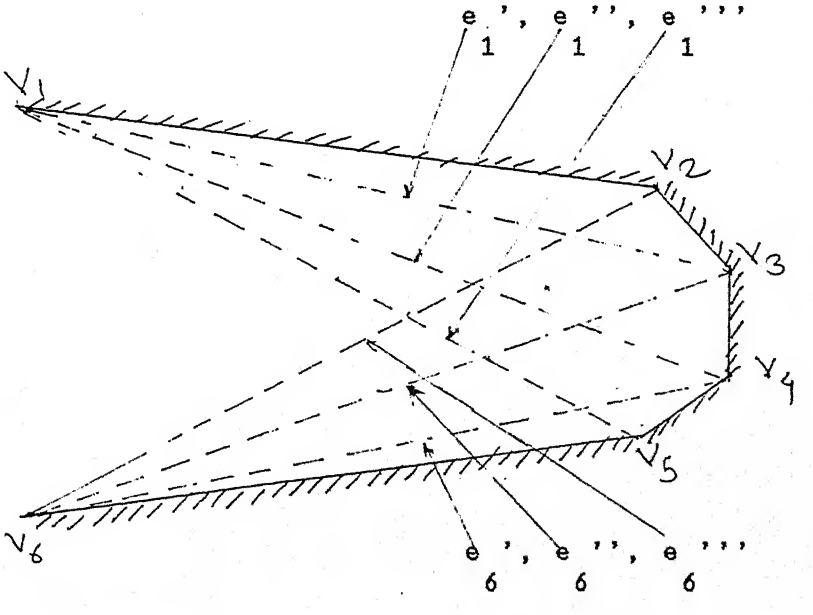

Fig. 2.2.2.2 Fork Pair Approximation in Bays

3) Fork Pair Rounded Corner Approximation :

It is done for uneven size forks, as in convex polygon description (ref. section 8, chapter 4). In Fig. 2.2.2.2, f_1 is the large fork and f_2 is the small fork of the part of polygon $V_1 - V_2 - V_3 - V_4 - V_5 - V_6$. The approximation lines e_1', e_1'', e_1''' from the upper side of the polygon and e_6', e_6'', e_6''' from the lower side of polygon, form the possible approximations. Of all the approximations, the approximations with minimum area approximation and with the approximated area equally divided on either sides, are selected. For the approximated area being equally divided on either sides, in Fig. 2.2.2.2, if the approximation $e_1'-e_6'''$ has minimum area then, the areas $V_1 - V_2 - V_3$ and $V_6 - V_5 - V_4 - V_3$, should be approximately equal.

4) Rounded corner at a fork :

It is the approximation given in section 10 of the chapter 4. It is exactly the same as that given in the part two of the current section.

2.3 Niche of bays and bay analysis in profile description :

After the identification of bays and the analysis of the bays up to the convex polygon description stage as expounded in the previous chapters, the shape knowledge extracted from the profile is in the following state.

The profile model is in the form of a convex hull. The convex hull is a union of the approximated original profile and the bays of the profile. The bays are decomposed in to their constituent convex polygons (CCPs). The descriptions of the CCPs of the bays and the profile are present in the profile model. The bays have

diverse geometrical and topological relations with the CCPs of the profile. The geometrical and topological relations among the bays and the profile are important for nesting. The formulation and analysis of these relationships are given in the next section.

The bay identification and analysis is performed after the projection relation analysis, proposed in the section 3.2 of the present chapter. The bay analysis, as stated earlier, differs very little from the profile analysis. It consists of the profile analysis, with the differences stated in section 2.2.1, up to and inclusive of projection relation analysis.

2.4 Bay Merging :

In the course of nesting, some of the identified bays may not be useful. It may happen that, a strong match of some other projections and bay features may preclude the utilisation of some of the bays. Such a situation is illustrated in Fig. 2.4.1. A very good match of the dominant projections P_1, P_2 and the bay B_1 forces an allocation which wastes the area of the bay B_2. Such a situation may also arise for highly complicated shapes. It may also happen that a matching bay is not found at all in the complimentary profiles formed during the allocation. To obtain a shape match match in such situations, it is required to merge some of the bays into the profile. After merging a bay in to the profile, the new profile, referred to as 'Bay Merged Profile'(BMP) henceforth, is subjected to shape analysis to obtain its description.

A model of the profile in which a number of BMP versions of the profile are formed by merging combinations of bays in to the profile, can generate descriptions to satisfactorily handle the

cases described above.

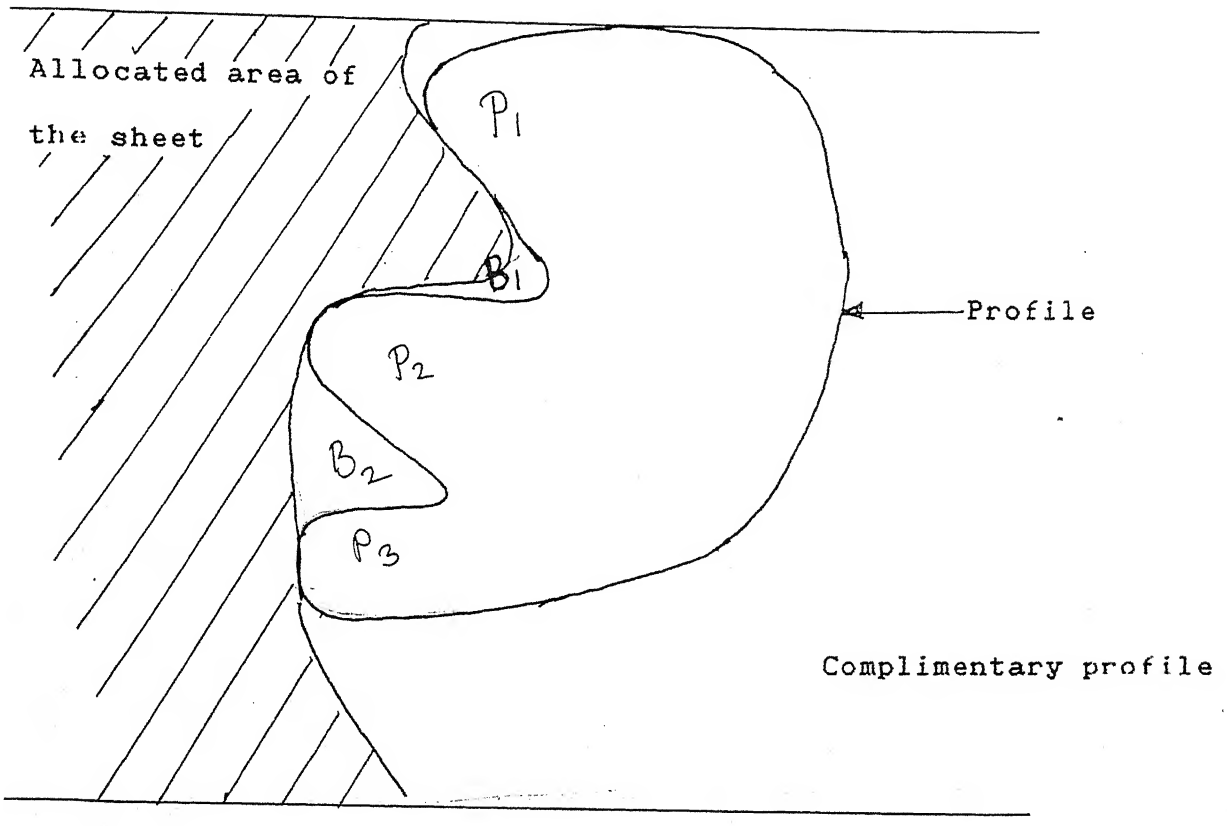

Fig. 2.4.1 Need to Merge Bays

3. Profile Description :

Description of a profile, as stated earlier, is an enumeration. The geometrical and the topological relations among the CCPs and bays, along with the CCP description, constitute the profile description. All the CCPs do not play an equal role in description. The CCPs, which project out of the profile and form bays between them are more important for nesting. These CCPs, called projections, are identified on the basis of their topological relations.

3.1 Topological relations among the CCPs :

3.1.1 Basic Idea of topological relations :

Topological relations are the connectivity relations among the CCPs, indicating the neighbourhood of the CCPs. Classically, these relations would be represented by an adjacency graph of the CCPs; where in the individual CCPs are the nodes of the graph and the existence of a shared edge between two CCPs producing an edge of the graph between the two nodes. Such a graph, does not satisfactorily model the relationships among the CCPs. In Fig. 3.1.1.1, CP_1 and CP_2 are two CCPs. In part (a), they share an edge; and hence they would be depicted as neighbours in the adjacency graph. In part (b) they do not share an edge. They are separated by a thin wedge. Here, they would not have any neighbourhood relationship between them. This does not discern between the neighbourhood relation of CP_1 with CP_2 and some other distant CCP. Also, an adjacency graph does not distinguish between the two situations depicted in parts (a) and (b) of Fig. 3.1.1.2. These two cases are distinctly different, and should be represented distinctly from one another.

Different types of neighbourhood relations are defined in the present work, which overcome these drawbacks. They represent actual connectivity relations more accurately than the adjacency graph.

3.1.2 Basis of the neighbourhood relations :

The neighbourhood relations should incorporate the following concepts :

1) The importance of a shared edge, from the perspective of both the CCPs in the relation. The importance of the shared edge may be different in the them. In Fig. 3.1.1.2(a), the shared edge is more important in the CP_1 than in CP_2. The neighbourhood of CP_1 is more important to CP_2 that that of CP_2 to CP_1.

2) Tunneling effect : Two CCPs may not share an edge, but they may be separated by a thin wedge(ref. Fig. 3.1.1.1). The CCPs CP_1 and CP_2 in part (b) of the figure should be considered as neighbours. It can be viewed as a tunneling of the neighbourhood relationship across a barrier. This maintains a continuity of the neighbourhood relation as the two CCPs move apart. The quantity representing the neighbourhood effect should reduce as the separation between the CCPs increases.

3) Geometrical location of the neighbourhood relation : A CCP may share more than one edge with other CCPs. In Fig. 3.1.2.1, CP_1 is a neighbour of CP_2 and CP_3. The neighbourhood relations of CP_1 with CP_2 and CP_3 are exactly located in the plane of the figure. They can be said to act along the lines L_2 and L_3. L_2 and L_3 are the perpendicular bisectors of the respective shared edges.

Definition of neighbourhood relations, henceforth referred to as N relations, incorporating the concepts stated above, is based on the following discussion. The profile model consists of the unapproximated CCPs, which are the result of the decomposition. The skeletons of the CCPs form a geometrical tree. The edges of

the CCPs in combination with the skeletons form a geometrical graph, henceforth referred to as the CCP - skeleton graph. A CCP - skeleton graph is illustrated in Fig. 3.1.2.2. The cycle $C_1-C_2-C_3-C_4-C_5-C_6-C_7-C_8-C_1$, passes through the CCPs CP_1, CP_2, CP_3. The shaded area is the area enclosed with in the cycle. The area $C_1-C_2-C_8$ is a subarea of the cycle. It is the area of the cycle associated with the CCP CP_1. The subarea $C_1-C_3-C_4-C_5$ is associated with the CCP CP_2. The cycle establishes a neighbourhood relation between CP_1 and CP_2, tunneling through CP_3. In CP_1, the area $C_1-C_2-C_8$ is associated with the cycle, out of the total area of the polygon. The area $C_1-C_2-C_3-C_4-C_5-C_6-C_7-C_8$ is the subarea of the cycle, linking CP_1 with CP_2. There may exist more than one cycles connecting two given CCPs. The cycle with the minimum enclosed area is the cycle on which the neighbourhood relation definition is based. Let the cycle $C_1-C_2-C_3-C_4-C_5-C_6-C_7-C_8$ be the minimum area cycle for the CCPs CP_1 and CP_2 in the Fig. 3.1.2.2. Let the areas in the Fig. 3.1.2.2 be denoted by,

A_c = area of the cycle $C_1-C_2-C_3-C_4-C_5-C_6-C_7-C_8-C_1$;

A_1 = area of the polygon $C_1-C_2-C_8$;

A_2 = area of the polygon $C_3-C_4-C_5$;

A_3 = area of the polygon $C_1-C_2-C_3-C_5-C_6-C_7-C_8$;

A_4 = area of the polygon $C_2-C_3-C_4-C_5-C_6-C_7$;

A_5 = area of CP_1 ; A_6 = area of CP_2 .

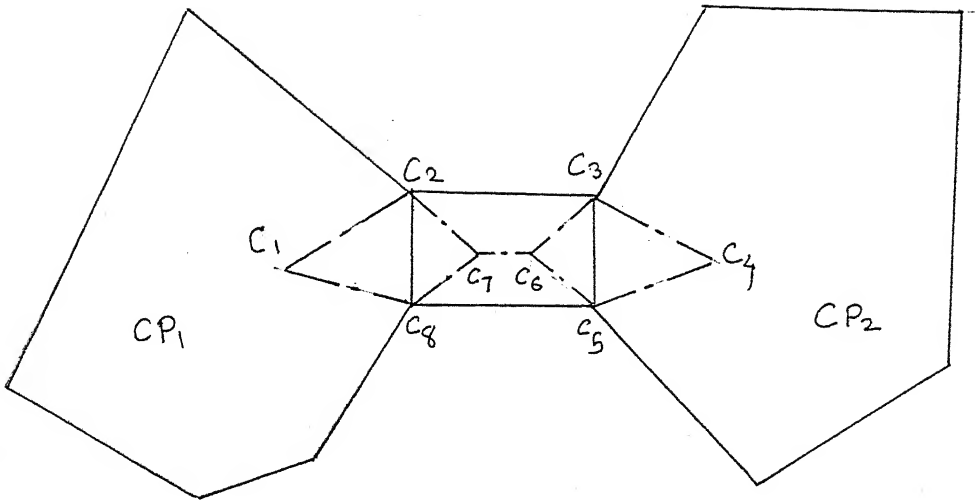

Fig. 3.1.2.2 Cycle Defining Neighbourhood Relations

3.1.3 Type one neighbourhood relations :

A neighbourhood relation between two CCPs, CP_1 and CP_2 of Fig. 3.1.2.2, can be defined from the perspective of CP_1, to indicate how important is CP_2 as a neighbour to CP_1. It is called 'Type One Neighbourhood Relation' between CP_1 and CP_2, henceforth abbreviated as N1 relation between CP_1 and CP_2, represented symbolically as $N(CP_1, CP_2)$.

$N(CP_1, CP_2)$ is defined as

$$N(CP_1, CP_2) = (A_{1\,3} / A_{1\,5}) * (A_{1\,3} / A_{1\,5});$$

acting along a line of action joining the centers of the edges of CCPs, C_2-C_8 of CP_1 and C_3-C_5 of CP_2. It is shown in Fig. 3.1.2.2, as the line L.

It can be seen that N_1 is not commutative, i.e. $N_1(CP_1, CP_2) = N_1(CP_2, CP_1)$. $N_1(CP_1, CP_2) = (A_1 / A_2) * (A_4 / A_6)$; acting along the line of action L.

3.1.4 Type two neighbourhood relations :

A neighbourhood relation between the CCPs CP_1 and CP_2 of the Fig. 3.1.2.2 can be defined so as to indicate a global perspective of the relation, rather than the perspective from one of the CCPs as in N_1. It is called the 'Type Two Neighbourhood Relation', henceforth abbreviated as N_2 relation, represented symbolically by $N_2(CP_2, CP_1, CP_2)$.

$N_2(CP_2, CP_1, CP_2)$ is defined as

$$N_2(CP_2, CP_1, CP_2) = (A_1 + A_2) / A_c ;$$

It is taken to be acting along the line of action L, which joins the centers of the two interacting regions of the two edges involved in the N_2 relation. If the said regions are collinear, then it is the same as that of $N_1(CP_1, CP_1, CP_2)$.

N_2 is commutative, i.e. $N_2(CP_2, CP_1, CP_2) = N_2(CP_2, CP_2, CP_1)$.

3.1.5 Overall neighbourhood relations :

The overall neighbourhood relation between the two CCPs CP_1 and CP_2 of the Fig. 3.1.2.2, is a triad acting along the line of action L i.e.,

$$N(CP_1, CP_2) = \{N_1(CP_1, CP_2), N_2(CP_1, CP_1, CP_2), N_2(CP_2, CP_1, CP_2)\}.$$

The N relation between two CCPs has a unique line of action. Two CCPs may share at most one edge. It can be seen in Fig. 3.1.5.1, that the two CCPs CP_1 and CP_2 must interact through the shared edge only. The cycle C_1, is the minimum area cycle. Any other cycle, such as C_2, would have a larger area than cycle C_1, the cycle through the shared edge.

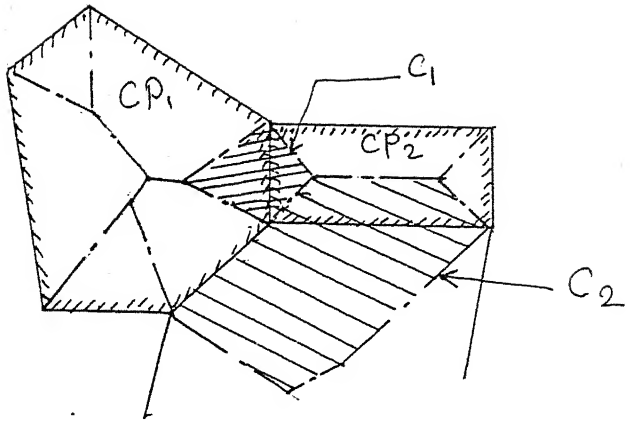

Fig. 3.1.5.1 Minimum Area Cycle

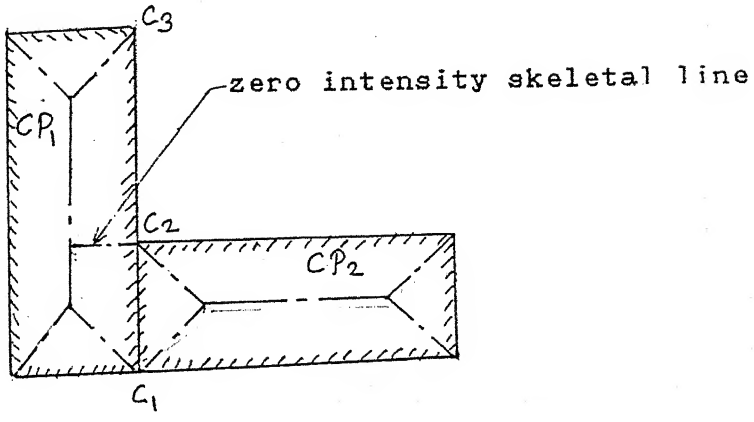

Fig. 3.1.5.2 Ambiguity in Edge Sharing

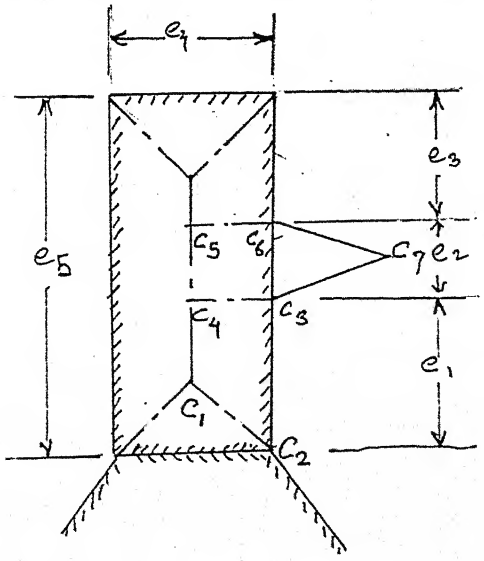

Fig. 3.1.5.3 N1 Relation with Exterior

An edge of a CCP, which it shares with another CCP, may be contained in the edge of the second CCP. In Fig. 3.1.5.2, the edge C_1-C_2 of CP_2 is contained in the edge C_1-C_3 of CP_1. The edge C_1-C_3 of CP_1 thus is shared with more than one CCP or with exterior. The edge C_1-C_3 is divided by introducing a vertex with 180 degrees interior angle at C_2. It gives rise to a zero intensity skeletal line, shown dashed in the figure. Thus the N relations of CP_1 with CP_2 and the other CCPs or the exterior interacting through edge C_1-C_3, are appropriately determined.

Two CCPs in an N relation, may share a vertex, rather than an edge. In such a case, the line of action is defined as the line passing through the common vertex, with inclination equal to the average of the inclinations of the skeletal lines of the two CCPs emanating from the vertex.

The N relation may be extended to cover the interaction between a CCP and the exterior of the profile. In absence of a bay analysis, the exterior may be treated as a polygon with very large area. The interaction of the CCP CP and the exterior is shown in Fig. 3.1.5.3. Only a definition of the N_1 relation is meaningful for C_p and the exterior. As the skeleton of the exterior is not defined, definition of N_2 is not feasible.

In Fig. 3.1.5.3, five different N_1 relations can be defined for CP and exterior. They are between edge e_1 - exterior, e_2 - exterior, e_3 - exterior, e_4 - exterior and e_5 - exterior.

$N_1(e_1, \text{exterior}) = \text{Area}(C_1\text{-}C_2\text{-}C_3\text{-}C_4) / \text{Area}(CP)$; along L_1 ;

$N_1(e_2, \text{exterior}) = (\text{Area}(C_3\text{-}C_4\text{-}C_5\text{-}C_6) / \text{Area}(C_1\text{-}C_2\text{-}C_3\text{-}C_4\text{-}C_5\text{-}C_6\text{-}C_7))$
$* (\text{area}(C_3\text{-}C_4\text{-}C_5\text{-}C_6) / \text{Area}(CP))$; along L_2 .

N_1 relations of e_1, e_3 and e_4 with the exterior are similar top

that of e_1.

3.2 Projections of the profile :

All the CCPs of a profile may not be equally important for nesting. The CCPs which project out of the profile are the important CCPs for nesting. Such CCPs are called the projections of the profile.

3.2.1 Projection identification :

The projection identification is based on the N relations of a CCP in a profile. A Projection would typically have a large peripheral track exposed to the exterior of the profile. In Fig. 3.2.1, the CCP CP is a projection of the profile. It has multiple N_1 relations with the exterior, N_{1i}, i = 1,...,n; where n is the number N_{1i} relations between CP and exterior.

For a projection, $\sum_i N_{1i}$ is close to one. Projections are identified on the application of the corresponding fuzzy qualitative predicate to all the CCPs in the profile.

3.2.2 Interrelations of projections :

For further analysis, only the projections are considered rather than all the CCPs. The projections, linked together by the N_2 relations form a geometrical graph. The graph and its constituent trees and strings, are henceforth referred to as projection graph, projection trees and projection strings respectively.

The important N relation for the identification of strings, trees and graphs is the N_2 relation. An N_2 relation of value almost equal to one indicates a N_2 relation linking two projections in to a string.

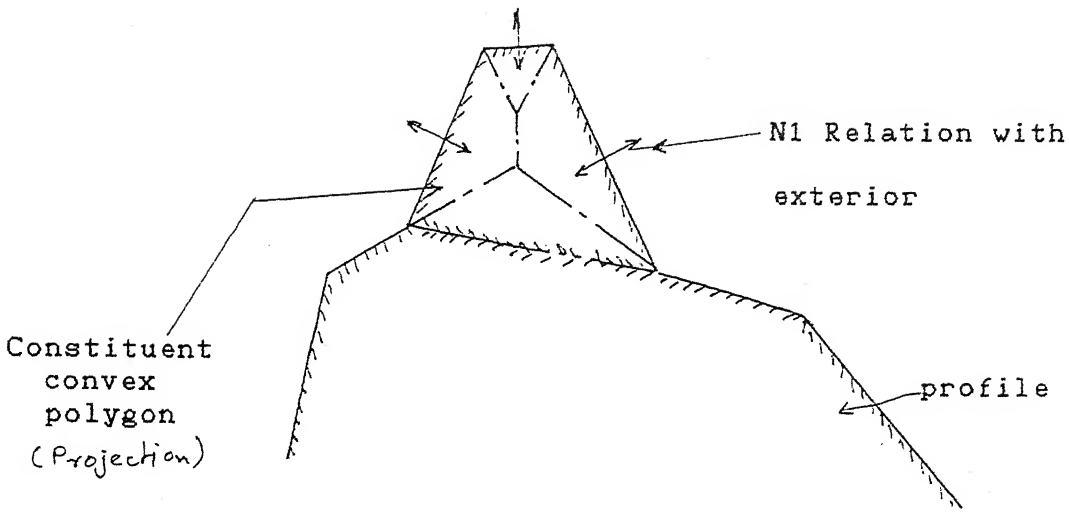

Fig. 3.2.1 Projections and N1 Relations with Exterior

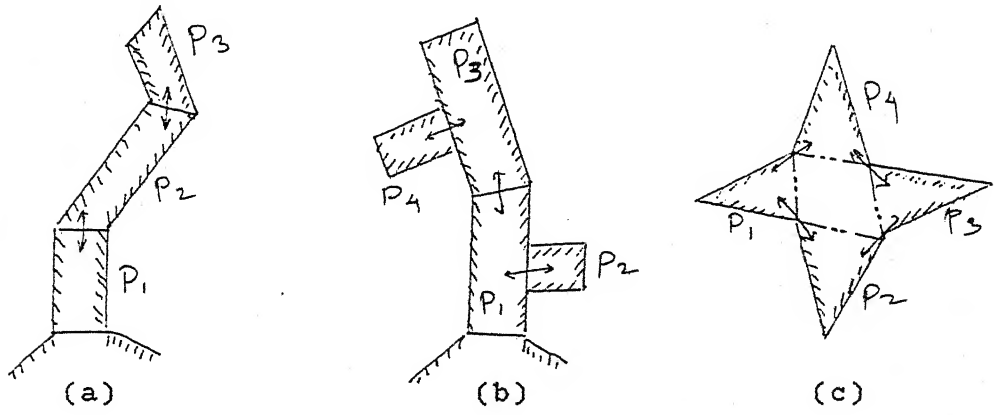

Fig. 3.2.2.1 N-Relations among Projections

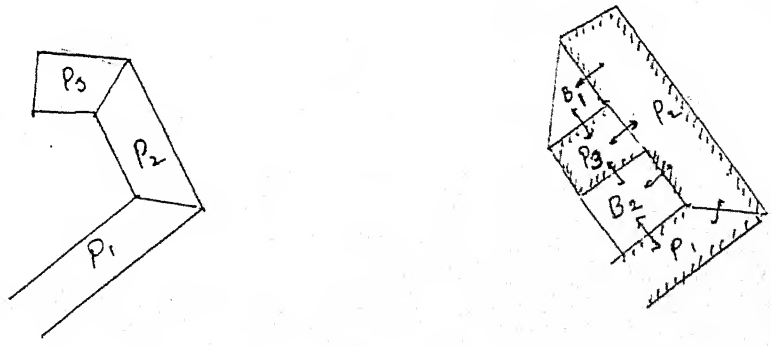

(a) Projection String (b) Projection Tree

Fig. 3.2.2.2 Distinction between Projection Strings & Trees

Various projection N interrelations are illustrated in Fig. 3.2.2.1. In part (a) the projections P_1, P_2 and P_3 form a projection string. In part (b) P_1, P_2, P_3 and P_4 form a tree. In part (c) P_1, P_2, P_3 and P_4 form a cycle i.e. a graph.

The distinction between projection strings and trees may not be as clear as in Fig. 3.2.2.1. The Fig. 3.2.2.2 shows an ambiguous case. The projection P_2 is only linked to P_1. But this is definitely not a string but a tree. Such cases are identifiable by the presence of two bays B and B', between P_1 and P_2. They may be treated as trees by dividing the projection P_1 in to two at one of the concave vertices of the profile on P_1.

3.3 Integration of bay analysis and the profile :

The integration of bays in to the profile model is done after projection analysis. The bays are analysed up to and inclusive of projection relations. Since the bays are also treated as profiles, they may have projections, called the bay-projections. These bay-projections are in contact with the projections of the profile. The first step in integration of bays is the formation of N relations of the bays and projections. The N relations forge links between various CCPs of profile and its bays. Again a geometric graph, called the Bay - Profile N relation graph, is formed by the N relations. The process of forming the N relations between the bay-projections and the projections (of the profile), is the same as that of the N relation formation between the CCPs of the profile as given earlier.

The model of the profile now consists of the projections, bays, and the bay - profile N relation graph. For a complex profile, with a large number of intermingled bays and projections, the

graph is extremely complex. A thorough analysis of such a graph is beyond the scope of the present work. Some of the complexities of a profile may have been removed by the approximations in the profile decomposition. In spite of it, the bay - profile N relation graph may remain very complex.

The model of the profile, at this stage is that of a geometrical graph i.e. a graph in which the nodes and the links are geometrical entities which bear strict positional relations in addition to the topological relations embodied by the graph. The geometrical relations are elaborated in the next section. A shape matching based on the description of a profile at this stage involves an inexact partial matching of a graph, and then the matching of the geometrical aspects of the relations. Inexact matching of a graph has been explored by Shapiro and Haralick [33]. The concepts developed by them could be explored and extended for a shape matching algorithm. It is not attempted in the present work.

The complexities are sought to be reduced by approximations. The secondary features such as the bay-projections and the low intensity projections on the projections are deleted by merging the bays between the secondary projections. Thus the bay-projections are approximated out of the profile model. The profile model at this stage, consists of simple strings of bays and projections. Subgraphs, if they exist, are among the members of a string. An example of such a string relation and a subgraph is given in Fig. 3.3.1. In part (a), the projections P_1, P_2 and P_3 form a string with bays B_1 and B_2. In part (b), a subgraph is

formed among the bay B_1 and the projections P_1 and P_2. Thus, in the further work, the bays and projections will be deemed to be only first order features, and an absence of any second order features will be assumed.

As the shape matching for nesting is likely to be inexact and as it is to a containment matching, i.e. the profile is to be contained in the complimentary profile, some of the bays may not be utilised at all. To facilitate a match under such circumstances, it is desirable to merge bays in to the profile in combinations and analyse the shape of the resulting profile (ref. section 2.3). A multitude of approximated models of the profile are formed by merging the bays in to profile in all possible combinations. The profile is now represented as a number of approximated models.

3.4 Geometrical relations :

The N relations are fixed in the plane of the figure. They act along their particular lines of action. The geometrical relations encode the geometrically located nature of the N relations and the relative location and the orientations of the CCPs or projections and bays. The geometrical nature of the N relations has already been elaborated earlier. The relative locations and relative orientations of the CCPs are quite easy to formulate. It is done by establishing a local co-ordinate system on each of the CCPs and storing the transformations between the local co ordinate systems. The co-ordinate systems are polar co-ordinate systems. This selection helps in ensuring the independence of the description with respect to the mirror imaging transformation. The axes of the co-ordinate systems are the feature axes. The important feature

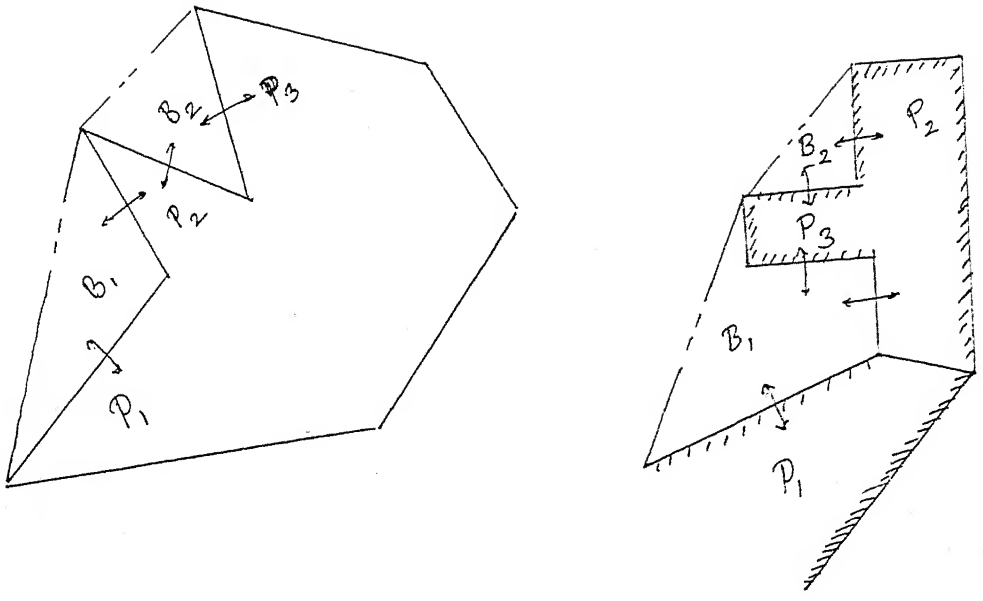

(a) (b)

Fig. 3.3.1 N-Relation among Bays and Projections

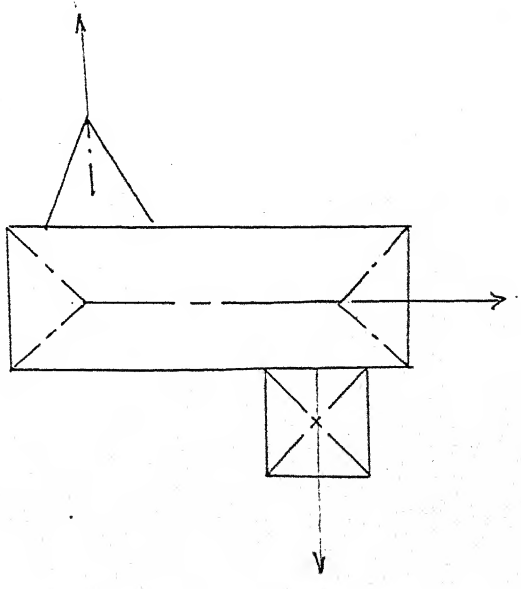

Fig. 3.4.1 Geometrical Relations

axes are selected to form the zero angle direction of the polar co-ordinate system. The zero angle directions are taken to be those which point towards the exterior of the profile and the convex hull of the profile. Thus multiple co-ordinate systems are associated with every CCP. In Fig. 3.4.1, a simple profile is shown. It is composed of the CCPs C_1, which is a rectangle, C_2 which is a triangle and C_3 which is a square. The feature axes for all the three are drawn dotted in the figure. Each of these feature axes can function as the co-ordinate axis direction. In the figure, only one co-ordinate system has been drawn for each of the CCPs. Ray O_1-O_1' is the co-ordinate axis for C1. Ray O_2-O_2' is the co-ordinate axis for C_2. Ray O_3-O_3' is the co-ordinate axis for C_3. The transformations between the pairs of local co-ordinate systems can be written down trivially. The lines of action of the N relations have also been shown in the figure.

The complete polygon description constitutes of the N-relation graph, the descriptions of the CCPs, and the geometrical relations.

4. Example of Profile Description :

The profile, given in chapter 3, section 16 (ref. Fig. 16.4, chapter 3) is again taken as the example for profile description.

1) The N-relations of the CCPs are taken. They are very simple as there are only three CCPs. The N-relations of the CCPs, their lines of action and the cycles of the N-relations, are shown in Fig. 4.1. As all the three CCPs have strong N-relations with the exterior, all are termed as projections.

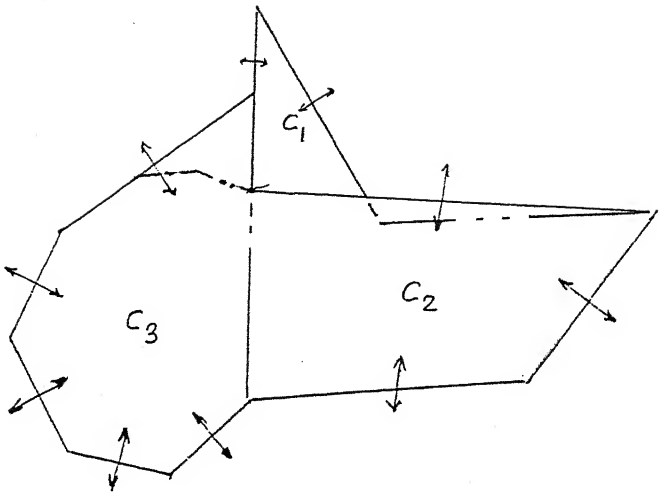

Fig. 4.1 N - Relations among CCPs

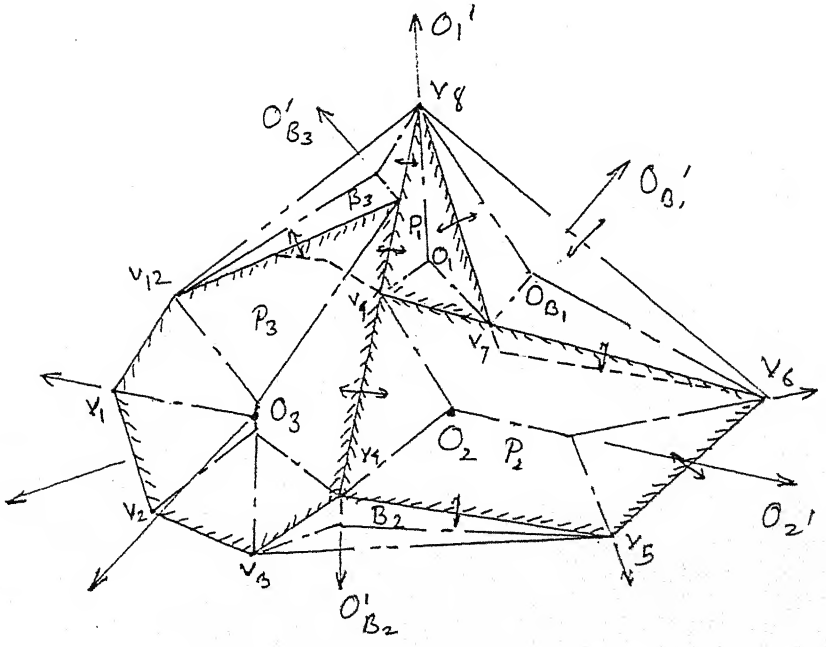

Fig. 4.2 All Relations among CCPs

The profile, after identification of bays and the N-relations of all the projections and bays, is shown in Fig. 4.2. There are three projections, P_1, P_2 and P_3 (corresponding to CCPs C_1, C_2 and C_3 respectively); and the bays B_1, B_2 and B_3 are interspersed among the projections.

The resulting bay-projection strings are :

$P_1 - B_1 - P_2$, $P_2 - B_2 - P_3$, $P_3 - B_3 - P_1$, $B_1 - P_2 - B_2$, $B_2 - P_3 - B_3$, $B_3 - P_1 - B_1$;
$P_1 - B_1 - P_2 - B_2$, $P_2 - B_2 - P_3 - B_3$, $P_3 - B_3 - P_1 - B_1$, $B_1 - P_2 - B_2 - P_3$, $B_2 - P_3 - B_3 - P_1$, $B_3 - P_1 - B_1 - P_2$;
$P_1 - B_1 - P_2 - B_2 - P_3 - B_3$.

The strings $P_1 - P_2$ and other such strings are not considered as they are not bay-projection strings. They are not peripheral and hence do not influence nesting allocation.

The local co-ordinate systems for the bays and projections also have been shown in Fig. 4.2 in the form of arrows. The origins of the local co-ordinate systems are the locations of the unifork center, indicated by O_i in the figure. Projection P_1 has only one important feature axes. The zero angle direction of the local co-ordinate system (polar) is directed along the feature axis $O_1 - V_8$, and directed towards V_8 from O_1, pointing towards the exterior of the profile. P_2 has one important feature axis $O_2 - O_2'$. P_3 has multiple feature axes of comparable importance; $F_{3\,13} - V_{13}$ (reversed to be directed from V_{13} to F_3) is the most important, $F_{1\,2} - V_3$, $F_{2\,2} - V_1$, $F_{1\,3} - V_1$ and $F_{3\,12} - V_3$ are the other less important feature axes. The approximate symmetry axes formed by combinations of feature axes $F_{1\,2} - V_1$, $F_{2\,1} - V_2$, $F_{1\,3} - V_3$ and $F_{3\,12} - V_3$, i.e. $O_3 - O_3'$ is the most important feature axis, hence the best candidate for local co-ordinate direction. For the bays, the symmetry axes formed by

combinations of the feature axes form important feature axes. Thus for B1, Ob_1-Ob_1' is the local co-ordinate direction. Similarly, for B2 and B3, Ob_2-Ob_2' and Ob_3-Ob_3' form the local co-ordinate directions.

The N-relationship graph, the geometrical aspects of the N-relations, the geometrical relations between the local co ordinate systems, along with the CCP descriptions given in the earlier chapters, constitute the description of one 'version' of the profile. The bays are then merged in to the profile in combinations and the same exercise is carried out. The bay merged profiles (BMPs) are illustrated in Fig. 4.3.

The shape descriptions of all the BMPs forms the complete description of the profile.

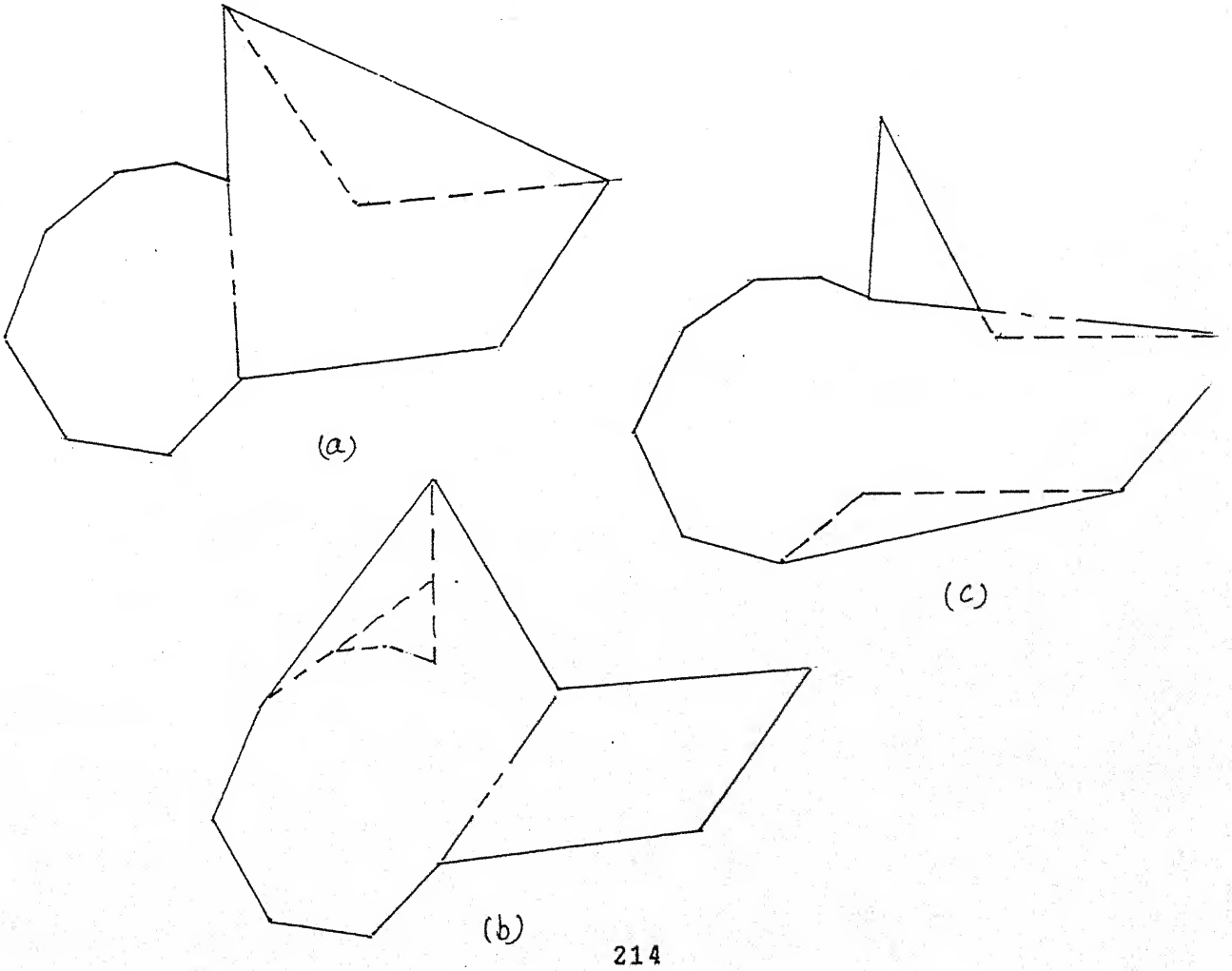

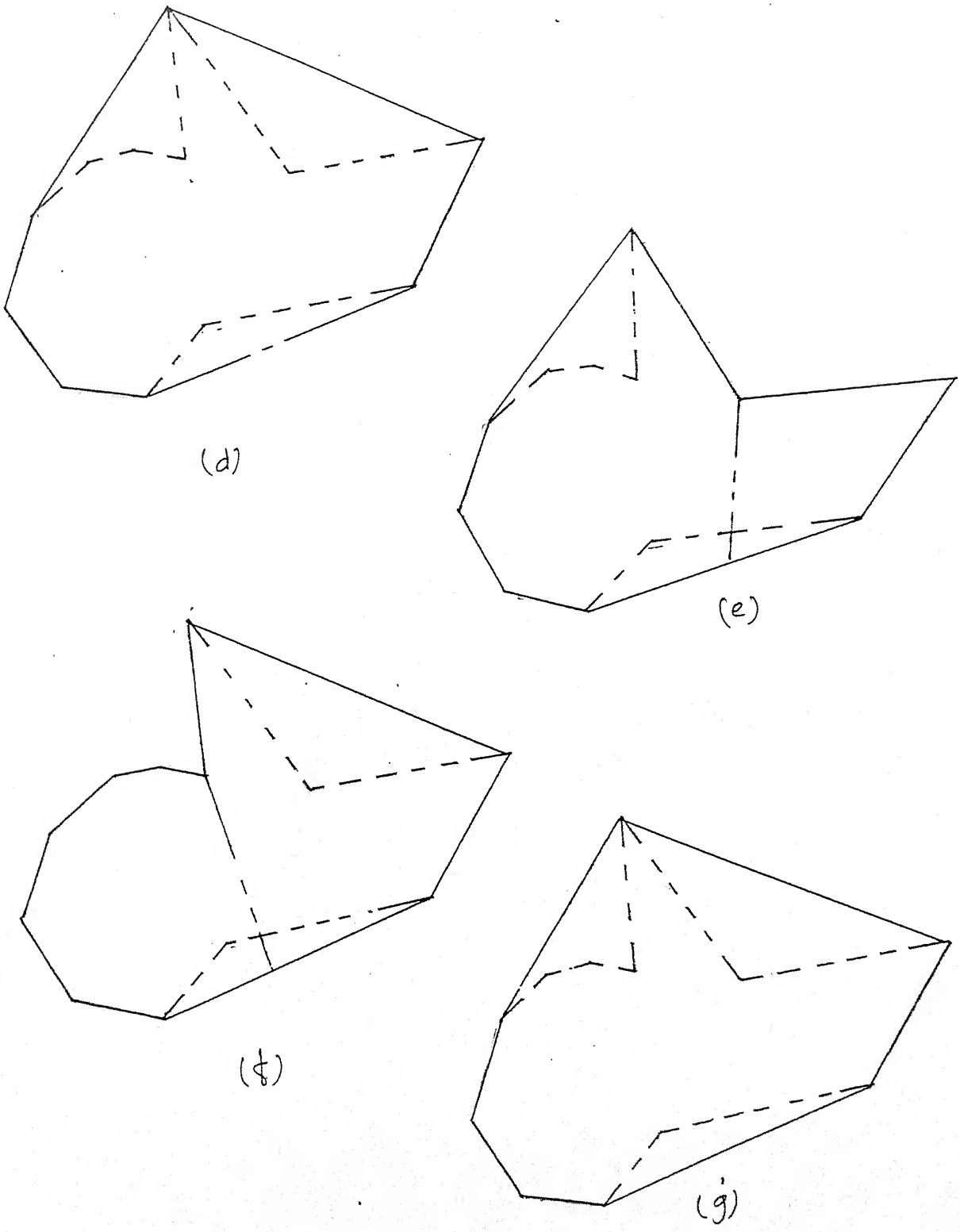

Fig. 4.3 Bay Merged Profile Versions

Chapter 6

CONCLUSIONS

1. Summary :

The aim of the thesis has been a full design automation, rather than an implementation of an interactive programme for nesting allocation. Shape analysis has been recognised to be crucial to any fully automatic nesting solution. Hence the basic thrust of the work is on shape analysis consistent with human perception of shape.

The problem of analysis of an arbitrary two dimensional profile is solved by decomposing the profile in to a set of convex polygons. The description of the constituent convex polygons, their inter-relations, and the boundary features, such as projections and bays generated thereof, form the description of the shape of the profile. Thus the shape description problem has been subdivided in to subproblems which have been solved independently. The shape description generated thereby will form the basis for further development of shape matching and nesting algorithms.

The subproblems and their solutions :

Polygon Decomposition : Pattern Recognition and computational geometry. In profile decomposition, which is a standard Computational Geometry / Pattern Analysis problem, the aim of the decomposition has been modified from a decomposition in to minimum number of polygons in to a decomposition optimising a heuristic function which reflects consistency with human perception. The skeleton and skeletal interactions of the concave vertices guide the decomposition cuts. A decomposition algorithm, based on the

skeleton, and approximations, has been proposed. It is a heuristically guided space search algorithm. The heuristics have been developed as fuzzy membership functions. Hence it also fits in to a fuzzy paradigm.

Convex Polygon Description : A scheme has been developed for a meaningful approximate description of an arbitrary convex polygon. It is based again on the special features of the skeleton of the convex polygon, such as the convexity of the radius of the skeletal circle as a function of the distance along the skeleton. The classification of the convex polygons, which is the basis of the description, is a fuzzy classification.

Profile Description : The proposed profile description is based on the geometrical and topological inter-relations of the constituent convex polygons. Features of the profile useful for nesting, such as projections, bays and their strings are recognised on the basis of these relations. An enumeration of these features along with the inter-relations, and the description of the constituent convex polygons is the profile description. The proposed algorithm generates multiple approximate descriptions. The further work on shape matching and nesting algorithms should be based on the profile description.

Shape matching and nesting algorithms have not been developed due to the time constraint on the thesis work. A thorough study of nesting algorithms has not been done; rather, the shape analysis approach has been pursued fully. The emphasis in the present work has been on the development of a complete conceptual framework for shape analysis and concomitant shape matching. The proposed framework can completely handle any non-selfintersecting polygon

with competence. The algorithms in the work have not been worked down to last details at places; but the problems have been reduced to standard problems in literature, for which complete solutions are known.

The present work is seen to be a fundamental work on two dimensional geometry. The approach developed in this work can be applied to diverse two dimensional geometry problems. As an illustration, an auxiliary problem in manufacturing automation, has been solved. The conceptual algorithm giving a complete solution has been given in the appendix.

2. Scope for Further Work in the Problem :

Since the present work is a conceptual framework development rather than a development of an algorithm, some of the standard problems to which the solution has been reduced, need to be studied further, for the purpose of an selection of the exact algorithm for the solution of the standard problem.

For the fuzzy logical operators and fuzzy inferencing, it is suggested that the generalised modus ponens developed by Didier and Prade [14], be followed. In addition, the fuzzy logical operators may be fine tuned by experimentation.

The heuristic functions / the fuzzy qualitative predicates proposed in the present work also should be improved and fine tuned by experimentation over a wide range of shapes. Particularly, the qualitative predicates for the proximity and size of the forks, in a convex polygon, need extra attention.

In profile decomposition, apart from cuts based on the skeletal interaction, the cuts generated by extending the edges meeting at

the concave vertex should be explored.

In the profile description, the projection-bay graphs have been analysed only after merging the bays required to reduce the complex graph to a set of strings. For a complete shape analysis, a thorough explorative study of the graphs may be done for a possible classification, as done in convex polygon description.

The shape description model is strictly additive in nature; i.e. the constituent convex polygons are only added to form the final profile. The concept of developing an additive as well as a subtractive model, wherein the enveloping approximations made for the sake of simplicity, may be considered to be the approximation minus the differential area between the approximation and the original shape, seems to be a good avenue for further work.

The whole shape description has been divided in to mutually exclusive set of subproblems. It has been assumed that the subproblems are mutually exclusive, but in reality it is not so. The subproblems do affect one another; e.g. In giving the CCP description, the exposure to the exterior should be considered while deciding the dominating features of the CCP. These cross effects should be studied, and explored further. For shape matching algorithms, the concepts developed by Shapiro and Haralick [33] may be found useful. Before proposing a nesting algorithm, a thorough study of nesting strategies, vis a vis the range of shapes, sizes, number of profiles, and the distribution of shape and size on the number of profiles must be done. For nesting based on shape matching, clustering is an important nesting strategy. The potential of the shape matching approach would be more apparent in an implementation which allows

clustering of the profiles in to simpler shapes and allocation of the clusters.

The possible cross-effects of the shapes of other profiles have not been considered in the present work; e.g. If a profile has a feature such as a bay, which is quite small and there are no projections which may possibly fit this bay in the other profiles, then it would be better to merge this bay in to the profile, rather than considering it to be a bay and there by cmplicating the analysis. Also, it would be better to approximate the features of a small profile, as the increase in nesting efficiency would not amount to much; and the complexity of the problem would be reduced. Such cross-effects, if considered, would greatly enhance the usefulness of any nesting implementation.

3. Generalisation of the work :

Polygons with holes can be handled through the clustering approach, by allocating small profiles in the holes; otherwise, holes do not play any part in nesting. After allocating small profiles in the holes, the remaining area should be merged in to the profile and shape analysis should be continued for the merged profile.

As mentioned earlier, curved boundary handling in the present work is not completely satisfactory. For a fully complete development capable of handling any two dimensional shape, curves should be handled as curves and not as linear approximations. The present work can not be directly extended to profiles with curved boundaries as the profile decomposition depends on concave vertex elimination; and also, in convex polygon description, the 'number

of sides' play an important role in the analysis. An investigation in to the curvature along the boundary of the profile might lead to a method to extend the present approach to curved profiles, as the change of sign of curvature and any discontinuity in curvature indicate the presence of a concavity.

Extension of the shape analysis to 3-D solids is extremely difficult. It is suggested that the skeleton could again play a vital role in 3-D analysis, as it does in 2-D analysis. A 3-D shape analysis using skeleton of 3-D solids has been mooted in [26]. It could be used as a starting point for the study of 3-D shapes.

APPENDIX

Auxiliary problem solved by shape analysis approach

1. Statement of Problem :

The generation of the machining sequence for a prismatic solid, of polygonal cross-section to be machined on a milling center, by end, peripheral or face milling, or by trepanning operations, from a bar of some standard cross-sections such as rectangular, hexagonal or circular.

2. Discussion on the approach to the problem :

This problem can be considered to be a two dimensional geometrical problem. The considerations of feasibility of the machining sequence from clamping of the work piece, the cutting forces minimisation and the optimality of the machining sequence for minimum time etc. can be imposed later, on the solution to the geometric problem. The geometrical problem must be completely solved first indicating the areas to be removed, the tools required to remove the areas, and the sequence of the removal of the area.

The basic approach to the problem will follow the following sequence.

1) Generate a minimum area envelope of the cross-section of a standard shape.

2) Identify the areas to be removed, by taking the differential area between the cross-section and the envelope. Disjoint components of the differential area are taken as different irregular profiles to be removed. These areas are referred to as profiles henceforth, to maintain consistency with the terminology

used in the thesis.

3) It may be noted that a the milling cutters considered in the problem, in one pass or in multiple, overlapping or non-overlapping passes, cut and remove rectangular areas. Hence the profiles should be decomposed in to rectangular constituents which may overlap. The constituents may also be triangular in shape. The machining of the triangular primitives is explained later. Each of the constituent primitives is cut by a milling cutter in one machining operation. To obtain a minimum number of machining operations, the number of primitive constituents should be minimum.

4) To obtain a feasible machining sequence, the rectangular constituents should be ordered on the basis of their exposure to the exterior, or their external visibility. The exterior referred here is the exterior of the polygon composed of the cross-section and the parts of the profiles yet to be removed, it is referred to as the intermediate cross-section henceforth.

5) The feasibility of each of the machining operations should be checked for the accessibility of the primitive at the time of removal, and the basic feasibility of machining such a primitive. For example, a pocket may not be accessible as the tool holder may interfere with the work-piece, a triangular notch can not be machined by a milling operation. A machining sequence which has been checked for the feasibility of all the machining operations in it, is referred to as a verified machining sequence.

6) A number of machining sequences may be possible. Some of which may turn out to be infeasible from clamping and other

considerations. A completely automated process planning should then consider the force analysis also. That is out of the purview of the present work which is strictly geometrical in nature. The geometrically feasible verified machining sequences may be all displayed to the user and the user may be asked to select one the machining sequence which is deemed to be the best for the clamping and other considerations.

Each of these steps is elaborated upon in the following sections.

3. Standard Envelope Generation :

This problem is not a very difficult one. A convex hull of the cross-section can be taken and the envelope may be built around it, on the basis of the available standard cross-sections and their sizes. Identification of the disjoint differential areas between the cross-section and the envelope is again a simple problem.

4. Decomposition :

The profile (the profile is the area to be machined away) may be decomposed in to convex polygons. Each of the convex polygons may then be decomposed in to rectangles and triangles quite trivially. This decomposition may not be optimal but it can form the basis of a solution methodology which can completely solve the problem and exactly identify and indicate the polygonal cross-sections which can not be machined by milling. The feasibility of the machining sequences which may be obtained from the decompositions, are discussed in the next section. A decomposition which can give a feasible machining sequence is called a feasible decomposition. Multiple feasible decompositions may be formed, and an optimal decomposition may be selected from the set of the feasible

decompositions. The heuristics for guiding the decomposition process should be based on the cutting considerations.

5. Feasibility of a Machining Sequence :

The feasibility of a machining sequence is the feasibility of the constituent machining operations. A machining operation is fully identified when the milling cutter required to remove the primitive under consideration is identified. At a stage in the determination of the machining sequence, a primitive may be in the situations shown in the Fig. 1.

A rectangular primitive, with atleast one side fully exposed to the exterior of the intermediate cross-section (ref. step 4 of section 2) may be milled by approaching the rectangle from that side, as shown in the part (a) of figure 1. Tentatively select a milling cutter, from those available, for the rectangle. Determine the area swept by the cutter as it approaches the rectangle. If the swept area does not intersect with the intermediate cross-section, then the machining operation is feasible.

A rectangle with only a part of a side exposed to the exterior of intermediate cross-section, necessarily needs a milling operation followed by a trepanning operation. The feasibility of this operation again depends upon the interference of the swept area of the cutter with the intermediate cross-section and also upon the position of the exposed boundary segment (Fig. 1(b)).

A triangle which has two sides exposed, may be machined as shown in part (c) of the figure 1. A triangle with only one side exposed to the exterior, can not be milled. The rest of the feasibility considerations are the same as the ones given earlier.

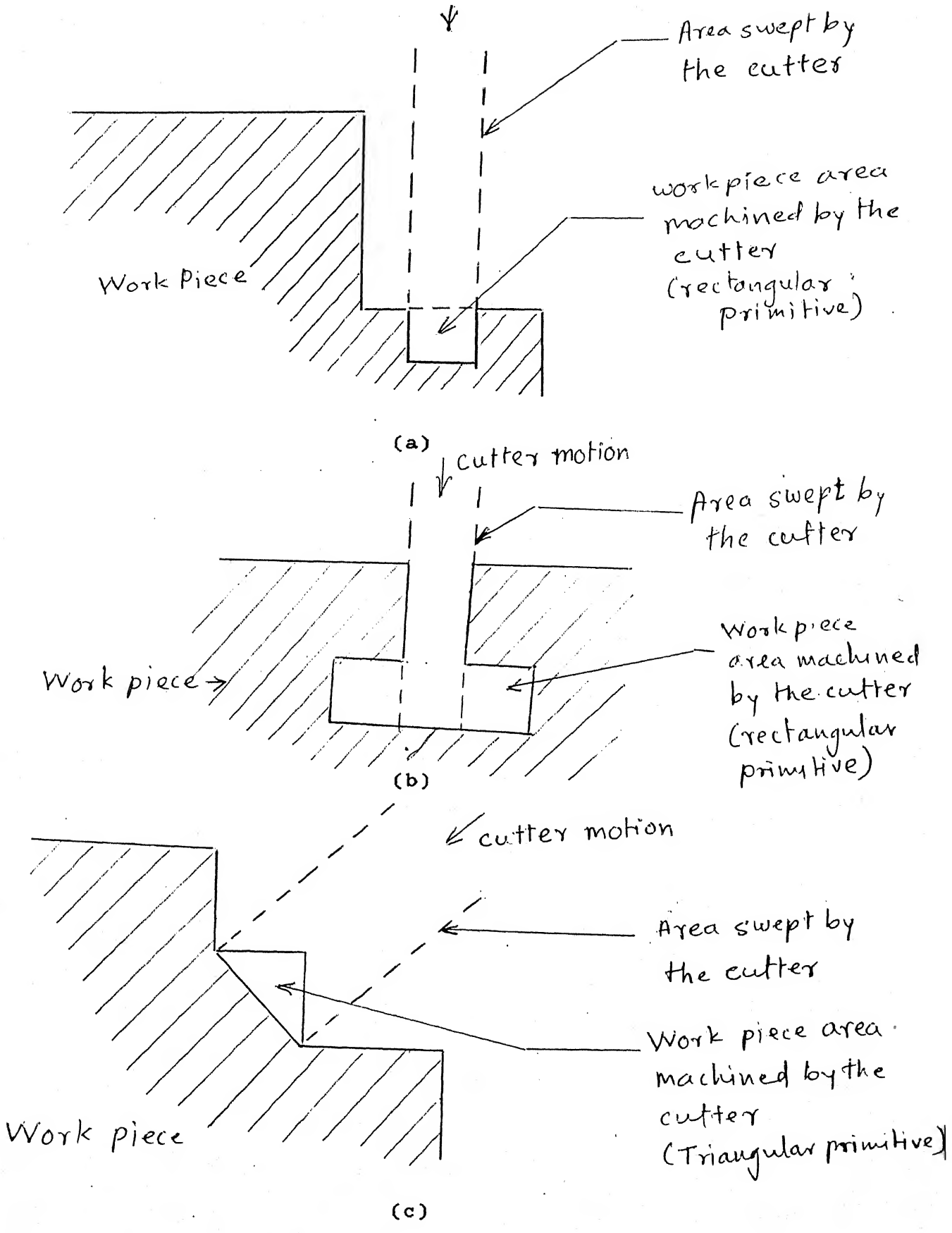

Fig. 1. Area Primitives and Milling Operation

6. Machining Sequence :

The neighbourhood relations of the primitives form a graph (similar to the CCP-N relation graph given in section 3 of the chapter 5) The neighbourhood relations may be the adjacency relations i.e. the existence of a shared edge between two primitives, instead of the N-relations developed in the thesis. Determination of a machining sequence is the determination of a hierarchy in the graph, in terms of the necessity of the prior removal of a primitive with respect to the other primitives. The directed graph formed by the imposition of the hierarchy, and after an exhaustive machining operation feasibility check (verification), gives the set of feasible machining sequences. The verified and directed primitive neighbourhood relation graph is henceforth abbreviated as VDPN graph.

The primitives which are directly exposed to the exterior of the envelope may be removed first and hence they form the roots of the graph. In Fig. 2, primitives A and B are directly exposed to the exterior of the envelope. They form the roots of the graph. Any of them can be removed first. If A is removed, then B is exposed to the exterior of the intermediate cross-section. Note that C is not exposed to the exterior for a feasible machining operation with just the removal of A. After the removal of B any of C and D can be removed in any order. If C is removed first, then D is removed, and finally E is removed by a trepanning operation. Similarly, if B had been removed in the first step rather than A, the graph could again have been followed similarly.

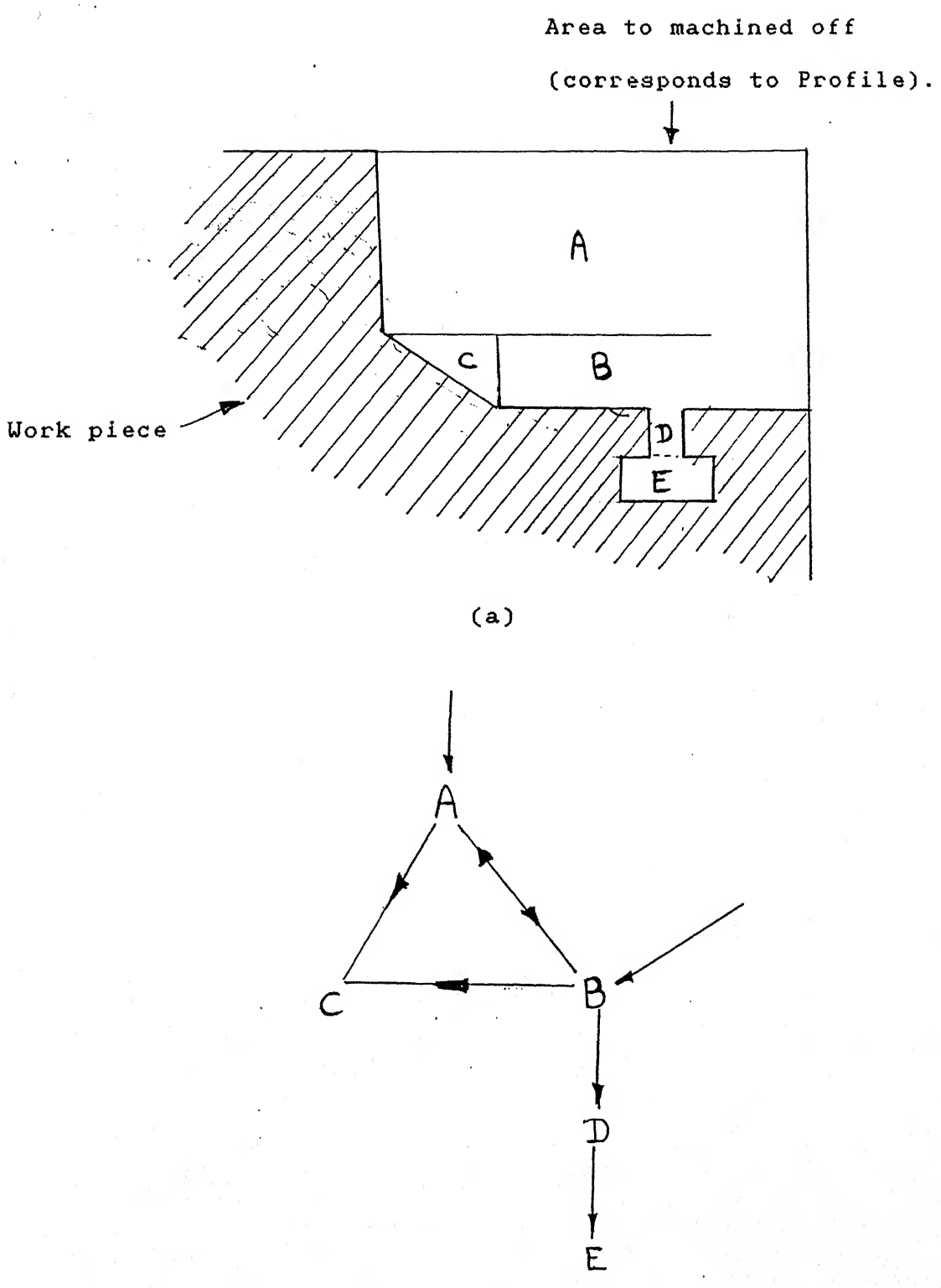

Fig. 2 Example of Automated Milling Geometric Process Planning

At each of these steps, the feasibility of a machining operation must be checked before deciding upon the set of the possible candidates for removal. A VDPN graph must contain all the primitive nodes present in the primitive N-relation graph; otherwise it indicates the infeasibility of the production of the object by a set of only milling operations, for the given set of cutters. It may be noted that a set of cutters is associated with every primitive, and thus every requisite machining operation is identified. The exact assignment of a unique cutter to every machining operation may be done later, on the basis of the optimality of the machining operation for simultaneity of machining operations and minimisation of the overall machining time. The VDPN graph for the object in figure 2(a), obtained after the hierarchy imposition and feasibility check is illustrated in the part (b) of the Fig. 2.

The paths from the roots to the leaf nodes of the VDPN graph, give the priority constraints for machining operations. A set of paths which completely spans the primitive nodes gives a set of feasible machining sequences. The set of all the sets of such spanning paths, give the complete set of feasible machining operation sequences. The machining sequences ABCDE, ABDEC, ABDCE, BACDE, BADEC, BACDE are the feasible machining sequences for the object in figure 2.

The set of the feasible machining sequences may be processed further for the determination of an optimal machining sequence. The possibility of simultaneous machining operations is indicated by the subpaths, within the set of paths giving a machining

sequence, which do not intersect i.e. which do not have any common primitive nodes.

7. Conclusions :

The basic concepts developed in the thesis, of decomposing the profile in to a set of constituent primitives and forming a neighbourhood relation graph to structure the shape of the profile, have been successfully applied in a diverse geometrical problem of automatic process planning. Thus the universality of the methodology has been demonstrated. It may be concluded that the method developed in the thesis has a very good potential for the solution of a lot of diverse geometrical problems encountered in mechanical engineering.

REFERENCES

1. Ahuja Narendra, Schachter Bruce J., "Pattern Models", John Wiley and Sons, 1983.

2. Albano, " A Method to Improve Two Dimensional Layout", Computer Aided Design, Vol. 9, no. 1, Jan. 1977, pp. 48 - 52.

3. Albano and Adamowicz, "Nesting Two Dimensional Shapes in Rectangular Modules", Computer Aided Design, Vol. 8, no. 1, 1976, pp 27 - 33.

4. Albano and Sappupo, "Optimal Allocation of Two Dimensional Irregular Shapes using Heuristic Search Methods", IEEE Trans. System, Man and Cybernetics, Vol. SMC-10, no. 5, May 80, pp 242 - 248.

5. Arcelli C. and G. Sanniti di Baja, "Shape Splitting Using Maximal Neighourhoods" , Proceedings of the 6th International Conference on Pattern Recognition, 1982, pp. 1106 - 1108.

6. Bailleul J., Tiabia K. and Soenen R., "Nesting of Two Dimensional Irregular Shapes in Anisotropic Materials", in "Advances in CAD/CAM", Ed. T. M. R. Ellis and O. I. Semenkov, Proceedings of IFIP/IFAC Conference on Programming Research and Operation Logistics in Advanced Manufacturing Technology, PROLAMAT 82, North Holland 83, pp 191 - 202.

7. Bjorklund Carolyn M. and Pavlividis T., "Global Shape Analysis by K-Syntactic Similarity", IEEE Trans. Pattern Analysis and Machine Analysis, Vol. PAMI-3, no. 2, March 1981, pp 144 - 154.

8. Blum Harry, "A Transformation for Extracting New Descriptions of Shapes", in "Symposium on Models for Perception of Speech and Visual Form", Cambridge, MA: MIT Press, 1964.

9. Blum Harry and Nagel Roger N., "Shape Description Using Weighted SAT Features", Pattern Recognition, Vol. 10, pp. 167 - 180.

10. Cai Yuzu, Liu Lujun, Wang Wei, Sun Jianwen, "An Expert System for Automatic Allocation of Two Dimensional Irregular Shapes", in "Expert Systems in CAD", Ed. John S. Gero, Proceedings of IFIP WG5.2, Working Conference on Expert Systems in CAD, North Holland 87, pp 407 - 419.

11. Chazelle Bernard M. "Computational Geometry and Convexity" PhD. Thesis, Department of Computer Science, Carnegie Melon University.

12. Deo Narsingh, "Graph Theory with Applications to Engineering and Computer Science", Englewood Cliff, N.J., Academic Press, 1979.

13. Duboise Didier and Prade Henri, "Fuzzy sets and Systems, Theory and Applications" Academic Press 1980.

14. Duboise Didier and Prade Henri, "Possibility Theory, An Approach to Computerised Processing of Uncertainty", Plenum Press 1988.

15. Duda R. O. and Hart P. E., "Pattern Classification and Scene Analysis", New York : Wiley, 1973.

16. Fu K. S., "Syntactic Methods in Pattern Recognition", New York : Academic Press, 1974.

17. Fu K.S., Srinivasan R. and Liu C.R., "Extracting Manufacturing Details from Geometric Models", Computers & Industrial Engineering, Vol. 9, No. 2, pp 125-133.

18. Henderson Thomas C. and Davis Larry C., "Hierarchical Models and Analysis of Shapes", Pattern Recognition, Vol. 14, no. 1-6, pp. 197 - 204.

19. Kandel Abraham, "Fuzzy Mathematical Techniques with Applications" New York, John Wiley 1982.

20. Kandel Abraham, " Fuzzy Techinques in Pattern Recognition", John Wiley and Sons 1982.

21. Lee D. T., "Medial Axis Transform of a Planar Shape", IEEE Trans. Pattern Analysis and Machine Intelligence, Vol. PAMI-4, no. 4, pp. 363 - 369.

22. Maheshwari Jagdish, "Computer Aided Nesting of Irregular Shapes", M.Tech. Thesis, Dept. of Mechanical Engg, IIT Kanpur, March 87.

23. Massone L. and Morasso P., "SCULPTOR - 2: Representing, Generating, and Editing Smooth Planar Shapes", in "Artificial Intelligence Methodology, Systems, Applications", Ed. W. Bibel and B. Petkoff, Proceedings of International Conference on Artificial Intelligence: Methodology, Systems, Applications (AIMSA '84), North Holland 1985.

24. Pavlividis T., "Algorithms for Shape Analysis of Contours and Waveforms", IEEE Trans. Pattern Analysis and Machine Intelligence, Vol. PAMI-2, no. 4, July 1980, pp. 301 - 312.

25. Pavlividis T., "Structural Pattern Recognition", New York : Springer Verlag, 1977.

26. Pizer Stephen M., Oliver William R., Bloomberg Sandra H., "Hierarchical Shape Description via Multi-resolution SAT", IEEE Trans. Pattern Analysis and Machine Intelligence, Vol. PAMI-9, no. 4, July 1987, pp 507 - 517.

27. Rong Kwei Lee, "A Part Feature Recognition System for Rotational Parts", International Journal of Production Reasearch, Vol. 26. No. 9, pp 1451-1475.

28. Sangal Rajeev, "Programming Paradigms in Lisp", Forthcoming by McGraw Hill Book Co.

29. Seng - Beng Ho and Charles R. Dyer, "Shape Smoothing using Medial Axis", IEEE Trans. Pattern Analysis and Machine Intelligence, Vol. PAMI-8, no. 4, July 1986, pp 512 - 520.

30. Shapiro Linda G., "A Strucural Model of Shape", IEEE Trans. Pattern Analysis and Machine Intelligence, Vol. PAMI 2, no. 2, Mar. 1980, pp 111 - 126.

31. Shapiro Linda G., "Recent Progress in Shape Decomposition and Analysis", in "Progress in Pattern Recognition 2", Ed. Kanal Laveen N., Rosenfeld Azriel, North Holland 1985 pp. 113 - 123.

32. Shapiro Linda G. and Haralick Robert M., "Decomposition of Two Dimensional Shapes by Graph - Theoretic Clustering", IEEE Trans. Pattern Analysis and Machine Intelligence, Vol. PAMI-1, no. 1, Jan. 1979, pp 10 - 20.

33. Shapiro Linda G. and Haralick Robert M., "Structural Description and Inexact Matching", IEEE Trans. Pattern Analysis and Machine Intelligence, Vol. PAMI-3, no. 5, Sept. 1981, pp 504 - 519.

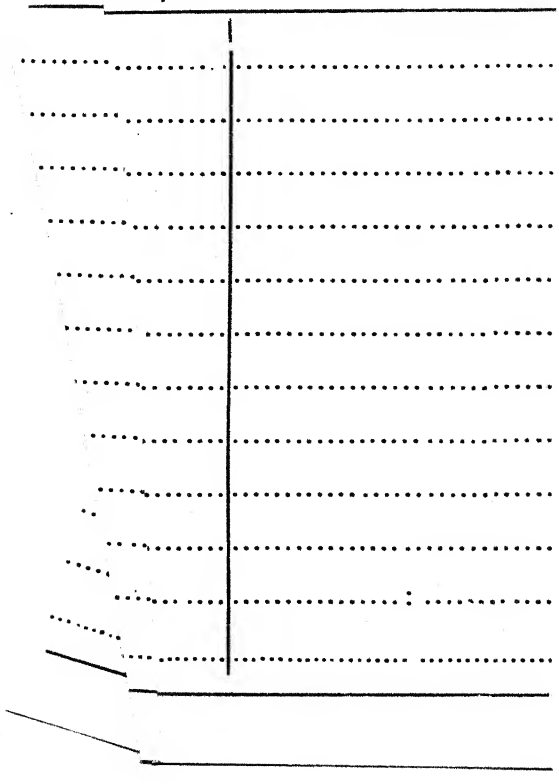

ME-1989-M-RAN-DEV